Platelets: Their Exploitation and Elimination

Lucy Anne Coupland

THE AUSTRALIAN NATIONAL UNIVERSITY

THE JOHN CURTIN SCHOOL
OF MEDICAL RESEARCH

A thesis submitted for the Degree of
Doctor of Philosophy at
The Australian National University

MARCH 2011

Table of Contents

Declaration

All experimental work presented in this thesis has been performed and analysed by the author unless stated otherwise. Initial assistance was provided by Dr Ben Quah with FACS machine settings and i.v. injections, by Mrs Anna Bezos with organ dissections and cell culture techniques and by Ms Megan Glidden with i.v. injections. Mrs Debbie Howard assisted in the bone marrow transplantation process and Ms Anna Browne in the collection of peritoneal macrophages. Dr Deborah Cromer performed the mathematical modelling of platelet and erythrocyte lifespans. Examination of organs for evidence of CFSE toxicity was undertaken by Professor Jane Dhalstrom of ACT Health.

This thesis conforms to The Australian National University guidelines and regulations. The work presented in this thesis has not been submitted for the purpose of obtaining any other degree at this, or other universities.

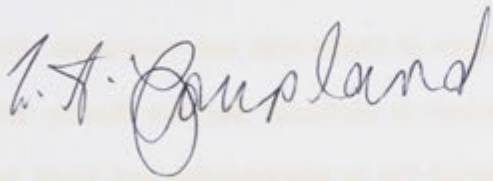

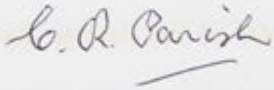

Lucy A. Coupland
(Author)

Professor Christopher R. Parish
(Supervisor)

Cancer and Vascular Biology Group
Division of Immunology and Genetics
The John Curtin School of Medical Research
The Australian National University

THE AUSTRALIAN NATIONAL UNIVERSITY

THE JOHN CURTIN SCHOOL
OF MEDICAL RESEARCH

MARCH 2011

Acknowledgements

Embarking on a PhD provided me with an opportunity to change career paths and to undertake a significant intellectual challenge. I was extremely fortunate to enlist a supervisor of Chris Parish's calibre and thank my referees Dr's Jennifer Byrne and James D'Rozario for securing Chris' interest in me as a PhD candidate. Chris is not only a superb scientist whose intellectual capacity and memory are to be envied, but he is also a very decent person displaying high morals and ethics, being approachable and understanding, but also infusing enthusiasm and confidence into his staff and students. I cannot thank Chris enough for the opportunities he has provided, and the time he has invested in me throughout my PhD candidature.

I would also like to thank my principal advisors Dr's Ben Quah and Hilary Warren for providing much appreciated encouragement along the way. Anna Browne, Anna Bezos, Megan Glidden and Julia Ellyard provided technical advice and assistance when required, but more importantly, they provided a greatly needed supportive and fun-filled environment particularly when experiments failed. The assistance of Dr Harpreet Vohra, Mick Devoy, Anne Prins and Cathy Gillespie, of the Microscopy and Cytomtery Resource Facility, and Cathy Edwards of Multimedia was invaluable. The help of the staff of the Animal Services Division, in particular Barbara Bourke and Nyasa Fook was also greatly appreciated. I would like to acknowledge and thank the NH&MRC for the Dora Lush Scholarship enabling me to undertake this PhD.

Finally, this work is dedicated to my parents, Anne and Bill, who have always believed in and encouraged my every ambition, to my husband, Robert, who has been in the background providing emotional, financial and domestic support for the duration of this candidature, and to my son, Timothy, a constant source of love, energy, happiness and enthusiasm.

Abbreviations

-/-	knockout
ACD	Acid citrate dextrose
ADP	Adenosine diphosphate
ANU	Australian National University
BSCG	Buffered saline citrate glucose
°C	Degrees celsius
C3	Complement component 3
CFSE	Carboxyfluorescein diacetate succinimidyl ester
CRC	Colo-rectal carcinoma
CV	Coefficient of variation
CVF	Cobra venom factor
DMSO	Dimethyl sulfoxide
ECM	Extracellular matrix
EDTA	Ethylenediaminetetraacetic acid
EGF	Epidermal growth factor
EMT	Epithelial to mesenchymal transition
ENU	*N*-ethyl-*N*-nitrosourea
FACS	Fluorescence-activated cell sorting
FcγR	Receptor for the Fc portion of IgG
FCS	Fetal Calf Serum
FITC	Fluorescein isothiocyanate
FSC	Forward scatter
g	Relative centrifugal force
GAG	glycosaminoglycan
Gp	Glycoprotein
HA	Hyaluronic acid

HGF	Hepatocyte growth factor
hr	hour/s
HS	Heparan sulphate
HSPG	Heparan sulphate proteoglycans
ICAM	Inter-cellular adhesion molecule
IgG	Immunoglobulin G
IL	Interleukin
i.p.	Intraperitoneal
i.v.	Intravenous
IVIg	Intravenous pooled immunoglobulin
ITP	Immune thrombocytopenic purpura
JAM	Junctional adhesion molecules
JCSMR	The John Curtin School of Medical Research
KO	Knockout
L	Litre
LAMP	Lysosomal-associated membrane protein
LLC	Lewis lung carcinoma
M	Molar
mAb	Monoclonal antibody
MEM	Minimal essential media
mg	Millgrams
μg	Microgram/s
MHC	Major histocompatibility complex
MHM	Multiple-hit model
min	Minute/s
μL	Microlitres
μM	Micromolar
mM	Millimolar

MMP	Matrix metalloprotease
NK cell	Natural killer
NKT cell	Natural killer T cell
PBS	Phosphate buffered saline
PDGF	Platelet-derived growth factor
PE	Phycoerythrin
PerCP	Peridinin chlorophyll protein complex
PMV	Platelet-derived microvesicles
P-Sel	P-Selectin
PSGL-1	P-selectin glycoprotein ligand 1
PSN	Penicillin streptomycin neomycin
RBC	Red Blood Cell, Erythrocyte
RNA	Ribonucleic acid
RT	Room temperature
SEM	Standard error of the mean
SIRPα	Signal regulatory protein α
SSC	Side scatter
TEM	Trans-endothelial migration
TGF	Transforming growth factor
TNF	Tissue necrosis factor
TPO	Thrombopoietin
TPO-R	Thrombopoietin receptor
VEGF	Vascular endothelial growth factor
VCAM	Vascular cell adhesion molecule
vWF	Von Willebrand factor
WBC	White blood cells, leukocytes
WT	Wild type

Abstract

Platelets are cytoplasmic fragments present in large numbers within the bloodstream that contain a multitude of proteins. For a long time, platelet function was believed to be limited to the essential functions of haemostasis and thrombosis. However, it has become clear in the last decade that platelets play significant roles in both innate and adaptive immunity, inflammatory responses including leukocyte migration, tissue regeneration and angiogenesis. Parallelling the revelation of the diverse physiological functions of platelets, however, has been the association of exacerbated platelet function with numerous thrombotic and chronic inflammatory diseases. Until our knowledge of platelet biology is more comprehensive, the prevention of platelet-associated pathologies will remain a challenge of inhibiting pathology-associated platelet reactions whilst preserving those essential for normal function. The aims of this thesis, therefore, were to examine in detail the following three platelet-associated biological processes: (i) The role of platelets in tumour cell metastasis, in particular, the kinetics and interrelationship of the pro-metastatic role of platelets and the anti-metastatic role of NK cells, and the relevant contributions to the metastatic process of platelet P-selectin and endothelial P-selectin. (ii) The determinants and mechanisms of antibody-mediated platelet elimination, as seen in the medical condition known as immune thrombocytopenic purpura (ITP), and the role of inhibitory self-recognition systems in this process. (iii) The factors influencing platelet and erythrocyte lifespan by establishing appropriate experimental and analytical methodologies.

The results of work described in Chapter 3 have demonstrated that the lung metastasis of both B16F1 melanoma cells and 4T1.2 breast cancer cells is promoted by platelets and inhibited by NK cells. Moreover, in the B16F1 metastasis model, platelets were demonstrated to promote lung metastasis by a process that is independent of NK cells and, likewise, the action of NK cells was unaltered in the presence or absence of platelets. Additionally, the role of platelets and NK cells in the metastatic process were

shown to be chronologically distinct with the pro-metastatic action of platelets occurring within 1 hr, and the anti-metastatic action of NK cells occurring between 1 hr and 24 hr following tumour cell injection. Intriguingly, unlike B16F1 melanoma lung metastasis, B16F1 liver metastasis appeared not to be reliant upon platelets, in fact, in the absence of platelets liver metastasis was increased most likely due tumour cells, unable to adhere to the lung capillary bed without the assistance of platelets, being swept into downstream organs. Furthermore, the pro-metastatic roles of both platelet-derived and endothelial-derived P-selectin in lung metastasis, and endothelial-derived P-selectin in liver metastasis, was demonstrated. P-selectin may, therefore, represent a key target for therapies aimed at preventing tumour metastasis in multiple organs.

In Chapter 4, it was demonstrated in a mouse model of ITP using rat mAbs specific for various murine platelet surface proteins, that ITP induction was dependent upon the platelet protein targeted by the antibody and the antibody isotype, it was not determined by the density of mAb binding or the level of platelet antigen saturation. Additionally, the mechanism of platelet elimination in this model of ITP occurred principally via FcγR-mediated phagocytosis but was also shown to occur, in a limited number of instances, through complement-mediated destruction or through an FcγR- and complement-independent process of platelet fragmentation. An exploration into the role of the self-recognition protein pair CD47:SIRPα in this model of ITP revealed that some antibodies that were incapable of inducing ITP in WT mice were capable of inducing ITP in CD47-deficient mice. Furthermore, administration of an activating mAb specific for SIRPα *in-vivo* not only prevented, but reversed rat IgG1 mAb-induced, FcγR-mediated ITP. This treatment effect was isotype specific, however, as SIRPα mAb treatment was unable to prevent ITP induced by rat IgG2b mAbs suggesting that SIRPα inhibits the signalling capacity of low-affinity rather than high-affinity FcγRs. The results of these studies give a greater understanding of the pathogenic pathways of

ITP and how self-recognition systems may be manipulated to prevent antibody-mediated ITP.

The aims of work presented in Chapter 5 were to establish an *in-vivo* platelet and erythrocyte labelling method using CFSE, determine the most appropriate mathematical model for lifespan analysis, and apply both to the study of factors that control platelet and erythrocyte lifespans. Control and platelet-deficient *c-mpl-/-* and Bcl-X_L mutant mice were injected with CFSE and platelet and erythrocyte fluorescence followed over time. Data sets were analysed using linear, exponential, multiple-hit and lognormal mathematical models. It was found that *in-vivo* CFSE labelling of platelets and erythrocytes requires no post-collection processing, proved to be stable, non-toxic and non-immunogenic, and the lifespans obtained were highly reproducible. Mathematical modelling revealed the lognormal model gave a robust fit to control and extreme data sets when either extrinsic or intrinsic factors determined lifespan. Using these methods, platelet lifespans were found to be significantly shortened in thrombopoietin-receptor deficient mice independent of blood loss, and the anti-apoptotic protein Bcl-X_L was shown to play a role in prolonging erythrocyte lifespans. Thus, the simultaneous study of platelet and erythrocyte lifespans using *in-vivo* CFSE labelling with lognormal modelling yielded insights into common intrinsic and extrinsic platelet and erythrocyte lifespan determinants and provides an improved methodology for use in this field of research.

The experimental data presented in this thesis has shed some light on three aspects of platelet biology, namely, proving their NK cell independent role in the promotion of tumour cell metastasis that closely resembles their role in assisting leukocyte migration; identifying not only likely determinants and mechanisms of antibody-mediated platelet destruction but also an inhibitor of this process that may have therapeutic potential; and the development of robust methods that may be used to

better understand those factors influencing the production, lifespan and senescence of platelets. As with most research, whilst the results presented in this thesis have answered some questions, they have also raised many more upon which future research may be based.

Publications resulting from this thesis

Coupland LA, Cromer D, Davenport MP, Parish CR.

A novel fluorescent-based assay reveals that thrombopoietin signaling and Bcl-X_L influence, respectively, platelet and erythrocyte lifespans.

Exp Hematol. 2010 Jun;38(6):453-461.e1. Epub 2010 Mar 16.

Conferences organised during candidature

2008

Member of Organising Committee, Annual Scientific Meeting of the Australasian Society of Immunology, Canberra Convention Centre.

2009

Conference Convenor and Member of Scientific Panel, Annual Scientific Meeting of the Australian Vascular Biology Society, John Curtin School of Medical Research.

Conferences attended during candidature

2007

Haematology Society of Australia and New Zealand Annual Scientific Meeting, Gold Coast Convention Centre (Poster presentation)

2008

Canberra Region Annual Scientific Meeting (Poster presentation)

International Vascular Biology Meeting, Darling Harbour Convention Centre, Sydney (Poster presentation)

2009

Australian Society of Immunology Annual Scientific Meeting, Gold Coast, Jupiter's Casino (Oral Presentation).

2010

Australian Vascular Biology Society Annual Scientific Meeting, Lorne Victoria.

2011

Australian Vascular Biology Society Annual Scientific Meeting, Bowral, NSW (Poster presentation and oral presentation awarded a prize).

Chapter 1

Literature Review

1.1 Introduction

Cancer is one of the greatest contributors to morbidity and mortality in developed countries with estimates that 1 in 3 males and 1 in 4 females within the Australian population will be diagnosed with cancer before the age of 75 (Australian Institute of Health and Welfare 2010). Approximately 40% of those individuals will succumb to their disease within 5 years despite treatment (Australian Institute of Health and Welfare 2008). The principle cause of cancer-associated mortality is metastasis, the spread of cancer from the initial site of occurrence, known as the primary, throughout the body forming secondary tumours.

Metastasis occurs via the bloodstream, known as the haematogenous route, or via the lymphatic vessels. Due to the nature of the circulatory system, haematogenous metastasis results in the dissemination of metastasising tumour cells to multiple organs with the most common sites being the liver, lungs, bone and brain (National Cancer Institute; Liotta 1992). It is these multiple secondary sites of tumour growth that present the greatest threat to life and the greatest challenge for treatment. Hence, elucidating the mechanisms of metastasis and designing therapies to prevent its occurrence are imperative to the overall goal of reducing cancer-related deaths.

The relationship between an increased risk of thrombosis (blood clots) and malignant cancer has been long recognised, being first described by Bouillard in 1823 and later by Trousseau in 1865 (Bouillard and Bouillaud 1823; Trousseau 1865). These initial observations stimulated a great amount of research into the many components of coagulation and their role in metastatic disease. Platelets were first demonstrated to promote metastasis by Gasic et al in 1968 (Gasic *et al.* 1968). Many studies performed since then have confirmed the pro-metastatic role of platelets with the purported mechanisms of action including the formation of a thrombus around the

tumour cell thus affording protection from haemodynamic stresses, linking tumour cells to the vascular endothelium via adhesion molecules, assisting the migration of tumour cells across the blood vessel wall through the releases of deradative enzymes, and the provision of growth and angiogenic factors enabling the establishment of secondary tumours (Karpatkin and Pearlstein 1981; Karpatkin 2002; Erpenbeck and Schon 2010). The evidence was sufficiently compelling for clinical trials of various anti-platelet agents to be conducted in individuals with cancer. Conflicting results, however, have cast a shadow of doubt over this potential avenue of therapy (Akl *et al.* 2007; Kuderer *et al.* 2007). Other laboratory-based research has suggested the only role for platelets in metastasis is the formation of a protective cloak around the tumour cells thus preventing immune-cell mediated tumour-cell killing (Nieswandt *et al.* 1999; Palumbo *et al.* 2005).

The full repertoire of platelet activities in health and disease is still being unravelled. For a long time, platelet function was believed to be limited to haemostasis (the arrest of bleeding) and thrombosis, however, it has become clear in the last decade that platelets play a significant role in immunity, inflammation, wound healing, and angiogenesis (new blood vessel formation). The molecular events involved in these platelet functions are complex and still being determined.

This thesis revisits the role of platelets in haematogenous tumour cell metastasis and, thus, the following sections provide background information on the diversity of platelet functions, the ultra-structural and molecular characteristics of the haematogenous metastatic process with a comparison made to that of leukocyte migration, and the evidence for and against a role for platelets in haematogenous metastasis. The chapter concludes with a summary of the aims of the PhD project.

1.2 Platelet Structure and Function

Although platelets were Initially thought to have a role only in thrombosis and haemostasis, they have subsequently been shown to participate in wound healing, angiogenesis and immune-related activities such as defence against pathological microorganisms, and activation and assisted migration of immune cells. The following sections briefly review the structure and functions of platelets.

1.2.1 Platelet Structure

Platelets circulate within the bloodstream and consist of small, discoid, anucleate, cytoplasmic fragments released by megakaryocytes from within the bone marrow or the lung capillary bed (Zucker-Franklin and Philipp 2000). In the resting state, the surface of the platelet contains numerous pores that function as entrances to the open canalicular system, an elaborate internal, tubular, membraneous network. Within the platelet cytoplasm are mitochondria, some endoplasmic reticulum and 3 types of storage granules - α granules, dense granules and lysosomes. The contents of platelet granules are considerable and listed in Table 1.1 (Reed 2002).

Alpha-granules are the largest and most numerous of the platelet secretory granules making up approximately 10% of the platelet volume and numbering 50-80 per platelet. The contents of α-granules are either synthesised by the megakaryocyte and packaged prior to platelet formation, or endocytosed by the megakaryocyte or platelet. Significant heterogeneity exists in the content of α-granules and subpopulations of granules have been observed within the α-granules (Blair and Flaumenhaft 2009). In comparison, dense granules constitute approximately 1% of platelet volume and

Table 1.1: Platelet granule contents

α-granules	***Membrane-bound proteins*** P-selectin αIIβ3 (GpIIb-IIIa) αVβ3 GpVI Fc receptors PECAM-1 (CD31) GpIb-IX-V CD9 CD36 Glut3 Fibrocystin L CD109 ***Adhesion & Coagulation*** vWF Tissue factor Fibrinogen Fibronectin vitronectin Factor V + multimerin Factor XI Factor XIII Factor VIII Prothrombin HMW kininogens Plasminogen activator-inhibitor-1 (PAI-1) α2-antiplasmin Histidine-rich glycoprotein Protease nexin-II	***Pro-angiogenic & Wound Repair*** Vascular endothelial GF-A Vascular endothelial GF-C Basic fibroblast GF Platelet-derived GF Epidermal GF Insulin-like GF-1 Hepatocyte GF Angiopoietin CXCL12 MMPs-1, 3 & 9 Gas6 β thromboglobulin Osteonectin Protease nexin-II Heparanase ***Angiogenesis Inhibitors*** Thrombospondin-1 CXCL-4 (PF4) Angiostatin Endostatin Tissue inhibitors of MMPs -1 & -4 ***Coagulation Inhibitors*** Antithrombin C1 inhibitor Tissue factor pathway inhibitor Protein S Protease nexin-2 Plasmin and plasminogen	***Pro-inflammatory & Immune Modulating Factors*** Platelet-derived GF CXCL-1,-4, -5, -7, -8, -12 CCL-2, -3, -5 Transforming GF-β β-thromboglobulin CD40L ***Antimicrobial Host Defence*** CXCL4, CXCL7, CCL5 Thymosin β4 C3, C4 precursor Factor D IgG ***Complement Regulators*** Platelet factor H C1 inhibitor β1H globulin ***Protease Regulation*** α1-antitrypsin α2-macroglobulin
Dense granules	***Platelet Activation*** ADP ATP Serotonin ***Nucleotides*** GTP GDP	***Ions*** Phosphate Pyrophosphate Calcium Magnesium	***Wound healing & Vasodilation & Constriction*** Serotonin Histamine ***Membrane proteins*** LAMP 3 (CD63) LAMP 2 P-selectin
Lysosomes	***Membrane Proteins*** LAMP 1 LAMP 2 LAMP 3 (CD63)	***Degradative Enzymes*** Acid hydrolases (x13) Cathepsin D Cathepsin E	

Table generated from data presented in (Israels et al. 1992; Henn et al. 1998; Reed 2002; Mezzano et al. 2008; Blair and Flaumenhaft 2009)

number approximately 7 per platelet. Lysosome numbers are very few (Reed 2002; Blair and Flaumenhaft 2009).

1.2.2 Platelet Function in Thrombosis and Haemostasis

Due to their small size and shape, platelets are marginalised by the blood flow to the lumenal surface of the blood vessels where they are most likely to come into contact with damaged endothelium (Plow and Ginsberg 1999). Intact endothelium secretes several factors that inhibit coagulation and platelet activation. Those factors preventing platelet activation include nitric oxide, prostaglandin I_2 and adenosine diphosphatase. When the endothelium is damaged, however, the secretion of these factors is down-regulated and the non-thrombogenic nature of the endothelium is reversed (Karsan and Harlan 1999). The reaction of platelets to exposed subendothelial matrix is complex with the underlying mechanisms varying according to the prevailing shear forces (Jackson 2007). The following sections describe, in a simplified way, the reaction of platelets when they interact with components of the subendothelial matrix exposed through injury.

1.2.2.1 Platelet Adhesion

Platelets express on their surface several receptor proteins that bind to components of the extracellular matrix (Table 1.2 lists the major platelet receptors and their ligands). The receptors with the greatest roles in platelet adhesion are GpIb-IX-V, GpVI, GpIa-IIa and GpIIb-IIIa (Plow and Ginsberg 1999; Lopez and Berndt 2002).

The initial contact between platelets and the subendothelial matrix involves the formation of platelet membrane tethers extending from the point of adhesion to the endothelium. These tethers may be transient and entail GpIb-IX-V binding to vWF which triggers a conformational change in GpIIb-IIIa to an active state enabling it to

bind fibronectin and vWF (Jackson 2007). Whilst the signalling induced by GpIb-IX-V binding to vWF results in GpIIb-IIIa activation, it does not induce granule secretion. More stable adhesive interactions with the endothelium are mediated by GpVI or GpIa-IIa binding to collagen and it is these interactions that induce sufficient signalling to induce granule secretion (Plow and Ginsberg 1999; Lopez and Berndt 2002).

1.2.2.2 Platelet Activation, Spreading and Aggregation

Platelets may be activated by platelet adhesion receptors binding their ligands (e.g., GpVI to collagen), agonists released from nearby platelets binding their G-coupled protein receptors on platelets (e.g. ADP and thromboxane A2), or soluble substances produced as a result of injury interacting with their platelet receptors (e.g. thrombin and adrenaline). The complete process of platelet activation includes cytoskeletal rearrangement and shape change, calcium mobilisation, integrin activation and granule secretion.

Following adhesion and activation, platelets spread on the damaged endothelial surface essentially forming a pavement. The additional membrane provided by the open canalicular system and α-granules results in a 2- to 4-fold increase in platelet surface area following activation (Blair and Flaumenhaft 2009). Following the release of granule contents, in particular ADP and thromboxane, and the generation of thrombin, additional platelets are recruited and activated and may either bind to the endothelium or to the initially adherent platelets thus forming a 3-dimensional thrombus. These platelet-platelet interactions are dependent upon GpIb-IX-V and GpIIb-IIIa (Patel *et al.* 2003; Furie and Furie 2004; Jackson 2007).

Table 1.2: Major platelet receptors

Receptor Family	Receptor	Ligands
Integrin - β3 Family	$\alpha_{IIb}\beta_3$ (GpIIb-IIIa) 50,000 - 80,000 copies	Fibrinogen, von Willebrand factor (vWF), fibronectin, vitronectin and thrombospondin
	$\alpha_v\beta_3$ 50-100 copies	Fibronectin, fibrinogen, laminin, collagen, PECAM-1, vitronectin, osteopontin, bone sialoprotein? [a]
Integrin - β1 Family	$\alpha_2\beta_1$ (GpIa-IIa) 2,000-4,000 copies	Collagen
	$\alpha_5\beta_1$ (GpIc-IIa) <1000 copies	Fibronectin
	$\alpha_6\beta_1$ (GpIc'-IIa) <1000 copies	Laminin
C-type lectin-like	CLEC-2	Podoplanin
EGF repeat containing receptor	PEAR1	Not yet identified
Immunoglobulin Superfamily	GpVI ~1000 copies	Collagen
	FcγRIIA (human)	IgG
	FcεRI (human)	IgE
	JAM-1	JAM-1 on other platelets or endothelium
	ICAM-2 ~3,000 copies	$\alpha_L\beta_2$ on leukocytes or other platelets
	PECAM-1 (CD31)	PECAM-1 (CD31) on other platelets, leukocytes or endothelium, $\alpha_v\beta_3$, heparan sulfate proteoglycans
	CD47	Thrombospondin, SIRPα

[a] The role of platelet $\alpha_v\beta_3$ is unknown, however, on other cell types the ligands for $\alpha_v\beta_3$ include those listed.

Table 1.2: Major platelet receptors (continued)

Receptor Family	Receptor	Ligands
Leucine-Rich Repeat Family	GpIb-IX-V 30-40,000 copies	vWF, P-selectin, Mac-1, thrombin, HMW kininogen, Factors XI and XII
Selectins	P-selectin [b]	PSGL-1, GpIb
Tyrosine Kinase Receptors	c-mpl	Thrombopoietin
TNF-Receptor Superfamily	CD40	CD40 ligand (CD40L)
	CD40L	CD40 on endothelium and immune cells, GpIIb-IIIa on platelets, and α5β1 on endothelial cells
Seven Transmembrane Receptors	PAR1 (human)	Thrombin, granzyme A, trypsin, plasmin
	PAR3 (mice)	Thrombin
	PAR4 (humans & mice)	Thrombin, trypsin, cathepsin G
	$P2Y_1$ and $P2Y_{12}$	ADP
	TXA_2/PGH_2	Thromboxane
	PGI_2, PGD_2 and PGE_2	Prostaglandin I_2, Prostaglandin D_2, Prostaglandin E_2
	PAF - receptor	Platelet-activating factor
	LA - receptor	Lysophosphatidic acid
	Chemokine receptors	CXC & CC chemokines
	V_{1a} receptor	Vasopressin
	A_{2a} receptor	Adenosine
	β_2-Adrenergic receptor	Adrenaline
	5-HT_{2A} receptor	Serotonin
	D3 and D5 receptors	Dopamine

Table generated from data presented in by (Clemetson 2002; Tomiyama et al. 2002; Nanda et al. 2005; von Hundelshausen and Weber 2007; May et al. 2009)

1.2.2.3 Thrombus Stabilisation

The binding of fibrinogen and vWF by GpIIb-IIIa receptors (up to 80,000 per platelet), in addition to the formation of the fibrin meshwork through cleavage of fibrinogen by thrombin, results in the stabilisation of platelet aggregates and the formation of a haemostatic plug (Woulfe *et al.* 2002). Additional proteins involved in thrombus stability include glycoprotein VI, PEAR1, P-selectin and interactions between Eph kinases and ephrins (Merten and Thiagarajan 2000; Goto *et al.* 2002; Prevost *et al.* 2002; Herrera-Galeano *et al.* 2008). Figure 1.1 depicts the role of platelets in thrombosis and haemostasis.

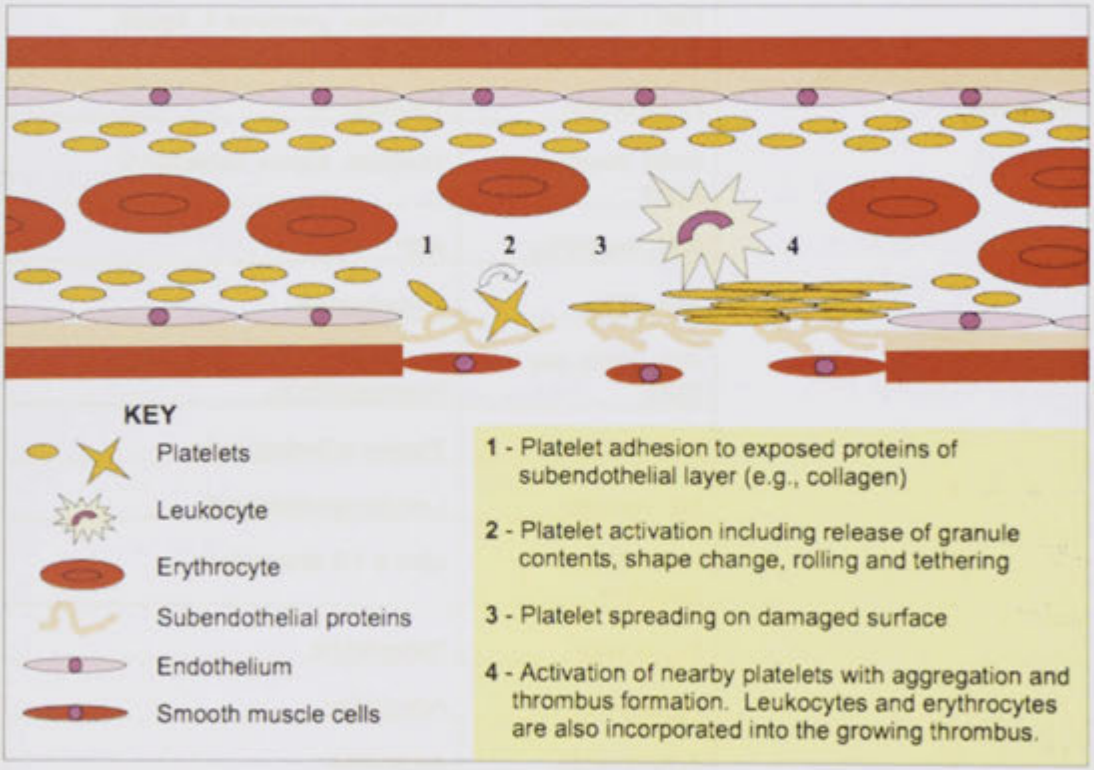

Figure 1.1: Platelet function in thrombosis and haemostasis

1.2.3 Platelet Function in Tissue Repair and Angiogenesis

The wound-healing effects of platelets are well recognised. Preparations of platelet releasate are used in several clinical scenarios, such as the healing of chronic ulcers in

diabetics, bone fractures and periodontal surgery amongst others, as they have been found beneficial in promoting tissue regeneration (Nurden *et al.* 2008; Blair and Flaumenhaft 2009).

Following injury, a host of activities take place that ultimately result in the repair of injured tissue. These activities include thrombosis and haemostasis (reviewed in section 1.2.2), the removal of damaged cells by phagocytosis, the remodelling of the extracellular matrix (ECM), and the growth of new tissue and its associated vasculature. Platelets release a multitude of factors that contribute to each of these steps including chemokines, cytokines, degradative enzymes, and growth factors that promote cell division, growth and differentiation . Of equal importance, platelets also release factors that regulate these processes thus ensuring they are 'switched- off' when the repair process is complete (Blair and Flaumenhaft 2009). The activators and regulators of wound repair released by platelets are included in Table 1.1.

1.2.4 Platelet Function in Inflammation and Immunity

In addition to their functions in haemostasis and wound healing, platelets have significant roles in the promotion of an inflammatory response and in antimicrobial defence. Due to their relative abundance in the bloodstream, platelets are capable of a rapid response to stimuli and accumulate at sites of infection in response to chemotactic signals. Platelets promote inflammation at the site of injury or infection by producing the key inflammatory cytokine, IL-1β, through rapid mRNA translation; by expressing CD40L that induces an inflammatory response in, and matrix degradation by nearby endothelial cells; by increasing vascular permeability through the release of histamine and serotonin from dense granules and through the production of prostaglandins D_2 and E_2; and by enhancing leukocyte recruitment through the release

of numerous chemokines and cytokines from α-granules (see Table 1.1) (Henn *et al.* 1998; Klinger 2002; May *et al.* 2002; Weyrich and Zimmerman 2004).

Platelets also provide protection from invading micro-organisms through direct action against pathogens, or indirectly by assisting other components of the immune system. They are capable of binding to antibody-bound pathogens via Fc receptors (in humans, not mice), and to complement-coated pathogens via complement receptors. Through the expression of CD40L, platelets have been demonstrated to promote adaptive immunity by activating dendritic cells. They can also recognise pathogen-associated molecular patterns via platelet Toll-like receptors. Following binding, platelets internalise micro-organisms or antigens into phagosomes. Alternatively, the binding of pathogens may stimulate platelet activation and the release of toxic oxygen metabolites and proteins capable of killing bacteria, fungi and protozoa as well as encapsulating the pathogen within a thrombus (Klinger 2002; Weyrich and Zimmerman 2004; Elzey *et al.* 2005; von Hundelshausen and Weber 2007).

Platelets also cooperate with other components of the immune system in the clearance of pathogens through the promotion of complement activity and the recruitment, activation and assisted migration of effector cells of both the innate and adaptive immune systems (Yeaman and Bayer 2002; Weyrich and Zimmerman 2004; von Hundelshausen and Weber 2007).

1.3 Tumour Metastasis

Tumour cell types display a preference for certain tissues to which they will metastasise, for example, prostate cancer frequently metastasises to the bone, whereas colon cancer metastasises to the liver and lung, and uveal melanoma generally metastasises to the liver (Nguyen *et al.* 2009). Furthermore, tumour

metastasis may occur via the lymphatic or haematogenous pathways with some cancers appearing to have a predilection for one over the other, while other cancers take advantage of both routes (Cao 2005). The following sections discuss the factors believed to influence the location of metastatic spread of tumour cells and the mechanisms of haematogenous metastasis. Lymphatic metastasis will not be considered as it is a distinct field of research and was not investigated in this body of work. It is worth mentioning, however, that tumour cells invading the lymphatic system may eventually enter the bloodstream via the lymphatic ducts, where lymph is deposited into the blood, and thence become widely dispersed (Wong and Hynes 2006).

1.3.1 Determinants of Tissue Preference for Metastatic Spread

Two dominant theories have been proposed for the mechanisms dictating the pattern of metastatic spread of tumour cells. The two theories are not mutually exclusive and each is supported by significant experimental evidence. The following sections discuss each of the proposed theories.

1.3.1.1 Mechanical Forces and Vascular Anatomy

One of the earliest theories proposed by Rudolf Virchow in 1858 and reinforced by James Ewing in 1928 is that the final destination of circulating tumour cells is determined by the dynamics of blood flow and the anatomy of the vasculature (Virchow 1858; Ewing 1928). Indeed, the majority (60%) of metastases can be predicted on the basis of the anatomy of the vasculature alone (Liotta 1992). The basis of the theory is that tumour cells will be carried within the venous system draining the primary tumour and carried to the first capillary bed that is encountered. As tumour cells usually have a greater diameter than the lumen of the capillaries, the tumour cells are arrested at these sites and subsequently metastasise to nearby tissue. The dynamics of the blood

flow within the capillaries will also force a small proportion of tumour cells through the narrow vessels on to the next capillary bed. The pattern of colorectal carcinoma (CRC) metastasis is consistent with this theory. As blood returns from the colon, the first capillary bed encountered is within the liver and this is the organ most frequently affected by CRC metastasis. The next capillary bed encountered is within the lungs, the second most likely site of CRC metastasis (Chambers *et al.* 2002; Nguyen *et al.* 2009). Similarly, in a detailed study of the pattern of metastatic spread of B16 melanoma cells in mice, both initial and secondary metastases occurred in the first capillary bed encountered with there being no evidence of organ selectivity (Alterman *et al.* 1985).

Based on the data outlined above and numerous autopsy studies, it has been widely accepted that the initial and predominant determining factor of the pattern of metastatic spread is the anatomy of the vasculature downstream of the primary tumour site with size restrictions within capillary beds trapping circulating tumour cells (Chambers *et al.* 2002; Nguyen *et al.* 2009).

1.3.1.2 Seed and Soil Hypothesis

In 1889, Steven Paget proposed the 'Seed and Soil' hypothesis for the organ preference of tumour cell metastasis following the study of numerous breast cancer patients (Paget 1889). He found that the preference for liver metastasis in breast cancer could not be explained by vascular anatomy and blood flow alone. He wrote "When a plant goes to seed, its seeds are carried in all directions, but they can only live and grow if they fall on congenial soil." He proposed that the liver, therefore, must be "receptive" to the metastasising breast cancer cells whereas other organs are not. Much research in this area has revealed that the gross structure of, and surface molecules on, endothelium varies between organs and influences the metastatic

pattern of certain tumour types (Pauli *et al.* 1990; Nguyen *et al.* 2009). Furthermore, reciprocal interactions between tumour cells and cells of the target organ determine whether tumour cells will adhere, extravasate, migrate, survive and grow (Chambers *et al.* 2002; Ben-Baruch 2008).

An extension of the 'Seed and Soil' hypothesis, proposed in 2005, is that soluble factors released by cells of the primary tumour prepare specific tissues for the attachment and invasion of circulating tumour cells. Thus, based on this hypothesis, the primary tumour establishes a "pre-metastatic niche" (Kaplan *et al.* 2005; Psaila and Lyden 2009).

1.3.2 Mechanisms of Haematogenous Metastasis of Tumour Cells

The processes involved in haematogenous metastasis are complex and include numerous steps. For the purpose of clarity, the metastatic process will be broken down into two sections, namely, (i) detachment from the primary tumour and migration into the bloodstream and (ii) extravasation from the bloodstream and invasion of a distant organ.

1.3.2.1 Detachment from Primary Tumour and Migration into Bloodstream

Metastasis was initially believed to occur as a result of increasing tumour size and pressure forcing tumour cells into the bloodstream. However, following intense research, it has become clear that metastasis is an active process involving changes in cell behaviour beyond those of tumourigenesis (Liotta 1992). The behavioural changes associated with metastatic tumour cells include detachment from the primary tumour mass, invasiveness, resistance to apoptosis and migration to other locations within the body. This phenotypic switch is consistent with that seen in some normal biological

processes and has been termed the 'epithelial to mesenchymal transition' (EMT) (Guarino *et al.* 2007; Tse and Kalluri 2007; Kalluri and Weinberg 2009).

1.3.2.1.1 Epithelial to Mesenchymal Transition (EMT)

EMT is associated with developmental processes including implantation, embryogenesis and organ development; inflammatory processes including wound healing and tissue regeneration; and tumour cell progression to a metastatic phenotype. Figure 1.2 depicts the morphological and molecular changes associated with EMT.

EMT is believed to constitute one of the key events transforming a tumour cell to the metastatic phenotype and is induced, in the case of many carcinomas, by hepatocyte growth factor (HGF), epidermal growth factor (EGF), platelet-derived growth factor (PDGF) and transforming growth factor-beta (TGF-β) released from the tumour stroma (Kalluri and Weinberg 2009). In the epithelial state, cell-cell interactions are maintained by specific adhesion molecules such as E-cadherin and syndecan and cell-ECM interactions are mediated by integrins. However, during the transition of a tumour cell to a mesenchymal and metastatic phenotype these proteins are lost through down-regulation, mutations affecting function, or an increase in protease cleavage (Sanderson 2001; Guarino *et al.* 2007; Tse and Kalluri 2007; Kalluri and Weinberg 2009).

Once separated from the tumour mass, an individual tumour cell can migrate through tissues, a process which involves repeated cycles of the following series of events:-

(i) pseudopod formation at the leading edge of the migrating cell

(ii) focal contact between the ECM and cell adhesion molecules

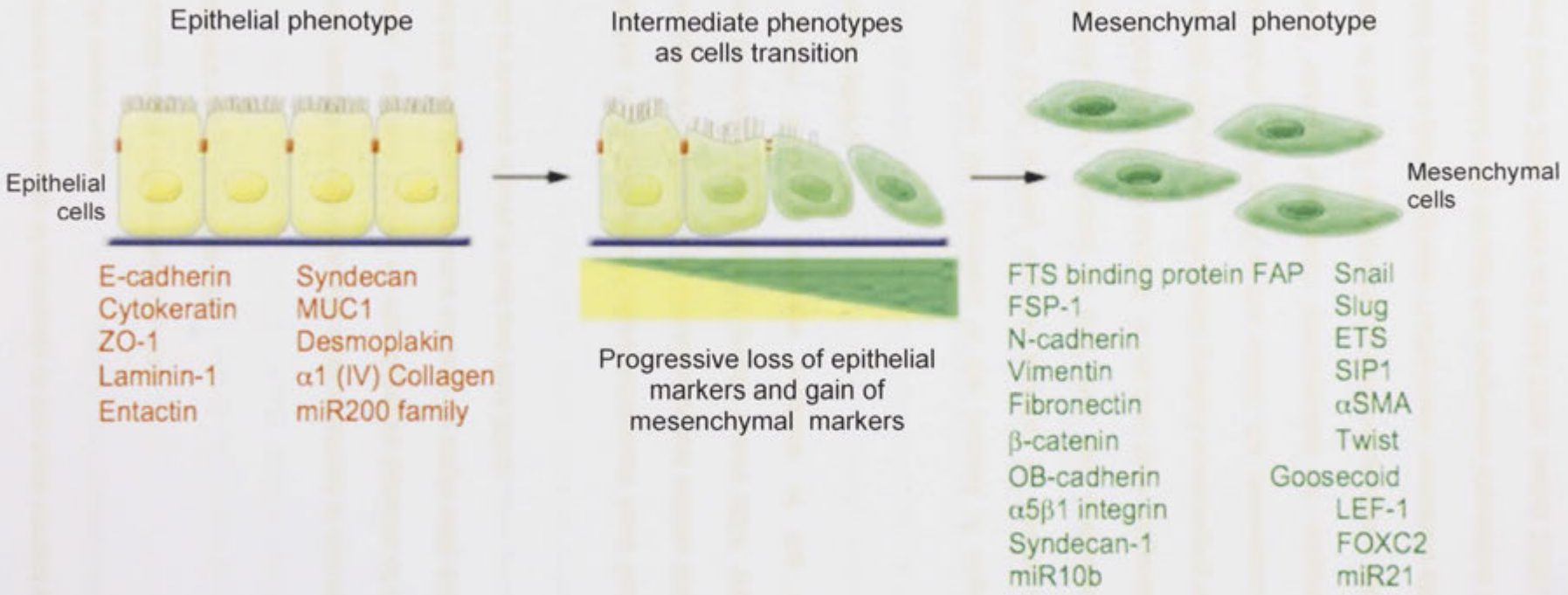

Figure 1.2: Morphological and Molecular Changes Associated with Epithelial to Mesenchymal Transition

from Kalluri R. and Weinberg, RA. *J. Clin. Invest, 2009*

(iii) recruitment and release of proteases at the focal contact points with digestion of ECM components

(iv) contraction of the cell cytoskeleton, and

(v) detachment of the rear of the cell.

This multi-step process of migration has been observed in non-neoplastic as well as neoplastic cells. Detailed studies on the migratory patterns of cells within tumours have revealed that migration may occur not only as single cells, but also collectively as chains, sheets or clusters of cells (Friedl and Wolf 2003).

Numerous factors within the tumour microenvironment have been demonstrated to influence the migratory behaviour of tumour cells and include chemokines (autocrine motility factor, stromal-derived factor-1), growth factors (EGF, lysophosphatidic acid, insulin-like growth factor-1), cleavage products of the ECM and matrix metalloproteases (MMPs).

Chemo-attractants may be generated in the process of migration following the digestion of the ECM, or they may be secreted by nearby cells. Platelets and macrophages are major sources of EGF that has downstream effects on cell proliferation, differentiation and survival. It has also been suggested that platelets and macrophages may establish a chemotactic gradient encouraging tumour cell migration into the vasculature. In support of this notion, the chemotaxis of carcinoma cells towards blood vessels has been demonstrated in response to EGF, with overexpression of the EGF receptor being demonstrated in a variety of tumour cells and associated with a poor prognosis. Furthermore, metastatic ability can be induced in non-metastatic tumour cells through the exogenous expression of the EGF receptor (Condeelis and Segall 2003; Friedl and Wolf 2003; Herbst 2004). Interestingly, all of

the growth factors released by the tumour stroma and demonstrated to induce EMT in carcinoma cells are also released by platelets.

The tumour-associated vasculature is very leaky and, therefore, may not represent a major barrier to tumour escape. Once tumour cells cross the blood vessel wall, however, they encounter the high mechanical stress associated with the shear forces generated by blood flow. Using intravital imaging, comparisons have been made of the ability of poorly metastatic and highly metastatic carcinoma cell lines to enter the bloodstream. The poorly metastatic tumour cells were fragmented by the shear forces within the bloodstream, whereas tumour cells derived from the highly metastatic carcinoma remained intact. The robust nature of the highly metastatic carcinoma cells under shear force was attributed to an increased expression of cytokeratins and a resistance to apoptosis induction (Condeelis and Segall 2003).

1.3.2.1.2 The Association between Inflammation and Cancer

The previous section alludes to a role for inflammation in metastasis promotion through the induction of EMT by platelets and components of the immune system. There is, in fact, a growing body of evidence suggesting that inflammation, mediated by platelets and immune cells, is essential for tumour progression.

Inflammation is an orchestrated response to tissue injury or infection. The role of platelets in tissue repair and inflammation was reviewed in sections 1.2.3 and 1.2.4. Other key players in the inflammatory process which may play a role in EMT and metastasis include thrombin, a product of the coagulation cascade, which promotes monocyte adhesion to endothelial cells (DiCorleto and de la Motte 1989). It is also a potent mitogen and has recently been demonstrated to induce migration of retinal pigment epithelial cells by stimulating the expression of chemokines (Palma-Nicolas *et*

al. 2010). Neutrophils recruited to the sites of injury or inflammation by platelets release additional pro-inflammatory cytokines to enhance the recruitment and activation of additional effector cells, including monocytes and macrophages. Following their activation, macrophages take over as the predominant source of tissue repair factors controlling cell proliferation, angiogenesis, ECM restructuring and phagocytosis of damaged cells. Mast cells also play a major role by contributing inflammatory mediators and growth factors to the wound site.

The inflammation associated with wound healing is self-limiting due to the rapid production of anti-inflammatory cytokines that supercede the pro-inflammatory cytokines. Dysregulation of this highly controlled response, or continued exposure of the tissue to injury, however, can lead to a chronic inflammatory state. The persistence of inflammation is believed to have the potential to promote tumourigenesis in pre-neoplastic cells. Additionally, the conditions associated with chronic inflammation may induce cancer progression through the promotion of an EMT in tumourigenic cells (Coussens and Werb 2002; Grivennikov and Karin 2010).

1.3.2.2 Extravasation and Invasion of Distal Organs by Tumour Cells

Once inside the vasculature, metastasising tumour cells must withstand the mechanical stresses created by the immense force of blood flow within the varying diameters of the blood vessels, escape destruction by circulating cells of the immune system, attach to the wall of a distant capillary bed resisting the inherent shear forces, migrate through the vessel wall and proliferate to establish a viable secondary tumour. This process as a whole represents a significant challenge to tumour cells as numerous studies demonstrate that less than 10% of cells entering the circulation succeed in establishing a secondary tumour (Liotta *et al.* 1974; Liotta 1992; Meyer and Hart 1998; Geiger and Peeper 2009). At which stage, or stages of the metastatic

process the majority of cells fail is a matter of debate. *In vivo* microscopy studies have provided insights into the ultrastructural events associated with tumour cell extravasation. The subsequent section therefore reviews the findings of videomicroscopy studies of tumour cell metastasis.

1.3.2.2.1 Ultrastructural Analysis of the Extravasation of Tumour Cells

A morphological study of the fate of 3 different mouse tumour cell lines (Lewis lung carcinoma, 16c mammary adenocarcinoma and B16 melanoma) injected into the tail vein of mice demonstrated the following common steps of lung invasion (Crissman *et al.* 1988):

(i) In less than 1 minute: Tumour cells were seen to arrest within the lung capillary bed following contact with endothelial cells. A size restriction within the vessel appeared to have an impact upon the initial lodgement of the tumour cells within the vessel. This initial lodgement was temporary, however, as those tumour cells that were unable to initiate an interaction with the endothelium passed through the capillary bed.

(ii) Within 2 min: Platelet activation and aggregation around the tumour cell was observed. A small number of platelets were observed in contact with tumour cells prior to their interaction with the endothelium, although the platelets appeared not to be involved in the initial contact with the vessel wall. Platelet aggregation was seen to continue for 1-4 hours with thrombus formation eventually causing vessel occlusion. Those platelets in close association with the tumour cells were observed to undergo shape change and degranulation, and the tumour cells were observed to develop extensions that became intimately associated with, and projected into, the platelet thrombus. The degree of interaction between the tumour cells and the endothelial cells increased over time. The platelet thrombus remained until the tumour cells had established contact with the sub-endothelial matrix.

(iii) 4 hours: Endothelial cell separation was observed, with cytoplasmic extensions of the tumour cells reaching the subendothelial matrix. Marked thinning of the endothelial cytoplasm was seen adjacent to tumour cells and the authors concluded that endothelial cells play an active role in this step, little destruction of endothelial cells being observed. The tumour cells then appeared to disrupt inter-endothelial cell junctions and gain access to the basement membrane.

(iv) 8-24 hours: The tumour-cell associated thrombus dissolved during this period and flow was re-established within the vessel. Tumour cells were also found attached to the subendothelial matrix.

(v) 24 hours: Tumour cell division was noted at at this time point with the development of intravascular nodules. The proliferating tumour cells caused further displacement of nearby endothelial cells and maintained their attachment to the basement membrane.

(vi) 3 – 8 days: The basement membrane of the capillary was dissolved under tumour nodules by the tumour cells and extravasation was achieved. No single tumour cells were observed to penetrate the basement membrane.

(vii) Observed interactions between tumour cells and circulating immune cells
Particular attention was paid to interactions between tumour cells and cells of the immune system prior to extravasation. A slight increase in the number of lymphocytes associating with the tumour cells was seen in the first 24 hours post injection, however, there were no direct interactions observed. An increased number of polymorphonuclear cells were seen to associate with Lewis lung carcinoma cells during the first 24 hours with occasional degenerative changes in the tumour cells observed (Crissman *et al.* 1988).

A subsequent series of detailed *in vivo* video-microscopy studies used a variety of models of murine carcinoma, sarcoma and melanoma and examined liver and lung

metastasis using a novel cell accounting procedure (Chambers *et al.* 2001). These studies revealed that tumour cells were highly efficient at survival within the circulation and that more than 80% of tumour cells injected intravenously extravasated through the capillary bed of a distant organ. In contrast, they were inefficient at survival, growth and persistence following extravasation, with only ~8% of injected tumour cells establishing a macroscopic secondary tumour. The observed outcomes for extravasated tumour cells were death through apoptosis or immune destruction, dormancy or successful proliferation (Chambers *et al.* 2001).

The authors of this work found that the majority of tumour cells were arrested in organs due to size restrictions within the first capillary bed encountered and the ability to extravasate was common to tumour cells with both high and low metastatic capacity. In contrast to the previous study by Crissman *et al.*, they did not observe initial growth of tumour cells within the blood vessels (Chambers *et al.* 2001).

1.3.2.3 Comparison of Molecular Events Associated with Leukocyte and Tumour Cell Extravasation

In vivo microscopy studies, along with those examining the process of tumour cell extravasation at the molecular level, reveal remarkable similarities to those of leukocyte extravasation in response to inflammation or injury (Miles *et al.* 2008).The following section, therefore, provides a comparison at the molecular level of leukocyte and tumour cell extravasation including adhesion and attachment to the vessel wall, transendothelial migration, and migration through the pericyte layer, basement membrane and underlying tissue. In section 1.3.2.3.4 our current understanding of the ultrastructural and molecular mechanisms of tumour cell metastasis to the liver are reviewed and compared with leukocytes. The process of leukocyte extravasation is depicted in Figure 1.3 and Table 1.3 lists the adhesion proteins implicated in tumour cell metastasis along with their purported mechanisms of action.

1.3.2.3.1 Adhesion and Attachment to the Blood Vessel Wall

In the case of inflammation, the endothelium is activated by the release of cytokines, such as IL-1, -6, -8, -12 and TNF-α by tissue-resident macrophages. It is conceivable that establishment of a pre-metastatic niche by tumour cells results in similar changes to the endothelium. Endothelial cell activation results in the expression of P- and E-selectin on their lumenal surface. Leukocytes flowing past a site of inflammation or injury, adhere to and roll along the endothelial surface of the blood vessel. This initial contact may be mediated by the following interactions:

(i) P- selectin on activated endothelial cells binding to sialyl Lewis^{X} or sialyl Lewis^{a} carried by PSGL-1 on leukocytes;

(ii) E-selectin on activated endothelial cells binding to sialyl Lewis$^{X \text{ or } a}$ carried by PSGL-1, or to L-selectin on leukocytes;

(iii) L-selectin on leukocytes binding endothelial cell-heparan sulfate proteoglycans (HSPG);

(iv) CD44 on leukocytes binding hyaluronic acid (HA) on the endothelium and

(v) the α4β1 integrin on endothelial cells binding to L-selectin on leukocytes (Liu and Kubes 2003; Bonder *et al.* 2006; Parish 2006; Ruffell and Johnson 2009).

During the process of rolling, leukocytes come into close proximity to chemokines, such as IL-8, produced by tissue-resident macrophages and presented by endothelial heparan sulfate to leukocyte receptors. This process activates leukocyte β1 and β2 integrins, such as α4β1 (VLA-4), αLβ2 (LFA-1) and αMβ2 (Mac-1), which mediate firm adherence of leukocytes to the endothelium via interactions with members of the immunoglobulin superfamily, such as ICAM-1, ICAM-2, VCAM-1 and PECAM-1 (Luscinskas *et al.* 1994; Parish 2006).

Contact between tumour cells and the endothelium has been shown to occur through size restriction, however, this contact also seems to involve molecular interactions common to leukocyte-endothelial adhesion. Thus, P-, E- and L-selectin, CD44, HA, $\alpha 4\beta 1$, $\alpha L\beta 2$, ICAM-2, VCAM-1 and PECAM-1 have all been demonstrated to promote metastasis in experimental models. Tumour cells often express sialyl Lewis^X or sialyl Lewis^a, carried by mucins, that interact with the selectin family members (Wahrenbrock *et al.* 2003). They may also aberrantly express CD44, thus enabling tumour cell rolling on P-selectin (Hanley *et al.* 2006), adhesion to fibrin (Alves *et al.* 2009) and adhesion and migration through interaction with HA on the endothelium (Mummert *et al.* 2003; Ponta *et al.* 2003). Alternatively, HA expressed on the surface of tumour cells may bind to endothelial CD44 or ICAM-1 (Zhang *et al.* 1995). Furthermore, tumour cells have been found to express the integrins $\alpha 4\beta 1$ and $\alpha L\beta 2$ thus potentially mediating binding to cell adhesion molecules on the endothelium following activation (Taichman *et al.* 1991; Wang *et al.* 2005). It should be noted that the above findings were dependent upon the tumour cell type studied and are unlikely to be common to all tumour cell types.

1.3.2.3.2 Transendothelial Migration (TEM)

Both leukocytes and tumour cells commence migration across the vessel wall by first crossing the endothelium. This may occur between endothelial cells (paracellular pathway) or through endothelial cells (transcellular pathway). Both of these pathways require significant morphological changes within the leukocyte/tumour cell and the endothelial cells that, in the case of leukocytes, are initiated by integrin:immunoglobulin superfamily member binding (Carman *et al.* 2007; Hidalgo and Frenette 2007; Nakhaei-Nejad *et al.* 2007; Aghajanian *et al.* 2008). A protrusive leading edge rich in the integrin $\alpha L\beta 2$ is formed on the leukocyte with a contractile rear and ventral membrane protrusions. Endothelial cells form protrusions at the cell surface, rich in the

integrin ligands VCAM-1 and ICAM-1, that are believed to promote firm adhesion between the leukocyte and endothelium (Nourshargh *et al.* 2010).

Leukocytes crawl along the endothelial surface probing for a migration permissive site. Once found, the bulk of the leukocyte follows the membrane protrusion to the basal side of the endothelial surface. The action of leukocyte crawling is associated with ICAM-1, VCAM-1 and E-selectin clustering and stimulates signalling events within endothelial cells that result in the reduction of endothelial cell junctions, in preparation for paracellular migration, or the formation of intracellular pores, in preparation for transcellular migration (Nourshargh *et al.* 2010).

VE-cadherin is important in maintaining contact between endothelial cells and must be temporarily inactivated through tyrosine phosphorylation to permit leukocyte, and presumably, metastatic tumour cell migration. Cytoskeletal contraction within the endothelial cells also assists in the creation of a permissible space. Several proteins present in endothelial junctions have been shown to assist transendothelial leukocyte migration and include PECAM-1, ICAM-2, junctional adhesion molecules (JAM-A, JAM-B, JAM-C), CD99 and endothelial-cell selective adhesion molecule (ESAM). The mechanism of transcellular migration is not fully understood but is known to involve the formation of a vesiculovacuolar organelle around the leukocyte that transports its contents to the abluminal side of the endothelial layer. The vesicle-associated membrane protein (VAMP) has been implicated in this process (Nourshargh *et al.* 2010).

Our understanding of tumour cell TEM is not as extensive as that of leukocytes. It has been demonstrated, however, that the interactions between integrins on the tumour cells and their immunoglobulin superfamily member receptors on the endothelium, the

down-regulation of cadherin expression by endothelial cells and cytoskeletal reorganisation within both endothelial and tumour cells are all integral to the process of tumour cell TEM (Miles *et al.* 2008).

1.3.2.3.3 Migration through the Pericyte Layer, Basement Membrane and Underlying Tissue

Following transendothelial migration, leukocytes and tumour cells must cross the pericyte layer and the basement membrane of the blood vessel. Migration across the pericyte layer may occur via the transcellular or paracellular routes, however little is understood about the underlying mechanisms. The basement membrane consists of a dense network of laminin, collagen type IV and heparan sulfate proteoglycans and is manufactured by endothelial cells and pericytes (Parish *et al.* 2001; Parish 2006; Nourshargh *et al.* 2010). It represents a significant barrier to the migrating lymphocyte and tumour cell. There is no consensus regarding the process of leukocyte migration across the basement membrane although there is evidence for the existence of permissive sites for migration within the basement membrane (Nourshargh *et al.* 2010). Additionally, there is significant evidence to suggest that both leukocytes and endothelial cells remodel the basement membrane through the release of proteases (including matrix metalloproteases (MMP), serine-, cysteine- and aspartic proteases) and heparanase thus generating a migratory pathway (Hulett *et al.* 2000). Unpublished data from the Parish Laboratory (in collaboration with Professor Michael Hickey, Monash University) using intra-vital microscopy in an *in vivo* inflammatory model demonstrated that the heparanase inhibitor PI-88 did not prevent leukocyte adhesion to the blood vessel wall but did prevent migration through the vessel wall.

Proteases and heparanase have also been implicated in tumour cell migration across the blood vessel wall. Cancer cells are able to degrade the ECM through the sequential actions of enzymes such as MMPs, serine and cysteine proteases and

Figure 1.3: The Process of Leukocyte Extravasation.

In response to cytokines produced by tissue-resident macrophages, pre-formed P-selectin is rapidly expressed on the surface of endothelial cells. E-selectin may also be expressed following transcription (not shown). The interaction between P-selectin and its ligand, PSGL1, on leukocytes initiates rolling on the endothelium which is further stabilised by L-selectin binding to endothelial-cell heparan sulfate proteoglycans (HSPGs), such as syndecan. Chemokines, such as CXC-chemokine ligand 8 (CXCL8), produced by tissue-resident macrophages are presented by heparan sulfate (HS) to receptors on leukocytes. This process activates leukocyte integrins thus enabling them to bind their endothelial ligands, such as $\alpha_L\beta_2$ binding to ICAM-1, and results in more stable leukocyte adhesion. Transendothelial migration may occur via the paracellular or transcellular pathways and involves extensive morphological changes within the leukocytes and endothelial cells. Once leukocytes have completed transendothelial migration, they interact with chemokines presented by HSPGs such as perlecan in the underlying basement membrane. In order to traverse the subendothelial basement membrane, leukocytes deploy various proteases and the heparan-sulfate-degrading enzyme heparanase to solubilise the basement membrane components. During basement membrane solubilisation, heparanase releases growth factors associated with basement membrane HSPGs.

Key: HS, heparan sulfate; ICAM1, intercellular adhesion molecule 1; CXCL8, CXC chemokine 8 or IL8.

From Parish, CR. *Nature Reviews Immunology 6, 633-643, 2006*

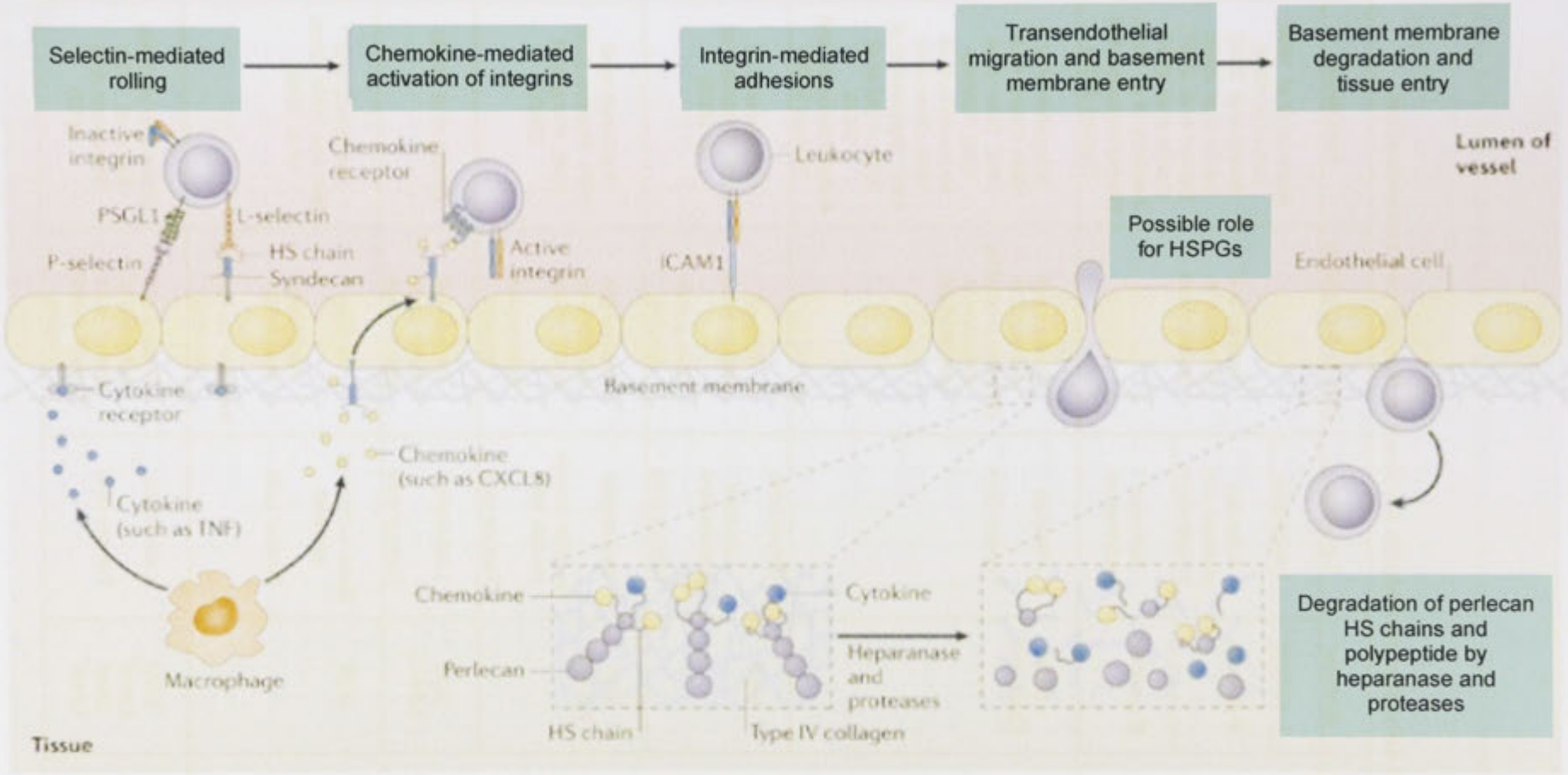
Selectin-mediated rolling
Chemokine-mediated activation of integrins
Integrin-mediated adhesions
Transendothelial migration and basement membrane entry
Basement membrane degradation and tissue entry
Inactive integrin
PSGL1
P-selectin
L-selectin
HS chain
Syndecan
Chemokine receptor
Active integrin
Leukocyte
ICAM1
Lumen of vessel
Possible role for HSPGs
Endothelial cell
Basement membrane
Cytokine receptor
Chemokine (such as CXCL8)
Cytokine (such as TNF)
Macrophage
Tissue
Chemokine
Perlecan
HS chain
Type IV collagen
Cytokine
Heparanase and proteases
Degradation of perlecan HS chains and polypeptide by heparanase and proteases

Table 1.3: Cell adhesion molecules involved in tumour cell extravasation.

Protein Family	Member	Location	Role in Metastasis	Reference
Selectins	L-selectin	Leukocytes	Tumour cell adhesion to endothelium	(Mannori *et al.* 1995; Kim *et al.* 1998; Borsig *et al.* 2002; Laubli *et al.* 2006; Barthel *et al.* 2007; Garcia *et al.* 2007; Tremblay *et al.* 2008; Konstantopoulos and Thomas 2009)
	P-selectin	Activated platelets and endothelium		
	E-selectin	Activated endothelium		
Integrins	$\alpha IIb\beta 3$ (GpIIb-IIIa)	Platelets Tumour cells	Tumour cell adhesion to platelets promoting adhesion to endothelium	(Karpatkin *et al.* 1988; Chang *et al.* 1992; Chen *et al.* 1992; Felding-Habermann *et al.* 1996; Chen *et al.* 1997; Bakewell *et al.* 2003; Patel *et al.* 2003; Konstantopoulos and Thomas 2009)
	$\alpha v\beta 3$	Osteoclasts Activated endothelium Tumour cells	Tumour angiogenesis Osteopontin binding	(Samanna *et al.* 2006; Somanath *et al.* 2009)
	$\alpha 4\beta 1$ (VLA-4)	Leukocytes Vascular smooth muscle cells Tumour cells	Tumour cell adhesion to endothelium Osteopontin binding	(Taichman *et al.* 1991; Bayless *et al.* 1998; Wang *et al.* 2005)
	$\alpha L\beta 2$ (LFA-1)	Leukocytes Tumour cells	Tumour cell adhesion to endothelium	(Wang *et al.* 2005)
	$\alpha 6\beta 4$	Basal surface of epithelia Tumour cells	Motility Apoptosis resistance Invasion via laminin binding	(Rabinovitz and Mercurio 1996; Chen *et al.* 2009)
Carbohydrate moieties	Sialyl Lewis^X Sialyl Lewis^a	Leukocytes Tumour cells	Tumour cell adhesion to endothelium through selectin binding	(Takada *et al.* 1993; Kim *et al.* 1998; Gassmann *et al.* 2010)

Table 1.3: Cell adhesion molecules involved in tumour cell extravasation (cont.)

Protein Family	Member	Location	Role in Metastasis	Reference
Immunoglobulin Superfamily	JAM-C	Endothelial cell junctions Tumour Cells	Tumour cell adhesion to endothelium and migration	(Santoso *et al.* 2005; Fuse *et al.* 2007)
	VCAM-1	Activated endothelium	Tumour cell adhesion via interactions with $\alpha 4\beta 1$ and sialyl Lewis^x	(Zetter 1993)
	PECAM-1	Endothelial cells Platelets Macrophages Leukocytes Osteoclasts Tumour Cells	Angiogenesis Thrombus formation Tumour cell adhesion to endothelium via homotypic interaction or via integrins	(Roos 1991; Sheibani and Frazier 1999; Gong and Chatterjee 2003)
	ICAM-1	Activated endothelium Leukocytes	Tumour cell adhesion to endothelium via integrins	(Tang and Honn 1994)
CD44 family	Numerous variant isoforms	Lymphoid and epithelial cells Tumour cells	Adhesion to endothelium Prevention of apoptosis Invasion Angiogenesis Motility and chemotaxis Growth factor binding Promotion of receptor tyrosine kinase activation	(Anborgh *et al.*; Kennel *et al.* 1993; Wang *et al.* 2005; Hanley *et al.* 2006; Samanna *et al.* 2006; Orian-Rousseau 2010)
Platelet glycoproteins	GpIb-IX-V	Receptor for vWF	Tumour cell adhesion to endothelium and basement membrane	(Jain *et al.* 2007)
Heparan sulphate proteoglycans	Perlecan Syndecan-1	Secreted by vascular endothelial and smooth muscle cells Expressed by tumour cells	Tumour cell invasion, migration, growth and angiogenesis	(Cohen *et al.* 1994; Jiang *et al.* 2004; Khotskaya *et al.* 2009)

endoglycosidases. Numerous studies have linked altered MMP expression in different human cancers with poor prognosis, with up-regulation of MMPs leading to enhanced cancer cell invasion, while synthetic or natural inhibitors of MMPs inhibit metastasis (Curran and Murray 2000; Itoh and Nagase 2002). Studies in melanoma cells indicate that the binding of the integrin $\alpha v\beta 3$ to its ligand, osteopontin, increases the expression of MMP-2. Furthermore, CD44 and $\alpha v\beta 3$ were demonstrated to be critical for the positioning of activated MMP molecules on the surface of invasive tumor cells (Hofmann *et al.* 2000; Hofmann *et al.* 2000; Samanna *et al.* 2006). Similar to MMPs, heparanase expression is also elevated in numerous cancer types studied in comparison to the surrounding normal tissue and the level of expression correlates with metastatic potential (Parish *et al.* 2001; Vlodavsky and Friedmann 2001; Chen *et al.* 2008; Hoffmann *et al.* 2008; Mikami *et al.* 2008). In rats injected with the mammary adenocarcinoma cell line 13762 MAT, or in mice injected with the B16 melanoma cell line, inhibition of heparanase using the inhibitor PI-88 dramatically reduced experimental lung metastasis (Vlodavsky *et al.* 1994; Parish *et al.* 1999). Furthermore, the invasion of Matrigel by renal cell carcinoma cell lines, 786-O and Caki-2, and SMMC7721 human hepatocellular carcinoma was inhibited by down-regulating the expression of heparanase using antisense oligodeoxynucleotides or small interfering RNAs (Zhang *et al.* 2007; Mikami *et al.* 2008). Anti-sense oligonucleotides to heparanase also inhibited experimental metastasis of human hepatocellular carincoma in nude mice (Zhang *et al.* 2007).

1.3.2.3.4 Successful Establishment of a Secondary Tumour

Following invasion of a distant organ, to form a successful secondary tumour, a metastasising tumour cell must proliferate, induce angiogenesis and resist immune destruction. In one study of metastatic efficiency in the lung, the majority of tumour cells that succeeded in extravasation underwent apoptosis soon after arrival (Cameron *et al.* 2000). In another study, of the 80% of injected cells that were found to

successfully extravasate into the liver, 1 in 40 grew to form micrometastases (defined as 4-16 cells), with 1 in 100 of these going on to form macroscopic tumours. Thirty-six percent of the injected cells remained as single dormant cells, therefore, not undergoing apoptosis or proliferation. From the figures presented in this paper, it would appear that ~40% of cells that successfully extravasated did not survive to attain dormancy or proliferate into a micrometastasis and, therefore, presumably underwent apoptosis or immune-mediated destruction (Luzzi *et al.* 1998). The growth and survival of tumor cells following extravasation or a period of dormancy is determined by factors inherent to the tumour cells and also to the microenvironment into which they migrate, such as growth factors, hormones, proteins of the ECM and cytotoxic immune cells (Nicolson 1993; Bates *et al.* 1995; Townson and Chambers 2006; Waldhauer and Steinle 2008). The failure of tumour cells to grow beyond a microscopic tumour is most likely due to the inability to initiate angiogenesis (Naumov *et al.* 2006).

1.3.2.3.5 Site-Specific Mechanisms of Leukocyte and Tumour Cell Extravasation

The majority of studies analysing the mechanisms of leukocyte extravasation have been performed in cremasteric and mesenteric post-capillary venules and are, therefore, likely to be consistent with what occurs in the majority of locations within the body. However, significant differences exist, not only in the structure of the endothelium, but also the expression profiles of cell adhesion molecules in various organs including the liver, brain, lymphoid tissues and bone marrow (Girard and Springer 1995; Karsan and Harlan 1999; Liu and Kubes 2003; Lee and Kubes 2008). These differences in tissue-specific extravasation are most evident in leukocyte and tumour cell extravasation from the liver microvasculature. Within the liver, venous blood from the gastro-intestinal tract enters via the hepatic portal vein into the pre-sinusoidal venules, and arterial blood enters via the hepatic artery into the hepatic arterioles. The two merge within the sinusoids and exit via the post-sinusoidal venules into the central vein (Figure 1.4).

Leukocyte extravasation from the pre- and post-sinusoidal venules is believed to occur as in the cremasteric and mesenteric venules. However, due to the nature of the endothelium within the sinusoids, the mechanism of leukocyte extravasation in this region is quite different. The sinusoids are comparatively narrow, being as wide as the leukocytes themselves. The sinusoidal endothelium is discontinuous, contains pores known as fenestrations, and lacks basal lamina and tight junctions. It contains numerous bristle-coated micropinocytic vesicles and has a high endocytic activity. Sinusoidal endothelium also lacks Weibel-Palade bodies and, therefore, does not release P-selectin or vWF upon activation. Sinusoidal endothelium also does not express E-selectin, PECAM-1, CD34 or VE-cadherin, however, they do express a diversity of oligosaccharides, adhesion proteins and pathogen-associated recognition receptors and are highly efficient at receptor-mediated endocytosis. Leukocyte rolling does not occur within the sinusoids despite this being the greatest site of leukocyte extravasation during inflammation. The extravasation of leukocytes within the sinusoids is not only selectin-independent but it also appears to be β2-integrin independent. Within the post-sinusoidal venules, on the other-hand, leukocyte extravasation does include rolling and does appear to be P- and E-selectin dependent. The sinusoidal endothelium constitutively expresses ICAM-1 and the vascular adhesion protein VAP-1, both of which promote lymphocyte extravasation. The α4β1-integrin also appears to be involved in CD4+ T cell recruitment in the sinusoids. The liver sinusoids constitutively express HA at high levels and its involvement in neutrophil extravasation within the sinusoids via CD44 binding has been demonstrated following LS-induced hepatic injury (Braet and Wisse 2002; Liu and Kubes 2003; Klintman *et al.* 2004; McDonald *et al.* 2008; Vidal-Vanaclocha 2008).

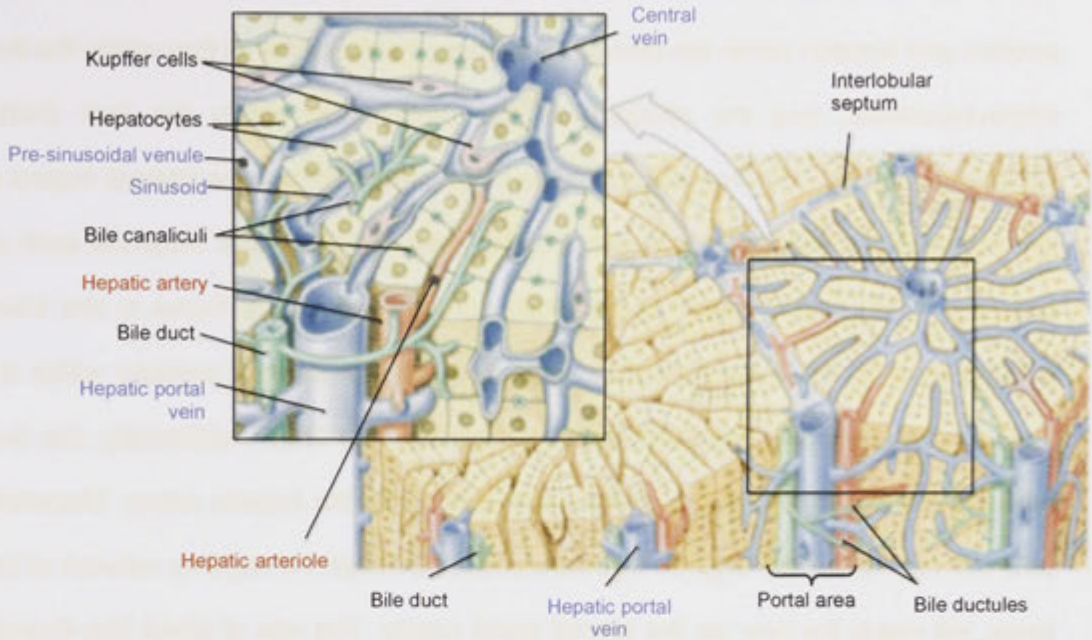

Figure 1.4: Histology of the Liver

Venous blood, returning from the gastro-intestinal tract (GIT), enters the liver via the hepatic portal vein. It travels from the pre-sinusoidal venules into the sinusoids, then exits via the post-sinusoidal venules (not shown) that empty into the central vein. Arterial blood, delivered via the aorta from the left ventricle, enters the liver via the hepatic artery and travels from the hepatic arterioles into the sinusoids, mixing with the venous blood from the GIT, and exits via the central vein.

From:

http://www.harford.edu/faculty/WRappazzo/BIO204/lecture/bio204lecturematerials.htm

with minor modification

The liver is the most common site of metastasis in gastro-intestinal cancers and the organ most commonly involved in haematogenous metastasis. This is likely due to its position and function within the circulatory system, the dynamics of flow within the liver microvasculature, and the structure of the endothelium within the liver (Vidal-Vanaclocha 2008). The liver filters venous blood returning from the internal organs of the abdomen via the portal vein with Kupffer cells ingesting toxic materials such as apoptotic cells, microorganisms, chemicals, drugs, and debris found in the blood passing through the liver. Metastatic cells derived from primary tumours within the abdominal viscera will, therefore, pass through the liver first. Additionally, the liver receives approximately 30% of the cardiac output via the hepatic artery. Metastatic cells derived from other organs, that have passed through the capillary network of the lungs, will reach the liver via the arterial blood supply. The rate of blood flow through the hepatic microcirculation is slow due to the extensive sinusoidal capillary network and due to the presence in and around the sinusoids of Kupffer and stellate cells. This slow flow rate will better enable tumour cells to adhere to the vessel walls of the hepatic microcirculation (Vidal-Vanaclocha 2008).

In vivo videomicroscopy studies on the fate of tumour cells delivered to the portal circulation showed that the majority were arrested within the pre-sinusoidal venules with few reaching the sinusoids. More than 90% of arrested CRC cells were eliminated by NK and Kupffer cells. In another study of liver metastasis using EL-4 lymphoma cells and C26 colon adenocarcinoma cells, the larger C26 cells were found to become lodged, without evidence of rolling, principally within the pre-sinusoidal venules with few entering the sinusoids, whereas the smaller EL-4 cells did adhere to the endothelium without interrupting blood flow, and a minority were observed to flow right through the hepatic circulation (Ding *et al.* 2001; Vidal-Vanaclocha 2008).

The adhesion molecules involved in liver metastasis include P- and E-selectin, CD44 and the sialyl Lewis^x and sialyl Lewis^a molecules. In a study using the murine carcinoma line H-59, the use of a monoclonal antibody to E-selectin reduced the number of liver metastases by 97% (Brodt *et al.* 1997). The intra-vital microscopy study mentioned in the previous paragraph also studied the role of P-selectin in the metastasis of EL-4 and C26 cells to the liver. Adhesion of the smaller EL-4 tumour cells was decreased in P-selectin-/- mice and in wild-type mice administered an anti-P-selectin antibody, however, this P-selectin effect on metastasis was not seen with the larger C26 cells (Ding *et al.* 2001). In a study comparing the lymphoma parental cell line RWA117-P with the liver-metastatic cell line, RAW117-H10, unlike sialyl Lewis^x the presence of sialyl Lewis^a was found to be much higher on the liver-metastatic line than the parental line and metastasis could be prevented by pre-treatment of the cells with sialidase (Kikkawa *et al.* 1998). Furthermore, the interaction between tumour cell CD44 and hepatic endothelial HA in metastasis to the liver of both B16 melanoma and Lewis lung carcinoma LL3 tumour cells was demonstrated when a synthetic HA-butyric acid molecule was administered prior to the intrasplenic implantation of the tumour cells (Coradini *et al.* 2004).

1.3.3 The Role of Platelets in Tumour Cell Metastasis

A wealth of evidence exists in the scientific literature linking platelets with the process of tumour cell metastasis. That they do play a role is not in doubt, however, whether this role is one of assisting tumour cell adhesion and migration across the blood vessel wall or of merely forming a barrier around tumour cells preventing immune cell-mediated killing has come into question. The following sections discuss the role of platelets in leukocyte extravasation and provide a review of the extensive research conducted in the area of platelets and tumour cell metastasis.

1.3.3.1 Leukocyte-Platelet Interactions as a Model of Haematogenous Tumour Metastasis

Platelets play a significant role in assisting leukocyte migration in response to injury and inflammation, a process that may resemble platelet-assisted tumour metastasis (Pitchford *et al.* 2003). Activated platelets express P-selectin on their surface and bind PSGL-1 on leukocytes within the circulation. This interaction results in activation of leukocyte β2 integrins and secretion of inflammatory cytokines (Wagner and Frenette 2008). Furthermore, since leukocyte:platelet complexes express a greater number of adhesion molecules and ligands than unactivated leukocytes alone, there is a greater chance of them interacting with activated endothelium.

Platelets have also been observed to roll along and adhere to activated endothelium via P-selectin (Frenette *et al.* 1995). A platelet layer forms over the endothelium and expresses P-selectin at a density higher than that of activated endothelium and, hence, leukocytes may be recruited more efficiently. Platelets also release chemokines, such as RANTES (CCL5), which promote leukocyte adhesion to the endothelium (Wagner and Frenette 2008).

Platelets have been demonstrated to play a significant role in the recruitment of leukocytes to sites of ischaemia/reperfusion injury. This occurs following the resumption of blood flow to an ischaemic organ and is associated with significant changes to the microvasculature that reflect changes seen in inflammation. Along with these changes, extensive tissue damage occurs, known as ischaemia/reperfusion injury, due to the release of reactive oxygen species by leukocytes recruited to the area (Salter *et al.* 2001). Leukocyte recruitment appears to be dependent upon the adhesion of platelets to the activated endothelium and the extent of ischaemia/reperfusion injury is significantly reduced following platelet depletion (Golino *et al.* 1987). The platelet proteins P-selectin and GpIIb-IIIa and the procoagulant

fibrinogen have been shown to be involved in ischaemia/reperfusion injury through the promotion of leukocyte adhesion and transendothelial migration (Massberg *et al.* 1999; Salter *et al.* 2001).

Platelets have recently been demonstrated to migrate into lung tissue in an experimental model of allergic asthma. This migration appeared to precede that of leukocytes and was not due to haemorrhage as erythrocyte antigens were not detected (Pitchford *et al.* 2003; Pitchford *et al.* 2008) Furthermore, endothelial cells have been shown to transport platelets transcellularly, in vesiculo–vacuolar organelles, to their basal surface (Feng *et al.* 1998; Feng *et al.* 2002). Platelets may assist leukocyte migration by degrading the basement membrane through the release of matrix metalloproteases and heparanase (Vlodavsky *et al.* 1992; Bartlett *et al.* 1995). The haemostatic effects of platelets also minimise bleeding and local tissue damage caused by extravasating leukocytes (Wagner and Frenette 2008).

1.3.3.2 Can Platelets Induce an EMT at the Primary Tumour Site?

Surprisingly, there is very little information on whether platelets are capable of enhancing the metastatic behaviour of tumour cells within the primary tumour. Theoretically, there is ample opportunity for platelets to interact with tumour cells at the primary tumour site. As a tumour grows it establishes its own blood supply through angiogenesis. Typically, tumour-associated blood vessels are ill-formed, tortuous and the lumenal surface consists of a mosaic of endothelium and tumour cells (Chang *et al.* 2000). Platelet adhesion to the vessel-associated tumour cells and release of granular contents has the potential of inducing an EMT, a process that would enhance the entry of tumour cells into the haematogenous circulation.

In studies determining the effect of platelet-derived microvesicles (PMV), released following platelet activation, on human lung cancer cell lines (A549, CRL 2066, CRL 2062, HTB 183, HTB 177), and breast cancer cell lines (MDA-231 and BT-549) it was demonstrated that the majority of the cell lines migrated towards PMV, with the level of reponse correlating with the metastatic capacity. Additionally, following exposure of the A549, HTB 177, MDA-231 and BT-549 cell lines to PMV, proliferation was enhanced, following activation of the MAPK p42/44 and AKT pathways, and in the A549 cells cyclin D2 mRNA was increased, thus increasing the invasive potential of these cells. Furthermore, matrix metalloprotease (MMP) expression was strongly upregulated in the A549, HTB 177, MDA-231 and BT-549 cells which was associated with enhanced chemoinvasion of Matrigel, an effect that could be reversed by the addition of an MMP inhibitor (Janowska-Wieczorek *et al.* 2005; Janowska-Wieczorek *et al.* 2006).

Unpublished work from Professor Parish's laboratory has demonstrated, using micro-array data and *in vitro* and *in vivo* studies, that platelets are capable of inducing a more aggressive phenotype in tumour cell lines. Using a Matrigel solubilisation assay, it was demonstrated that numerous tumour cell lines when exposed to washed, thrombin-activated platelet membranes were able to solubilise Matrigel proteins to a significantly greater extent than the tumour cell lines or platelet membrane preparations alone. When the human breast cancer cell line MDA-MB-231 cell line was studied further, the extent of Matrigel solubilisation was platelet membrane concentration dependent. Additionally, the tumour cells were observed to adopt an invasive phenotype when incubated with thrombin-activated platelet membranes (Figure 1.5). *In vivo* studies revealed that MDA-MD-231 and the MM170 cells were both significantly more metastatic when pre-incubated with thrombin-activated platelet membranes. Subsequent micro-array data have indicated that invasion-associated genes are upregulated in tumour cells following their incubation with activated platelets.

1.3.3.3 Platelets Can Promote Tumour Cell Extravasation and Invasion

Elucidating the mechanisms involved in tumour cell extravasation has involved the use of *in vitro* flow-chamber and Matrigel degradation models, as well as *in vivo* experimental metastasis models and intra-vital videomicroscopy. The experimental metastasis models usually involve the intravenous injection of tumour cells into the tail vein or the splenic or portal circulation of mice (Xue and Gao 1989; Panis *et al.* 1990; Elkin and Vlodavsky 2001). Due to the vascular anatomy, the first capillary bed encountered is within the lungs following tail vein injection and the liver following portal vein/intrasplenic injection. Less commonly, tumour cells are injected into the left cardiac ventricle, thus bypassing the lungs, and metastases assessed in the bone marrow or brain (Mandybur 1981; Arguello *et al.* 1988). Following a period of time sufficient to enable the growth of macroscopic metastases, the organs of interest are removed and the tumour burden enumerated. The role of a specific cell type or protein may be determined in this model through the use of knockout or transgenic mice, by pre-treating mice with blocking or depleting antibodies, and by the administration of peptide mimetics, protein-specific enzymes or pharmaceutical agents. It is acknowledged that this model does not replicate the true-to-life situation in that a bolus of 1-200,000 tumour cells is unlikely to occur at any one time in the course of metastatic disease. Additionally, the endothelium in the experimental animals is 'naïve' in that soluble factors, possibly released by the primary tumour in order to establish a pre- metastatic niche, are absent. In spite of these short-comings, and in the absence of a superior model, the experimental metastasis models described enable the assessment of the molecular interactions associated with tumour cell extravasation within the intact vascular system and its inherent shear forces, and within the complex milieu of the haematogenous and immune systems.

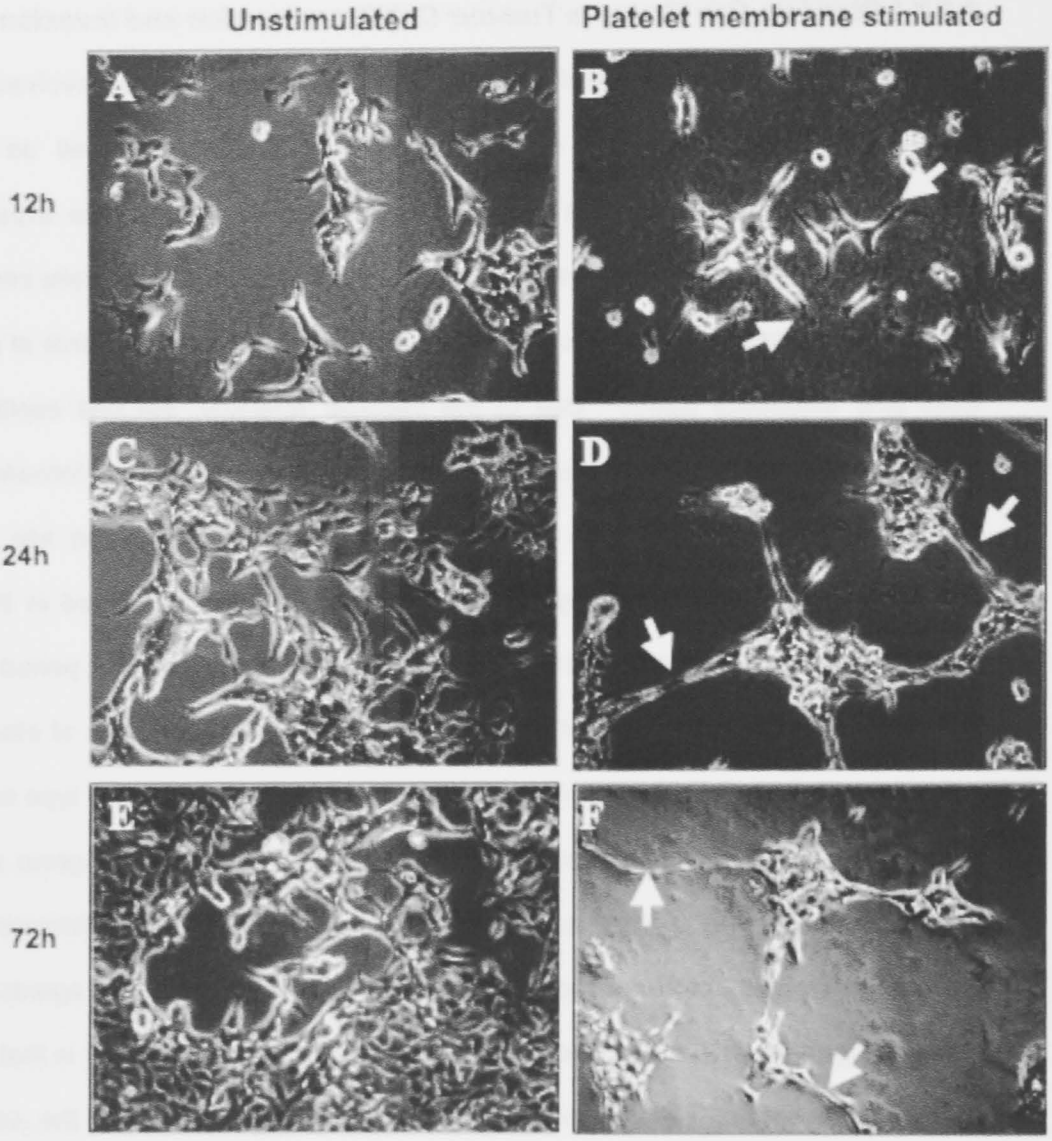

Figure 1.5: The adoption of an invasive phenotype by MDA-MB-231 tumour cells when cultured on Matrigel in the presence of thrombin-activated human platelet membranes.

A, C and E: Phase contrast images of MDA-MB-231 tumor cells cultured for 12, 24 and 72 hr, respectively, on a thin layer of Matrigel.

B, D and E: Morphology of MDA-MB-231 tumour cells cultured on Matrigel for 12, 24 and 72 hr, respectively, in the presence of thrombin-activated human platelet membranes (5×10^8 platelet equivalents/ml). Arrows in (**B**) indicate visible holes in the matrix produced by invading tumour cells whereas arrows in (**D**) and (**E**) highlight long cellular connections between aggregates of tumour cells not seen in control cultures.

Unpublished work of Jian-Hong Peng
PhD Student, Parish Laboratory

Many different tumour cell types have been demonstrated to have the ability to induce platelet activation and this correlates with their capacity to metastasise *in vivo* when injected intravenously (Karpatkin and Pearlstein 1981). Tumour cells may induce platelet activation through several mechanisms including: (i) activation of the coagulation pathway through the constitutive expression of tissue factor or cancer procoagulant, with the coagulation pathway resulting in the production of the potent platelet activator, thrombin; (ii) release of TNF-α or IL-1β by tumour cells resulting in expression of tissue factor by endothelial cells and associated dowregulation of thrombomodulin, thus creating a prothrombotic environment at the vascular wall; (iii) direct activation of platelets by tumour cells through the release of agonists, such as ADP or thrombin, or by direct binding of tumour cells to platelets (Noble and Pasi 2010).

Numerous experimental studies have demonstrated the requirement of platelets for successful metastasis of i.v. injected tumour cells. Ultrastructural studies *in vivo* have also demonstrated that tumour cells arrested in the vasculature are surrounded by platelets and fibrinogen (Karpatkin and Pearlstein 1981; Erpenbeck and Schon 2010). When anti-platelet agents are administered, or when platelet levels are experimentally lowered *in-vivo,* tumour cell metastasis is inhibited (Gasic *et al.* 1968; Karpatkin and Pearlstein 1981; Gasic 1984; Honn *et al.* 1992; Tzanakakis *et al.* 1993). Furthermore, mice genetically deficient in circulating platelets, the thrombin receptor PAR4, fibrinogen or the Gαq protein required for platelet activation have a reduced susceptibility to metastasis formation (Palumbo *et al.* 2000; Camerer *et al.* 2004; Palumbo *et al.* 2005). In particular, the platelet-specific adhesion proteins GpIIb-IIIa and P-selectin have consistently been shown to promote metastasis. As a result of the importance of these two molecules in tumour metastasis and leukocyte migration in

ischaemia/reperfusion injury, the following sections discuss the normal function of these two proteins and the evidence for their role in tumour cell metastasis.

1.3.3.4 Role of the Integrin αIIbβ3 (GpIIb-IIIa) in Tumour Metastasis

Integrins are heterodimeric receptors consisting of α and β subunits that are generally involved in cell-ECM interactions or cell-cell adhesion. In addition to their adhesive function, which is activated by inside-out signalling, they are involved in cell communication through outside-in signalling. Several members of the integrin family have been implicated in metastasis as shown in Table 1.2.

The protein αIIbβ3, also known as GpIIb-IIIa, is the most highly expressed receptor on the surface of resting platelets with approximately 50,000 copies/platelet, this number increasing to approximately 80,000 upon platelet activation. The role of GpIIb-IIIa in platelet function is to cross-link platelets through the binding of soluble macromolecular ligands, thus forming a stable clot. Ligands for GpIIb-IIIa include fibrinogen, von Willebrand factor (vWF), fibronectin, vitronectin and thrombospondin (Hato *et al.* 2002; Coller and Shattil 2008) .

Consistent with other members of the integrin family, until activated through inside-out signalling, GpIIb-IIIa has a low affinity and avidity for its ligands. Inside-out signalling through GpIIb-IIIa may be triggered by other platelet adhesion receptors binding their ligands (e.g., GpIb-IX-V binding to vWF or GpVI binding to collagen), by agonists released from nearby platelets binding their G-coupled protein receptors (e.g., ADP and thromboxane A2), or by substances produced as a result of tissue injury (e.g., thrombin and adrenaline). This inside-out signalling modulates within 1 second the ligand-binding affinity of GpIIb-IIIa through conformational change and increases the

mobility of the protein to allow clustering, thus increasing adhesive function (Hato *et al.* 2002; Coller and Shattil 2008).

Outside-in signalling occurs through a conformational change induced in the cytoplasmic domains of GpIIb-IIIa following ligand binding. The subsequent signalling cascades lead to changes in cytoskeletal reorganization thus permitting platelet spreading to enhance adhesion, granule secretion and clot retraction (Hato *et al.* 2002; Coller and Shattil 2008).

There is a significant amount of evidence implicating GpIIb-IIIa in the promotion of tumour cell extravasation. Inhibition of GpIIb-IIIa adhesion using blocking monoclonal antibodies or small molecules significantly reduces the interaction between platelets and tumour cells, as well as *in vivo* experimental metastasis (Bastida *et al.* 1987; Grossi *et al.* 1987; Amirkhosravi *et al.* 1999). Similarly, using a mouse strain deficient in β3 integrins, bone metastasis of B16 melanoma was significantly inhibited (Bakewell *et al.* 2003). Using bone marrow chimeras, it was demonstrated that the β3 integrins exerted their prometastatic effect via platelets, with GpIIb-IIIa being the dominant β3 integrin expressed by platelets. Subsequent pharmacological inhibition of GpIIb-IIIa also significantly reduced metastases (Bakewell *et al.* 2003). In separate studies, GpIIb-IIIa binding to tumour cells was shown to occur via recognition of fibronectin and von Willebrand factor *in vitro* and GpIIb-IIIa blockade prevented tumour cell–platelet interactions *in vitro* and experimental metastasis *in vivo* (Karpatkin *et al.* 1988; Amirkhosravi *et al.* 1999).

GpIIb-IIIa expression is normally restricted to platelets, megakarocytes and some haemopoietic progenitors, however, numerous tumour cells have been found to express GpIIb-IIIa, and in doing so, increase their metastatic potential through

enhanced platelet and endothelial interactions (Chen *et al.* 1992; Nierodzik *et al.* 1992; Oleksowicz *et al.* 1995; Chen *et al.* 1997). Furthermore, the level of expression of GpIIb-IIIa by a variety of B16 melanoma lines correlated with their ability to induce platelet activation and to form lung colonies. In addition, the level of GpIIb-IIIa expression increased following stimulation with thrombin, which was associated with an increased ability of the tumour cells to adhere to fibronectin and the subendothelial matrix (Chang *et al.* 1992; Wojtukiewicz *et al.* 1992).

1.3.3.5 Role of P-selectin in Tumour Metastasis

The selectin family of adhesion molecules, consisting of P-selectin, L-selectin and E-selectin, are structurally related, transmembrane glycoproteins that recognise specific ligands which are generally sialo-fucosylated carbohydrate structures (Mannori *et al.* 1995).

P-Selectin is stored within the α-granules of platelets and the Weibel-Palade bodies of endothelial cells, both of which translocate to the surface within minutes following platelet/endothelial cell activation. Constitutive expression of P-selectin has been observed on the vascular endothelium of several organs with the highest levels seen in the liver and lungs (Eppihimer *et al.* 1996; Singh *et al.* 1999). The ligand for P-selectin, PSGL-1 (P-selectin glycoprotein ligand-1), is expressed by platelets, leukocytes and endothelial cells and carries the sialyl Lewis^{x} tetrasaccharide (Moore *et al.* 1994; Frenette *et al.* 2000). PSGL-1 is capable of binding all 3 selectins, although it binds P-selectin with the greatest affinity (Guyer *et al.* 1996; Li *et al.* 1996). Both platelet- and endothelial-derived P-selectin mediate the initial tethering of leukocytes to the vascular wall during inflammation and aid stable thrombus formation following vessel wall injury (McEver *et al.* 1995; Furie and Furie 2004).

Several studies using experimental metastasis to the lung have demonstrated a role for P-selectin in the promotion of metastasis through enhancement of tumour cell interactions with the blood vessel wall. This effect is generally attributed to the binding of platelet P-selectin to various carbohydrate ligands on the tumour cell surface (Kim *et al.* 1998; Kim *et al.* 1999; Garcia *et al.* 2007). In contrast, the relative contribution of endothelial P-selectin in tumour cell metastasis to the lung is not clear. As mentioned in section 1.3.2.3.4, a study of EL-4 lymphoma metastasis to the liver demonstrated a marked P-selectin effect which was attributed to endothelial P-selectin, however, the relative contributions of platelet P-selectin and endothelial P-selectin in this model were not delineated (Ding *et al.* 2001).

It should be noted that unpublished results from Professor Parish's Laboratory demonstrated a potential cooperative role for P-selectin and GpIIb-IIIa in the promotion of metastasis by platelets. When incubating the human breast cancer cell line MDA-MD-231 with washed, thrombin-activated, platelet membranes, it was found that interactions between platelet membranes and tumour cells and activation of Matrigel solubilisation could be prevented only when antibodies to P-selectin and GpIIb-IIIa were used in combination. Antibodies to GpIbα, PECAM-1 and $\alpha 2\beta 1$ were also tested in isolation and in combination with the antibody to P-selectin but had no inhibitory effects. These results are supported by the findings of Yu *et al.* who demonstrated that the binding of the highly metastatic human hepatoma cell line, MHCC97, to ECM in an *in vitro* adhesion assay was enhanced by platelets and could be significantly reduced by mAbs to GpIIb-IIIa and P-selectin (Yu *et al.* 2002).

1.3.3.6 The Pro-Metastatic Effects of the Tumour Cell-Platelet Interaction

The potential pro-metastatic effects of circulating tumour cells associating with platelets include the following (Karpatkin and Pearlstein 1981; Honn *et al.* 1992; Vlodavsky *et al.* 1992; Erpenbeck and Schon 2010):

(i) A platelet-coated tumour cell may be better able to withstand the shear stresses within the circulation and more likely to become arrested within the capillary bed.

(iii) Platelet adhesive proteins may interact with the endothelium creating a stable platform for subsequent tumour cell migration.

(iv) Platelet-derived proteases and heparanase may assist in the migration of tumour cells across the vessel wall, particularly the subendothelial basement membrane.

(v) Platelet-derived growth and angiogenic factors may assist the subsequent growth of tumour cells and the establishment of secondary tumours.

Other research, however, has suggested that the only role platelets play in promoting metastasis is the protection of tumour cells from destruction by NK cells through physical impedence and the downregulation of NK function by PDGF interacting with the inhibitory receptor NKG2D (Nieswandt *et al.* 1999; Palumbo *et al.* 2005; Kopp *et al.* 2009).

1.4 Conclusions

Platelets, despite their small size, contain a remarkable armoury of proteins that not only promote thrombosis, haemostasis and tissue repair but also attack invading microorganisms, initiate an inflammatory response, and activate cells of the immune system. Furthermore, activated platelets attract and bind leukocytes, including NK cells, within the circulation assisting their migration across the blood vessel wall.

The small amount of research conducted on the role of platelets at the primary tumour site indicates that they are capable of inducing genes involved in invasion, proliferation and angiogenesis. In contrast, the evidence indicating a role for platelets in tumour cell extravasation, that parallels their role in leukocyte migration, is substantial. In the light of this wealth of evidence, it is hard to conceive that the only role for platelets in the metastatic process is to form a protective cloak around tumour cells preventing their destruction by NK cells. Platelet adhesion proteins involved in leukocyte migration have unequivocally been shown to promote tumour cell metastasis, moreover, L-selectin, present on leukocytes, including NK cells, has been shown to have an independent and synergistic effect with P-selectin in promoting metastasis (Borsig *et al.* 2002; Lejtenyi *et al.* 2003). Furthermore, leukocytes are readily incorporated into, and capable of migrating through, a thrombus (Sheikh *et al.* 2004; Wohner 2008). The timing within the metastatic process of the actions of platelets and NK cells on tumour cells has not been determined and may resolve these conflicting data.

1.5 Experimental Aims of this PhD

In light of the evidence and controversy regarding the role of platelets in tumour cell extravasation detailed above, initially this PhD project planned to address the following aims:

(i) To establish the kinetics of the pro-metastatic role of platelets and the anti-metastatic role of NK cells in an experimental model of tumour cell metastasis, and to determine whether platelets have a role in promoting metastasis beyond that of preventing NK cell-mediated tumour cell killing.

(ii) To determine the relative contributions of platelet-derived and endothelial-derived P-selectin in promoting metastasis.

(iii) To establish an improved methodology enabling the *in vivo* monitoring of platelet production and lifespan for use when trialling anti-platelet therapies or investigating the cause of abnormal platelet numbers.

During the research under these aims, however, it was observed that the use of a mAb specific for the platelet protein GpIIb-IIIa *in vivo* resulted in the elimination of >95% of platelets and, upon reviewing the literature on the mechanisms of antibody-mediated platelet depletion (provided in Chapter 4), it was felt that a contribution could be made to this field of research. The project aims were extended, therefore, to include the following:

(iv) To investigate the different mechanisms of platelet depletion using monoclonal antibodies to a variety of platelet proteins.

(v) To explore the potential regulatory pathways that determine whether an anti-platelet antibody causes platelet depletion or not.

(vi) To establish whether these regulatory systems can be manipulated to prevent antibody-mediated depletion as seen in the medical condition known as immune thrombocytopenic purpura (ITP).

It was hoped that the results of this work would better define the role of platelets and NK cells in tumour cell metastasis, the mechanisms and regulation of antibody-mediated platelet elimination, and provide improved techniques for the study of the determinants of platelet production and lifespan. The greater aim of this work was to contribute to the significant bank of knowledge on the mechanisms of haematogenous metastasis and ITP, and in so doing, aid the quest to find more effective therapies for the treatment of both conditions.

Chapter 2

Materials and Methods

The following chapter details the materials and experimental methods used to obtain the results described in chapters 3, 4 & 5.

2.1 General reagents

2.1.1 Media, buffers and anti-coagulant solutions

Acid Citrate Dextrose (ACD)

Sodium citrate 25 g/L, citric acid 14 g/L and glucose 20 g/L in purified, deionised, sterile water, pH 4.5.

Alpha Minimal Essential Medium (alpha MEM)

Minimum Essential Medium (MEM) Alpha Medium powder (Invitrogen, Carlsbad, CA) in purified, deionised, sterile water.

Bouin's Solution

Acetic acid 5% (v/v), formaldehyde 9% (v/v), picric acid 0.9% (v/v) in purified, deionised, sterile water.

Buffered Saline Citrate Glucose (BSCG)

NaCl 6.78 g/L, sodium citrate 4 g/L, Na_2HPO_4 1.2 g/L, KH_2PO_4 0.2 g/L, EDTA 0.34 g/L and glucose 2 g/L in purified, deionised, sterile water.

EDTA (5mM) in PBS

EDTA 1.46 g/L in phosphate buffered saline

F15 Medium

F15 MEM powder (Gibco BRL, Grand Island, NY) 9.61g/L and $NaHCO_3$ 2.2 g/L in purified, deionised, sterile water.

Hank's Balanced Salt Solution

NaCl 8 g/L, KCl 400 mg/L, $MgSO_4.7H_2O$ 100 mg/L, $MgCl_2.6H_2O$ 100 mg/L, $CaCl_2$ 112 mg/L, glucose 1 g/L, phenol red 20 mg/L, $NaH_2PO_4.2H_2O$ 78 mg/L, KH_2PO_4 60 mg/L in purified, deionised, sterile water.

Phosphate Buffered Saline (PBS)

NaCl 8 g/L, $NaH_2PO_4.2H_2O$ 0.35 g/L and $Na_2HPO_4.2H_2O$ 1.25 g/L in purified, deionised, sterile water.

Penicillin Streptomycin Neomycin (PSN) Antibiotics

Penicillin G 300 mg/L, streptomycin sulphate 500 mg/L, neomycin sulphate 500 mg/L in purified, deionised, sterile water.

RPMI-1640

RPMI powder (Gibco BRL, Grand Island, NY), $NaHCO_3$ 2 g/L in purified, deionised, sterile water.

Red Blood Cell Lysis Buffer

7.65 g/L NH_4Cl and 2.06g/L Tris in purified, deionised, sterile water, pH 7.2.

Trypsin/EDTA

0.04% (w/v) Trypsin and 0.02% (w/v) EDTA in purified, deionised, sterile water.

2.2 Animals

The strain, phenotype, background and source of all mice used are detailed in Table 2.1. Approval for all experimental procedures conducted on these mice was obtained from the Animal Experimentation Ethics Committee of the Australian National University. The mice were housed within PC2 facilities. Daily care and breeding of the mice was conducted by the staff of the Animal Services Division, the Australian National University or the candidate.

2.3 Antibodies

Table 2.2 details the antibodies used. The 1B5 mAb against mouse GpIIb-IIIa was kindly provided by Professor Barry Coller (The Rockefeller University, New York, USA) (Lengweiler *et al.* 1999). All other antibodies were purchased from commercial sources.

Table 2.1: Mouse strains used in experimental procedures

Mouse Strain	Background	Phenotype	Source	Reference
C57BL/6	B6	WT	Animal Resources Centre, Perth, Australia	NA
C57BL/6 (CD45.1)	B6	CD45.1 congenic strain	Animal Resources Centre, Perth, Australia	NA
BALB/c	BALB/c	WT	Animal Resources Centre, Perth, Australia	NA
P-selectin-/-	C57BL/6	Absence of P-selectin	Dr Michael Hickey, Monash University, Melbourne, Australia	(Kuligowski *et al.* 2006)
c-mpl-/-	C57BL/6	Lack thrombopoietin receptor 5-15% normal platelet numbers	Dr Warren Alexander, WEHI, Melbourne, Australia	(Alexander *et al.* 1996)
Plt20	BALB/c	Mutation in Bcl-X_L 30% normal platelet numbers	Dr Ben Kyle, WEHI, Melbourne, Australia	(Mason *et al.* 2007)
C3-/-	C57BL/6	Absence of C3 component of complement system	Professor Marina Botto, Imperial College, London, UK	(Wessels *et al.* 1995)
FcRγ-/-	C57BL/6 or BALB/c	Absence of common gamma chain of all Fc receptors	Dr Mark Hogarth, Burnett Institute, Melbourne, Australia	(Takai *et al.* 1994)
β_2M-/-	C57BL/6	Absence of β_2 microglobulin associated with MHC Class I	Dr Guna Karupiah, JCSMR, ANU, Canberra, Australia	(Zijlstra *et al.* 1990)
B6.129S7-Cd47tm1Fpl/J	C57BL/6	Absence of CD47	Jackson Laboratories, Maine, USA	(Lindberg *et al.* 1996)
B6.129S4-Itgamtm1Myd/J	C57BL/6	Absence of CD11b (Mac-1)	Jackson Laboratories, Maine, USA	(Coxon *et al.* 1996)
NOD-scid IL2 Rγ	NOD	Absence of NK, B and T cells	Jackson Laboratories, USA	(Shultz *et al.* 2005)
NOD/scid	NOD	Absence of B and T cells	Animal Resources Centre, Perth, Australia	NA

Table 2.2: Antibodies Used in Experimental Procedures

Antigen (CD)	Molecule	Species	Raised in	IgG isotype	Clone	Source	Catalogue No.
Purified mAbs							
CD11b	Mac-1/CR3	mouse	rat	IgG2a,	M1/70	BD	553308
CD31	PECAM-1	mouse	rat	IgG1	Pec.H3	Emfret	M120-0
CD41/61	GpIIb/IIIa	mouse	hamster	IgG3	1B5	Barry Coller	NA
CD41/61	GpIIb/IIIa	mouse	rat	IgG1	Leo.A1	Emfret	M022-0
CD41/61	GpIIb/IIIa	mouse	rat	IgG2b	Leo.H4	Emfret	M021-0
CD42a	GpIX	mouse	rat	IgG1	Xia.B4	Emfret	M051-0
CD42b	GpIbα	mouse	rat	IgG1	Xia.G7	Emfret	M042-0
CD42b	GpIbα	mouse	rat	IgG2b	Xia.G5	Emfret	M040-0
CD42d	GpV	mouse	rat	IgG1	Gon.C2	Emfret	M060-0
CD42d	GpV	mouse	rat	IgG2a	Gon.G6	Emfret	M061-0
CD47	IAP	mouse	rat	IgG2a	miap301	BD	555297
CD49b	GpIa	mouse	rat	IgG1	Sam.H9	Emfret	Custom made
CD49b	GpIa	mouse	rat	IgG2b	Sam.G4	Emfret	M070-0
CD62L	L-selectin	mouse	rat	IgG2a	MEL-14	BD	553148
CD62P	P-selectin	mouse	rat	IgG1	RB40.34	BD	553741
CD172a	SIRPα	mouse	rat	IgG1	P84	BD	552371
CD200 R	OX2 R	mouse	rat	IgG2a	OX-110	BioLegend	123902
	Isotype control		rat	IgG1	A110-1	BD	553993
	Isotype control		rat	IgG1	R3-34	BD	553922
	Isotype control		rat	IgG2a	54447	R&D	MAB006
	Isotype control		rat	IgG2b	141945	R&D	MAB0061
	Isotype control		hamster	IgG3	E36-239	BD	551386
FITC Conjugated mAbs							
CD62P	P-Selectin	Mouse	Rat	IgG1	RB40.34	BD	553744
CD71	Transferrin R	Mouse	Rat	IgG1	C2	BD	553266
CD45.2	LCA	Mouse	Mouse	IgG2a	104	BD	553772
CD3	CD3	Mouse	Rat	IgG2b	17A2	BD	555274
	Isotype control		Rat	IgG1	R3-34	BD	554684

Table 2.2: Antibodies Used in Experimental Procedures (continued)

Antigen (CD)	Molecule	Species	Raised in	IgG isotype	Clone	Source	Catalogue No.
PE-Conjugated mAbs							
CD31	PECAM-1	Mouse	Rat	IgG2a	MEC13.3	BD	553373
CD41	GpIIb	Mouse	Rat	IgG1	MWReg30	BD	558040
CD200	OX2	Mouse	Rat	IgG2a	OX-90	BioLegend	123807
	IgG2a	Rat	Mouse	IgG2b	RG7/1.30	BD	558067
	TER-119	Mouse	Rat	IgG2b	TER119	BD	553673
CD45.1	LCA	Mouse	Mouse	IgG2a	A20	BD	553776
CD161c	NK1.1	Mouse	Mouse	IgG2a	PK136	BD	553165
Miscellaneous mAbs							
CD4-APC	L3T4	Mouse	Rat	IgG2a	RM4-5	BD	553051
CD8a-APC AF780	Ly-2	Mouse	Rat	IgG2a	53-6.7	eBioscience	47-0081-82
CD45.2-PercP	Ly-5.2	Mouse	Mouse	IgG2a	104	BioLegend	109828
CD11b-PercP	Mac-1 α chain	Mouse	Rat	IgG2b	M1/70	BD	550993
CD45R-Pacific Blue	B220	Mouse	Rat	IgG2a	RA3-6B2	BD	558108

2.4 Flow cytometry equipment and software

Samples were analysed on either a Becton Dickinson FACSort or Becton Dickinson LSR Fortessa machine using BD CellQuest™ software (Franklin Lakes, NJ) and FlowJo software (Tree Star Inc., Ashland OR).

2.5 Platelet and erythrocyte enumeration

Mice were placed in a restrainer and approximately 1 mm of the tail tip removed using surgical scissors. 5 μL whole blood was collected from the tail vein and thoroughly mixed into 45 μL ACD. To prevent blood loss from the wound of thrombocytopenic mice, or when platelet and erythrocyte kinetics were performed, lignocaine gel was applied topically for pain minimisation and the tail tip cauterised.

Platelet and erythrocyte numbers were determined via flow cytometry within 30 min of collection using the method of Alugupalli *et al* (Alugupalli *et al.* 2001). Briefly, 10 μL blood/ACD was added to 990 μL PBS containing 10 μL rainbow fluorescent reference beads (Becton Dickinson, Catalogue No. 556291). Platelet and erythrocyte gates were determined using their characteristic log forward and log side scatter parameters. These parameters were confirmed when establishing the method using antibodies to GpIIb-IIIa (clone MWReg30) and glycophorin A (clone TER119). Samples were passaged through the FACS machine until 1000 reference beads had been collected, representing 10 μL of the solution. Platelet and erythrocyte numbers were calculated per μL blood by multiplying the number of events in the platelet or erythrocyte gate by a factor of 100 (multiplied by 1000 to account for the blood sample dilution factor, and divided by 10 as 10 μL of diluted sample was analysed).

2.6 Staining of platelets for cell surface markers

From the tail tip of mice, 5 μL samples of whole blood were collected into 100 μL of 5mM EDTA in PBS. Samples were centrifuged at 350*g* for 5 min at room temperature to pellet RBCs and WBCs. The platelet-rich supernatant from each sample was collected and centrifuged at 1210*g* for 10 min at room temperature and the supernatant removed. Antibodies directed against the surface markers of interest were added, or an appropriate isotype control, and incubated in the dark for 30 min at 37°C. Samples were washed twice with PBS prior to FACS analysis or addition of a fluorescent-conjugated secondary antibody. Following incubation with the secondary antibody for 30 min in the dark at room temperature, 2 wash steps were repeated prior to analysis using flow cytometry.

2.7 Platelet-assisted tumour cell metastasis

2.7.1 Tumour cell lines, culture, injection and assessment of tumour burden

2.7.1.1 B16-F1 mouse melanoma cell line

B16-F1 melanoma cells were cultured in F15 medium supplemented with 10% foetal calf serum, 0.1% PSN and 1% glutamine and passaged 4 times prior to preparation for injection. Cells were washed twice with PBS following lifting with EDTA/Trypsin and resuspended in HBSS for injection. A dose of 1-2 x 10^5 cells in 200 μL was injected into the tail vein of mice. Mice were culled 14 days following injection of tumour cells, the lungs +/- livers were then removed and placed into 10% formalin. The preserved organs were dissected into separate lobes and tumours counted under a dissecting microscope.

2.7.1.2 Mouse breast cancer cell line - 4T1.2

This cell line was kindly provided by Dr Robin Anderson (Peter MacCallum Cancer Institute, Melbourne) and routinely cultured in alpha MEM supplemented with 10% foetal calf serum, and 0.1% PSN. Cells were passaged 3 times prior to preparation for injection. Cell were washed twice with PBS following lifting with EDTA/Trypsin and resuspended in HBSS for injection. A cell dose of 1-2 x 10^5 in 200 μL was injected i.v. into BALB/c mice. Mice were culled 14 days following tumour cell injection, the lungs +/- the livers removed and placed into Bouin's solution. The preserved organs were dissected into separate lobes and tumours counted under a dissecting microscope.

2.7.2 Depletion of platelets in mice

To deplete mice of platelets, 20 μg of a mAb specific for mouse GpIIb-IIIa, clone 1B5, was diluted in 150 μL of PBS and injected i.v. via the tail vein.

2.7.3 Depletion of NK cells in mice

To deplete mice of NK cells, 50 μL of a rabbit polyclonal anti-asialo GM1 antiserum (#986-10001, Wako Pure Chemical Industries, Osaka, Japan) was mixed with 100 μL of 0.9% saline and injected i.v. via the tail vein at the time points indicated.

To confirm the selective depletion of NK cells, mice were injected with the anti-asialo serum or PBS i.v. via the tail vein and the spleens removed 1 hr and 48 hr following injection. The spleens were mashed, the cells washed, stained with mAbs specific for

NK1.1, CD45.2, CD3 and B220 in addition to the viability dye Hoechst 33258, then analysed using flow cytometry (Figure 3.5).

2.7.4 Generation of P-selectin bone marrow chimeras

This experiment was performed on two separate occasions with the bone marrow make-up of the chimeras described in Chapter 3, Tables 3.1 and 3.2 .

2.7.4.1 Bone marrow Collection

Donor mice were euthanased via cervical dislocation and the femurs and tibias dissected. The marrow was extracted by flushing the lumen of the bones with RPMI-1640. The cellular extract was then filtered 3 times through a 70 μm filter, placed on ice and a cell count performed. Cells were centrifuged at 300*g* for 5 min at 4°C and resuspended in PBS at a concentration of 1 x 10^7 cells/mL in preparation for injection.

2.7.4.2 Mouse irradiation and marrow transplantation

Irradiation of the mice and injection of bone marrow preparations were performed by Mrs Debbie Howard. Recipient mice were placed in containers and irradiated with 1000 rads from a cobalt-60 source. Within 4 hr of irradiation the mice were injected i.v. with 2 x 10^6 bone marrow cells. Mice received prophylactic antibiotic therapy of neomycin and polymyxin in their drinking water for 6 wk following irradiation.

2.7.4.3 Measurement of CD45 allotype

Four to 6 wk following irradiation, 7 μL of blood was collected from the tail vein of each bone marrow recipient mouse into 20 μL of ACD. Following the addition of 150 μL of cold red cell lysis buffer, samples was incubated for 20 min at room temperature. Samples were then centrifuged at 300*g* for 5 min, the supernatant removed, CD45.1-

PE and CD45.2-FITC antibodies added and the samples incubated on ice in the dark for 25 min. Samples were washed twice with PBS to remove excess antibody and resuspended in PBS for subsequent analysis using flow cytometry. Leukocytes were gated using their characteristic log SSC and linear FSC. The percentages of CD45.1-PE and CD45.2-FITC positive cells were determined for each mouse.

2.7.4.4 Metastasis experiment in P-selectin chimeras

Experimental lung metastasis with B16-F1 melanoma cells were conducted in the P-selectin chimeras as described in section 2.7.1.1 ≥ 6 weeks post irradiation.

2.8 Immune-mediated depletion of platelets

2.8.1 Effect of mAbs directed against various platelet antigens on platelet numbers

Mice were injected i.v. with 20 μg of various antibodies (detailed in Table 2.2) specific for the platelet antigens GpIIb-IIIa, GpIbα, GpIX, GpIa, GpV and PECAM-1. Platelet numbers were determined, as described in Section 2.5 prior to, 2- and 24 hr post mAb injection. In a subset of experiments, mice were injected i.v. with 50 μg of a mAb specific for either SIRPα or the CD200R (OX2R) 1 hr prior to, or 1 hr post injection of the anti-platelet mAbs.

2.8.2 Analysis of platelets for degree of mAb binding

2.8.2.1 In vitro studies

To determine the extent of anti-platelet mAb binding to the surface of platelets, 200 μL of whole blood was collected from the tail vein of mice into 4 mL of 5mM EDTA in PBS, 5ml of PBS added, the sample spun at 1210*g* for 10 min at room temperature and the

supernatant discarded. The platelet, leukocyte and RBC pellet was resuspended in 8 mL of PBS and aliquoted. The *in vivo* dose of mAb administered to mice was 10 μg/mL of blood and, therefore, a range of mAb concentrations that equated to 2.5 – 40 μg/mL of blood, was added to the samples. The samples were then incubated at 37°C for 30 min, washed with PBS prior to the addition of a secondary FITC-conjugated antibody directed against rat IgG1 and the samples incubated on ice in the dark for 30 min prior to washing twice with PBS and analysis using flow cytometry.

2.8.2.2 In vivo studies

In the case of anti-platelet mAbs that failed to depleted platelets *in vivo* their extent of binding to platelets was determined by collecting 5 μL of whole blood in duplicate from the tail tip of mice into 100 μL 5mM EDTA in PBS 2 hr following mAb injection. A further 130 μL of PBS was added to each sample prior to centrifugation at 1210*g* for 10 min at room temperature. The pellet was washed in PBS prior to the addition of a FITC-conjugated antibody directed against rat IgG1. The samples were incubated on ice in the dark for 30 min prior to washing twice with PBS and analysis using flow cytometry.

2.8.3 Depletion of complement using cobra venom factor (CVF)

Mice were depleted of C3 by administering an intra-peritoneal injection of 50 μL of CVF (500 μg/mL) (Venom Supplies, Tanunda, South Australia), diluted in 0.9% saline 18 hr prior to injection of mAbs directed against platelet antigens.

2.8.4 Macrophage uptake of antibody-bound platelets

2.8.4.1 Macrophage isolation

Peritoneal macrophages were collected from euthanased mice into ice-cold 0.9% saline, centrifuged at 400*g* for 10 min at 4°C, resuspended in PBS and labelled for 20 min on ice with a mAb to PerCP conjugated mAb specific for CD11b (BD Biosciences, cat # 550993). The cells were then washed twice, resuspended in RPMI-1640 containing 1% FCS and kept on ice.

2.8.4.2 Platelet isolation, CFSE-labelling and incubation with mAbs

Platelets were isolated from 1 mL of whole blood collected from 5 mice via retro-orbital bleed through heparinized capillary tubes into BSCG. The blood was initially centrifuged at 300*g* for 5 min at room temperature to pellet erythrocytes and leukocytes. Platelets were then pelleted from the plasma by centrifugation at 1210*g* for 10 min at room temperature. The platelet pellet was resuspended in 5 mL of PBS and 5 μL of a 1 mM solution of CFSE in DMSO then added whilst the tube was being slowly vortexed. The platelets were incubated with CFSE in the dark for 5 min at room temperature prior to 3 washes in PBS/1% FCS and resuspension in 650 μL of PBS. Aliquots (200 μL) of the platelet preparation were then incubated with 3.35 μg of an IgG1 mAb specific for GpIX, GpIIb-IIIa or an isotype control for 30 min at 37°C (thus maintaining an equivalent platelet:mAb ratio as the *in vivo* concentration of 10 μg/mL of whole blood), and washed with PBS prior to resuspension in 750 μL of RPMI-1640 containing 1% FCS. A platelet count was performed on the residual platelet preparation via FACS analysis as described in section 2.5.

2.8.4.3 Co-Incubation of macrophages and antibody-bound platelets

Platelets and macrophages were co-incubated at a ratio of 20:1, respectively, for 1 hr at 37°C prior to analysis by flow cytometry. CD11b+ cells were gated and analysed for the level of CFSE fluorescence.

2.8.5 Platelet disintegration *in vitro* following incubation with antibodies directed against platelet antigens.

Whole blood (100 μL) from the tail tips of mice was collected into 2 mL of BSCG, diluted with 5 mL of PBS, centrifuged at 1210*g* for 10 min at room temperature, the pellet resuspended in 5mL of PBS and centrifuged again. The platelet, leukocyte and RBC pellet was resuspended in 1 mL of Hanks solution and aliquoted in 200 μL volumes. To each sample 0.2 μg of the anti-platelet antibody of interest was added (thus maintaining an equivalent platelet:mAb ratio as the *in vivo* concentration of 10 μg/mL of whole blood), the samples were incubated at 37°C for 30 min and washed twice with PBS prior to resuspension in Hanks solution. Each sample was further aliquoted into two wells and a FITC conjugated mAb specific for P-selectin or an isotype control added (2.5 μg/mL) Following incubation in the dark for 30 min at room temperature and two subsequent washing and centrifugation steps, the samples were analysed using flow cytometry.

2.9 Platelet and erythrocyte lifespan studies in mice using CFSE-labelling

2.9.1 *In vivo* CFSE labelling

Carboxyfluorescein diacetate succinimidyl ester (CFSE - Molecular Probes, Carlsbad CA) was dissolved in DMSO to prepare a stock solution of 10 mM. Immediately prior to injection into the lateral tail vein, 50 μL of stock CFSE was mixed with 100 μL of PBS. The solution was injected slowly over ~30 seconds.

2.9.2 Platelet and erythrocyte lifespan analysis

To determine the lifespan of platelets in mice, blood samples were collected at 1, 24, 48, 72, 96 and 120 hr following injection of CFSE as described in section 2.5. To define the platelet population from background debris when platelet numbers were low, such as in the *c-mpl-/-* and Plt20 mutant mice, a PE-conjugated anti-mouse GpIIb-IIIa antibody (clone MWReg30) was added to the ACD at a concentration of 2 μg/mL. Samples were analysed as described in Section 2.5 with PE positive platelets gated for subsequent CFSE labelling analysis.

To determine the lifespan of erythrocytes in mice, blood samples were collected at 1, 5, 10, 20, 30, 40 and 50 days following CFSE injection as described in section 2.5. Erythrocytes were gated based upon their characteristic log forward and side-scatter parameters for subsequent CFSE labelling analysis.

To determine the extent of CFSE labelling of platelet and erythrocyte populations at each time point, fluorescence was measured on the FL-1 channel of the flow cytometer, with the percentage of CFSE positive platelets and erythrocytes being followed over time to determine lifespan, and the total cumulative number of CFSE negative platelets and erythrocytes followed over time to determine bone marrow production rates. See Figure 5.1 for more details of analytical method used.

2.9.3 CFSE immunogenicity studies

To determine the immunogenicity of CFSE, mice were injected with a second dose of CFSE 12 weeks after the first dose. Erythrocyte kinetics were repeated and compared with results from the initial erythrocyte lifespan studies in these mice.

2.9.4 CFSE toxicology studies

To determine whether i.v. injection of CFSE caused any hepato- or nephrotoxicity, one mouse was injected with 155 μL of PBS (PBS control), two mice were injected with 92 μL of DMSO mixed with 63 μL of PBS (DMSO control), and two mice were injected with 50 μL of 10mmM CFSE stock in 42 μL of DMSO and 63 μL of PBS. One mouse from each experimental group was culled 24 hr post CFSE injection and the kidneys and livers were collected and fixed in 10% formalin. The remaining mice were culled 10 days post CFSE injection and the organs removed and fixed. The organs were paraffin-embedded, sectioned and H&E stained prior to examination by an independent anatomical pathologist.

2.9.5 Comparison of old and young erythrocytes

Age-associated changes in erythrocytes were also studied using *in vivo* CFSE labelling. Following the injection of mice with CFSE, blood samples were collected, as described in Section 2.5, on day 10 and day 40 post CFSE injection. A comparison was made of the mean forward scatter (Mean FSC) and the co-efficient of variation of the side scatter (CV of SSC) of newly generated versus aged erythrocytes. Aged erythrocytes were defined as erythrocytes that were CFSE-bright 40 days following CFSE injection. Newly generated erythrocytes were defined as erythrocytes that were CFSE-dull 10 days following CFSE injection (Figure 5.6).

2.9.6 Mathematical modelling of platelet and erythrocyte lifespan data

This work was done in collaboration with Professor Miles Davenport, University of New South Wales and Dr Deborah Cromer, Oxford University, UK. Dr Cromer was responsible for modelling the lifespan data generated by the candidate.

2.9.6.1 Lifespan modelling methods

In order to estimate the platelet and red cell lifespans from the experimental data it was assumed that the percentage of CFSE labelled cells within each mouse was fitted by either a linear or exponential curve, or by a curve derived from a lognormal distribution which was termed the 'lognormal model' (Murphy and Francis 1969; Dowling *et al.* 2005). A linear distribution would arise if all cells had exactly the same lifespan. An exponential distribution would generally arise if the death of platelets occurs at a defined "rate", possibly as a result of an external event. A log-normal distribution is likely to arise when the majority of platelets have a particular lifespan, which can vary slightly from its mean value.

It was assumed that cell lifespans have a distribution given by a function $f(\tau)$ (and therefore that a proportion, $f(\tau)$, of cells have a lifespan of τ time units). If *F%* of such cells were labelled initially with CFSE, the percentage of labelled cells one would observe in circulation *t* time units after labelling is given by:

$$S(t) = \frac{F}{C}\int_{t}^{\infty}\left(1-\int_{0}^{s} f(\tau)d\tau\right)ds \qquad \text{(S1)}$$

where *C* is a normalising constant (Murphy and Francis 1969).

For a linear distribution:

$$f_{lin}(\tau) = \begin{cases} 1 & \tau = L \\ 0 & otherwise \end{cases},$$

where L gives the lifespan of cells. The number of CFSE labelled cells observed in circulation at time x after labelling is:

$$S_{lin}(t) = \begin{cases} \frac{F(L-x)}{L} & x < L \\ 0 & \text{otherwise} \end{cases}. \quad \text{(S2)}$$

For an exponential distribution:

$f_{exp}(\tau) = \alpha e^{-\alpha\tau}$,

where α gives the decay rate of the cells. The number of CFSE labelled cells observed in circulation x time units after labelling is then given by

$$S_{exp}(t) = Fe^{-\alpha x}. \quad \text{(S3)}$$

Note that since $f_{exp}(\tau)$ represents the lifespan distribution of cells there is a factor of α at the front to ensure that the area under the curve is equal to one. $S_{exp}(t)$ gives the observed number of labelled cells present at time t after labelling and has the familiar constant term at the front.

For a log-normal distribution:

$$f_{ln}(\tau) = \frac{1}{\sqrt{2\pi}st} e^{-\frac{(\ln(t)-m)^2}{2s^2}},$$

where m and s are defined in terms of the mean, μ, and the standard deviation, σ, of cell lifespans via

$\mu = e^{m+\frac{s^2}{2}}$ and $\sigma = \sqrt{e^{2m+s^2}(e^{s^2}-1)}$.

The number of CFSE labelled cells one would observe in circulation x time units after labelling is given by

$$S_{in}(t) = \frac{F}{2}\left[1 - te^{-x_1}(1 - erf(x_2)) - erf(x_2 - \frac{s}{2})\right] \quad \text{(S4)}$$

where $x_1 = m + s^2/2$ and $x_2 = \frac{\ln(t) - m}{s\sqrt{2}}$ (Dowling *et al.* 2005).

Equations S2, S3 and S4 were fitted to experimental platelet and red blood cell data to determine average cell lifespans. Matlab®'s non-linear least squares estimator `lsqnonlin` was used to perform the fitting.

2.9.6.2 Statistical analysis

Comparisons were performed using the Student's t-test when the standard deviation (SD) of the two groups was comparable (calculated with the F-test), and the Mann Whitney test or non-parametric t-test was used when the SD between the two groups was significantly different. Significance of the t-tests or Mann Whitney test is given as a 2-tailed P-value. Statistical software used included Microsoft Excel (Version 11.2.3) and InStat (Version 3.0).

Chapter 3

Platelets and P-selectin control tumour cell metastasis in an organ-specific manner and independently of NK cells

3.1 Abstract

The pro-metastatic role of platelets has long been recognised with many mechanisms having been proposed such as platelets shielding tumour cells from destruction by intravascular natural killer (NK) cells and P-selectin expressed by activated platelets aiding the interaction of blood-borne tumour cells with the endothelium. The following chapter describes the results of investigations into the kinetics of the pro-metastatic role of platelets and the anti-metastatic role of NK cells in experimental models of 4T1.2 breast cancer lung metastasis and B16F1 melanoma lung and and liver metastasis. Furthermore, the relevant contributions of platelet P-selectin and endothelial P-selectin in B16F1 melanoma lung and liver metastasis were determined. The results of this work have demonstrated that the lung metastasis of both B16F1 melanoma cells and 4T1.2 breast cancer cells is promoted by platelets and inhibited by NK cells. Moreover, in the B16F1 metastasis model, the prometastatic role of platelets and the antimetastatic role of NK cells were shown to be chronologically distinct, and that platelets promote lung metastasis by a process that is independent of NK cells. Intriguingly, unlike B16F1 melanoma lung metastasis, B16F1 liver metastasis appeared not to be reliant upon platelets. Furthermore, the pro-metastatic roles of both platelet-derived and endothelial-derived P-selectin in lung metastasis, and endothelial-derived P-selectin in liver metastasis, was demonstrated. P-selectin may, therefore, represent a key target for therapies aimed at preventing tumour metastasis in multiple organs.

3.2 Introduction

Metastasis poses the greatest threat to life following a diagnosis of cancer and the greatest challenge for successful treatment. Tumour cells may spread from the primary tumour into the lymphatics or the bloodstream or both, however, for dissemination to organs such as the liver, lung and brain, tumour cells must ultimately enter the bloodstream (Wong and Hynes 2006). The process of haematogenous tumour cell metastasis includes the migration of tumour cells from the primary tumour, intravasation, survival within the bloodstream, adhesion to and migration across the blood vessel wall, and survival and growth within a distant organ into a secondary tumour. The likelihood of a tumour cell successfully completing the metastatic process is low, being <10% (Liotta 1992). At what stage or stages of the metastatic process tumour cells fail, however, is a matter of debate.

Platelets have long been implicated in haematogenous metastasis with the first experiments definitively demonstrating an association being published in 1968 (Gasic *et al.* 1968). Since then a multitude of studies have demonstrated that platelets, and adhesion proteins expressed by platelets, promote tumour cell metastasis (*for a recent review see* Erpenbeck and Schon 2010) through mechanisms analogous to the role platelets play in assisting leukocytes across the blood vessel wall in inflammation (Pitchford *et al.* 2003; Pitchford *et al.* 2005; Wagner and Frenette 2008). The proposed mechanisms by which platelets promote metastasis include: (i) the formation of a thrombus around the tumour cells within the bloodstream - this has several potential advantages including prolonging the survival of tumour cells within the bloodstream from shear stresses and immune cell attack, increasing the effective size of the tumour cell thus enhancing the likelihood of arrest in downstream capillary beds due to a size restriction, and inducing ischaemic changes in endothelial cells following arrest; (ii) the promotion of adhesion to the blood vessel wall via platelet-specific proteins including P-

selectin and GpIIb-IIIa; (iii) the release from platelets of permeability factors and degradative enzymes to assist tumour cell migration across the blood vessel wall; and (iv) the release from platelets of angiogenic and other growth factors to assist in the establishment of a secondary tumour (Karpatkin 2002; Erpenbeck and Schon 2010). Other research has suggested, however, that the only role platelets play in promoting metastasis is to shield tumour cells from NK cell attack (Nieswandt *et al.* 1999; Palumbo *et al.* 2005), and to impair NK cell function via the inhibitory effects of platelet-derived TGF-β on the NK cell activating receptor NKG2D (Kopp *et al.* 2009).

The role of NK cells in detecting and destroying cancerous cells has been extensively studied. *In vitro* studies have shown that NK cells are capable of killing human- and animal-derived tumour cells without prior sensitisation (Herberman *et al.* 1975; Kiessling *et al.* 1978). Additionally, in experimental metastasis models conducted in mice genetically deficient of NK cells or experimentally depleted of NK cells, a substantial increase in tumour metastases was observed (Gorelik *et al.* 1984; Nieswandt *et al.* 1999; Kim *et al.* 2000; Palumbo *et al.* 2005), whilst enhancing NK cell function decreased metastases (Hanna and Fidler 1980; Riccardi *et al.* 1980). The cytolytic function of NK cells against stressed or cancerous cells, mediated principally by perforin/granzyme mediated apoptosis, is regulated by the balance of signals transmitted by killer inhibitory- and killer activating- receptors. NK cells also release immunoregulatory cytokines which stimulate the anti-tumour actions of the adaptive immune system (Smyth *et al.* 2002; Vivier *et al.* 2008).

Platelets express numerous proteins that are involved in thrombus formation and leukocyte migration and many of these have also been implicated in tumour cell metastasis. In particular, the adhesion molecule P-selectin, that is expressed by activated platelets and endothelium and has a pivotal role in leukocyte migration, has

been strongly implicated in the metastatic process. An assumption has been made, however, that platelet-derived P-selectin is responsible for the promotion of tumour cell metastasis, with the potential contribution of endothelial-derived P-selectin being largely ignored. Furthermore, in the face of the wealth of experimental evidence indicating that platelets promote the adhesion to and migration across the blood vessel wall of metastasising tumour cells, it is hard to conceive that the role of platelets in tumour cell metastasis is limited to the inhibition of NK cell effector function. The aims of the work described in this chapter, therefore, were to confirm the key role played by platelets in tumour cell metastasis, investigate the relationship between the pro-metastatic activity of platelets and the anti-metastastic action of NK cells and determine the importance of both endothelial-derived and platelet-derived P-selectin in tumour cell metastasis.

3.3 Results

3.3.1 Establishing the optimum experimental metastasis assay and platelet depletion procedure

The experimental metastasis assay took some time to establish, with the predominant problem being an unacceptable variation in the number of metastases between mice within the same experimental group. This is a significant problem experienced by many groups (personal communication, Professor Israel Vlodavsky), however, it was possible to overcome when the following measures were taken: (i) the vial containing the tumour cell preparation was gently but thoroughly mixed with a pipette immediately prior to being drawn into a syringe and (ii) the volume of tumour cell suspension drawn up into a syringe each time was sufficient for one mouse only, not for several mice as is recommended (Elkin and Vlodavsky 2001), this step alone dramatically decreasing the degree of variation in metastatic foci observed in recipient mice.

The optimum tumour cell number for the experimental metastasis assay was determined by injecting C57BL/6 mice with varying numbers of B16F1 melanoma cells i.v. via the tail vein (Figure 3.1). Two weeks later the mice were culled, the lungs removed and the number of lung metastases in each individual lobe ascertained under a dissecting microscope. In choosing the cell number to inject, consideration was given to the welfare of the mice, the tumour cell number that would reliably give sufficient tumours to obtain meaningful results, and to adhere as closely as possible to the 'true-to-life' conditions of metastasis by using as low a cell number as possible. A tumour cell number of 1×10^5 tumour cells/mouse was initially chosen, however, in some experiments this cell number proved too low to produce sufficient numbers of metastases and hence the cell number was increased in subsequent experiments to 2×10^5 tumour cells/mouse. In experiments where NK cells were depleted, the tumour burden in mice was greatly enhanced and, therefore, the tumour cell number was reduced in these experiments to 1×10^5 tumour cells/mouse.

Following the establishment of the experimental metastasis assay in mice, the 1B5 hamster monoclonal antibody specific for the mouse platelet glycoprotein, GpIIb-IIIa, was obtained as a means of determining the role of platelets in tumour cell metastasis (Lengweiler *et al.* 1999). Intravenous administration of 20 μg of the 1B5 mAb per mouse resulted in the depletion of >95% of the platelet population (Figure 3.2A and B). The platelet depleting effect occurred within 5 min of mAb administration, lasted for approximately 40 hr and was followed by a thrombocytosis which at 120 hr resulted in an approximate 2-fold increase in platelet numbers above baseline levels (Figure 3.2C and D). The 1B5 antibody proved useful in tumour metastasis experiments as a means of depleting platelets rapidly and reliably at different stages of the metastatic process and, thereby, determining the role of platelets at different stages of the tumour metastatic process.

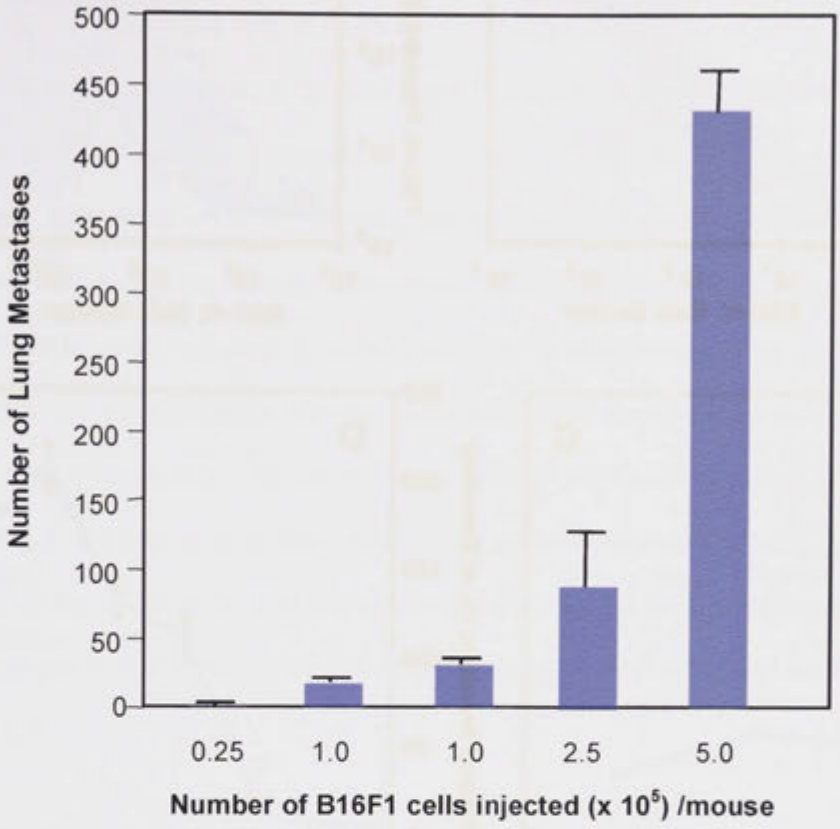

Figure 3.1 – Determining the optimum tumour cell number for use in experimental lung metastasis assays. C57BL/6 mice (n=5) were injected i.v. with various numbers of B16F1 melanoma cells then culled 14 days later and the lungs extracted and fixed in formalin. The number of tumours within each lung lobe was counted under a dissecting microscope. The results of 2 experiments using 1 x 10^5 cells/mouse are shown to demonstrate the reproducibility of the assay. The mean and SEM are presented. In subsequent experiments, tumour cell numbers of 1-2.0 x 10^5 cells/mouse were used.

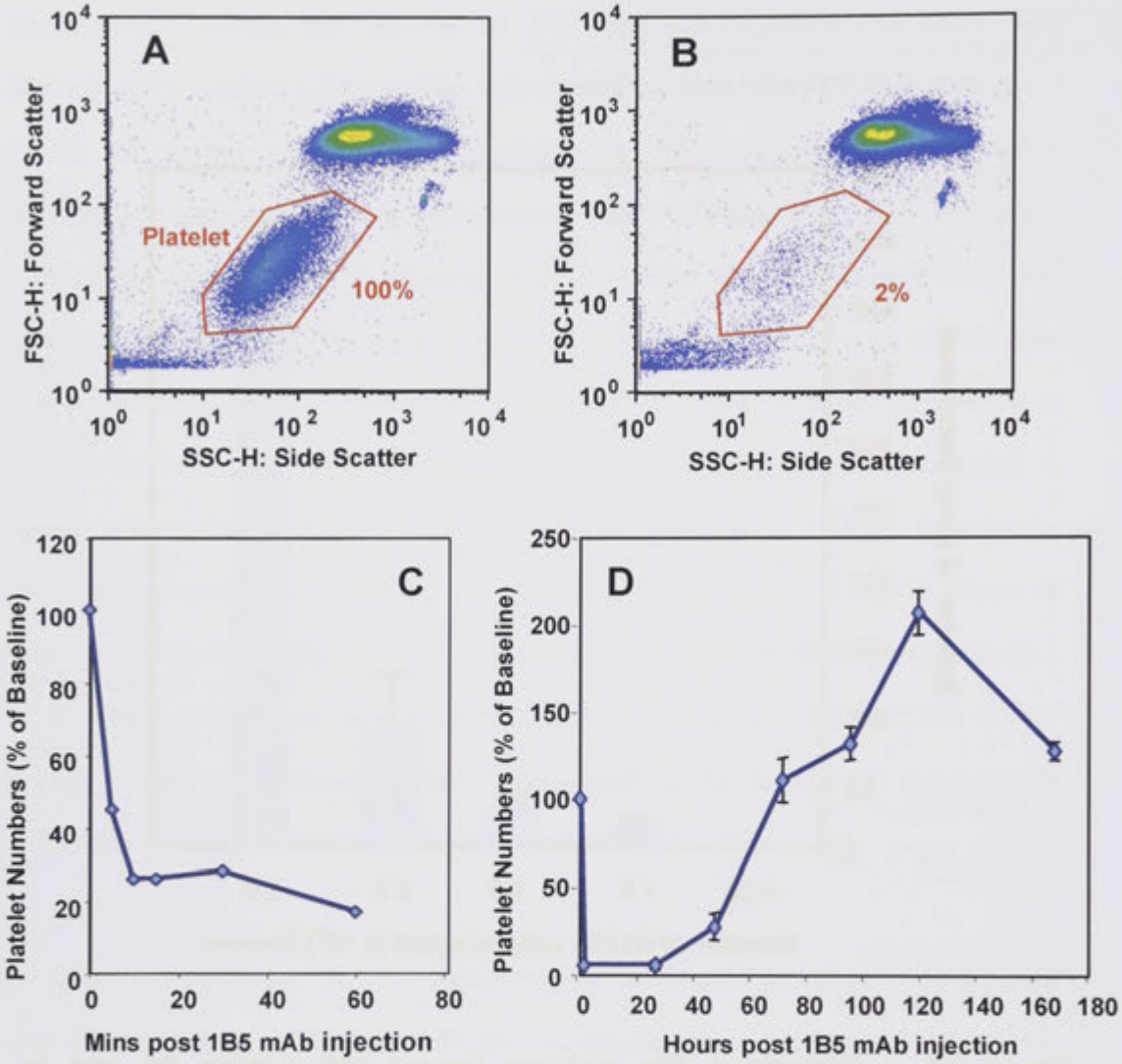

Figure 3.2 – Rapid and transient depletion of platelets *in vivo* using a hamster mAb (1B5) specific for mouse platelet glycoprotein GpIIb/IIIa. Whole blood was collected from C57BL/6 mice and analysed via flow cytometry **(A)** at baseline and **(B)** 2 hr following i.v. injection of 20 μg of the 1B5 mAb. Platelet populations were identified based on their characteristic log forward- and side-scatter parameters (red gated area) and platelet numbers were determined by the inclusion of a known concentration of reference beads in each sample. **(C-D)** C57BL/6 mice were injected with the 1B5 mAb and platelet numbers monitored over a period of (C) 60 mins (n=1) and (D) 7 days (n=3).

3.3.2 Platelets are required for the lung metastasis of B16F1 melanoma and 4T1.2 breast cancer cells

In order to determine the role of platelets in the lung metastasis of B16F1 melanoma and 4T1.2 breast cancer cells, C57BL/6 and BALB/c mice were injected with 20 μg of the 1B5 mAb or an isotype control 1-3 hr prior to the injection of 1 x 10^5 B16F1 melanoma cells or 2 x 10^5 4T1.2 cells, respectively. Fourteen days later the lungs were removed and tumour burden determined. When C57BL/6 mice were injected with the 1B5 mAb, which resulted in >95% reduction in platelet numbers, prior to B16F1 melanoma cell administration, tumour metastases were undetectable compared to the control mice (Figure 3.3). Similarly, when BALB/c mice were injected with the 1B5 mAb, which resulted in a similar reduction in platelet numbers (>95%), prior to the injection of the 4T1.2 cells, a highly significant reduction in lung metastases was seen in comparison to the control mice (i.e., metastases 6% level of control mice, $p < 0.05$) (Figure 3.3).

To confirm that the antimetastatic effects observed were due to a lack of platelets rather than a non-specific effect of the depleting antibody, the metastasis experiments were repeated in two mouse strains genetically deficient in platelets. In the case of the B16F1 melanoma, tumour cells were injected into C57BL/6 *c-mpl-/-* mice (contain ≤15% normal platelet numbers) whereas the 4T1.2 tumour cells were injected into BALB/c Plt20 mutant mice (contain ~30% normal platelet numbers). In the *c-mpl-/-* mice a significant reduction in lung metastases was observed in comparison to their heterozygous (*c-mpl+/-*) littermates (i.e., metastases 17% level of control mice, $p<0.05$) (Figure 3.3). In contrast, with the Plt20 mutant mice, no significant change in tumour metastasis numbers was observed compared with the wild type BALB/c mice (Figure 3.3). Collectively these data suggest that a substantial depletion in circulating platelets (≥85%) is required for tumour lung metastasis to be inhibited.

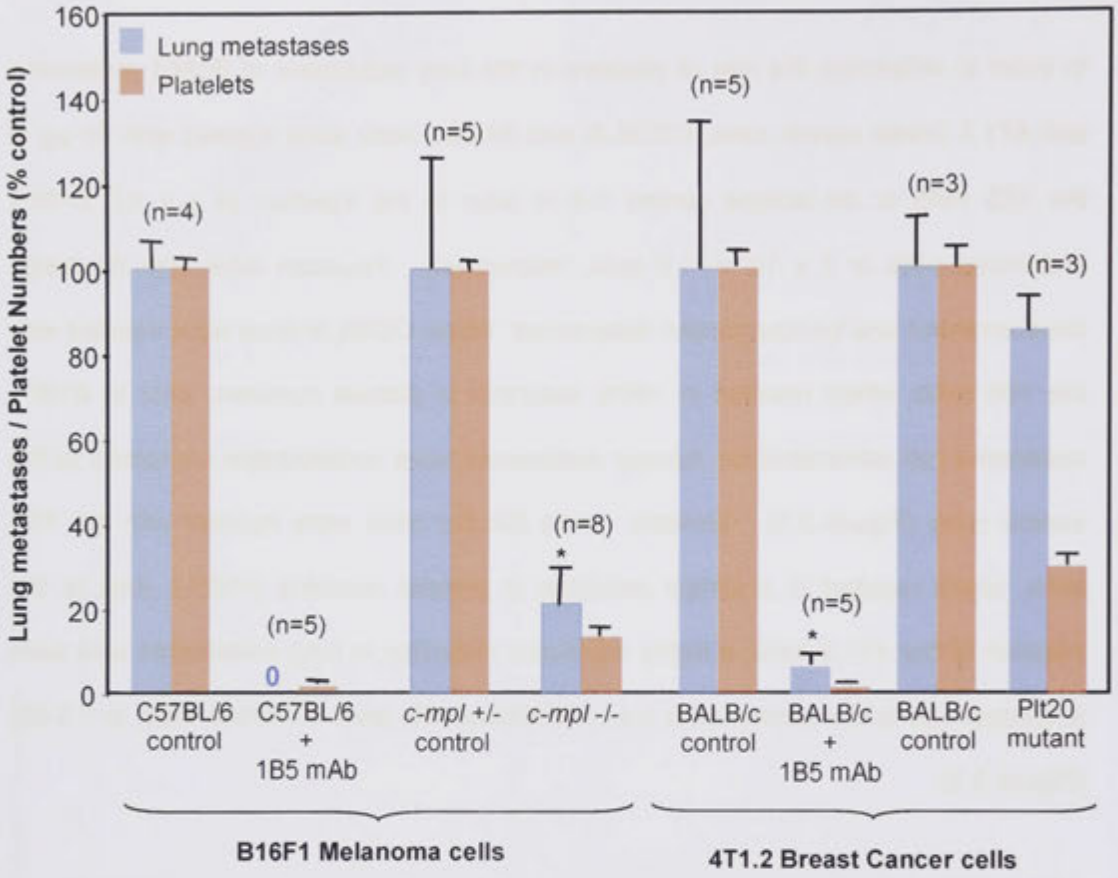

Figure 3.3: Substantial platelet depletion is required to reduce the lung metastasis of B16F1 melanoma and 4T1.2 breast cancer cells in mice. Two approaches were used to determine the role of platelets in the haematogenous metastasis of B16F1 melanoma and 4T1.2 breast cancer cell lines (i) C57BL/6 and BALB/c mice were depleted of platelets (>95%) using the GpIIb/IIIa mAb (1B5) 3 hr prior to i.v.injection, via the tail vein, of 1 x 10^5 B16F1 melanoma or 2 x 10^5 4T1.2 cells, respectively. (ii) C57BL/6 *c-mpl-/-* mice (~15% of normal platelet numbers) and their *c-mpl+/-* littermates (normal platelet numbers), and BALB/c Plt20 mutant mice (~30% normal platelet numbers) were injected i.v. with 1 x 10^5 B16 cells or 2 x 10^5 4T1.2 cells, respectively. Lungs were removed 14 days following tumour cell injection and the number of metastases counted. Significant reductions in metastasis numbers relative to controls are shown as *$p \leq 0.05$.

3.3.3 Platelets are only required at a very early stage of B16F1 melanoma lung metastasis

The kinetics of platelet involvement in B16F1 melanoma lung metastasis was determined by depleting platelets from mice using the 1B5 mAb to GpIIb-IIIa at varying time points before and after injection of B16F1 melanoma cells (Figure 3.4). These experiments showed that the depletion of platelets 3 hr prior to the injection of B16F1 tumour cells resulted in an almost total absence of lung metastases in all mice, whereas platelet depletion 1 hr, 3 hr and 24 hr following the injection of B16F1 melanoma cells did not reduce the number of lung metastases in comparison to experimental controls (Figure 3.4).

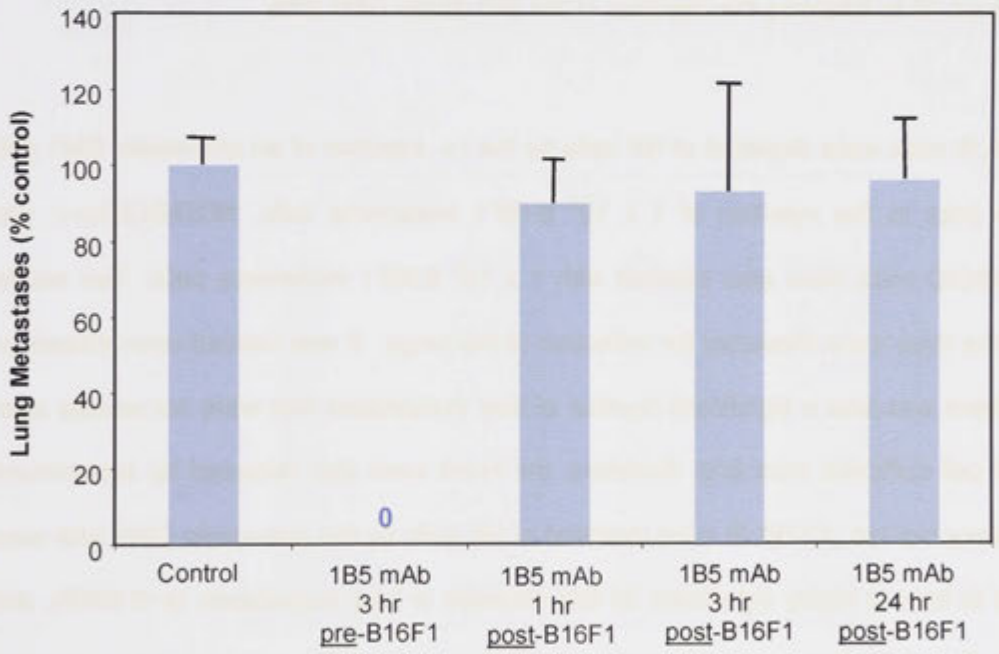

Figure 3.4: Platelets are only required at a very early stage of B16F1 melanoma metastasis. C57BL/6 mice (n=4-5) were depleted of platelets using the 1B5 mAb to GpIIb/IIIa at 3 hr prior to- and 1 hr, 3 hr and 24 hr post-injection of 1 – 2 x 10^5 B16F1 melanoma cells via the tail vein. The results were obtained from several experiments, each experiment including a control group. Lung metastases were determined as described in Figure 3.2.

3.3.4 NK cells strongly inhibit metastasis and mask the influence of platelets on liver and lung metastasis

Experiments were undertaken to determine whether B16F1 melanoma metastasis is susceptible to NK cell control using two different experimental models. NOD/SCIDγc-/- mice, which are genetically deficient in NK cells (and are also lymphocyte deficient), NOD/SCID controls (NK cell sufficient but lacking T and B cells) and antibody depletion of NK cells in C57BL/6 mice using a rabbit anti-asialo GM1 polyclonal antibody. Preliminary experiments showed that splenic NK cells were depleted by ~80% 1 hr following injection of the anti-asialo GM1 pAb whereas NKT, T and B cell splenic numbers were not affected (Figure 3.5). A similar level of NK cell depletion (77%) was observed 48 hr following the injection of the anti-asialo GM1 pAb.

C57BL/6 mice were depleted of NK cells by the i.v. injection of an anti-asialo GM1 pAb 48 hr prior to the injection of 1 x 10^5 B16F1 melanoma cells. NOD/SCIDγc-/- and NOD/SCID mice were also injected with 1 x 10^5 B16F1 melanoma cells. Two weeks later the mice were dissected for collection of the lungs. It was noticed upon dissection that there was also a significant number of liver metastases that were not usually seen in NK cell sufficient mice and, therefore, the livers were also removed for assessment of tumour burden. C57BL/6 mice depleted of NK cells by the anti-asialo GM1 pAb were found to have a highly significant 33-fold increase in lung metastases ($p<0.0005$), and a significant 54-fold increase in liver metastases ($p<0.05$) compared to untreated control mice (Figure 3.6A). Similarly, NOD/SCIDγc-/- mice were found to have a much higher tumour burden in the liver (58-fold higher than controls, $p<0.005$) and the lungs (3-fold higher than controls, $p<0.05$) than the NOD/SCID controls (Figure 3.6A). It should be noted that based on a macroscopic examination, except for sporadic renal metastases, there was no evidence of tumour metastases in other organs of NK cell depleted C57BL/6 and NK cell deficient NOD/SCIDγc-/- mice.

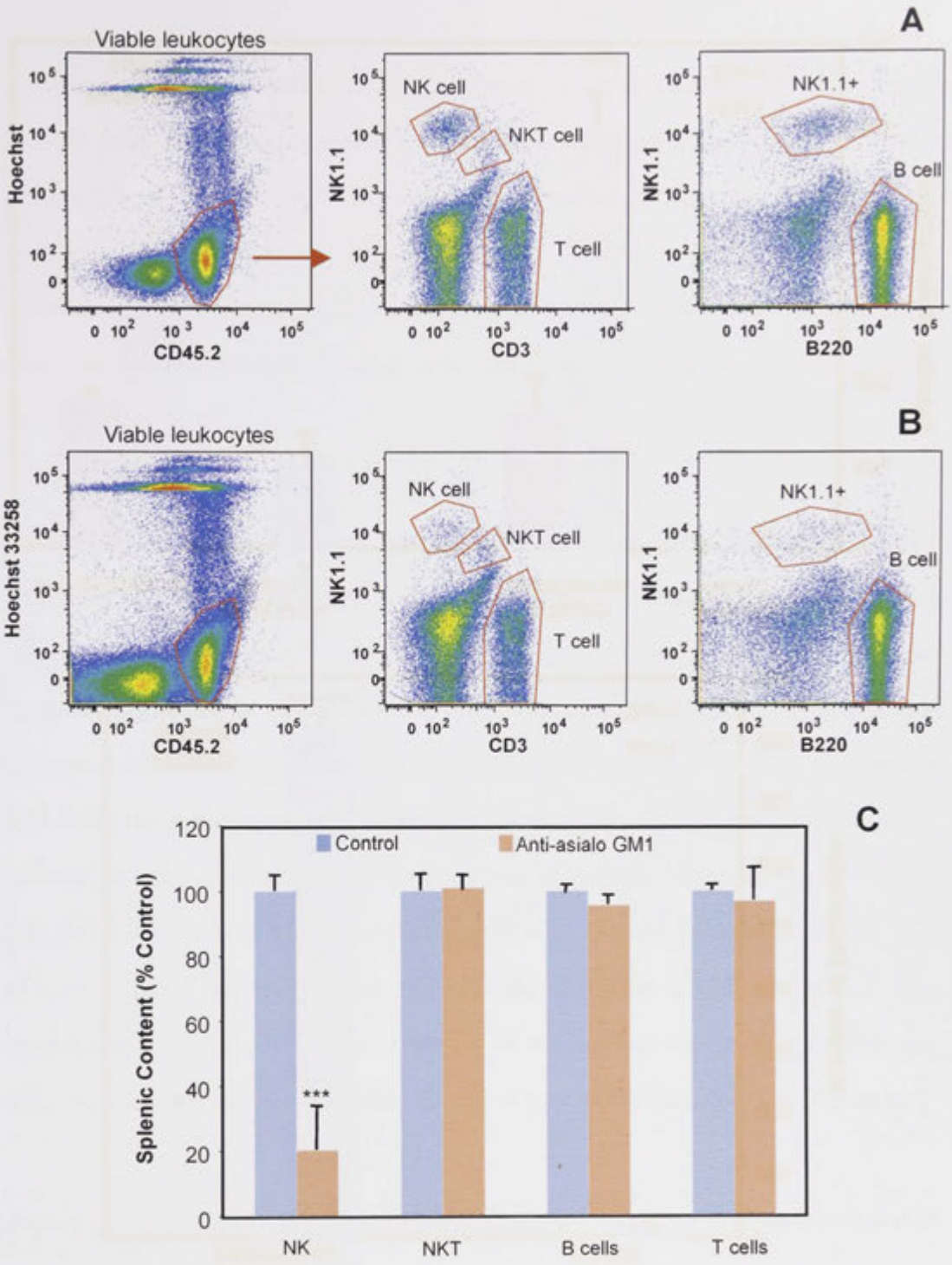

Figure 3.5: Injection of an anti-asialo GM1 pAb selectively depletes the majority of splenic NK cells within 1 hr. C57BL/6 mice (n=3) were injected with 50 μL of an anti-asialo GM1 pAb i.v. then 1 hr later spleens were removed, cells extracted, stained with mAbs specific for CD45.2, NK1.1, CD3 and B220, and then analysed using flow cytometry. **(A)** Gating strategy used to detect the different viable leukocyte populations in spleens from untreated mice and **(B)** in spleens from mice treated with the anti-asialo GM1 pAb. **(C)** A comparison of splenic leukocyte populations 1 hr following treatment with the anti-asialo GM1 pAb. Significant reduction in NK cells relative to controls is shown as ***$p \leq 0.0005$.

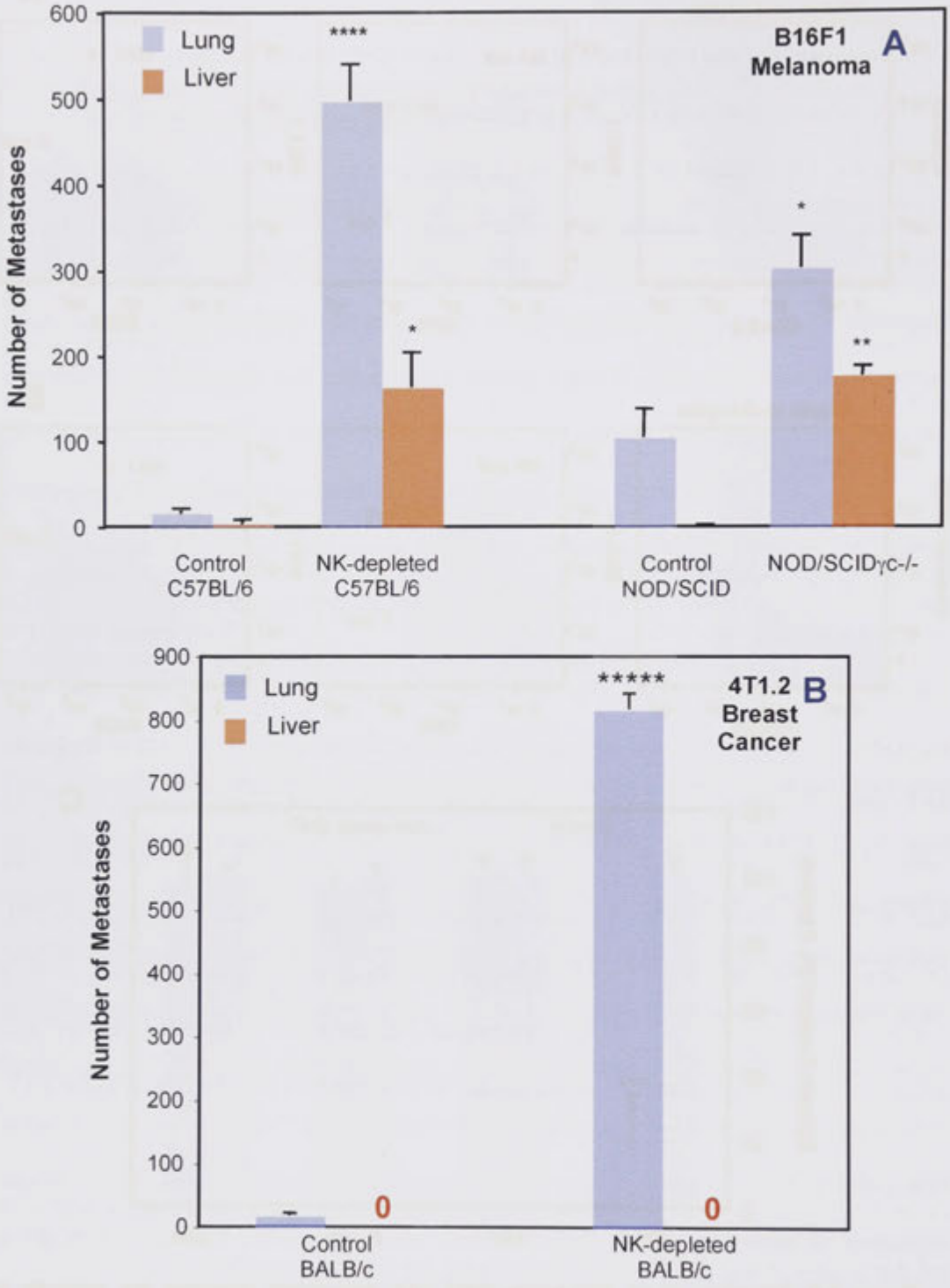

Figure 3.6: The metastasis of B16F1 melanoma and 4T1.2 breast cancer cells is inhibited by NK cells. (A) Tumour metastases in C57BL/6 mice depleted of NK cells by i.v injection of an anti-asialo GM1 pAb 48 hr prior to tumour cell injection and in NOD/SCIDγc-/- mice (n=5) genetically deficient in NK cells. Mice were injected with 1 x 10^5 B16F1 melanoma cells i.v. via the tail vein. **(B)** Tumour metastases in BALB/c mice (n=5), depleted of NK cells by i.v injection of an anti-asialo GM1 pAb 48 hr prior to the injection of 2 x 10^5 4T1.2 breast cancer cells i.v. via the tail vein. Fourteen days after tumour cell injection the lungs and livers were collected from all mice and tumours counted. Significant changes in numbers of metastases relative to controls are shown as *p≤0.05, **p≤0.005, ***p≤0.0005 and *****p≤0.000005.

To assess whether the metastasis of 4T1.2 tumour cells is also susceptible to NK cells, BALB/c mice were injected i.v. with the anti-asialo GM1 pAb to deplete NK cells 48 hr prior to the i.v. injection of 2 x 10^5 4T1.2 cells. Two weeks later the lungs and livers were collected and assessed for tumour burden. The NK-cell depleted mice had a dramatically higher tumour burden in their lungs than the control mice (47-fold higher than controls, $p<0.000005$), however, liver metastases were not found in either group of mice (Figure 3.6B).

The respective roles of platelets and NK cells in the metastatic process was then assessed by depleting C57BL/6 mice of NK cells 48 hr prior to B16F1 melanoma injection and/or platelets 24 hr prior to tumour cell injection. Two weeks later the number of metastases in the liver and lungs was determined. When compared with untreated control mice, mice depleted of platelets had no detectable lung metastases and liver metastases appeared but were sporadic and few in number (Figure 3.7). In contrast, in mice depleted of NK cells there was a dramatic increase in both lung (46 fold, $p<0.005$) and liver (66±11 tumours versus 0 in controls) metastases (Figure 3.7). In mice depleted of both NK cells and platelets, there was a 48% decrease in lung metastases compared with mice depleted of NK cells alone ($p<0.05$), which was accompanied by a concomitant 42% increase in liver metastases ($p<0.05$) (Figure 3.7).

Overall these studies imply that NK cells dramatically mask the metastatic potential of tumour cells and that platelets may assist lung but not liver metastasis.

3.3.5 The anti-metastatic effect of NK-cells occurs later and independent of platelets

In order to resolve the relationship between the pro-metastatic action of platelets and the anti-metastatic role of NK cells we investigated the kinetics of the anti-metastatic

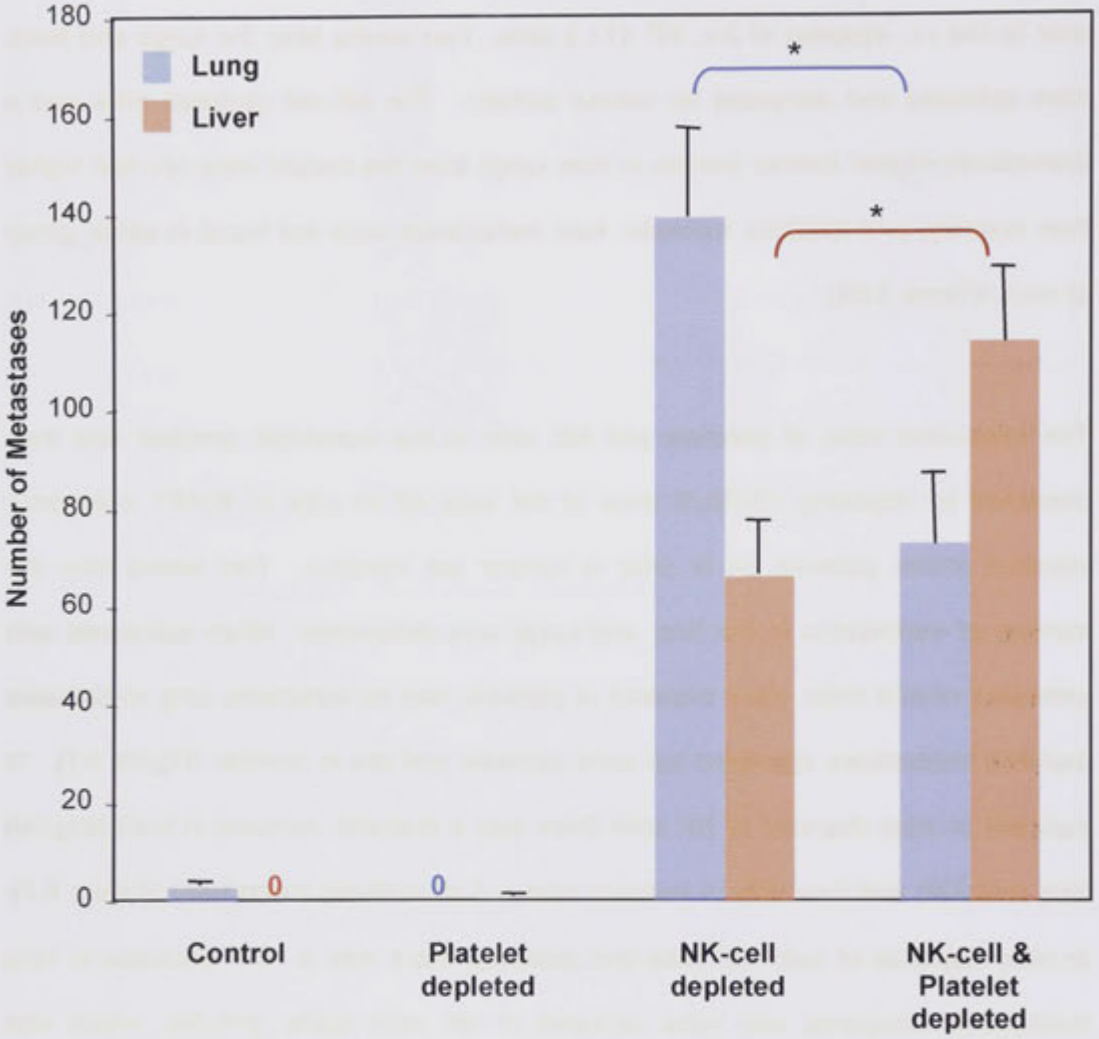

Figure 3.7: Interplay between platelet and NK cell depletion on B16F1 melanoma lung and liver metastasis. C57BL/6 mice (n=5) were depleted of NK cells (anti-asialo GM1 pAb) 48 hr prior to and/or platelets (GpIIb-IIIa specific mAb 1B5) 1 day prior to i.v. injection of 1 x 10^5 B16F1 melanoma cells. Fourteen days later the mice were culled and lungs and livers collected for determination of metastasis numbers. Significant changes in metastasis numbers are shown as *$p \leq 0.05$. This experiment was also performed using 2 x 10^5 B16F1 cells and identical metastasis trends were observed.

effect of NK cells. Thus, C57BL/6 mice were depleted of NK cells 48 hr prior to, and 1 hr or 24 hr following the i.v. injection of 2 x 10^5 B16F1 melanoma cells. Two weeks later the liver and lungs were collected and metastases counted. When the NK cell-depleting antibody was administered 48 hr before or 1 hr after tumour cell injection there was a comparable dramatic enhancement in lung and liver metastasis. In contrast, this enhancement in tumour metastasis did not occur if the NK cell depleting pAb was given 24 hr after the tumour cells (Figure 3.8A). These data imply that NK cells exert their action after tumour cells lodge in the vasculature of target organs. Since NK cell depletion is rapid (<1 hr, Figure 3.5), it appears that NK cells exert their anti-metastatic effect between 1 hr and 24 hr following tumour cell injection.

To determine whether the kinetic profile of NK cell inhibition of tumour metastasis changes in the absence of platelets, the above experiment was repeated in mice that were additionally depleted of platelets 24 hr prior to i.v. injection of 1 x 10^5 B16F1 melanoma cells (Figure 3.8B). The outcome of this experiment was very similar to when platelets were present (Figure 3.8A), supporting the view that NK cells exert their anti-metastatic effect independent of platelets.

3.3.6 Endothelial P-selectin plays a critical role in lung and liver metastasis

Having demonstrated that the mechanism by which platelets promote metastasis was not through the inhibition of NK cell function, experiments were performed to determine the contribution of the adhesion protein P-selectin (P-sel), but more specifically the relative contributions of platelet-derived and endothelial-derived P-sel, to the metastatic process.

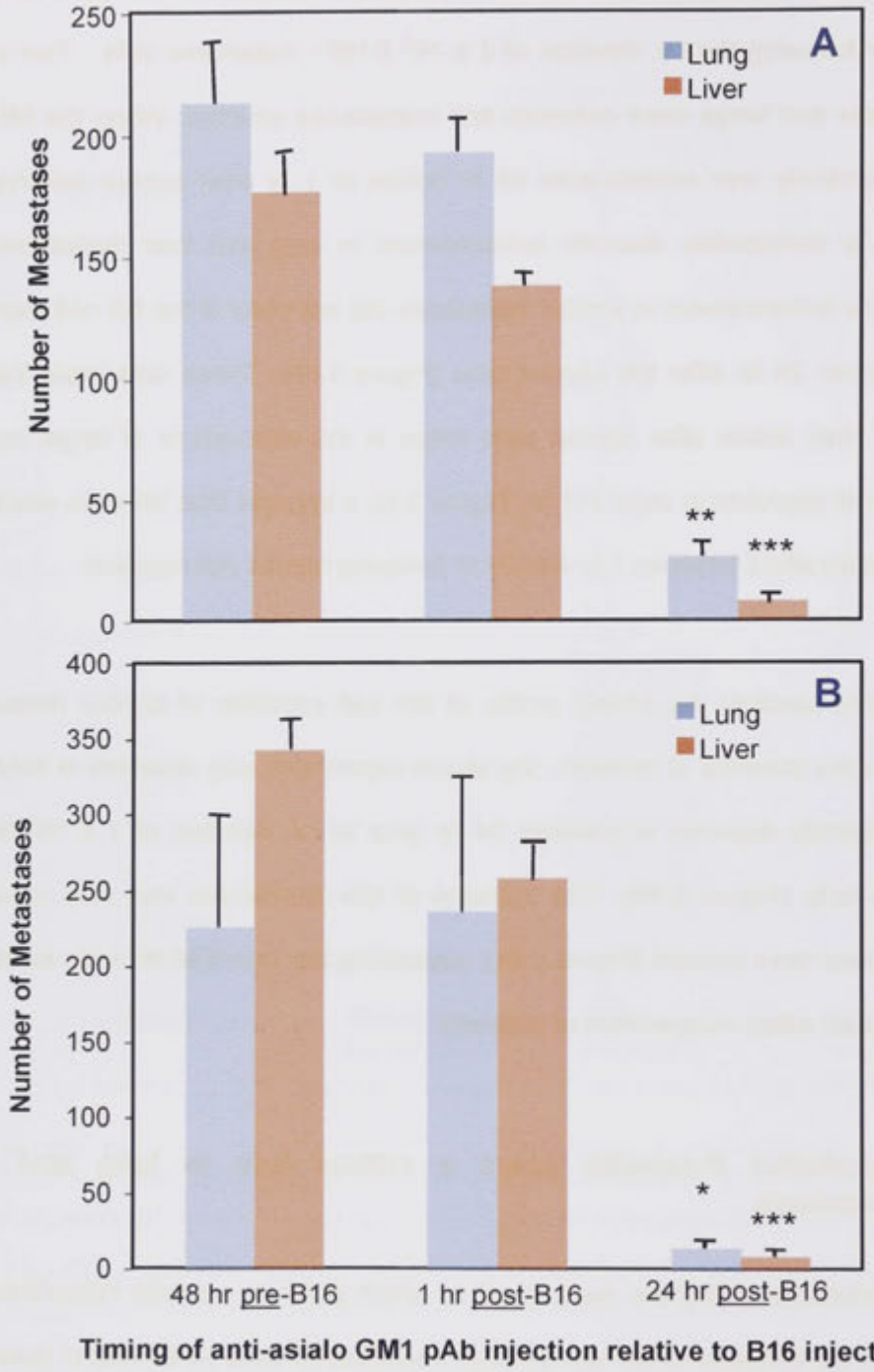

Figure 3.8: NK cell control of B16F1 lung and liver metastasis occurs between 1 and 24 hr after tumour cell injection in a platelet independent manner. (A) Lung and liver metastasis in C57BL/6 mice (n=5), depleted of NK cells by i.v injection of an anti-asialo GM1 pAb 48 hr pre- and 1 hr and 24 hr post-injection of 2 x 10^5 B16F1 melanoma cells i.v. via the tail vein. **(B)** As above, however, all mice were depleted of platelets by the injection of an anti-GpIIb-IIIa mAb (1B5) 24 hr prior to the injection of 1 x 10^5 B16 melanoma cells. Significant reductions in metastasis numbers relative to NK depletion 48 hr pre-B16F1 tumour cell injection are shown as *$p \leq 0.05$, **$p \leq 0.005$ and ***$p \leq 0.0005$.

The role of P-sel in the metastasis of B16F1 tumour cells to the lung was determined following the i.v. injection of C57BL/6 wild type mice and C57BL/6 P-sel-/- mice with 1 or 2 x 10^5 B16F1 melanoma cells. Lung metastases in P-sel-/- mice were found to be 63% lower than in control wild type mice (Figure 3.9A), a reduction that was highly significant ($p<0.00005$).

As P-sel is expressed by both platelets and endothelial cells, P-sel bone marrow chimeras were generated in two separate transplant experiments. Congenic C57BL/6 mice expressing the CD45.1 allotype of the leukocyte common antigen were used as bone marrow donors or recipients thus introducing an easily measured marker of donor marrow engraftment as C57BL/6 mice carry the CD45.2 allotype. In the first transplant experiment platelet P-sel positive (P+) endothelium P-sel negative (E–) mice were generated by transplanting P-sel-/- mice (CD45.2) with wild type C57BL/6 (CD45.1) marrow; P–E+ mice were generated by transplanting C57BL/6 (CD45.1) mice with P-sel-/- marrow (CD45.2); and the control group (P+E+) consisted of wild type C57BL/6 (CD45.2) mice transplanted with C57BL/6 (CD45.1) marrow (Table 3.1). A second transplant experiment was performed to demonstrate reproducibility of the initial results and to ensure that residual host P-sel+ platelets were as low in number as possible. Thus, the platelet-deficient *c-mpl-/-* strain (CD45.2) was transplanted with P-sel-/- marrow (CD45.2), thereby generating P–E+ mice. A control group for these mice was generated using *c-mpl-/-* mice (CD45.2) as recipients of C57BL/6 (CD45.1) bone marrow. In this experiment, P+E– mice were generated by using P-sel-/- mice (CD45.2) as recipients of wild type C57BL/6 (CD45.1) bone marrow and the control group (P+E+) for these mice, as in the first experiment, consisted of wild type C57BL/6 mice (CD45.2) transplanted with C57BL/6 (CD45.1) marrow (Table 3.2).

Table 3.1 – Extent of Donor Marrow Engraftment and Platelet Numbers in P-selectin Bone Marrow Chimeras (Transplant Experiment 1)

Group [a]	BM Recipient	BM Donor	% Leukocyte CD45.1 Allotype [b]	Platelet Numbers/μL [b] ($x10^6$)
P+E+	C57BL/6 (CD45.2)	C57BL/6 (CD45.1)	82 ± 0.2	1.09 ± 0.01
P–E+	C57BL/6 (CD45.1)	P-Sel -/- C57BL/6 (CD45.2)	20.6 ± 0.4	1.18 ± 0.03
P+E–	P-Sel -/- C57BL/6 (CD45.2)	C57BL/6 (CD45.1)	80.1 ± 0.7	1.06 ± 0.01

Table 3.2 – Extent of Donor Marrow Engraftment and Platelet Numbers in P-Selectin Bone Marrow Chimeras (Transplant Experiment 2)

Group [a]	BM Recipient	BM Donor	% Leukocyte CD45.1 Allotype [b]	Platelet Numbers/μL [b] ($x10^6$)
P+E+	C57BL/6 (CD45.2)	C57BL/6 (CD45.1)	83.3 ± 0.4	1.37 ± 0.03
P+E–	P-Sel -/- C57BL/6 (CD45.2)	C57BL/6 (CD45.1)	78.6 ± 0.5	1.28 ± 0.03
P+E+	*c-mpl* -/- C57BL/6 (CD45.2)	C57BL/6 (CD45.1)	73.9 ± 0.7	1.22 ± 0.02
P–E+	*c-mpl* -/- C57BL/6 (CD45.2)	P-Sel -/- C57BL/6 (CD45.2)	<1.0 ± 0.1	1.49 ± 0.04

a '**P**' = Platelets; '**E**' = Endothelium; '**+**' = P-Sel positive; '**–**' = P-Sel negative

b Extent of donor marrow engraftment was measured by determining the proportion of CD45.1+ vs CD45.2+ leukocytes in whole blood, with the leukocyte phenotype and platelet numbers/μL being measured in whole blood via flow cytometry 4 wk following irradiation and bone marrow transplantation.

Platelet numbers and the extent of engraftment of donor bone marrow were determined in the P-sel chimeras 4 weeks following transplantation by measuring the C45.1+ versus CD45.2+ status of blood leukocytes by flow cytometry. Platelet numbers were also determined using flow cytometry and the results are presented in Tables 3.1 and 3.2. It was found that bone marrow engraftment, based on CD45 allotypes, was ~80%.

The various bone marrow chimeras were injected i.v. with 2 x 10^5 B16F1 melanoma cells and the lungs removed 2 weeks later for metastasis enumeration. The data from the two separate bone marrow chimera metastasis experiments are presented in Figure 3.9B. The selective absence of P-selectin on platelets substantially (77% Expt 1 and 78% Expt 2) and significantly ($p<0.005$ and $p<0.05$, respectively) reduced the number of lung metastases compared to control bone marrow chimeric mice. Similarly, the selective absence of endothelial P-selectin resulted in a comparable (69% Expt 1 and 74% Expt 2) and significant ($p<0.05$ and $p<0.005$, respectively) reduction in the ability of B16F1 tumour cells to metastasise to the lungs (Figure 3.9B).

Collectively these data indicate that <u>both</u> platelet and endothelial P-selectin are required for the lung metastasis of B16F1 melanoma cells.

The P-selectin knockout and bone marrow chimera experiments described above provided data on the role of platelet and endothelial P-selectin in B16F1 melanoma lung metastasis but in these experiments liver metastases were undetectable. In order to ascertain the role of P-selectin in B16F1 melanoma metastasis to the liver, C57BL/6 wild-type and P-selectin-/- mice were depleted of NK cells, thus providing conditions that increased the number of detectable liver metastases, and injected 48 hr later with 2 x 10^5 B16F1 melanoma cells. Two weeks later the lungs and livers were removed

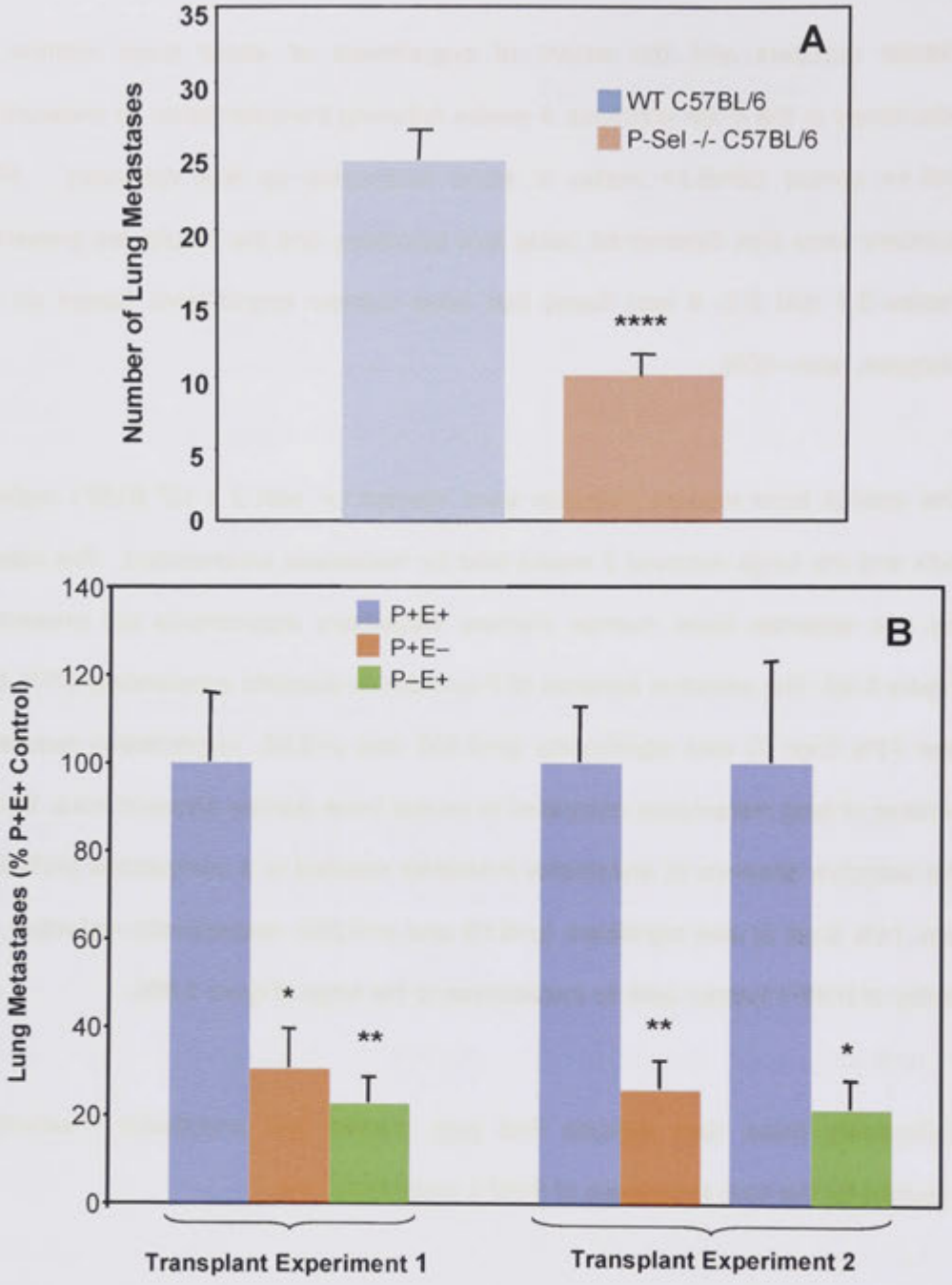

Figure 3.9: P-selectin on both platelets and endothelium is involved in the lung metastasis of B16F1 melanoma cells. (A) WT C57BL/6 (n=24) and P-selectin-/- (n=22) mice were injected i.v. with 1 x 10^5 B16F1 melanoma cells. Fourteen days later the lungs were removed and tumours counted. Data pooled from 2 experiments. **(B)** P-selectin bone marrow chimeras (n=5/group) were generated where the platelets (P–E+) or endothelium (P+E–) were P-selectin deficient. For more details see Tables 3.1 and 3.2. Following donor marrow engraftment, mice were injected i.v. with 2 x 10^5 B16F1 melanoma cells. Fourteen days later the lungs were removed and tumours counted. Panel B represents data from two separate transplantation and metastasis experiments. Significant reductions in metastasis numbers relative to WT (P+E+) controls are shown as *$p \leq 0.05$, **$p \leq 0.005$ and ****$p \leq 0.00005$.

and tumours counted. As seen in previous experiments with NK cell sufficient mice (Figure 3.9A), the number of lung metastases in the NK cell depleted P-sel-/- mice was reduced by 49% compared with NK cell depleted WT controls ($p<0.005$). The number of liver metastases in the NK cell depleted P-sel-/- mice was also found to be substantially (37%) and significantly reduced ($p<0.05$) (Figure 3.10A).

Previous data in this chapter suggests that platelets are probably not required for B16F1 liver metastasis (Fig. 3.7), implying that platelet P-sel does not play a role in liver metastasis. The question remained as to whether endothelial P-sel was required for liver metastasis and, in order to examine this possibility, C57BL/6 wild type and P-sel-/- mice were depleted of NK cells and platelets 48 hr and 2 hr, respectively, prior to the injection of 1×10^5 B16F1 melanoma cells. Fourteen days later the lungs and livers were removed and tumours counted. The platelet-depleted P-sel-/- mice were found to have significantly fewer liver (52%, $p<0.05$) and lung (65%, $p<0.05$) metastases than their platelet-depleted wild type controls (Figure 3.10B), supporting the conclusion that endothelial P-selectin is just as important for B16F1 melanoma liver metastasis as lung metastasis.

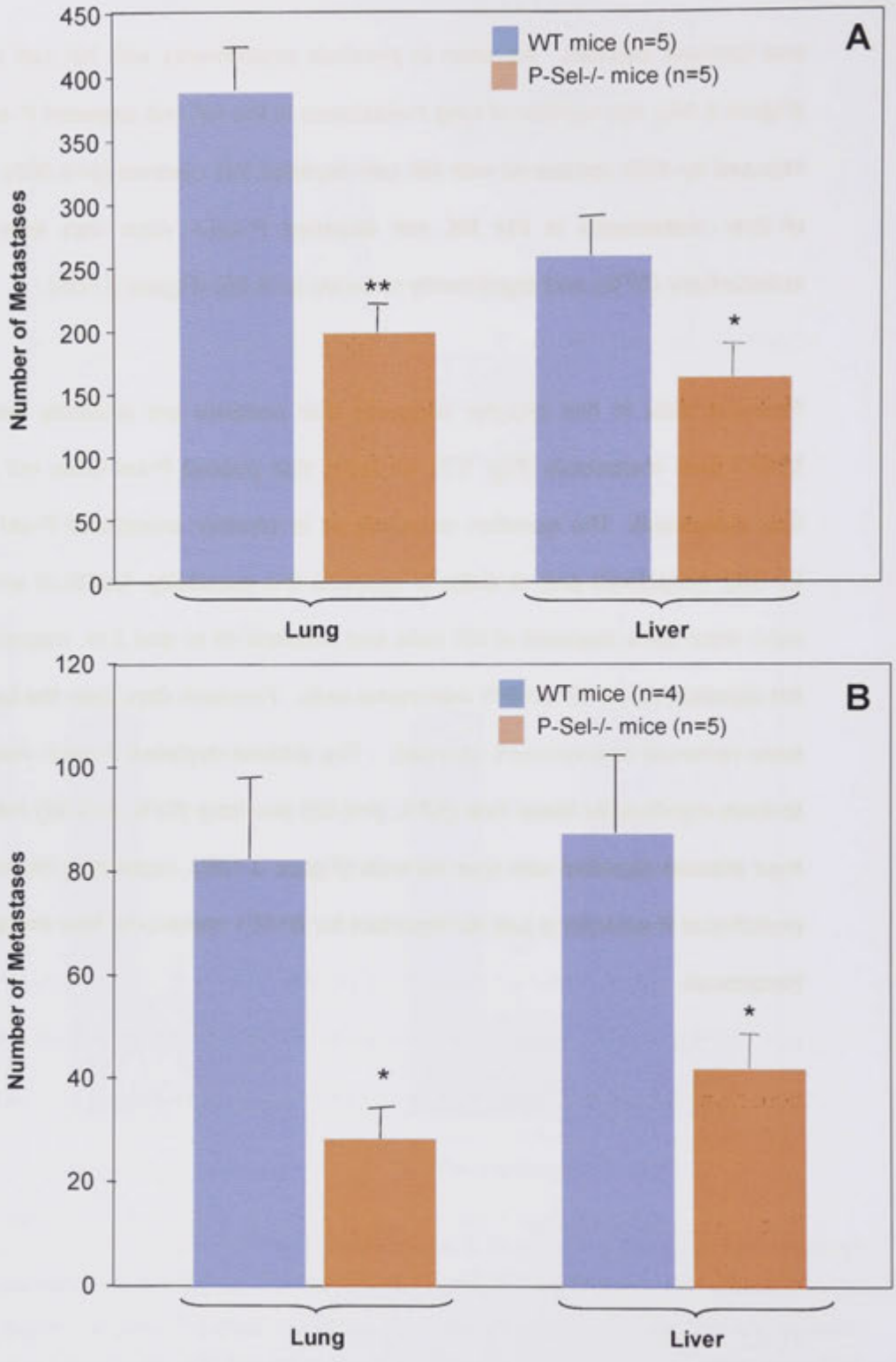

Figure 3.10: Endothelial P-selectin is involved in B16F1 melanoma metastasis to both the liver and lung. **(A)** WT C57BL/6 and P-selectin-/- mice were depleted of NK cells by injection of an anti-asialo GM1 pAb 48 hr prior to injection of 2 x 10^5 B16F1 melanoma cells. Fourteen days later the lungs and livers were removed and tumours counted. **(B)** As in (A), however mice were additionally depleted of platelets by the injection of an anti-GpIIb/IIIa mAb (1B5) 2 hr prior to injection of 1 x 10^5 B16F1 melanoma cells. Significant reductions in metastasis numbers relative to controls are shown as *$p \leq 0.05$ and **$p \leq 0.005$.

3.4 Discussion

The key findings of the work described in this chapter are that (i) platelets promote B16F1 melanoma and 4T1.2 breast cancer lung metastasis, (ii) the pro-metastatic effect of platelets is brief, lasting for only up to 1 hour following tumour cell entry into the circulation, (iii) the anti-metastatic action of NK cells occurs after the pro-metastatic actions of platelets and is not inhibited by platelets, (iv) platelets do not appear to be necessary for B16F1 melanoma liver metastasis, unlike B16F1 melanoma lung metastasis and (v) endothelial P-selectin plays an important role in both B16F1 melanoma lung and liver metastasis.

Studies on the kinetics of the prometastatic effect of platelets demonstrated that the time frame during which platelets are required for metastasis is very short in duration and early in the metastatic process. Essentially, platelets only play a role in the first hour following entry of tumour cells into the bloodstream. Beyond that, their assistance is not required for successful metastasis (Figure 3.4). These results support the broadly accepted model of the role of platelets in metastasis, namely, that platelets mediate the initial interaction of tumour cells with the blood vessel wall via platelet adhesion proteins binding to their endothelial ligands (Erpenbeck and Schon 2010).

The susceptibility of B16F1 melanoma and 4T1.2 breast carcinoma metastasis to NK cell inhibition was dramatically demonstrated using either the NOD/SCIDγc-/- mouse strain, which is genetically deficient in NK cells, or mice depleted of NK cells using an anti-asialo GM1 pAb (Figure 3.6). It was found that in both these models, depletion of NK cells resulted in a very substantial increase in lung metastases (3-33 fold). Interestingly, liver metastases were not usually seen in the B16F1 experimental lung metastasis model, however, in the absence of NK cells the number of liver metastases

was dramatically increased. The appearance of B16F1 tumour metastases in the liver of NK depleted mice, indicates that a significant proportion of B16F1 melanoma cells pass through the lung capillary beds to the left cardiac ventricle from where they are dispersed to multiple organs including the liver. In NK cell sufficient mice, these tumour cells are efficiently eliminated from the liver, however, in NK cell deficient mice the extent of tumour cell infiltration into hepatic tissue is revealed. Metastases were occasionally seen in the kidney in NK cell depleted mice, however, cerebral metastases could not be detected, nor was there any evidence of altered neurological function in any of the mice injected with B16F1 or 4T1.2 tumour cells (data not shown). Unlike B16F1 melanoma, liver metastases were not seen with 4T1.2 tumour cells in NK cell depleted mice. This observation may indicate that the 4T1.2 tumour cells are incapable of extravasating into, or surviving within, the hepatic environment. In support of this conclusion, a previous study of the metastatic tendency of this cell line following mammary gland injection, showed a predilection for the lungs, bone and lymph nodes with no liver metastases being found (Lelekakis *et al.* 1999).

The pro-metastatic effects of platelets and the anti-metastatic effects of NK cells were probed for evidence of an interrelationship by depleting mice of platelets, NK cells or both prior to the injection of B16F1 melanoma cells (Figure 3.7). The key finding of this experiment was that in mice depleted of both platelets and NK cells, there was a 48% reduction in the number of lung metastases compared to mice depleted of NK cells only. This result indicates firstly, that platelets promote B16F1 melanoma metastasis in the absence of NK cells and, secondly, that a substantial number of tumour cells were capable of extravasating in the absence of platelets, a result that was revealed only when NK cells were depleted, and may be due to the involvement of endothelial adhesion molecules or physical entrapment within small vessels. Furthermore, in the absence of platelets and NK cells, a concomitant 42% increase in liver metastases was observed, most likely due to a greater number of tumour cells passing through the

lungs due to a reduced ability to bind to the blood vessel wall. To further demonstrate the independence of the pro-metastastic role of platelets from the anti-metastatic role of NK cells, the kinetics of the NK cell effect on metastasis was studied in the presence and absence of platelets (Figure 3.8). Mice were depleted of NK cells 48 hr prior to- and 1 hr or 24 hr post-B16F1 melanoma cell injection. The experiment was repeated in mice that were additionally depleted of platelets 24 hr prior to B16F1 cell injection. The results of these two experiments were essentially the same in that the anti-metastatic effect of NK cells was seen to occur between 1 and 24 hr following tumour cell injection, whether or not mice were injected with the platelet depleting mAb (Figure 3.8). Collectively, these results unequivocally demonstrate that, in the B16F1 experimental metastasis model, platelets promote lung metastasis by a mechanism that is independent of NK cells. Furthermore, the roles of platelets and NK cells in the metastatic process were demonstrated to be chronologically distinct, with platelets acting to promote metastasis within the first hour of tumour cell entry into the bloodstream and NK cells exerting their anti-metastatic effects between 1 and 24 hr after tumour cell injection. Additionally, these experiments suggest that platelets play little or no role in B16F1 melanoma liver metastasis.

Some of these findings contrast with those of Nieswandt *et al* and Palumbo *et al*, both of whom examined lung metastasis in platelet-, NK cell- or platelet and NK cell-deficient mice (Nieswandt *et al.* 1999; Palumbo *et al.* 2005). Nieswandt *et al* studied the lung metastasis of CFS1/LacZ tumour cells and B16F10 melanoma cells in mice depleted of NK cells 1 week prior to the injection of tumour cells using the TM-β1 mAb to the interleukin 2 receptor β chain expressed constitutively by NK cells and activated T cells (Caligiuri *et al.* 1990), To deplete platelets, mice were injected with a polyclonal rabbit anti-mouse platelet serum 24 hr prior to tumour cell injection. In the absence of NK cells the number of lung metastases of the CFS1/LacZ fibrosarcoma increased

approximately 18-fold and B16F10 melanoma approximately 2-fold. In contrast, in our experiments with B16F1 melanoma, a 47-fold increase in lung metastasis was observed in NK cell depleted mice compared to control mice implying that the B16F10 melanoma cell line is not as susceptible to NK cell killing as the B16F1 melanoma cell line. Similar to our studies, Nieswandt *et al* noted the appearance of significant numbers of liver metastases in NK cell depleted mice injected with B16F10 melanoma cells, although these were not quantified. Consistent with our studies of B16F1 melanoma and 4T1.2 breast cancer lung metastasis, in the absence of platelets, lung metastasis of both CFS1 and B16F10 cells was virtually eliminated. In contrast to our findings, when mice were depleted of both platelets and NK cells, Nieswandt *et al* concluded that the prevalence of lung metastases was not significantly different to that seen in mice depleted of NK cells only. When examining their data for B16F10 melanoma, however, there was a reduction of ~25% in the mean number of lung metastases in the mice depleted of platelets and NK cells compared to mice depleted of NK cells alone, although the standard deviation in the number of metastases seen in the NK cell depleted mice was considerable which prevented this result from reaching statistical significance.

In a related study Palumbo *et al* depleted NK cells using an anti-asialo GM1 serum and, also, used the Gαq mutant mouse strain to study the role of platelets in tumour metastasis. The Gαq protein is involved in the activation of phospholipase C and increases in Ca2+ and protein kinase C activity in most cells. As Gαq is required for platelet activation this mouse strain has normal platelet numbers, however, thrombus formation is severely compromised (Offermanns *et al.* 1997; Palumbo *et al.* 2005). The ability of Lews lung carcinoma (LLC) cells and B16-BL6 melanoma cells to metastasise to the lung was virtually eliminated in Gαq-/- mice compared to controls and, through bone marrow transplantation, this effect on metastasis was demonstrated to be due to

bone-marrow derived cells. The authors attribute the pro-metastatic effect of Gαq to platelets but concede that the contribution of leukocytes to the metastatic process was not determined. Using quantitative analysis of residual nuclear radiolabelled LLC cells, the metastasis promoting effect of Gαq was shown to occur between 5 and 24 hr following intravenous injection of tumour cells. This result is, therefore, substantially different to our finding, i.e., that platelets act to promote metastasis within 1 hr following tumour cell entry into the bloodstream. A significant difference between the experimental models used by ourselves and Palumbo *et al.* was that platelets were absent in our model whereas platelets were present but had a signalling defect preventing their activation in the experiments conducted by Palumbo *et al.* The measurement of residual tissue radioactivity was also used to demonstrate that 24 hr following tumour cell injection Gαq-/- mice depleted of NK cells did not show a decrease in LLC lung metastases when compared to wild-type mice depleted of NK cells. The validity of results obtained using radionuclear labelled tumour cells are, however, questionable as the radioactivity measured does not give an indication of the number of cells going on to form tumours nor the reutilisation of radioactivity by neighbouring cells. Furthermore, Chambers *et al* have conducted several *in vivo* microscopy studies examining the process of lung and liver metastasis using both nuclear- and cytoplasmic-labelling of tumour cells and have found that, in comparison to cytoplasmic labelling, radioactive nuclear labelling rendered tumour cells more vulnerable to destruction *in vivo*. They found a significant decline in the number of nuclear-labelled tumour cells over the first 24 hr following i.v. injection of the tumour cells. When using cytoplasmic labelling, however, greater than 80% of injected tumour cells were demonstrated to successfully extravasate (Chambers *et al.* 2001).

Our studies into the kinetics of B16F1 lung metastasis indicate that the pro-metastatic effect of platelets occurs <1 hr after tumour cell injection (Figure 3.4) whereas the anti-

metastatic effects of NK cells occurs >1 hr after tumour cell entry into the bloodstream (Figure 3.8). *In vivo* microscopy studies of tumour cell extravasation, conducted by Crissman *et al*, have revealed that in less than 1 minute following injection, tumour cells contact endothelial cells of the lung capillary bed, with blood vessel size restrictions influencing the initial lodgement. This lodgement was, however, temporary and those tumour cells unable to initiate an interaction with the endothelium passed through the capillary bed. Also, within 2 min following tumour cell injection, platelets were seen to associate with the tumour cells with the formation of thrombi in which cellular extensions of tumour cells were noted. The thrombus remained until tumour cells established contact with the subendothelial matrix. At 4 hr following tumour cell injection, endothelial cell separation was observed, with cytoplasmic extensions of the tumour cells reaching the subendothelial matrix (Crissman *et al.* 1988). Chambers *et al.* demonstrated in their *in vivo* microscopy studies of the metastatic process of several tumour cell lines, that the greatest inefficiency in metastasis was seen to occur following extravasation (Chambers *et al.* 2001). The studies of B16F1 melanoma lung and liver metastasis presented in this chapter demonstrated that NK cells accounted for an ~98% reduction in the number of metastases, which occurred between 1- and 24 hr following tumour cell injection and was unchanged in the absence of platelets. Our results demonstrate, therefore, that the anti-metastatic effect of NK cells is not due to platelets either shielding tumour cells from NK cell attack or mediating molecular inhibition of NK cell effector function and, taken with the findings of Crissman *et al* and Chambers *et al*, would suggest that NK cells destroy tumour cells following their adhesion to the vasculature. It is possible that the interaction between tumour cells and the blood vessel wall activates the endothelium with the subsequent release of cytokines, such as TNF-α, that recruit NK cells. Such a sequence of biological events may account for the 1-hour delay observed before the onset of NK cell destruction of tumour cells.

Having demonstrated the NK cell independent role of platelets in tumour cell metastasis, the adhesion protein P-selectin, found in platelets and the endothelium, was investigated in the B16F1 melanoma experimental metastasis model using P-sel-/- mice. Consistent with previous research (Kim *et al.* 1998), the absence of P-selectin was found to significantly diminish lung metastasis. To determine the relative contributions to the metastatic process of platelet-derived and endothelial-derived P-selectin, the experimental B16F1 melanoma lung metastasis assay was performed in P-selectin deficient chimeric mice generated through bone marrow transplantation. These experiments revealed that both endothelial-derived and platelet-derived P-selectin contribute to the metastatic process to a similar extent.

To determine the role of P-selectin in B16F1 melanoma extravasation in the liver, wild type and P-selectin-/- mice were depleted of NK cells prior to the injection of B16F1 tumour cells into the tail vein, thereby preventing NK-cell mediated destruction of tumour cells. As seen previously, lung metastasis was significantly reduced in the absence of P-selectin, however, a significant reduction was also seen in liver metastases. As other experiments described in this chapter demonstrated that platelets were not required for B16F1 melanoma metastasis to the liver (Figure 3.7), endothelial-derived P-selectin was considered the predominant contributor to this process. To confirm this, the experiment was repeated but all mice were additionally depleted of platelets thus eliminating platelet-derived P-selectin. Under these circumstances endothelial P-selectin was indeed found to have a significant role in promoting metastasis to the liver and, consistent with the results obtained with the bone marrow chimeras, endothelial P-selectin was also found to promote B16F1 melanoma lung metastasis.

Resting platelets do not express P-selectin on their surface. The initial interactions between circulating tumour cells and platelets via P-selectin are reliant, therefore, upon prior platelet activation. Many tumour cell types are able to generate the protein thrombin, a potent pro-coagulant and activator of platelets, and thence have the capacity to recruit platelets via P-selectin:mucin interactions (VanDeWater *et al.* 1985; Rickles *et al.* 2003). Tumour cell:platelet interactions may also occur via other protein:ligand pairs in the process of haematogenous metastasis. Podoplanin is a sialomucin-like glycoprotein that has been identified on several tumour cells and interacts with the receptor CLEC-2 on platelets to induce their activation and promote experimental tumour metastasis (Suzuki-Inoue 2011). Additionally, the integrins GpIIb/IIIa on platelets and $\alpha V\beta 3$ on tumour cells have both been shown to participate in platelet:tumour interactions and to promote tumour metastasis in experimental animal models (Felding-Habermann *et al.* 1996; Trikha *et al.* 2002).

The endothelium of the liver and lungs constitutively express P-selectin and at levels higher than all other organs (Eppihimer *et al.* 1996; Singh *et al.* 1999), possibly to promote leukocyte migration and surveillance as these organs are exposed to high levels of pathogens, either inhaled or ingested. It is not surprising that the liver and lungs are susceptible to invasion by metastasising tumour cells given their locations within the circulatory system, the constitutive expression of P-selectin, and the fact that many tumour cells express mucins containing sialyl Lewis^x and sialyl Lewis^a that bind P-selectin (Kim *et al.* 1999). When relating the findings herein to those of Crissman *et al* obtained with *in vivo* videomicroscopy, it is possible that endothelial P-selectin plays a role in the initial temporary contact between tumour cells and the endothelium. This initial interaction would then be significantly strengthened by proteins on activated platelets, such as P-selectin, CLEC-2 and GpIIb-IIIa, and proteins of the coagulation cascade, such as fibrin. In the absence of platelets, however, the interaction between tumour cells and the endothelium within the lung capillary bed would appear insufficient

to support extravasation by a significant proportion of cells as is evident from the substantially reduced lung metastases occurring in platelet-depleted mice. In the liver, however, where the velocity of blood flow is comparatively slow, the interaction between endothelial adhesion proteins and tumour-cell ligands would appear sufficient to arrest tumour cells enabling their subsequent extravasation, with platelets not being required to aid endothelial adhesion. Numerous adhesion proteins expressed on tumour cells and by the endothelium have the potential to assist in the arrest of tumour cells and are detailed in Table 1.3.

Whilst the results of our experiments demonstrated that platelets are not required for B16F1 melanoma metastasis to the liver, it is possible that platelets play a minor role, which is difficult to quantify as platelet depletion appears to result in fewer tumour cells lodging in the lung vasculature and consequently more tumour cell entering the liver. To overcome this problem would require bypassing the lung capillary bed by injecting tumour cells directly into the left cardiac ventricle, hepatic artery or spleen in the presence and absence of platelets. The problem with this approach, however, is controlling post-injection internal haemorrhage in platelet-depleted mice.

In summary, the results of this work have demonstrated that the lung metastasis of both B16F1 melanoma cells and 4T1.2 breast cancer cells is promoted by platelets and inhibited by NK cells. Moreover, in the B16F1 metastasis model, the prometastatic role of platelets and the antimetastatic role of NK cells were shown to be chronologically distinct, and that platelets promote lung metastasis by a process that is independent of NK cells. Intriguingly, unlike B16F1 melanoma lung metastasis, B16F1 liver metastasis appeared not to be reliant upon platelets. The pro-metastatic roles of both platelet-derived and endothelial-derived P-selectin in lung metastasis, and endothelial-derived P-selectin in liver metastasis, was demonstrated. P-selectin may, therefore, represent a key target for therapies aimed at preventing metastasis in multiple organs.

Chapter 4

The fate of antibody-coated platelets: Can self-recognition systems be manipulated to treat ITP?

4.1 Abstract

Immune thrombocytopenic purpura (ITP) is a condition affecting all age groups and is characterised, in the majority of cases, by the binding of auto-antibodies to platelet surface proteins targeting them for elimination. The resulting low platelet numbers renders the individual susceptible to life-threatening haemorrhage. The following chapter describes the results of investigations into the various mechanisms of antibody-mediated platelet depletion in a mouse model of ITP and the paradox of why some anti-platelet antibodies do not induce ITP. Furthermore, the role of self-recognition inhibitory proteins on phagocytes in ITP development was investigated for potential treatment avenues. The results of this work have demonstrated that ITP induction was dependent upon the platelet protein targeted by the antibody and the antibody isotype, it was not determined by the density of mAb binding or the level of antigen saturation. Additionally, the mechanism of platelet elimination occurred principally via FcγR-mediated phagocytosis but was also shown to occur through complement-mediated destruction or through an FcγR- and complement-independent process of platelet fragmentation. An exploration into the role of the self-recognition protein pair CD47:SIRPα in this model of ITP revealed that some antibodies that were incapable of inducing ITP in WT mice were capable of inducing ITP in CD47-deficient mice. Furthermore, administration of an activating mAb specific for SIRPα *in vivo* not only prevented, but reversed rat IgG1 mAb-induced, FcγR-mediated ITP. This treatment effect was isotype specific, however, as SIRPα mAb treatment was unable to prevent ITP induced by rat IgG2b mAbs suggesting that SIRPα inhibits low-affinity rather than high-affinity FcγRs. The results of these studies give a greater understanding of the pathogenic pathways of ITP and how self-recognition systems may be manipulated to prevent antibody-mediated ITP.

4.2 Introduction

As detailed in Chapter 3, administration to mice of the hamster mAb, 1B5, specific for murine GpIIb-IIIa results in >95% depletion of platelets for a 36 hr period (Figure 3.2). Upon reviewing the literature on the mechanisms of antibody-coated platelet clearance, we found several significant findings that had not been followed up or interconnected and believed a contribution could be made to this field of research. The initial intention was to determine whether antibodies to platelet adhesion proteins could be used as therapeutic agents to prevent not only tumour cell metastasis, but also leukocyte migration in inflammation-mediated pathologies, such as asthma or reperfusion injury. This interest soon expanded to include potential therapeutic options for individuals with ITP.

In certain medical conditions and during pregnancy, platelets may be erroneously targeted by the immune system for destruction. When platelets are destroyed at a rate greater than that of production, affected individuals are left with low platelet numbers, a state known as thrombocytopenia, with the antibody-mediated form of this disorder being known as immune thrombocytopenic purpura (ITP). Individuals with severe ITP may experience extensive bruising, nose-bleeds, bleeding into the gums and oral mucosa and/or a purpuric (purple) rash due to microscopic bleeding into the skin. They are also at significant risk of a life-threatening internal haemorrhage.

ITP is considered a primary medical disorder when the diagnostic process has excluded any coexisting causative pathologies known to be associated with thrombocytopenia (e.g., human immunodeficiency virus or hepatitis C infection, systemic lupus erythematosis, hypothyroidism, lymphoma, leukaemia, anti-phospholipid syndrome and inherited disorders causing thrombocytopenia) or therapy-

related explanations for low platelet numbers (i.e., recent treatment with drugs such as quinidine, heparin, abciximab and many more) (Kereiakes *et al.* 1996; Cines and Blanchette 2002; Nurden *et al.* 2004). The incidence of ITP is estimated to be 1 new case per 10,000 individuals per annum and may occur at any age, although 50% of cases present in childhood. The disease course differs significantly between paediatric and adult cases. In children the majority of cases are of rapid onset, often there is a history of recent viral infection or immunisation, the disease course lasts from 3–12 months and usually resolves spontaneously. In adults, however, the condition has a slower onset, bleeding tends to be more severe and the disease course is more likely to be chronic, essentially life-long (Cines and Blanchette 2002; Cines and Blanchette 2006; Cooper and Bussel 2006; Provan *et al.* 2009).

Antibodies were demonstrated to be the pathological agent in the majority of ITP cases when transfusion of the plasma or IgG-rich fractions of plasma from patients with ITP into healthy individuals induced thrombocytopenia (Harrington *et al.* 1951; Shulman *et al.* 1965). The most commonly targeted platelet proteins for autoantibodies found in the serum of patients with ITP are GpIIb/IIIa, GpIb/IX, GpIa/IIa, GpV and GpIV, and it is not unusual for patients to have antibodies specific for several platelet proteins present in their serum (Cines and Blanchette 2002). The pathophysiology of ITP has until recently been considered to be due to the accelerated clearance of auto-antibody coated platelets by Fcγ-receptors on macrophages. However, more recently it has been shown in some individuals that the autoantibodies produced also induce apoptosis of megakaryocytes within the bone marrow, hence platelet production is reduced alongside accelerated platelet destruction (Chang *et al.* 2003; Houwerzijl *et al.* 2004; McMillan *et al.* 2004; Houwerzijl *et al.* 2006).

Treatment strategies differ between adults and children and also depend upon the severity of platelet depletion. The majority of paediatric cases are not treated unless platelet numbers are very low due to the likelihood of spontaneous resolution and the significant side-effects of therapy. For the duration of the thrombocytopenia, however, children must modify their behaviour to reduce the risk of injury and possible haemorrhage. In adult and paediatric cases with active bleeding, corticosteroid therapy is often given as an immunosuppressant. Corticosteroids also reduce bleeding through a direct effect on blood vessels. Pooled donor intravenous immunoglobulin (IVIg) is given as it appears to have several therapeutic actions including FcR blockade, neutralisation of autoantibodies, and engagement of the inhibitory FcγR, FcγRIIB, on macrophages (Samuelsson *et al.* 2001; Crow *et al.* 2006). More recently, agonists of the thrombopoietin receptor have been approved for use to boost platelet production by the bone marrow (Nurden *et al.* 2009). If the disease is refractory to these first-line treatment approaches, there are numerous second-line options including alternative immunosuppressive agents or splenectomy (Cines and Blanchette 2002; Chong 2009; Provan *et al.* 2009).

It is not uncommon for treatment failures to occur, perhaps reflecting the heterogeneity of ITP pathophysiology, and the side-effects of current treatment strategies carry significant risks and cause considerable morbidity (Cooper and Bussel 2006). It would stand to reason, therefore, that a comprehensive understanding of all possible mechanisms of immune-mediated platelet destruction is required before treatments can be administered with a reasonable expectation of success.

Previous studies in mice demonstrated that the antigen targeted by the antibody determines the mechanism of platelet depletion (Nieswandt *et al.* 2000). This group found that antibodies to GpIIb-IIIa caused FcγR-mediated clearance of platelets whilst

antibodies to GpIbα induced an FcγR-independent mechanism of depletion. Equally intriguing were the findings that antibodies to GpIX, GpV and CD31 did not cause significant platelet depletion (Nieswandt *et al.* 2000; Poujol *et al.* 2003). Additional studies from the same laboratory and their collaborators demonstrated that the administration of IVIg did not prevent platelet depletion following the administration of GpIbα-specific mAbs whereas it did prevent depletion following administration of GpIIb-IIIa-specific mAbs (Webster *et al.* 2006), thus confirming the FcR-independent mechanism of platelet depletion induced by the GpIbα-specific mAb.

Equally intriguing were the findings of accelerated platelet clearance in mice deficient of the immune effector cell inhibitory protein, SIRPα, or the widely expressed SIRPα ligand, CD47. (Yamao *et al.* 2002; Olsson *et al.* 2005). In an *in vitro* phagocytosis assay, Olsson *et al.* also demonstrated enhanced phagocytosis of IgG opsonised CD47 deficient platelets compared to WT platelets. Furthermore, the addition of a SIRPα-specific mAb increased the rate of WT platelet clearance to match that of CD47 deficient platelets. Unfortunately, the anti-platelet mAb (6A6) used in these studies is of unknown antigen specificity (Olsson *et al.* 2005).

When investigating the use of mAbs to deplete platelets for tumour metastasis studies (Chapter 3), we became aware of the intriguing findings of Nieswandt *et al* and Olsson *et al.*, particularly the inability of mAbs specific for certain platelet surface proteins to induce ITP. These findings prompted us to hypothesise that mAbs to platelet antigens that caused platelet depletion may be interfering with the interaction between CD47 and SIRPα and, if so, the system may be manipulated to prevent platelet depletion following antibody binding in ITP or when anti-platelet antibodies are administered as a therapeutic agent.

The aims of the work presented in this Chapter, therefore, were to:

(i) Investigate the different mechanisms of platelet depletion using rat IgG1 and IgG2b mAbs specific for a variety of murine platelet surface proteins.

(ii) Explore the potential regulatory pathways that determine why some anti-platelet antibodies do not cause platelet depletion.

(iii) Establish whether these regulatory systems can be manipulated to prevent antibody-mediated platelet depletion (ITP).

4.3 RESULTS

4.3.1 Induction and severity of ITP is platelet antigen and IgG subclass-dependent and is unrelated to the level of antibody binding

Initially a range of rat IgG1 mAbs specific for the murine platelet surface proteins GpIbα, GpIIb-IIIa, GpIa, GpV, GpIX and PECAM-1 were examined for their ability to induce ITP in C57BL/6 mice (Figure 4.1A, Table 4.1). Three different effects on platelet numbers were observed over a 24 hr period following mAb administration. First, a rapid depletion (within 2 hr of injection) of >50% of platelets was seen with the IgG1 mAbs specific for GpIbα and GpIIb-IIIa. Second, a slow but significant depletion in platelet numbers was seen with the GpIa-specific mAb and, to a lesser extent, the GpV-specific mAb. Third, little or no depletion of platelets was observed with the IgG1 mAbs specific for GpIX and PECAM-1 (Figure 4.1A, Table 4.1). BALB/c mice were also injected with the rat IgG1 antibodies specific for GpIbα, GpIIb-IIIa, GpIa, GpV and PECAM-1 (Table 4.1). The platelet depletion induced by the GpIbα- and GpIIb-IIIa-specific IgG1 mAbs was very similar to that seen in C57BL/6 mice, indicating the effects were not strain specific. However, a greater level of platelet depletion was observed in BALB/c mice with the mAbs specific for GpIa and GpV, with the PECAM-1-specific mAb also

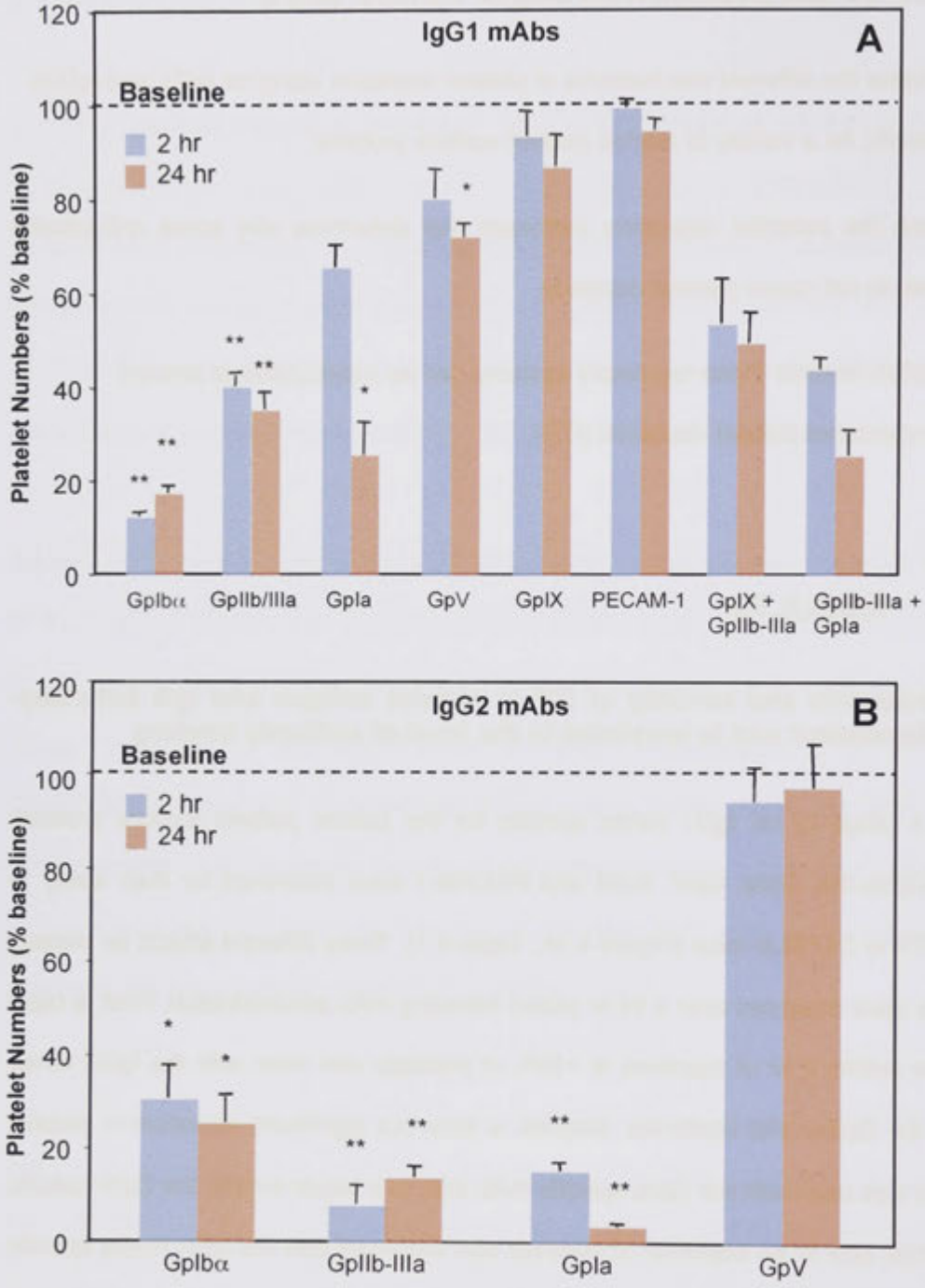

Figure 4.1 – Monoclonal antibodies against GpIbα, GpIIb-IIIa, GpIa and possibly GpV, but not GpIX or PECAM-1, can induce ITP in C57BL/6 mice. Data shown for (A) rat IgG1 and (B) rat IgG2a and IgG2b mAbs against mouse platelet surface molecules. Baseline platelet numbers were assessed in C57BL/6 mice (n=3) prior to i.v. injection of 20 μg of each mAb specific for a platelet surface molecule. Platelet numbers were assessed at 2 hr (blue) and 24 hr (red) post mAb injection. Bars represent SEM. Significant reductions in platelet numbers relative to baseline in mAb treated mice are shown as *p≤0.05, ** p≤0.005. When another mAb was combined with the GpIIb-IIIa mAb, comparison made to % reduction with the mAb specific for GpIIb-IIIa alone.

Table 4.1: The Level of Platelet Depletion Occurring in Wild-type and FcγR-/- Mice Following Injection of mAbs Specific for Different Platelet Proteins

Antibody Target	Antibody Isotype	Platelet numbers (% baseline) [a]	
C57BL/6 mice		**Wild-type mice [b]**	**FcγR -/- mice [b]**
GpIbα	IgG1	12.3 ± 0.9 ($p < 0.005$)	ND [c]
GpIbα	IgG2b	25.2 ± 5.4 ($p < 0.05$)	20.9 ± 1.5 ($p = ns$)
GpIIb-IIIa	IgG1	35.3 ± 3.8 ($p < 0.005$)	ND [c]
GpIIb-IIIa	IgG2b	7.8 ± 4.2 ($p < 0.005$)	78.4 ± 5.7 ($p < 0.005$)
GpIa	IgG1	25.6 ± 7.1 ($p < 0.05$)	ND [c]
GpIa	IgG2a	3.5 ± 0.6 ($p < 0.005$)	62.4 ± 4.1 ($p < 0.005$)
GpV	IgG1	72.1 ± 2. 9 ($p < 0.05$)	ND [c]
GpV	IgG2b	94.0 ± 7.2 ($p = ns$)	ND
GpIX	IgG1	86.9 ± 6.8 ($p = ns$)	ND
PECAM-1 (CD31)	IgG1	96.5 ± 2.7 ($p = ns$)	ND
BALB/c mice		**Wild-type mice**	**FcγR-/- mice**
GpIbα	IgG1	12.0 ± 2.1 ($p < 0.005$)	23.8 ± 2.9 ($p < 0.05$)
GpIIb-IIIa	IgG1	29.3 ± 3.2 ($p < 0.0005$)	104.5 ± 4.3 ($p < 0.005$)
GpIa	IgG1	9.0 ± 1.0 ($p < 0.0005$)	87.5% ± 9.6 ($p < 0.05$)
GpV	IgG1	39.5 ± 5.5 ($p < 0.05$)	107.8 ± 6.9 ($p < 0.005$)
PECAM-1 (CD31)	IgG1	86.3 ± 1.7 ($p < 0.05$)	ND

ND = Not determined

[a] Platelet numbers were measured at 2 hr and 24 hr following mAb injection and the lowest of these two measurements in WT mice is provided with statistical significance of the difference when compared to baseline platelet numbers. Platelet numbers in FcγR-/- mice at the equivalent time point are provided with statistical significance of the difference when compared to the WT value.

[b] Data mean ± SEM (n=3)

[c] Determined in BALB/c mice

Strong platelet depleting mAbs

Weak platelet depleting mAbs

Non-depleting mAbs

producing a small but significant reduction in platelet numbers in BALB/c mice that was not seen in C57BL/6 mice (Table 4.1).

To determine whether an increased level of platelet depletion occured when two mAbs specific for different platelet surface antigens were combined, 20 μg of the IgG1 mAb specific for GpIIb-IIIa and either the GpIa or the GpIX-specific IgG1 mAbs were injected simultaneously into C57BL/6 mice. The levels of platelet depletion observed, however, were not significantly greater than when the mAb to GpIIb-IIIa was administered alone (Figure 4.1 Panel A) suggesting that the mechanism of platelet depletion associated with administration of the GpIIb-IIIa specific IgG1 mAb was functioning at maximum capacity. Additionally these data indicated that the GpIX-specific mAb did not have inhibitory properties that could prevent ITP induced by the GpIIb-IIIa specific mAb.

A similar pattern of ITP induction was observed with the four rat IgG2 mAbs as was seen with the rat IgG1 mAbs of comparable antigen specificity, although there were some minor differences. Thus, when compared to their IgG1 counterparts, the IgG2b mAbs specific for GpIIb-IIIa and GpIa induced a more rapid and greater level of platelet depletion, whereas the IgG2b mAb specific for GpIbα induced somewhat less platelet depletion than the IgG1 mAb of comparable specificity. Similarly, the IgG2a mAb specific for GpV did not induce platelet depletion whereas the comparable IgG1 mAb was a weak platelet depletor (Figure 4.1B; Table 4.1). Unfortunately, rat IgG2 mAbs specific for GpIX and PECAM-1 could not be sourced.

The extent of mAb binding to the platelet surface was considered a potential explanation for the variation in the degree of ITP induced by the different mAbs. The level of platelet surface binding of all the IgG1 mAbs was, therefore, examined following incubation *in vitro* with C57BL/6 mouse platelets, with a mAb concentration

(10 μg/ml) being used *in vitro* that closely corresponded with the *in vivo* concentration of the mAbs (Figure 4.2A). This study showed that the mAb specific for GpIX bound platelets at the highest density followed, in order of decreasing density, by the mAbs specific for GpIbα, GpV, GpIIb-IIIa, GpIa and PECAM-1. Clearly the data indicate that the density of mAb binding to platelets is not a simple explanation for the ITP-inducing ability of the mAbs. For example, the GpIX-specific mAb, which does not induce ITP, exhibited the highest density binding, whereas the GpIIb-IIIa- and GpIa-specific mAbs that bind 3-6 fold less effectively than GpIX induced ITP. It is possible, however, that the level of expression of the protein on the platelet surface and, hence, the density of bound mAbs influenced *the rate* of platelet depletion. For example, 50-80,000 copies of GpIIb-IIIa are expressed on the platelet surface and, following the administration of a GpIIb-IIIa-specific mAb to mice, the majority of platelets were seen to be depleted within 2 hr. In contrast, 2-4,000 copies of GpIa-IIa are expressed on the platelet surface and, when a GpIa-specific IgG1 mAb was administered to mice, maximum platelet depletion was not observed until 24 hr following mAb injection.

To further validate the *in vitro* data, a comparison was made between the level of binding observed *in vitro* with that occurring when the mAbs were injected *in vivo*. Thus the level of platelet surface binding of the non-ITP inducing IgG1 mAbs specific for GpIX and PECAM-1 was determined 2 hours following *i.v.* injection into C57BL/6 mice. The level of platelet surface binding of the GpIX-specific mAb seen *in vivo* was identical to that obtained in the *in vitro* study whereas the level of binding of the mAb specific for PECAM-1 *in vivo* was less than that seen in the *in vitro* studies (Figure 4.2B). This result is not surprising as PECAM-1 is expressed not only on platelets but also on leukocytes and the vascular endothelium. These studies clearly demonstrate that the density of binding of mAbs to the platelet surface does not correlate with the ability of the mAbs to induce ITP when injected into mice.

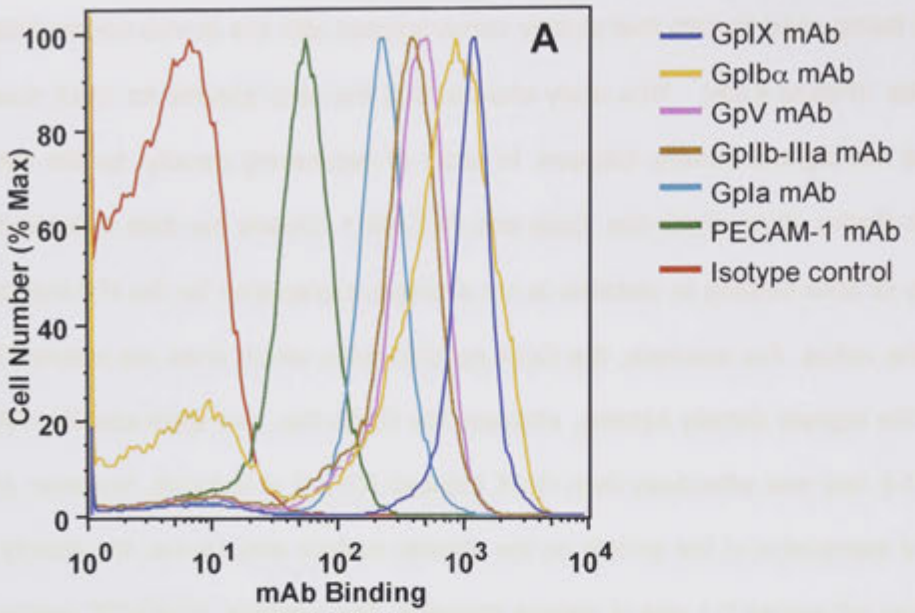

mAb Target Antigen	PECAM-1	GpIa	GpIIb-IIIa	GpV	GpIbα	GpIX
Fold-binding *vs* Isotype control	9.0	35.3	62.7	80.6	138.4	191.2

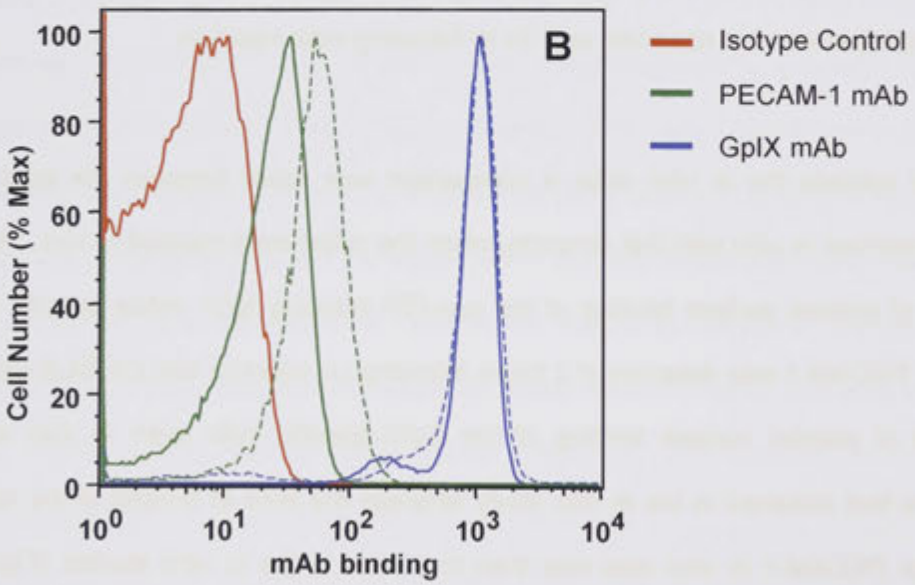

Figure 4.2 – Extent of mAb binding to platelets does not correlate with the ability of the mAbs to induce ITP. The extent of binding of the various rat IgG1 mAbs to their platelet target antigens was determined using **(A)** all IgG1 mAbs *in-vitro* and **(B)** the two IgG1 non-depleting mAbs *in-vivo* (solid lines) and *in-vitro* (dotted lines). For *in-vitro* studies washed whole blood from C57BL/6 mice was incubated with the mAbs (10 μg/ml) for 30 mins at 37°C and for *in-vivo* studies C57BL/6 mice were injected with 20 μg of each mAb and blood collected 2 hr later. Extent of mAb binding was determined by flow cytometry using a FITC-conjugated mouse anti-rat IgG1 mAb. Data in Table shows the level of *in-vitro* binding of all the IgG1 mAbs expressed as fold-binding *vs* isotype control as seen in Panel A.

Another possibility is that the level of antigen saturation by mAbs on the platelet surface influences the ability of a particular mAb to induce ITP. In order to test this possibility mouse platelets were incubated with a range of mAb concentrations *in vitro* and the level of antigen saturation determined at 10 μg/ml, the estimated *in vivo* concentration of the IgG1 mAbs following a dose of 20 μg/mouse, i.e., the mAb dose used for the ITP studies. It was found that at a mAb concentration of 10 μg/ml, GpIIb-IIIa and GpV were the least saturated, GpIX and GpIbα were almost saturated, and GpIa and PECAM-1 were beyond saturation (Figure 4.3). Thus, the degree of platelet antigen saturation also does not correlate with the ability of the different mAbs to induce ITP.

4.3.2 Induction of ITP by platelet-specific mAbs is predominantly FcγR dependent and is regulated at the macrophage level.

Since previous studies have suggested that FcγR play a key role in ITP, those antibodies causing significant platelet-depletion were administered to FcR common γ-chain deficient (FcγR-/-) mice. The IgG1 mAbs were tested in FcγR-/- mice on a BALB/c background as it was on this strain background that more severe ITP was observed with the IgG1 mAbs. The IgG2 mAbs were, in contrast, tested in FcγR-/- mice on a C57BL/6 background. In each case, comparisons of the level of ITP induction were made with wild-type (WT) mice of the same genetic background.

In FcγR-/- mice, the platelet depleting ability of all the ITP inducing mAbs was dramatically inhibited except those mAbs specific for GpIbα (Figure 4.4, Table 4.1). The extent of ITP induction observed following injection of both the IgG1 and the IgG2 mAbs specfic for GpIbα was essentially unchanged in FcγR-/- mice. Interestingly, the IgG2b antibody specific for GpIa still caused 37.6% depletion of platelets at 2 hr in FcγR-/- mice, although this value was significantly less than the 96.5% depletion seen

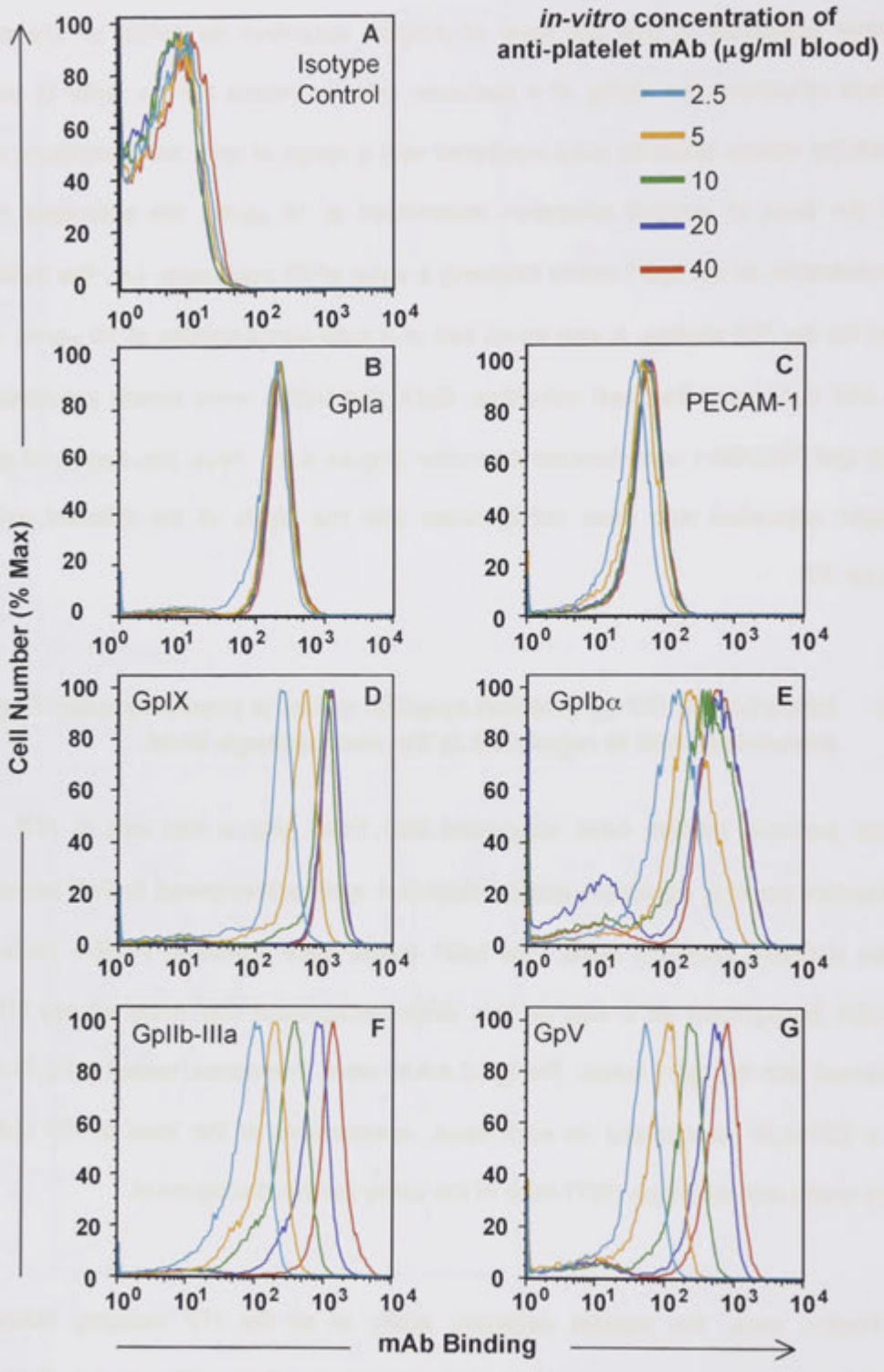

Figure 4.3 – Ability of IgG1 mAbs to saturate their target antigens does not correlate with their ability to induce ITP. Whole blood was collected from C57BL/6 mice and incubated for 30 min at 37°C with 2.5–40 μg/ml of the different platelet-specific rat IgG1 mAbs, 10 μg/ml corresponding to the approximate mAb concentration tested for ITP induction *in-vivo*. Antibody binding detected as in Figure 4.2.

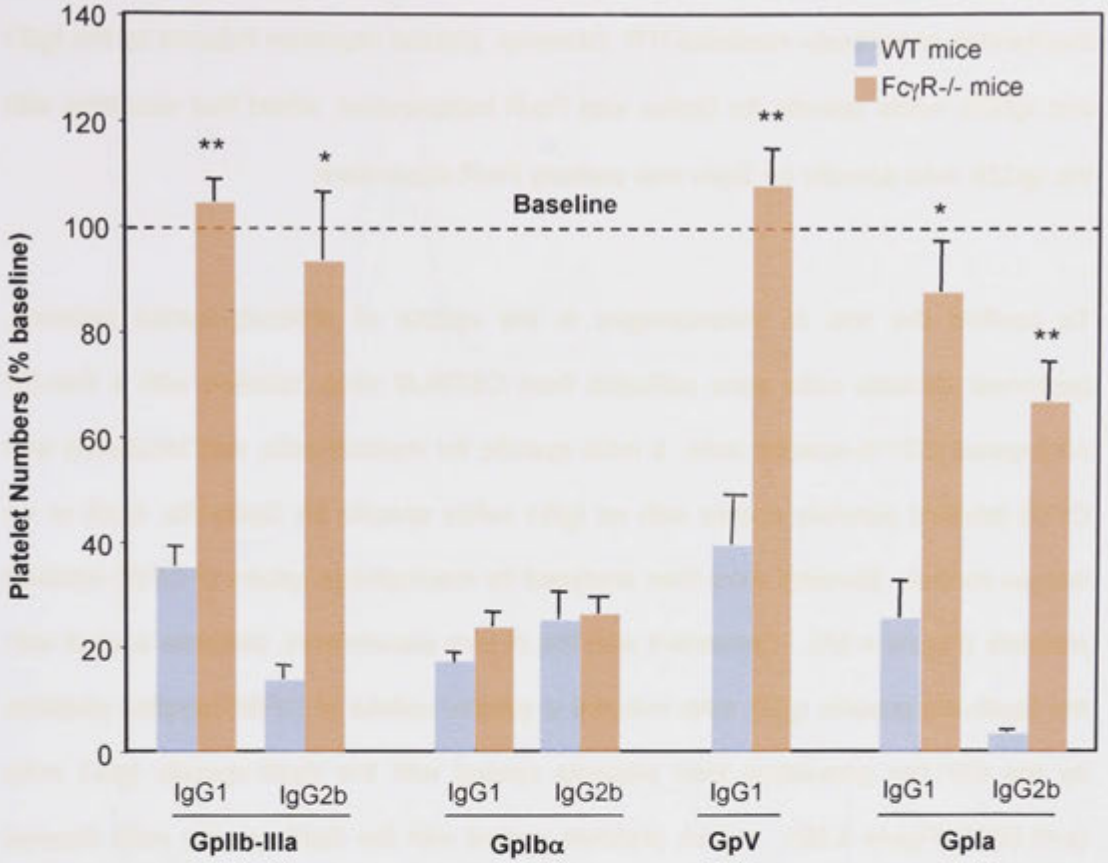

Figure 4.4 – Induction of ITP by platelet-specific mAbs is predominantly FcγR dependent. Baseline platelet numbers were performed on WT (blue) and FcγR-/- (red) mice (n=3) prior to i.v. injection of 20 μg of mAb to a platelet surface molecule. Data shows platelet numbers as a percentage of baseline at 24 hr post-injection of mAb. Bars represent SEM. Significant increases in platelet numbers in FcγR-/- mice relative to WT mice are shown as *p≤0.05, ** p≤0.005. IgG1 data was obtained from FcγR-/- on a BALB/c background as more severe ITP was observed in mice of this background with the IgG1 mAbs. IgG2b data was obtained from FcγR-/-mice on a C57BL/6 background. Control values were obtained from WT of the same background.

in WT mice (Figure 4.4, Table 4.1). These data imply that FcγR uptake is the principal mechanism of antibody-mediated ITP. However, platelet depletion induced by the IgG1 and IgG2b mAbs specific for GpIbα was FcγR independent, whilst that occurring with the IgG2b mAb specific for GpIa was partially FcγR dependent.

To confirm the role of macrophages in the uptake of antibody-coated platelets, peritoneal exudate cells were collected from C57BL/6 mice, labelled with a Per-CP conjugated CD11b-specific mAb, a mAb specific for myeloid cells, and incubated with CFSE-labelled platelets coated with rat IgG1 mAbs specific for GpIIb-IIIa, GpIX or an isotype control. Samples were then analysed for macrophage uptake of CFSE-labelled platelets (Figure 4.5A). Consistent with the *in vivo* experiments, platelets coated with the GpIIb-IIIa-specific IgG1 mAb induced a greater uptake of CFSE labelled platelets by the CD11b+ population than platelets coated with the GpIX-specific IgG1 mAb ($p<0.0005$)(Figure 4.5B). In fact, platelets coated with the GpIX-specific mAb showed only a slight increase in phagocyte uptake above background. These data suggest that FcγR-mediated ITP induced by the binding of the various anti-platelet antibodies occurs at the level of the macrophage, although additional *in vivo* experiments would be required to definitively demonstrate this point.

4.3.3 FcγR-independent mechanisms of ITP induction involve platelet disintegration or complement-mediated destruction

Following the demonstration that administration of the IgG1 and the IgG2b mAbs specific for GpIbα still induced ITP in FcγR-/- mice, alternative mechanisms of platelet destruction were investigated. To determine the role of complement in the platelet depletion induced by these antibodies, the GpIbα-specific IgG1 mAb was administered to C3-/- mice (Figure 4.6). These data demonstrated that complement had no role in the platelet depletion mediated by the IgG1 mAb specific for GpIbα.

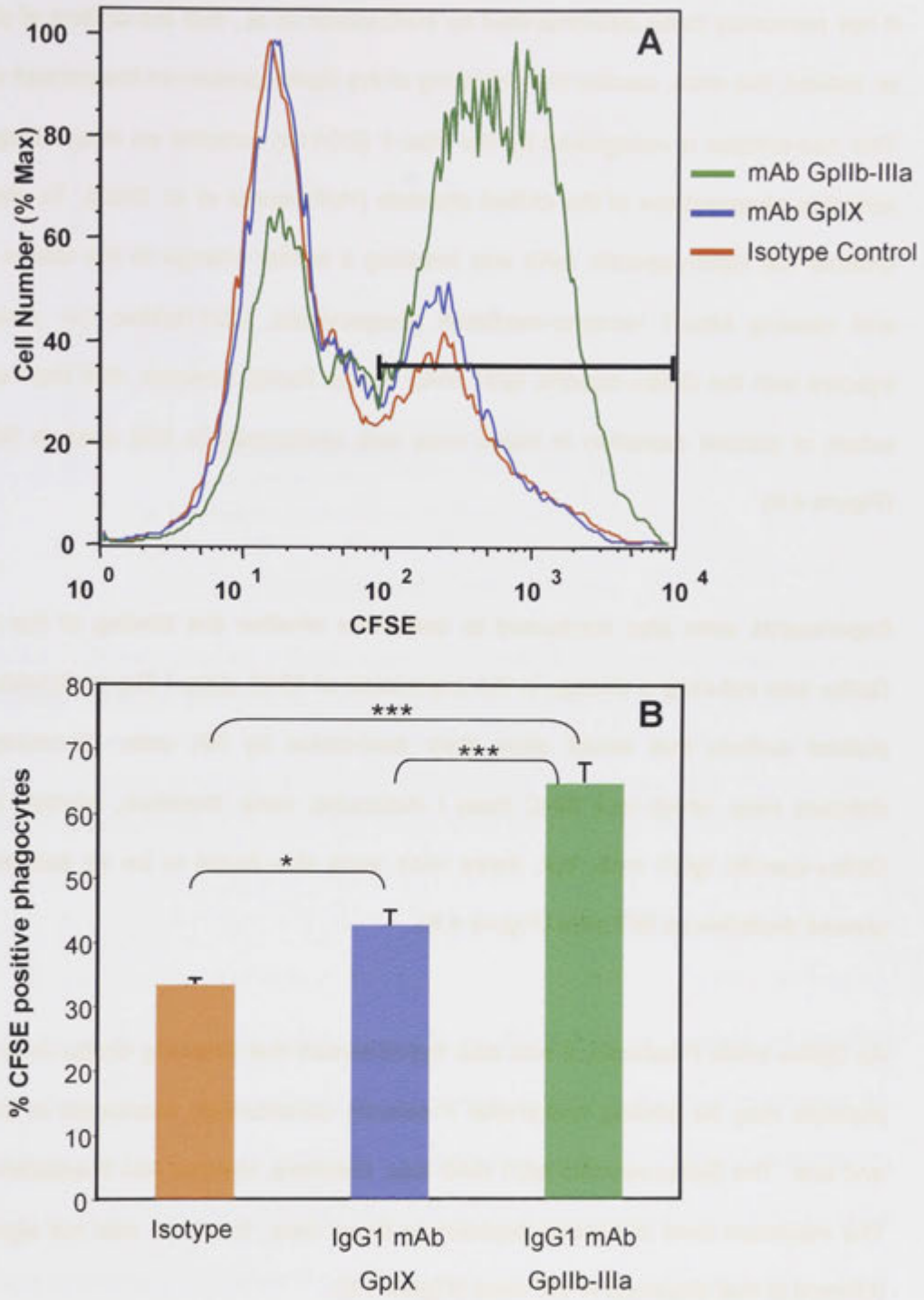

Figure 4.5 – Platelets are selectively opsonised for phagocyte uptake by an ITP inducing mAb specific for GpIIb-IIIa. Peritoneal exudate cells were collected from C57BL/6 mice, incubated with a Per-CP conjugated mAb specific for CD11b, then incubated for 60 min at 37°C with CFSE-labelled platelets coated with rat IgG1 mAbs specific for GpIIb-IIIa, GpIX or an isotype control. **(A)** Representative histogram of samples analysed by flow cytometry for platelet uptake by CD11b+ myeloid cells gated for detection of CFSE fluorescence. **(B)** Combined results from 2 separate experiments consisting of a total of 5 samples. Significant increases in the percentage of CFSE+ CD11b+ cells shown as *p<0.05 and ***p<0.0005.

It has previously been demonstrated by Hoffmeister *et al.*, that the chilling of platelets or, indeed, live mice, causes the clustering of the GpIbα protein on the platelet surface. This neo-antigen is recognised by the Mac-1 (CD11b) receptor on macrophages and activates phagocytosis of the chilled platelets (Hoffmeister *et al.* 2003). To determine whether the GpIbα-specific mAb was inducing a similar change to the GpIbα protein and causing Mac-1 receptor-mediated phagocytosis, CD11b(Mac-1)-/- mice were injected with the GpIbα-specific IgG1 mAb. It was found, however, that the maximum extent of platelet depletion in these mice was unchanged to that seen in WT mice (Figure 4.6).

Experiments were also conducted to determine whether the binding of the mAb to GpIbα was inducing a change in the expression of MHC class-I like molecules on the platelet surface that would allow their destruction by NK cells. β2-microglobulin deficient mice, which lack MHC class I molecules, were, therefore, injected with the GpIbα-specific IgG1 mAb, but, these mice were also found to be as susceptible to platelet depletion as WT mice (Figure 4.6).

As GpIbα binds P-selectin, it was also hypothesised that following GpIbα-mAb binding platelets may be binding endothelial P-selectin constitutively expressed in the lungs and liver. The GpIbα-specific IgG1 mAb was, therefore, injected into P-selectin-/- mice. The maximum level of platelet depletion in these mice, however, was not significantly different to that observed in WT mice (Figure 4.6).

To investigate whether the binding of the GpIbα-specific IgG1 mAb was causing direct activation and disintegration of platelets, washed whole blood was incubated for 30 min at 37°C with the GpIbα-specific IgG1 mAb, the GpIIb-IIIa-specific IgG2b mAb or the GpIa-specific IgG2b mAb and compared with a control sample containing no antibody.

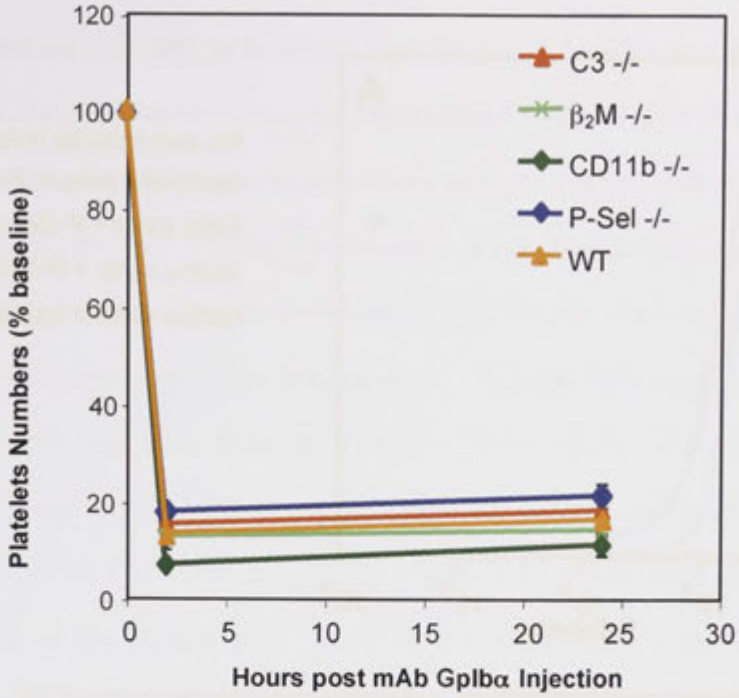

Figure 4.6 - ITP induction by a GpIbα-specific mAb does not involve complement, the macrophage receptor Mac-1, MHC-Class I-like molecules or P-selectin. Baseline platelet numbers were assessed for WT, C3-/-, CD11b-/-, β_2M-/- and P-Sel-/- C57BL/6 mice (n=3) prior to i.v. injection of 20 μg of an IgG1 mAb specific for GpIbα. Data shows platelet numbers as a percentage of baseline at 2 hr and 24 hr post-injection of mAb. Bars represent SEM.

Following this, a FITC-conjugated antibody to P-selectin, a marker of platelet activation, was added. The samples were then analysed by flow cytometry for changes in platelet size, based on forward and side scatter, and P-selectin expression. In contrast to all the other treatments, platelets incubated with the GpIbα-specific IgG1 mAb became weakly positive for P-selectin expression (Figure 4.7A) and were clearly reduced in size (Figure 4.7B) thus indicating that the binding of the mAb to GpIbα was causing platelet activation and fragmentation. This process was independent of complement as the platelets used in this experiment were washed free of serum, and ITP was demonstrated in complement deficient mice administered the GpIbα-specific IgG1 mAb (Figure 4.6).

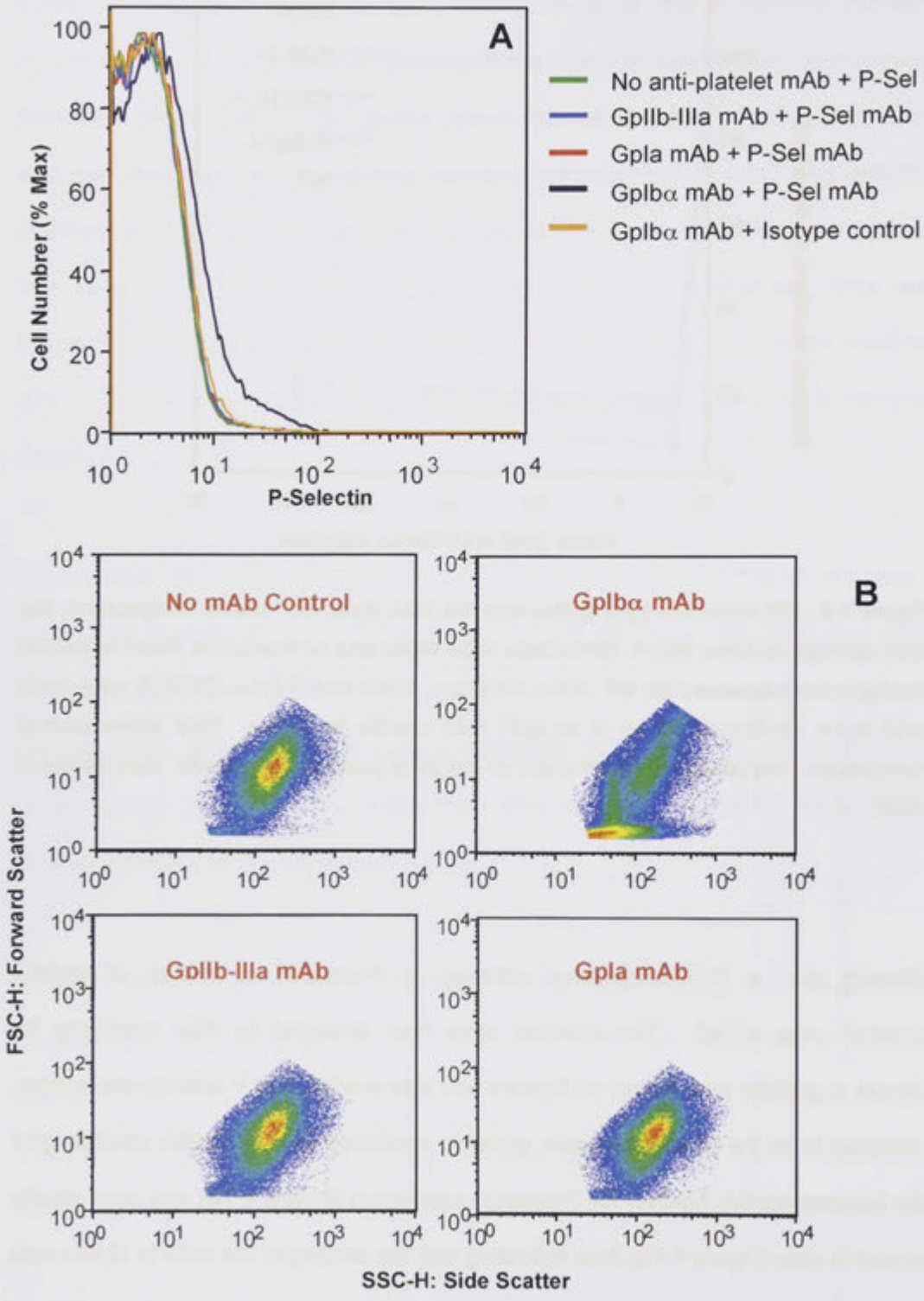

Figure 4.7 – The ITP-inducing GpIbα-specific mAb, but not ITP-inducing mAbs to other platelet surface molecules, directly activates platelets. Washed blood cells from wild-type C57BL/6 mice were incubated with rat IgG1 mAbs to GpIbα, GpIIb-IIIa or GpIa for 30 mins at 37°C followed by a FITC-conjugated rat IgG1 antibody specific for P-selectin, then analysed by flow cytometry for **(A)** surface expression of P-selectin and **(B)** alterations in platelet size (FSC) and granularity (SSC).

Since ITP induced by the IgG2b mAb specific for GpIa was found to be partially independent of FcγR, this antibody was administered to WT and FcγR-/- mice depleted of C3 using cobra venom factor to determine whether complement-mediated platelet destruction was involved. Indeed, the induction of ITP was completely inhibited in the complement-depleted FcγR-/- mice indicating that platelet depletion by this mAb is partially complement dependent (Figure 4.8). A small but significant increase in platelet numbers was also seen at 2 hr after GpIa IgG2b mAb administration in complement-deficient WT mice when compared with complement-sufficient WT mice (32.9% ± 1.7 *vs* 15.2% ± 1.8; $p < 0.005$) (Figure 4.8). These data demonstrate that administration of the GpIa-specific IgG2b mAb induces platelet depletion via FcγR-mediated phagocytosis and complement-mediated destruction.

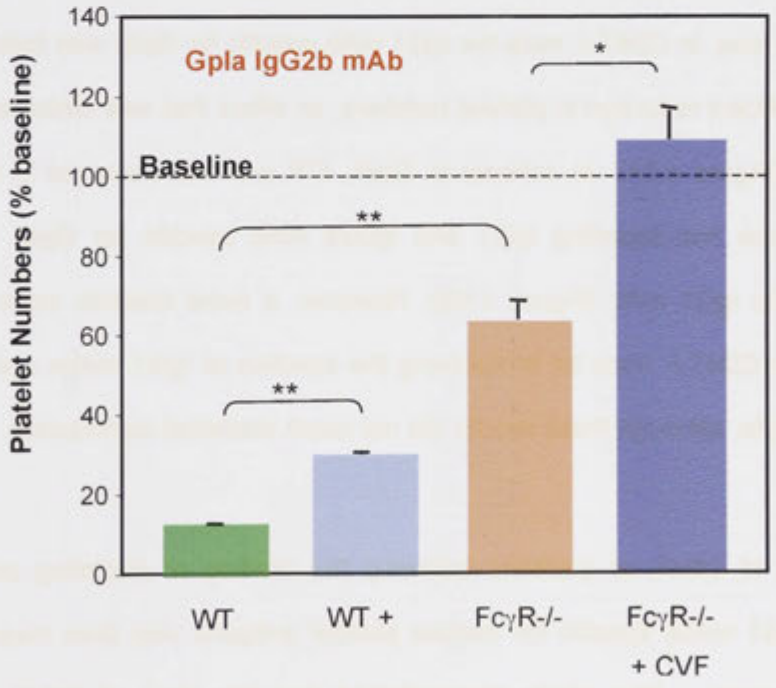

Figure 4.8 – Induction of ITP by rat IgG2b mAb to GpIa is both FcγR and complement dependent. C57BL/6 WT and FcγR-/- mice (n=3) were depleted of complement via i.p. injection of cobra venom factor (CVF) 18 hr prior to i.v. injection of 20 μg of an IgG2b mAb specific for GpIa. Baseline platelet numbers were performed prior to injection of the GpIa mAb. Data shows platelet numbers as a percentage of baseline at 2 hr post injection of mAb. Bars represent SEM. Significant increases in platelet numbers are shown as *p≤0.05 and **p≤0.005.

4.3.4 Engagement of the phagocytosis inhibitor, SIRPα, prevents IgG1-mediated, but not IgG2b-mediated, ITP

The important question remaining was why some platelet antigen-specific mAbs induce ITP via FcγR-mediated phagocytosis while others do not. The working hypothesis was that the interaction of the ITP inducing mAbs with their platelet surface antigens was causing the loss of a self-recognition molecule on the platelet surface and, in doing so, triggering phagocytosis following FcγR engagement. As earlier studies have shown that antibody-mediated platelet depletion is enhanced in CD47-/- mice (Olsson *et al.* 2005), we examined whether the CD47-SIRPα recognition system may regulate ITP in our experimental model. Thus, experiments were performed to ascertain the role of the self-antigen, CD47, on platelets and its receptor, SIRPα, on macrophages in regulating the depletion of antibody-coated platelets. Initially CD47-/- mice (n=3) were injected with rat IgG1 mAbs specific for various platelet antigens and platelet numbers determined over time. In CD47-/- mice the IgG1 mAb specific for GpIX was indeed able to induce a significant reduction in platelet numbers, an effect that was sustained for at least 48 hours (Figure 4.9A). In contrast to GpIX, ITP was not observed in CD47-/- mice receiving the non-depleting IgG1 and IgG2b mAb specific for GpV, nor the PECAM-1-specific IgG1 mAb (Figure 4.9B). However, a trend towards more severe ITP was seen in CD47-/- mice 24 hr following the injection of IgG1 mAbs specific for GpIIb-IIIa and GpIa, although these results did not reach statistical significance.

The expression of CD47 on platelets following the binding of depleting and non-depleting rat IgG1 mAbs specific for various platelet antigens was then investigated using flow cytometry. This study demonstrated that the level of CD47 surface expression was not reduced by any of the IgG1 mAbs compared with the level seen in the control sample. In fact, there appeared to be a slight increase in CD47 expression following anti-platelet mAb binding, although this increase did not correlate with the

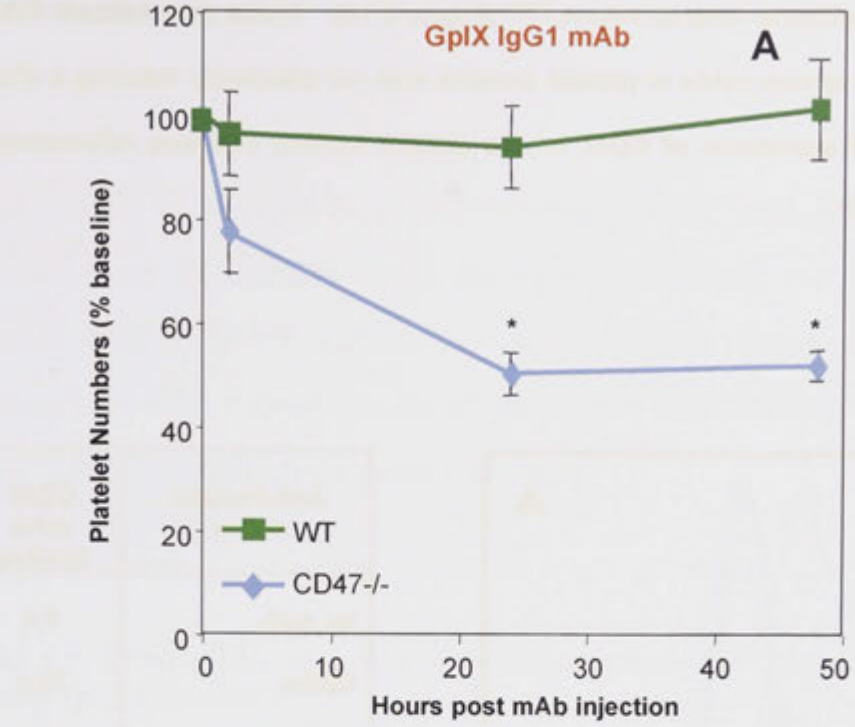

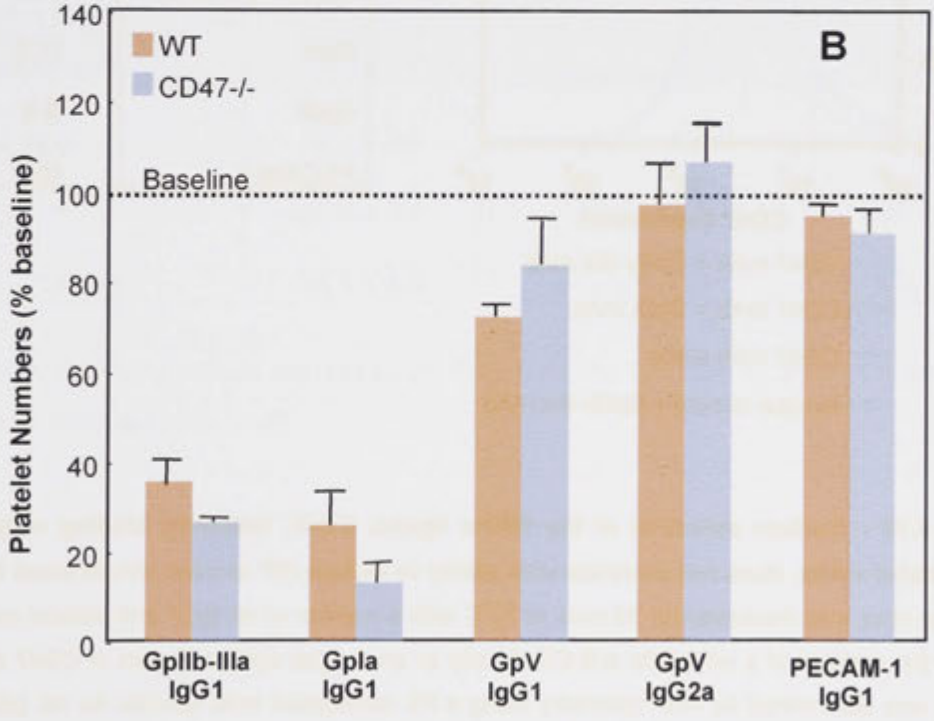

Figure 4.9 – GpIX specific mAb induces ITP in CD47-/- mice. (A) Wild-type (WT) and CD47-/- C57BL/6 mice (n=3) were injected i.v. with 20 μg of a GpIX-specific rat IgG1 mAb and platelet numbers measured prior to, 2, 24 and 48 hr post mAb injection. **(B)** Ability of mAbs specific for various platelet antigens (20 μg i.v.) to affect platelet numbers 24 hr after administration to WT and CD47-/- C57BL/6 mice. Significant decreases in platelet numbers between WT and CD47-/- mice are shown as *p≤0.05. Note that differences in panel B did not reach statistical significance.

ability of the particular mAb to induce ITP (Figure 4.10). These data indicate that the binding of the various mAbs to platelet proteins was not selectively inducing a change in the level of expression of CD47 on the platelet surface that was influencing the induction of ITP.

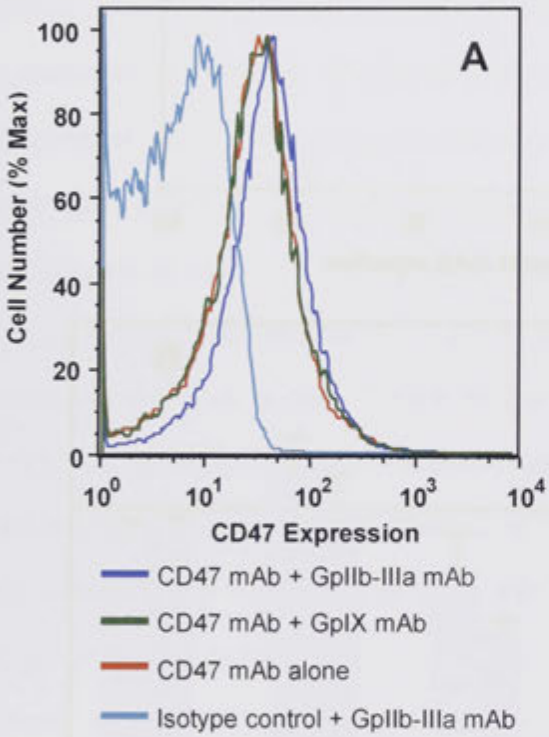

Anti-Platelet mAbs	CD47 mAb binding
No mAb	7.4
GpIbα	10.4
GpIIb-IIIa	10.1
GpV	11.2
GpIX	6.9
PECAM-1	10.5

Figure 4.10 – Surface detection of the SIRPα ligand, CD47, following binding of IgG1 anti-platelet mAbs, does not correlate with ability to induce ITP *in-vivo*. Whole blood from wild-type mice was incubated for 30 mins at 37°C with a number of rat IgG1 anti-platelet mAbs prior to the addition of a rat IgG2a anti-CD47 mAb or an isotype control. Extent of CD47 mAb binding was determined by flow cytometry using a PE conjugated mAb specific for rat IgG2a. **(A)** Representative FACS plot for samples incubated with IgG1 mAbs specific for GpIIb-IIIa and GpIX. Data in table shows the level of CD47 mAb binding in the presence of different anti-platelet mAbs expressed as fold-binding vs isotype control.

Since the data described in this Chapter suggest that phagocytosis-inhibitory receptors, such as SIRPα, may be controlling ITP severity, we examined the ability of a SIRPα activating mAb to inhibit ITP. It was found that injection of such a mAb 1 hr prior to the injection of 20 μg of the platelet-depleting rat IgG1 mAbs specific for GpIa (C57BL/6 mice), GpV (BALB/c mice) and GpIIb-IIIa (C57BL/6 mice) resulted in a complete inhibition of ITP induction ($p<0.05$ – $p<0.0005$ compared with isotype control)(Figure 4.11). Furthermore, the inhibition of ITP by SIRPα mAb treatment was similar to that observed in FcγR-/- mice (Table 4.2).

Table 4.2: Comparison of Ability of SIRPα Activation or FcγR Deficiency to Prevent IgG1-induced ITP.

Specificity of Anti-Platelet mAb (IgG1)	WT mice [a]	WT mice treated with SIRPα specific mAb [a]	FcγR-/- mice [a]
GpIIb-IIIa	35.3 ± 3.8	95.7 ± 6.5	104.5 ± 4.3
GpIa	25.6 ± 7.1	81.2 ± 8.9	80.5 ± 8.8
GpV (BALB/c)	39.5 ± 5.5	103.5 ± 1.6	107.8 ± 6.9

[a] Mean platelet numbers expressed as % of baseline (± SEM) at 24 hr following anti-platelet mAb injection (n=3).

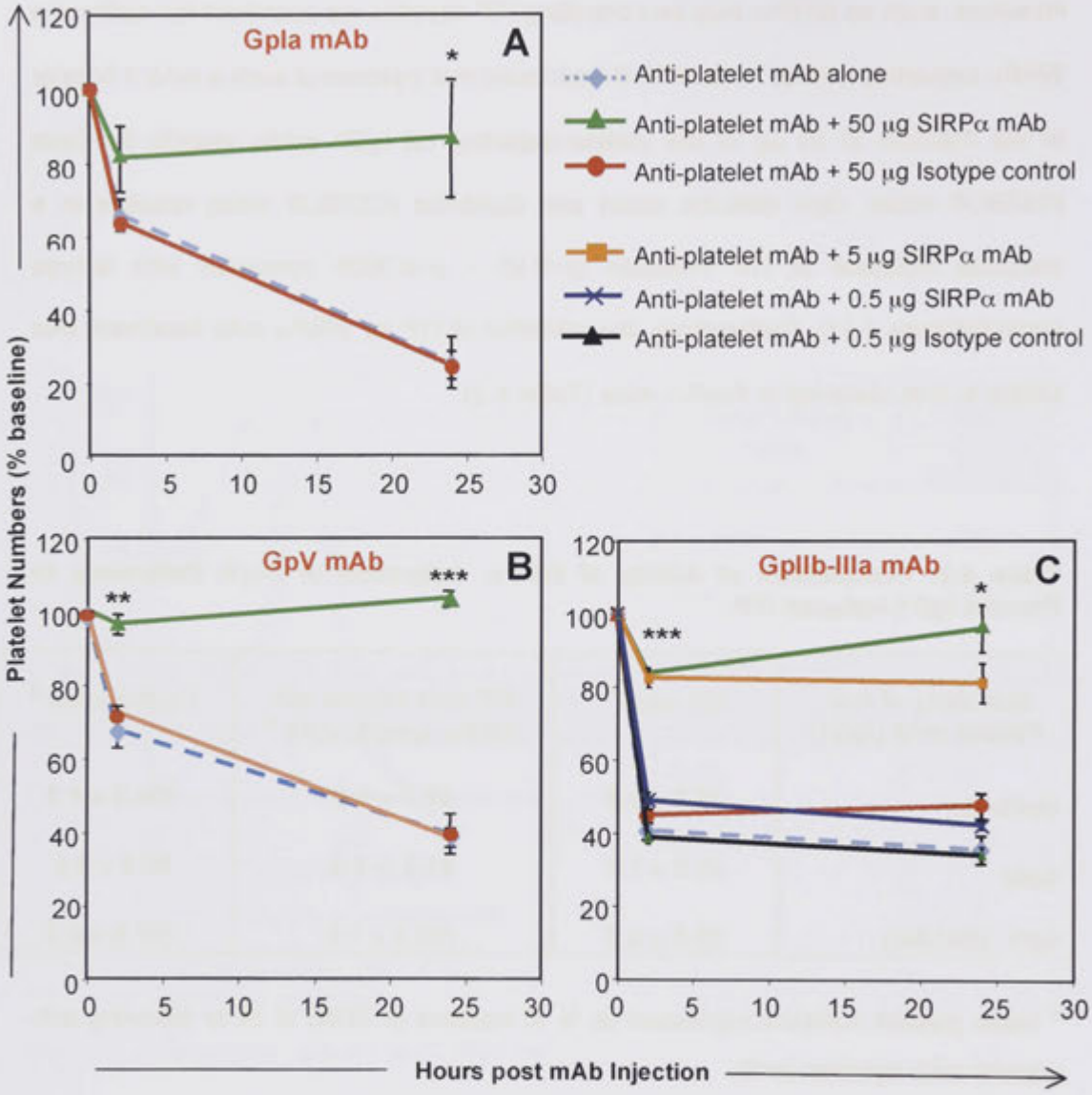

Figure 4.11 – Treatment with low concentrations of a SIRPα-specific mAb prevents FcγR-mediated ITP induced by rat IgG1 mAbs. **(A & B)** 50 μg of a rat IgG1 mAb to SIRPα or an isotype control was injected i.v. 1 hr prior to injection of 20 μg of a rat IgG1 mAb specific for **(A)** GpIa in C57BL/6 mice and **(B)** GpV in BALB/c mice. **(C)** C57BL/6 mice were injected i.v. with 50-, 5- or 0.5 μg of a SIRPα-specific mAb or 50 μg or 0.5 μg of an isotype control 1 hr prior to i.v. injection of 20 μg of an IgG1 mAb specific for GpIIb-IIIa. Platelet numbers were determined 1 hr prior to injection of the SIRPα mAb or the isotype control, and 2 hr and 24 hr following injection of the anti-platelet mAbs. Statistical comparisons made between equivalent doses of isotype control treated mice *vs* SIRPα-specific mAb treated mice are shown as *p≤0.05, ***p≤0.0005. Data for mice treated with anti-platelet mAbs alone (·····) from Figure 4.1A included to demonstrate reproducibility of ITP induced by each mAb.

The minimum dose of the SIRPα-specific mAb required to prevent ITP was also investigated in mice administered the GpIIb-IIIa-specific mAb. C57BL/6 mice were injected with 5 or 0.5 μg of the SIRPα-specific mAb 1 hr prior to injection of 20 μg of the IgG1 mAb specific for GpIIb-IIIa. The platelet preserving effect of the 5 μg dose of the SIRPα mAb was found to be similar to that observed with a 50 μg dose of the mAb, but a 0.5 μg dose was ineffective (Figure 4.11C).

To determine whether the SIRPα-specific mAb could reverse pre-existing ITP, C57BL/6 mice were injected with 20 μg of the GpIIb-IIIa-specific IgG1 mAb then 2 hr later with 50 or 5 μg of the SIRPα-specific mAb. Platelet numbers were determined at baseline, 1, 3 and 24 hr following injection of the GpIIb-IIIa-specific mAb. Platelet numbers were significantly increased following treatment with the SIRPα-specific mAb at 3 hr (both doses $p<0.05$) and 24 hr after injection of the GpIIb-IIIa-specific IgG1 mAb (5 μg $p<0.05$ and 50 μg $p<0.005$) compared with mice receiving an isotype control (Figure 4.12).

Additional experiments were conducted to determine whether the SIRPα-specific mAb could also prevent IgG2b mAb-induced ITP. Thus, WT C57BL/6 mice were injected with 50 μg of the SIRPα mAb or an isotype control 1 hr prior to the injection of 20 μg of the rat IgG2b mAb specific for GpIIb-IIIa. In stark contrast to the effect of SIRPα mAb treatment prior to the GpIIb-IIIa-specific IgG1 mAb, ITP was not inhibited by SIRPα mAb treatment prior to the IgG2b mAb administration (Figure 4.13A). The ability of SIRPα mAb treatment to prevent ITP induced by the GpIa-specific IgG2b mAb was also investigated. As ITP induced by this mAb was previously demonstrated to be both FcγR and complement-mediated (Figure 4.8), WT and FcγR-/-mice were depleted of complement using CVF and the WT mice subsequently injected with the SIRPα-

specific mAb or saline 1 hr prior to injection of the GpIa-specific mAb. However, as seen with the GpIIb-IIIa-specific IgG2b mAb, SIRPα mAb treatment prior to GpIa-specific IgG2b mAb administration did not result in ITP inhibiton (Figure 4.13B). These data contrast with the results seen in FcγR-/- mice administered these IgG2b mAbs (Figure 4.4) and implies that the inhibitory receptor, SIRPα, does not regulate the FcγR subclass that binds rat IgG2b mAbs.

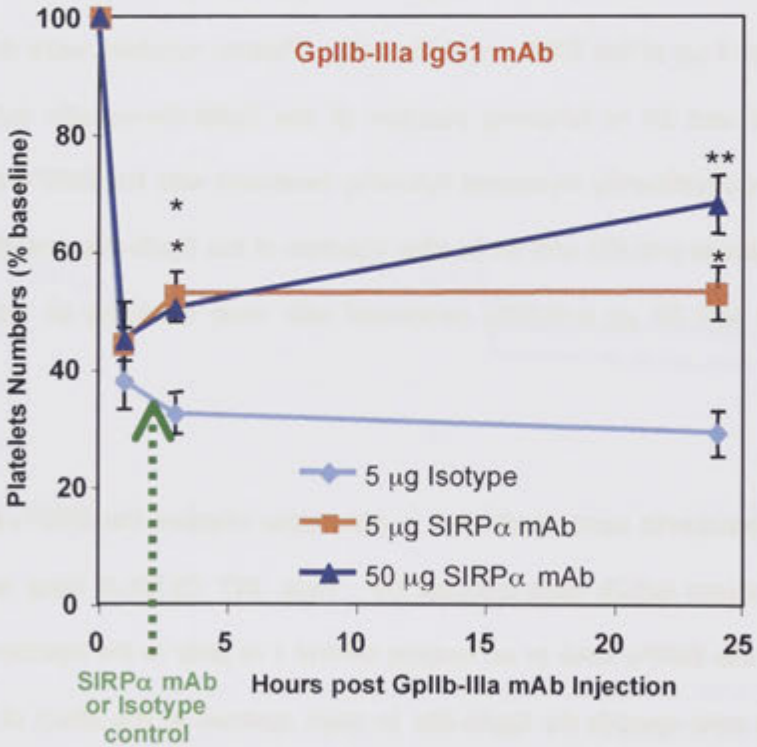

Figure 4.12 – SIRPα-specific mAb treatment can reverse ITP induced by a GpIIb-IIIa specific IgG1 mAb. C57BL/6 mice (n = 3) were injected i.v. with 20 μg of a rat IgG1 mAb specific for GpIIb-IIIa and 2 hr later with 50 or 5 μg of a SIRPα-specific mAb, or 5 μg of an isotype control. Platelet numbers were determined at baseline, 1, 3 and 24 hr post mAb GpIIb-IIIa injection. Significant increases in platelet numbers between the isotype control and the SIRPα-specific mAb treated mice are shown as *p≤0.05 and **p≤0.005.

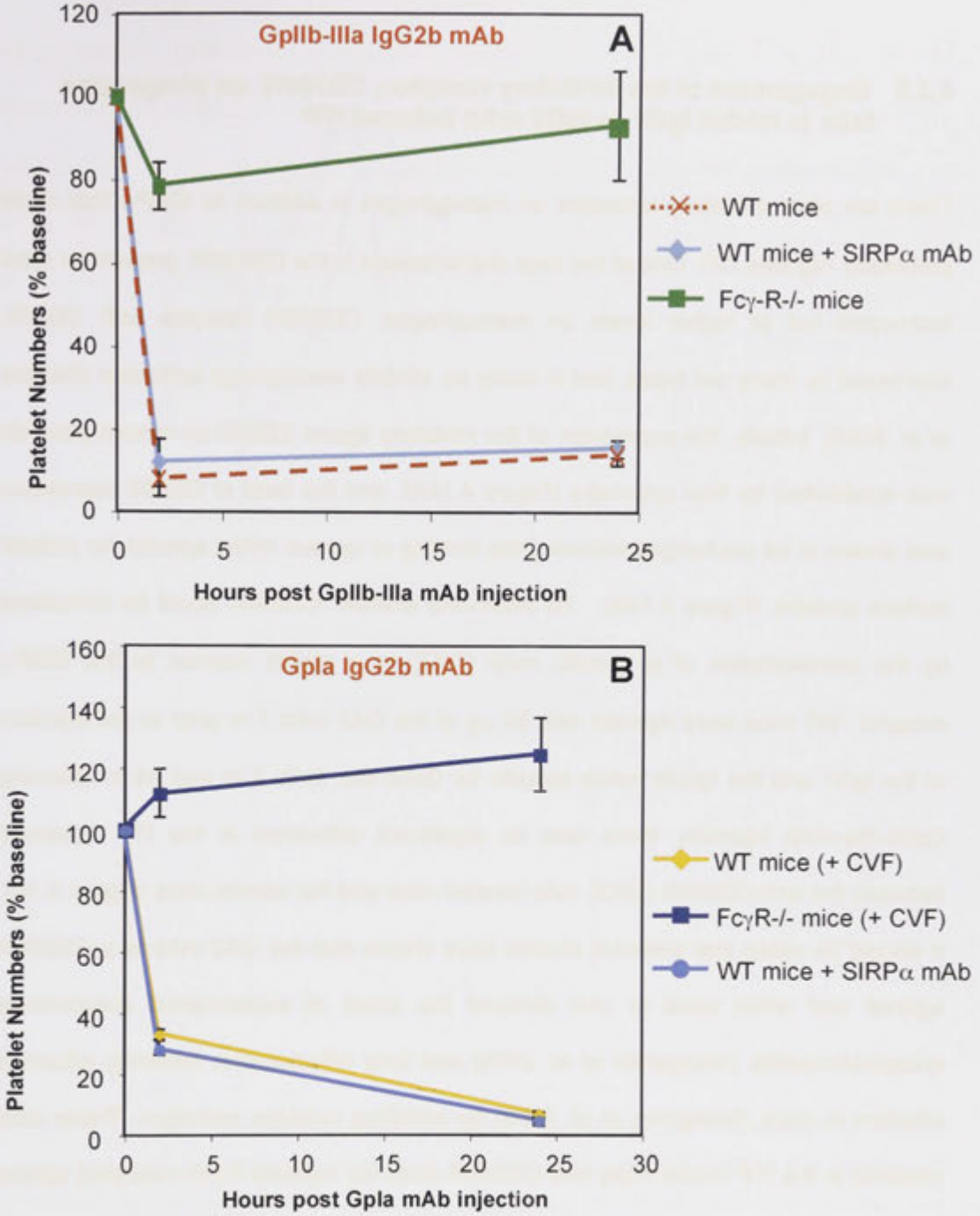

Figure 4.13 – SIRPα-specific mAb is unable to prevent ITP induced by rat IgG2b mAbs specific for GpIIb-IIIa or Gpla either alone or when combined with complement depletion. (A) ITP observed in WT C57BL/6 mice (n = 3) injected i.v. with 20 μg of a GpIIb-IIIa-specific rat IgG2b mAb in the presence or absence of a SIRPα-specific mAb (50 μg i.v.) injected 1 hr earlier. ITP induced by the GpIIb-IIIa mAb in FcγR-/- mice is included for comparison. **(B)** ITP observed in WT C57BL/6 mice depleted of complement by CVF and injected i.v. with saline or 50 μg of a SIRPα-specific mAb 1 hr prior to i.v. injection of 20 μg of a rat IgG2b mAb specific to Gpla. ITP induced by the Gpla-specific mAb in CVF treated FcγR-/- mice is included for a comparison. Platelet numbers were determined at baseline, 2 hr and 24 hr post injection of the mAbs to GpIIb-IIIa or Gpla. Data in (A) for WT mice (·····) from Figure 4.1B.

4.3.5 Engagement of the inhibitory receptor, CD200R, on phagocytes fails to inhibit IgG1 or IgG2 mAb induced ITP

There are other inhibitory receptors on macrophages in addition to SIRPα that could potentially regulate ITP. One of the best characterised is the CD200R, present on most leukocytes but at higher levels on macrophages. CD200R interacts with CD200, expressed by many cell types, and in doing so, inhibits macrophage activation (Barclay *et al.* 2002). Initially, the expression of the inhibitory ligand CD200 on mouse platelets was established by flow cytometry (Figure 4.14A), and the level of CD200 expression was shown to be unchanged following the binding of various mAbs specific for platelet surface proteins (Figure 4.14B). To determine whether CD200R could be stimulated by the administration of a specific mAb (OX2) in a similar manner to the SIRPα receptor, WT mice were injected with 50 μg of the OX2 mAb 1 hr prior to the injection of the IgG1 and the IgG2b mAbs specific for GpIIb-IIIa. Both 2 hr and 24 hr following GpIIb-IIIa-mAb injection, there was no significant difference in the ITP observed between the anti-CD200R (OX2) mAb treated mice and the control mice (Figure 4.15). It should be noted that previous studies have shown that the OX2 mAb is a CD200R agonist and when used *in vivo* delayed the onset of experimental autoimmune encephalomyelitis (Voulgaraki *et al.* 2005) and lung inflammation following influenza infection in mice (Snelgrove *et al.* 2008) by inhibiting cytokine secretion. These data obtained in the ITP model imply that CD200R does not regulate FcγR-mediated uptake of antibody-coated platelets by phagocytes.

4.3.6 ITP induction by the hamster mAb (1B5) to mouse GpIIb-IIIa involves FcγR and complement-independent platelet disintegration

The mechanism of platelet depletion induced by the hamster mAb (1B5) specific for mouse GpIIb-IIIa used to deplete mice of platelets for the metastasis studies described in Chapter 3, was also studied. As shown in Figure 3.2, this hamster antibody caused

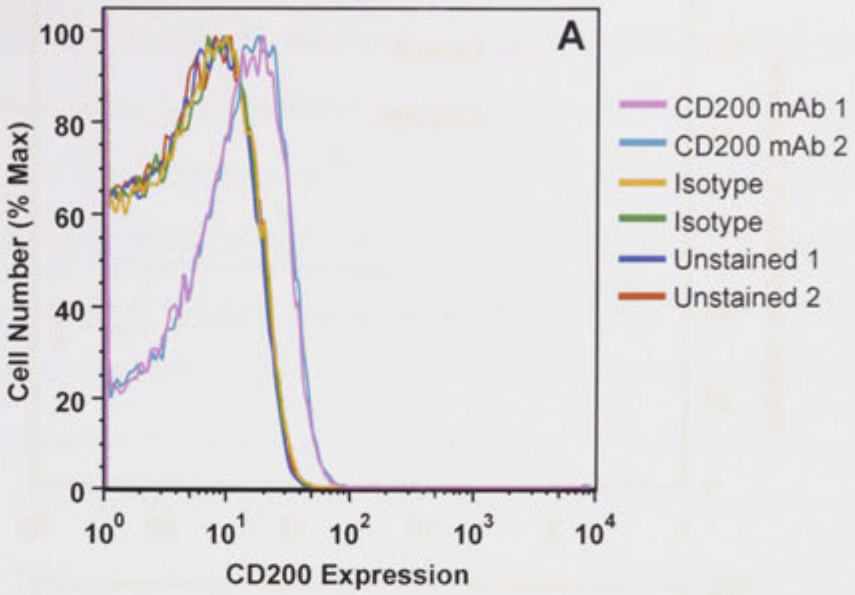

B

Anti-Platelet mAbs	CD200 mAb binding
No mAb	1.7
GpIbα	1.7
GpIIb-IIIa	1.8
GpIa	1.7
GpIX	1.8

Figure 4.14 – The inhibitory ligand CD200 is expressed on the surface of mouse platelets and the level of expression remains unchanged following the binding of various mAbs specific for platelet surface proteins. (A) Whole blood from WT mice was incubated with a PE-conjugated CD200-specific mAb or a PE-conjugated isotype control. Samples were then analysed by flow cytometry. Duplicate histograms for each treatment are shown. **(B)** Isolated platelets were incubated with various mAbs specific for platelet surface proteins for 30 mins at 37°C then incubated with a PE-conjugated CD200-specific mAb or a PE-conjugated isotype control and analysed by flow cytometry for the level of CD200 mAb binding. Data in table represents the level of CD200 mAb binding in the presence of different anti-platelet mAbs expressed as fold-binding vs isotype control.

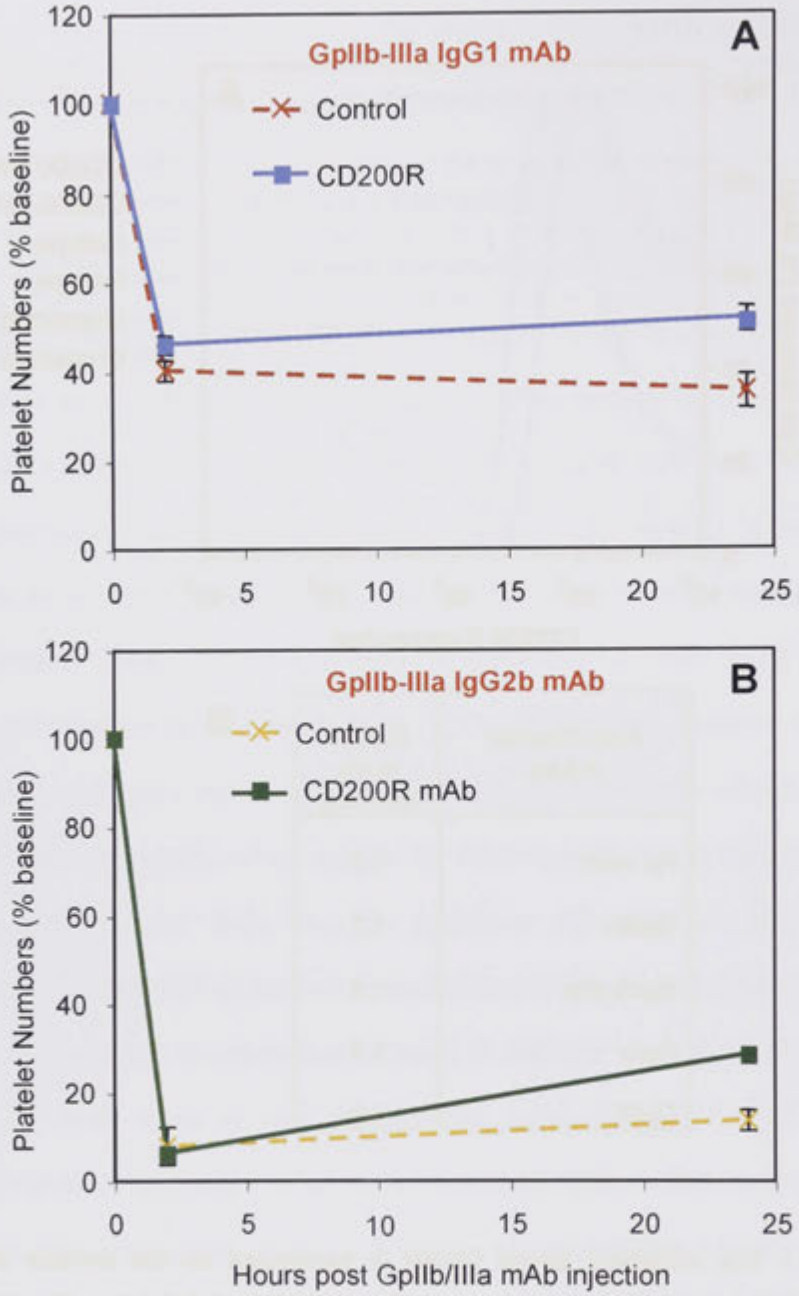

Figure 4.15 – Treatment with a CD200R-specific mAb does not prevent ITP induced by rat IgG1 and IgG2b mAbs specific for GpIIb-IIIa. WT C57BL/6 mice were injected with 50 μg of a CD200R-specific mAb (OX2) 1 hr prior to injection of **(A)** 20 μg of a GpIIb-IIIa-specific IgG1 mAb (n=3) or **(B)** 20 μg of a GpIIb-IIIa-specific IgG2b mAb (n=1). Platelet numbers were measured at 2 hr and 24 hr post GpIIb-IIIa mAb injection. Data for GpIIb-IIIa IgG1 mAb (– –) and GpIIb-IIIa IgG2b mAb (– –) in control mice taken from Figure 4.1.

rapid and extensive depletion of platelets when administered to mice. Experiments were performed to determine the contribution of FcγR, the FcγR regulatory protein, SIRPα, and complement in 1B5-mediated depletion of platelets. WT mice administered 20 μg of the 1B5 mAb experienced platelet reductions of ~95% 2 hr following mAb injection as seen in previous experiments. Administration of 50 μg of the SIRPα-specific mAb 1 hr prior to 1B5 mAb administration did not alter this outcome. When the 1B5 mAb was administered to FcγR-/- mice, 70% of platelets were depleted within 2 hr. This was significantly less depletion than that observed in WT mice ($p<0.005$). When FcγR-/- mice were depleted of C3 using CVF prior to injection of the 1B5 mAb the outcome was essentially unchanged from untreated FcγR -/- mice (Figure 4.16A).

The extent of platelet disintegration induced by the binding of the 1B5 mAb was also examined by incubating washed whole blood with the 1B5 mAb as in Figure 4.7. The platelet activating GpIbα-specific IgG1 mAb and the non-activating GpIIb-IIIa-specific IgG1 mAb were included as controls. The results of this experiment demonstrated that the 1B5 mAb did indeed induce platelet loss similar to, but to a lesser extent than that induced by the GpIbα-specific IgG1 mAb (Figure 4.16B). The 1B5 mAb therefore induces platelet depletion through both FcγR-mediated uptake and complement-independent platelet disintegration.

Figure 4.16 – ITP Induced by the hamster IgG3 mAb (1B5) specific for mouse GpIIb-IIIa occurs through an FcγR unaffected by SIRPα mAb treatment, with complement–independent platelet fragmentation also playing a role. (A) ITP induced by injection (20 μg i.v.) of the hamster GpIIb-IIIa-specific IgG3 mAb, 1B5, in WT mice in the presence or absence of a SIRPα-specific mAb (50 μg i.v.) administered 1 hr earlier, and in FcγR-/- mice either depleted or not depleted of complement by CVF (n=3). Platelet numbers were measured at baseline, 2 hr and 24 hr post injection of the 1B5 mAb. Significant increases in platelet numbers in both complement sufficient or deficient FcγR-/- mice compared to WT mice are shown as *p≤0.05 and **p≤0.005. **(B)** Washed whole blood from WT C57BL/6 mice was incubated with the GpIIb-IIIa-specific hamster IgG3 mAb 1B5, the GpIbα-specific rat IgG1 mAb, or the GpIIb-IIIa-specific rat IgG2b mAb for 30 min at 37°C, washed twice in PBS and then analysed by flow cytometry for a reduction in platelet numbers. Significant reductions in platelet numbers compared to the no mAb control, are shown as *p≤0.05 and **p≤0.005.

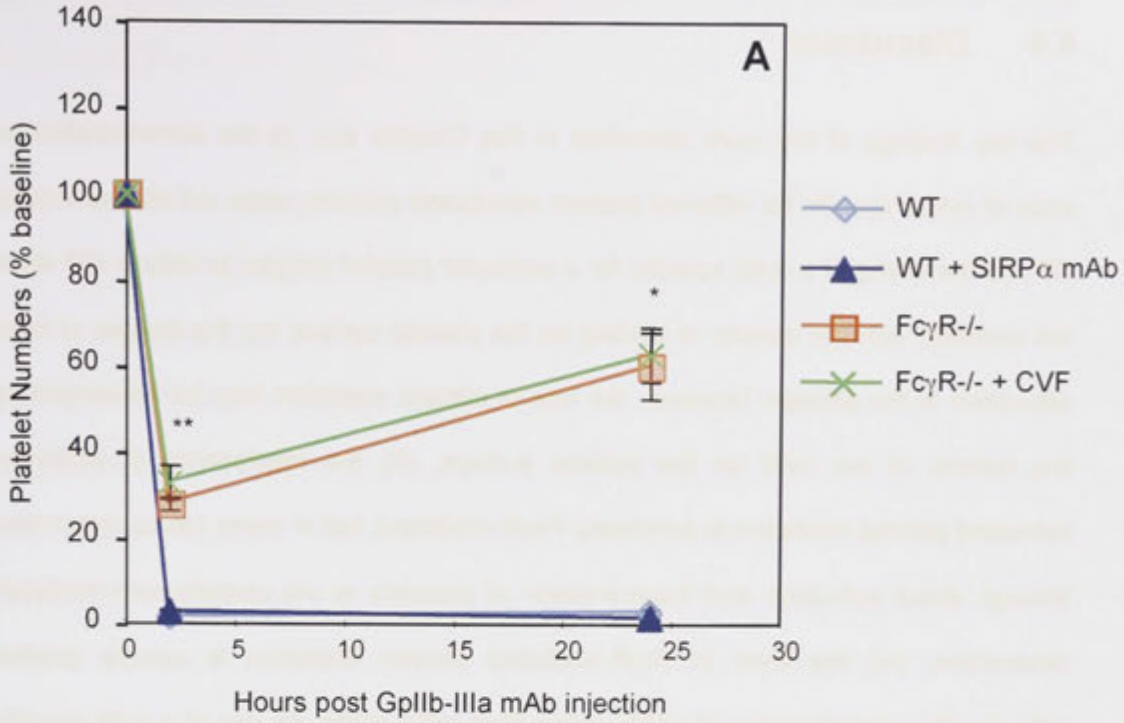
A
Platelet Numbers (% baseline)
140
120
100
80
60
40
20
0
0
5
10
15
20
25
30
Hours post GpIIb-IIIa mAb injection
**
*
WT
WT + SIRPα mAb
FcγR-/-
FcγR-/- + CVF

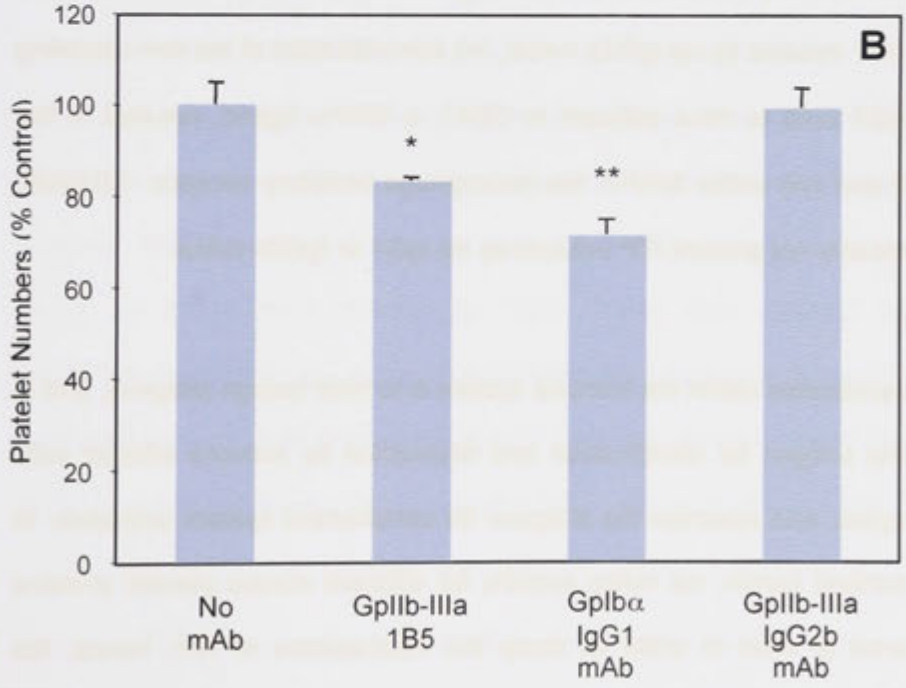
B
Platelet Numbers (% Control)
120
100
80
60
40
20
0
*
**
No mAb
GpIIb-IIIa 1B5
GpIbα IgG1 mAb
GpIIb-IIIa IgG2b mAb

4.4 Discussion

The key findings of the work described in this Chapter are: (i) the administration to mice of mAbs specific for different platelet membrane proteins does not always induce ITP, (ii) the ability of a mAb specific for a particular platelet antigen to induce ITP does not correlate with the density of binding on the platelet surface nor the degree of mAb saturation of the antigen, however, the rate of platelet depletion may be influenced by the density of the mAb on the platelet surface, (iii) the mechanism of antibody-mediated platelet depletion is principally FcγR-mediated, but in some cases may occur through direct activation and fragmentation of platelets or via complement-mediated destruction, (iv) the level of FcγR-mediated platelet depletion is usually greater following the administration of IgG2b mAbs than IgG1 mAbs, (v) use of a mAb specific for the phagocytosis inhibitory protein SIRPα *in vivo* not only prevented, but reversed rat IgG1 mAb induced, FcγR-mediated ITP, although the SIRPα mAb could not prevent FcγR-mediated ITP induced by rat IgG2b mAbs, (vi) administration of the non-depleting GpIX-specific IgG1 mAb to mice deficient in CD47, a SIRPα ligand, resulted in the induction of ITP and (vii) unlike SIRPα, the macrophage inhibitory receptor, CD200R, was found to probably not prevent ITP induced by rat IgG1 or IgG2b mAbs.

The function of antibodies within the immune system is to bind foreign antigens, and in doing so, tag the antigen for identification and destruction by immune effector cells such as phagocytes, and opsonise the antigens for complement system activation. In the studies described herein, rat mAbs specific for different mouse platelet proteins were administered to mice in order to study the mechanisms of ITP, hence, the elimination of antibody-coated self-antigens was under study rather than foreign antigens. Auto-reactive antibodies are a key feature of many autoimmune disorders

and, therefore, the findings of this work are relevant not only to ITP but to all antibody-mediated pathologies.

Three mechanisms of Ab-mediated platelet depletion were identified in these studies. The predominant pathway was found to be FcγR-mediated phagocytosis as ITP induction was inhibited in FcγR-/- mice with the majority of the mAbs under study. The second mechanism of platelet depletion identified was via the direct activation and fragmentation of platelets, a process that was independent of FcγRs, complement, Mac-1 and P-selectin. Antibody-mediated fragmentation of human platelets has previously been reported to occur in response to antibodies specific for CD9, GpIIb-IIIa, GpIV and an additional two unidentified platelet antigens and the mechanism of platelet activation in these studies was demonstrated to occur as a result of Fc:FcR interactions (Horsewood *et al.* 1991). Human platelets express FcR whereas mouse platelets do not (McKenzie 2002). Therefore, from the studies of mouse platelets presented herein, the binding of mAbs to GpIbα would appear sufficient to initiate signalling by this protein resulting in platelet activation and fragmentation. The third mechanism of Ab-mediated platelet depletion was through complement activity, however, this was seen to play a partial role with only one of the antibodies under study, an IgG2b mAb specific for GpIa. These data suggest that complement regulatory proteins on the surface of platelets are effective in preventing complement-mediated lysis and that steric hindrance of these regulatory proteins may have resulted in the complement activity induced by the IgG2b mAb specific for GpIa.

In order to further comprehend the implications of our data, it is necessary to have a thorough understanding of the function of the different FcγRs. Mice express four FcγR subtypes that vary in their interactions with IgG isotypes and may inhibit or activate cellular effector functions (Table 4.3). The nomenclature of the IgG subclasses is not

consistent between species, however, genetic, structural and functional studies have enabled the comparison of mouse and rat IgG subclasses and the FcγR with which they interact (Hulett and Hogarth 1994). Unfortunately, the same information is not available for hamster IgG isotypes. The rat mAbs used in the studies described in this Chapter included the IgG1, IgG2a and IgG2b isotypes. Rat IgG1 and IgG2a are reported to be most similar to murine IgG1 and bind to the murine low-affinity activating receptor, FcγRIII, and the murine low-affinity inhibitory receptor, FcγRIIB (Table 4.3). Rat IgG2b, on the other hand, is reportedly similar to murine IgG2a and binds the high-affinity activating receptor, FcγRI, the low-affinity activating receptor, FcγRIII, the low-affinity inhibitory receptor FcγRIIB, and, most likely, the recently identified intermediate-affinity activating receptor, FcγRIV (Nimmerjahn *et al.* 2005). The response of the effector cell is determined by the balance of the activation and inhibitory signals received via the different FcγRs (Ravetch and Bolland 2001).

Table 4.3: Murine Fcγ Receptors and Their Interactions

FcγR subclass	Effector Function	Mouse IgG Isotypes Bound	Equivalent Rat Isotype/s
I	Activating	IgG2a (high affinity)	IgG2b
IIB	Inhibitory	IgG1, IgG2b, IgG2a (low affinity)	IgG1, IgG2a, IgG2b
III	Activating	IgG1, IgG2b, IgG2a (low affinity)	IgG1, IgG2a, IgG2b
IV	Activating	IgG2a and IgG2b (intermediate affinity)	IgG2b (?)

Table generated from data presented in Fridman, 1991, Goding, 1996, and Nimmerjahn et al, 2005.

In the ITP studies described herein, a greater extent of FcγR-mediated platelet depletion was observed when IgG2b mAbs specific for GpIIb-IIIa and GpIa were administered to mice than was seen with their IgG1 counterparts. This result is consistent with the notion that rat IgG2b mAbs bind the murine high-affinity FcγR whereas IgG1 mAbs bind the low-affinity activating receptor, thus, a much stronger pro-phagocytic signal occurs in response to IgG2b mAbs. As platelets are flowing in the bloodstream past FcγR-bearing effector cells, high-affinity Fc:FcγR binding would more likely result in a sustained interaction between platelets and effector cells. In contrast, low-affinity Fc:FcγR binding may result in platelet release from the effector cell, although this is less likely if multiple low-affinity interactions occur. This effect may explain the different rates of platelet depletion observed when mice were administered the IgG1 mAbs specific for GpIIb-IIIa and GpIa. As GpIIb-IIIa is present on the surface of platelets in very high numbers, when bound by IgG1 mAbs, multiple low-affinity interactions with the effector cells would promote a sustained interaction with rapid platelet clearance. GpIa-IIa, however, is present on the platelet surface in low numbers and, therefore, interactions with low-affinity FcγR would be fewer in number, and, therefore, less likely to be sustained, resulting in a reduced rate of platelet clearance.

The lack of ITP induction observed following the administration of some IgG1 mAbs implied that platelet clearance by FcγRs was being inhibited. As platelet-depleting and non-platelet-depleting mAbs were of the same isotype, the potential mechanism of inhibition was considered to be other than inhibitory FcγR. Having demonstrated that the non-ITP inducing mAbs were binding to the platelet surface, in the case of the GpIX-specific mAb to a greater level than the ITP-inducing mAbs, we hypothesised that the gain or loss of a secondary signal on the platelet surface must also be required to trigger phagocytosis.

The self-recognition, inhibitory protein pairs CD47:SIRPα and CD200:CD200R were considered as possible regulators of FcγR-mediated depletion of antibody-coated platelets and, therefore, were investigated. It is useful to review the current understanding of the role of these regulatory protein pairs in the context of platelets and ITP, in order to better understand the implications of the data. CD47, also known as the integrin-associated protein (IAP), is a widely expressed membrane protein and present on the surface of platelets in association with GpIIb-IIIa (αIIbβ3) and GpIa-IIa (αIIβ1) (Chung *et al.* 1997; Chung *et al.* 1999). The receptor for CD47, SIRPα, is expressed on hematopoietic stem and/or progenitor cells, monocytes, granulocytes, and dendritic cells (Seiffert *et al.* 2001). CD47:SIRPα signalling in macrophages results in the activation of SHP-1 phosphatase which dephosphorylates myosin IIA preventing the formation of a phagocytic cup (Tsai and Discher 2008). The SIRPα:CD47 interaction has been demonstrated to regulate the half-life of platelets, with CD47-/- and SIRPα mutant mice having a shorter platelet lifespan than WT mice (Yamao *et al.* 2002; Olsson *et al.* 2005). Furthermore, CD47-/- mice were more sensitive to Ab-mediated ITP than wild-type mice when injected with a mouse IgG1 mAb, known as 6A6, to an unidentified platelet antigen. *In vitro* experiments using IgG opsonised platelets demonstrated an enhanced uptake of CD47-/- platelets, however, when SIRPα was blocked using a specific mAb, the rate of uptake of WT platelets increased to that of CD47-/- platelets (Olsson *et al.* 2005). A further piece of evidence implicating CD47 in the regulation of ITP was the finding that in a mouse model of ITP induced by shiga-toxin producing *E. coli* infection, CD47 expression on platelets was downregulated (Guo *et al.* 2009). CD200 is a member of the Ig superfamily and is expressed on thymocytes, neurons, endothelium, follicular dendritic cells in all lymphoid organs, a subset of CD34+ progenitor cells and at low levels on some smooth muscle cells and B lymphocytes. It is reportedly expressed in very low levels or absent on NK cells, monocytes, granulocytes and platelets in humans (Kretz-Rommel *et al.*

2008) but we found detectable levels of the protein on mouse platelets. The interaction between CD200 and CD200R inhibits the activation of, and cytokine secretion by granulocytes and macrophages (Hoek *et al.* 2000). To our knowledge, the role of CD200R in the inhibition of phagocytosis, has not been studied.

Following the demonstration that expression of CD47 on platelets was not reduced subsequent to the binding of the various IgG1 mAbs to platelet antigens, we hypothesised that steric hindrance of the interaction between CD47 and SIRPα, caused by antibody binding, was likely determining whether an IgG1 mAb caused platelet depletion or not, and that steric hindrance was more likely to occur with mAbs specific for proteins with which CD47 is closely associated. The data supports this hypothesis in that the IgG1 mAbs to GpIIb-IIa and GpIa, with which CD47 is known to associate, induced the most marked FcγR-mediated ITP. Furthermore, when CD47-/- mice were administered the non-platelet depleting GpIX-specific IgG1 mAb a significant reduction in platelet numbers of ~50% was observed. GpIX is a non-integrin and is not known to be associated with CD47. Consequently, binding of the mAb specific for this protein would not hinder the interaction between CD47 and SIRPα in WT mice. It is intriguing that a slow reduction over 24 hr in platelet numbers to 50% baseline was observed in the CD47-/- mice rather than a rapid reduction within 2 hr as seen with the GpIIb-IIIa-specific IgG1 mAb. This suggests that despite the significant level of binding of the GpIX-specific mAb to the platelet surface, only a proportion of these mAb are able to interact with FcRs. When reviewing the structure of the GpIb-IX-V complex (Figure 4.17), it is feasible that the large ectodomains of the 2 GpIbα chains impeded the interaction between bound GpIX-specific mAbs and FcγRs. This factor may also explain why the GpV-specific IgG1 and IgG2a mAbs were weak and non-depletors, respectively, in WT and also in CD47-/- mice. An alternative explanation for the partial induction of ITP by the GpIX-specific IgG1 mAb in CD47-/- mice and the lack

of ITP induction by the mAbs specific for GpV is the presence of additional inhibitory mechanisms controlling phagocytosis. This inhibitory effect may be due to differential binding of the mAbs to FcγRIIB. Although this was initially considered unlikely as the mAbs were of the same isotype, it is possible that differences in the glycosylation of the mAbs influences their binding affinity for the inhibitory FcγR (Raju 2008). It is interesting to note that BALB/c mice administered the IgG1 mAbs to GpV, GpIa and PECAM-1 had more severe ITP than that observed in C57BL/6 mice receiving these mAbs, suggesting strain differences in the expression of inhibitory FcγR or polymorphisms affecting their function (Jiang *et al.* 2000). To summarise this section, it is suggested that the lack of ITP induction by some anti-platelet IgG1 mAbs may have been due to the inability of Fc:FcR interactions to occur due to steric hindrance imposed by neighbouring surface proteins, differences between the mAbs in their affinity for inhibitory FcγR, and/or due to the ability of CD47:SIRPα interactions to occur thus inhibiting phagocytosis.

As ITP induction by an anti-platelet IgG1 mAb appeared to be determined by the balance of activating and inhibitory phagocytosis signals delivered via FcγRs and SIRPα, we investigated the possibility of preventing Ab-mediated ITP induction by pushing the balance towards an inhibitory phagocytosis signal. It has been previously observed that the *in vivo* administration of mAbs specific for receptors or their ligands may result in the activation of the receptor through cross-linking (Boyman *et al.* 2008). This appeared to be the case with the mAb specific for SIRPα as mice pre-treated with this antibody were resistant to ITP following administration of the IgG1 mAbs specific for GpIIb-IIIa and GpIa, in C57BL/6 mice, and GpV, in BALB/c mice. Treatment with the SIRPα mAb could not only prevent but also reverse IgG1 mAb-induced ITP.

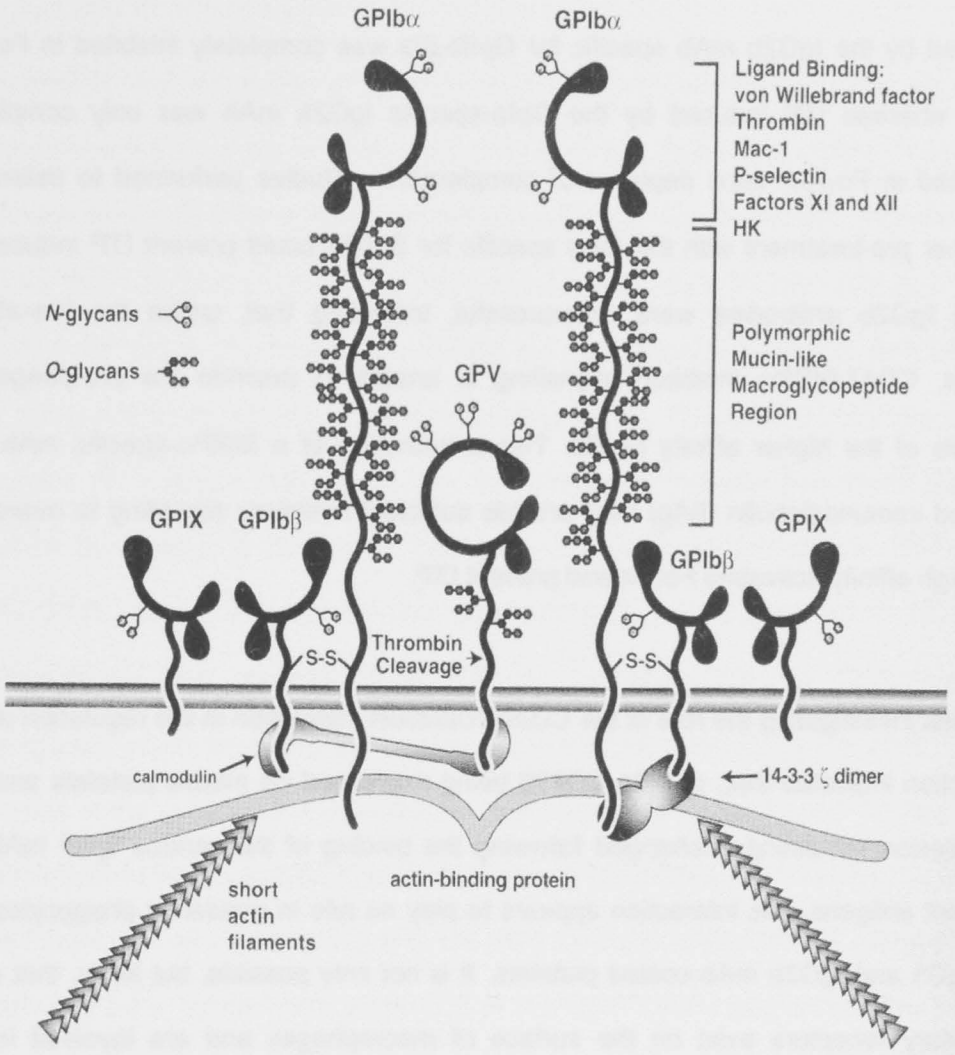

Figure 4.17: Structure of the GpIb-IX-V complex.

From Lopez, JA & Berndt, MC. *Platelets,* Elsevier Academic Press, 2002.

The IgG2b mAbs specific for GpIIb-IIIa and GpIa induced a greater level of platelet depletion than their IgG1 counterparts, probably due to high-affinity FcγR binding. ITP induced by the IgG2b mAb specific for GpIIb-IIIa was completely inhibited in FcγR-/- mice whereas ITP induced by the GpIa-specific IgG2b mAb was only completely inhibited in FcγR-/- mice depleted of complement. Studies performed to determine whether pre-treatment with the mAb specific for SIRPα could prevent ITP induced by these IgG2b antibodies were unsuccessful, indicating that, unlike the low-affinity FcγRs, CD47:SIRPα inhibitory signalling is unable to override the pro-phagocytic signals of the higher affinity FcγRs. The combination of a SIRPα-specific mAb with pooled immunoglobulin (IVIg) may provide sufficient inhibitory signalling to overcome the high affinity activating FcγRs and prevent ITP.

Studies investigating the role of the CD200:CD200R interaction in the regulation of ITP induction indicated that, despite CD200 being expressed on mouse platelets and this expression remaining unchanged following the binding of the various IgG1 mAbs to platelet antigens, this interaction appears to play no role in regulating phagocytosis of rat IgG1 and IgG2b mAb-coated platelets. It is not only possible, but likely, that other inhibitory receptors exist on the surface of macrophages and are involved in the regulation of phagocytosis induced by high-affinity FcγR engagement.

The hamster anti-mouse GpIIb-IIIa mAb, 1B5, belongs to the IgG3 isotype and was used in Chapter 3 to deplete mice of platelets for tumour metastasis studies. The relationship between hamster IgG isotypes and murine isotypes is unknown, however, data described in this Chapter demonstrated that platelet depletion induced by the 1B5 mAb occurs partially via complement independent platelet fragmentation and partially via FcγR-mediated phagocytosis. As 1B5 induced FcγR-mediated uptake could not be

prevented through pre-treatment with the SIRPα-specific mAb, this suggests the antibody binds to high-affinity FcγRs.

In conclusion, the destruction of antibody-bound platelets principally occurs via FcγR-mediated phagocytosis but may also occur through complement-mediated destruction or through an FcγR- and complement-independent process of platelet fragmentation. Use of a SIRPα-specific mAb *in vivo* can prevent or reverse IgG1 mAb-induced, FcγR-mediated ITP but is insufficient to override the pro-phagocytic signals delivered by IgG2 mAbs interacting with high-affinity activating FcγRs. The ligand for SIRPα, CD47, is present on platelets associated with the integrins GpIIb-IIIa and GpIa thus an attractive hypothesis is that mAb binding to these proteins sterically inhibit the SIRPα:CD47 interaction thereby removing the inhibitory phagocytosis signal. Based on this hypothesis, the capacity of an antibody to induce ITP via FcγR-mediated phagocytosis would, therefore, be determined in the first instance by the ability of the Fc portion of the antibody to overcome physical barriers and interact with FcγRs; in the second instance by the isotype and glycosylation of the mAb and, therefore, the affinity of the FcγRs with which it binds; and in the third instance, in the case of mAbs binding low-affinity FcγRs, by the steric hindrance of the CD47:SIRPα interaction. The results of these studies provide a greater understanding of the pathogenic pathways of ITP and how the self-recognition system, expressed by phagocytic cells may be manipulated to prevent antibody-mediated tissue damage.

Chapter 5

Monitoring platelet and erythrocyte lifespan kinetics using *in vivo* CFSE labelling

5.1 Abstract

The factors determining platelet and erythrocyte lifespan are not completely understood despite extensive study. The lack of success may be attributed to the methods used to measure lifespan kinetics, all of which require processing of cells prior to analysis, and the inconsistent and potentially inappropriate use of mathematical models for data analysis. The aims of this study were to establish an *in vivo* platelet and erythrocyte labelling method using CFSE, determine the most appropriate mathematical model for lifespan analysis, and apply both to the study of factors that control platelet and erythrocyte lifespans. Control and platelet-deficient *c-mpl-/-* and Bcl-X_L mutant mice were injected with CFSE and platelet and erythrocyte fluorescence followed over time. Data sets were analysed using linear, exponential, multiple-hit and lognormal mathematical models. It was found that *in vivo* CFSE labelling of platelets and erythrocytes requires no post-collection processing, proved to be stable, non-toxic and non-immunogenic, and the lifespans obtained were highly reproducible. Mathematical modelling revealed the lognormal model gave a robust fit to control and extreme data sets when either extrinsic or intrinsic factors determined lifespan. Using these methods, platelet lifespans were found to be significantly shortened in thrombopoietin-receptor deficient mice independent of blood loss, and the anti-apoptotic protein Bcl-X_L was shown to play a role in prolonging erythrocyte lifespans. Thus, the simultaneous study of platelet and erythrocyte lifespans using *in vivo* CFSE labelling with lognormal modelling yielded insights into common intrinsic and extrinsic platelet and erythrocyte lifespan determinants and provides an improved methodology for use in this field of research.

5.2 Introduction

The work described in this chapter arose when attempting to deplete mice of platelets for the purpose of tumour cell metastasis studies. Subsequent to the administration of an antibody treatment that we anticipated would reduce platelet numbers in mice, an unexpected increase in platelet numbers was observed. It was not clear whether the treatment had induced an increase in platelet production from the marrow or whether it had prolonged the lifespan of platelets within the bloodstream. Upon reading the literature, it became apparent that little progress had been made in identifying factors that determine the production, lifespan and destruction of platelets and it occurred to us that this lack of progress may be due to deficiencies in the methodologies available for measuring these parameters. It also became clear that prior work in this area focused on either platelet- or erythrocyte lifespans but not both despite the likelihood of there being molecular pathways common to both and the potential for one to affect the other. We, therefore, set out to establish a new method for the simultaneous *in vivo* labelling and tracking of platelets and erythrocytes, and to determine the most appropriate mathematical model for the analysis of platelet and erythrocyte lifespan data.

Previously, lifespan measurements have been achieved using radioisotopes, biotin-labelling or labelling with fluorescent compounds (Van Putten 1958; Goodman and Smith 1961; Hoffmann-Fezer *et al.* 1991; Heilmann *et al.* 1993; Michelson *et al.* 1996; Baker *et al.* 1997). The shortcomings of methods using radioisotopes include the risks to researchers associated with radiation and the difficulty of its disposal. Furthermore, methods that require *in vitro* labelling of isolated cells of interest prior to injection into the animal may cause cellular damage or activation that have the potential to influence lifespan. Biotin labelling *in vivo* has overcome these problems, but post-collection fluorescent labelling and centrifugation is required prior to analysis. Additionally, as biotin labels cell surface proteins there is the potential for interference with normal

function (Magnusson *et al.* 1998). Biotin has also been demonstrated to be highly immunogenic inducing anti-biotin antibodies, therefore, studies repeated in the same animal may be compromised (Berger 1975; Dale *et al.* 1994; Muzykantov *et al.* 1996).

In addition to the shortcomings of the labelling techniques mentioned above, published mathematical models for the analysis of platelet and erythrocyte survival data are numerous, of questionable suitability and applied inconsistently, thus comparisons between studies are difficult to perform (Lotter *et al.* 1986; Hoffmann-Fezer *et al.* 1993; Baker *et al.* 1997; Mason *et al.* 2007). The multiple-hit model (MHM) is recommended for use when analysing platelet survival data by the International Committee for Standardization in Hematology (1988), although it was not recommended for use when platelet survival time was very short (Lotter *et al.* 1986). The MHM assumes that lifespan is determined by the number and rate of damaging hits that platelets receive within the circulation (Murphy and Francis 1971). However, the advent of ENU (*N*-ethyl-*N*-nitrosourea) mutagenesis and genetically modified animals has resulted in the identification of intrinsic factors, such as pro- and anti-apoptotic proteins, that play a role in determining platelet lifespan kinetics (Carpinelli *et al.* 2004; Mason *et al.* 2007). Thus, a mathematical model that makes no prior assumptions about biological events and that is suitable for use with a diversity of survival times is preferable, as is a rapid and cost-effective method for the screening of lifespans in mutant animals to hasten progress in this field of research.

This chapter describes a safe, easy, reliable and cost-effective method for simultaneous *in vivo* labelling and measurement of platelet and erythrocyte lifespans and the application of this method in wild type, *c-mpl-/-* and Bcl-X_L mutant mice. The method is based on carboxyfluorescein diacetate succinimidyl ester (CFSE), a fluorescent dye that covalently links to intracellular molecules and overcomes the problems associated with previous labelling procedures (Quah *et al.* 2007). CFSE

labelling allows the simultaneous identification of both aged and young platelets or erythrocytes, and since it is non-immunogenic, allows repeat studies in the same animal to be performed. Mathematical modelling of the survival data obtained using the CFSE labelling procedure in the wild type and mutant mouse strains revealed that the lognormal model very accurately fits platelet and erythrocyte data, even when survival times were very short and, moreover, when lifespans were dictated by either cell intrinsic or extrinsic factors. The simultaneous analysis of platelet and erythrocyte lifespans in wild type, *c-mpl-/-* and Bcl-X_L mutant mice revealed that a lack of thrombopoietin signalling, known to dramatically reduce platelet production, was shown to also significantly shorten platelet lifespans independent of blood loss, and reduced Bcl-X_L signalling was demonstrated to decrease erythrocyte lifespans in conjunction with the previously established reduction in platelet lifespans.

5.3 Results

5.3.1 *In vivo* CFSE labelling of platelets and erythrocytes is stable, non-toxic and non-immunogenic

Initial studies investigated whether CFSE, a fluorescent dye that has been used extensively to label lymphocytes and follow their migration and proliferation, could be administered *in vivo* to label erythrocytes and platelets. A simple FSC/SSC gating strategy was used to identify platelets and erythrocytes with a PE-conjugated anti-GpIIb/IIIa antibody confirming platelet identity and reference beads being used to quantify platelet and erythrocyte numbers (Figure 5.1A). It was found that the intravenous injection of mice with CFSE resulted in the fluorescent labelling of platelets and erythrocytes present in the bloodstream at the time of injection (Figure 5.1B and 5.1C). Fluorescent labelling of both platelets and erythrocytes was highly stable

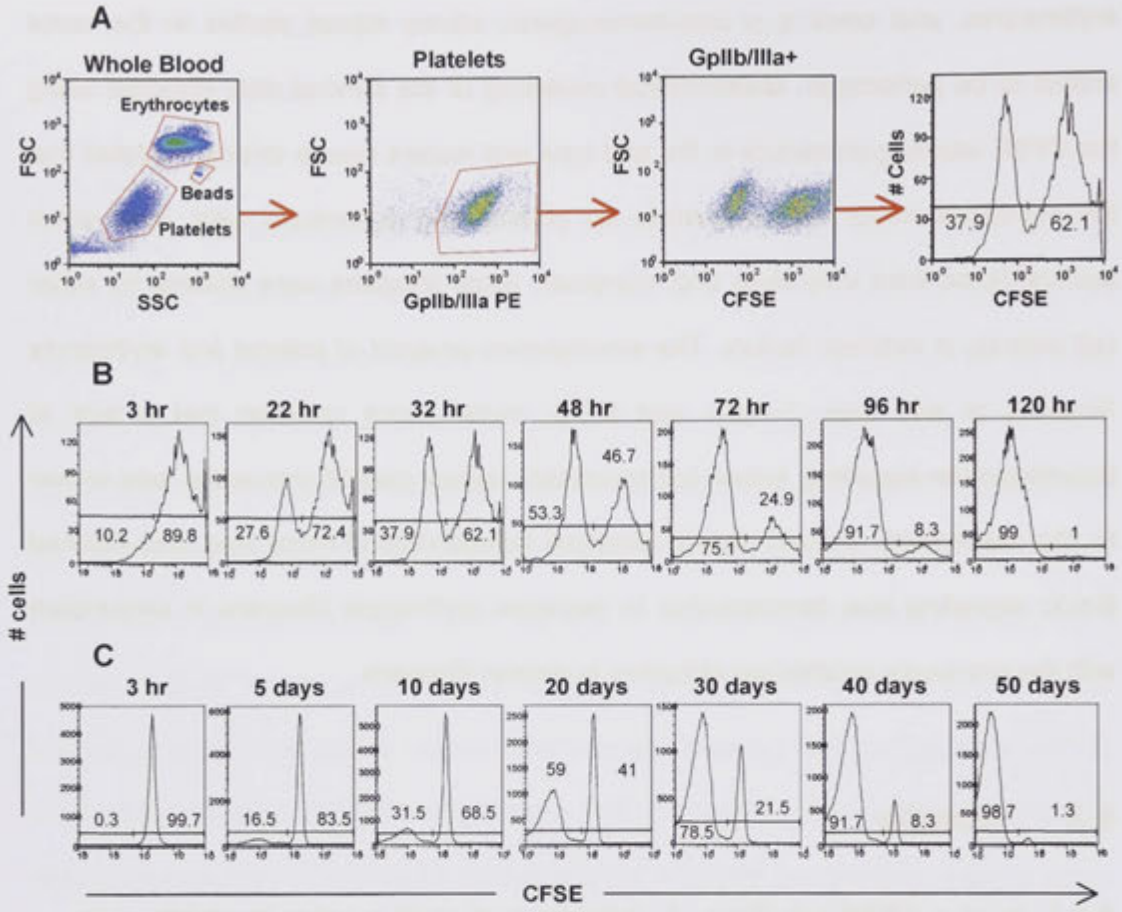

Figure 5.1: Flow cytometry analysis of carboxyfluorescein diacetate succinimidyl ester (CFSE)-labelled platelets and erythrocytes in mice for determination of lifespan. Following intravenous injection of CFSE into C57BL/6 mice, anticoagulated blood was collected at various time points, exposed to a phycoerythrin (PE)-conjugated monoclonal antibody to GpIIb-IIIa and analysed by flow cytometry. **(A)** Gating strategy for platelets using forward (FSC) and side scatter (SSC) parameters and GpIIb-IIIa-PE staining. CFSE bright and dull populations were then determined (data shown for 32 hours post-CFSE injection). **(B)** Characteristic CFSE profiles obtained with platelets at 3 hours to 120 hours following CFSE injection, demonstrating the appearance of a CFSE dull peak and the diminution of the CFSE bright peak. **(C)** Characteristic profiles obtained with erythrocytes. Numbers in flow cytometry histograms represent percentage of platelets **(B)** or erythrocytes **(C)** that are CFSE dull or CFSE bright.

allowing platelets to be tracked for 5 days (Figure 5.1B) and erythrocytes for 50 days (Figure 5.1C) post labelling. Furthermore, platelets and erythrocytes released from the bone marrow subsequent to the CFSE injection had a substantially lower level of CFSE fluorescence, thus enabling measurement of the rates of production and destruction of each cell type and allowing lifespans to be easily determined (Figure 5.1B and 5.1C). Mice were kept for 8 months following CFSE injection with no evidence of ill-health. Additionally, histological examinations performed by a pathologist at 1 and 10 days post CFSE injection showed no evidence of renal or hepatic toxicity. In a group of mice receiving a subsequent injection of CFSE 12 weeks after the first, an identical erythrocyte lifespan was obtained thus demonstrating the reproducibility of the labelling method and, importantly, the lack of immunogenicity of CFSE in C57BL/6 mice (Figure 5.2).

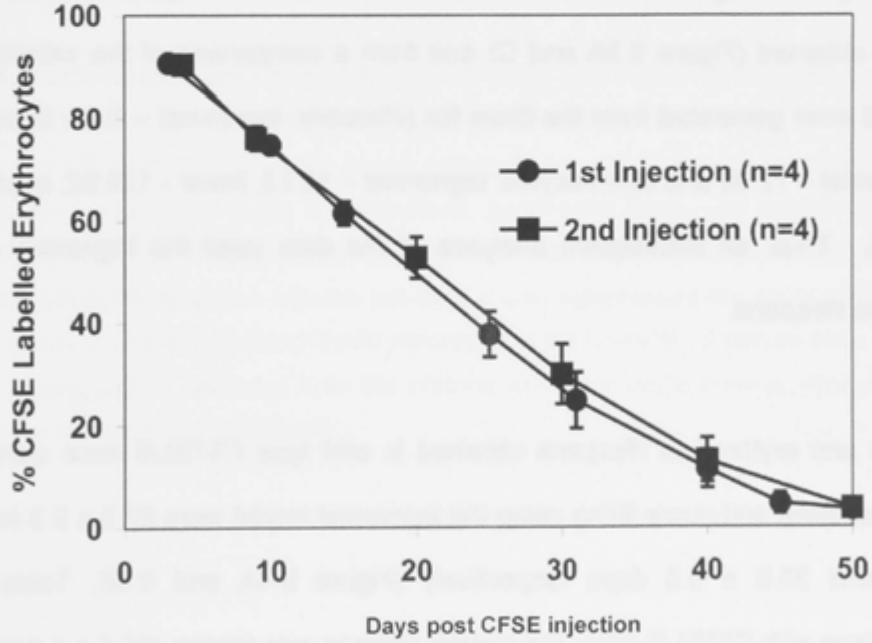

Figure 5.2: Reproducibility and lack of immunogenicity of the *in-vivo* CFSE-labelling procedure. C57BL/6 mice were given a second intravenous injection of CFSE 12 weeks after the first injection. Percentage of CFSE bright erythrocytes was determined at each time point following CFSE injection as outlined in Figure 5.1. The mean percent of CFSE bright erythrocytes for all mice is shown with error bars representing the standard error of mean (n=4).

5.3.2 Platelet and erythrocyte lifespans in wild type and platelet-deficient mouse strains

The availability of highly accurate platelet and erythrocyte tracking data, obtained using the CFSE-labelling method, allowed us to analyse various mathematical models of platelet and erythrocyte lifespans. Model fits to the percentage of CFSE labelled platelets and erythrocytes in C57BL/6 mice assuming a linear fit (yellow), exponential fit (red) and lognormal model (green) are shown in Figure 5.3A (platelets) and Figure 5.3C (erythrocytes). The corresponding lifespan distributions of platelets are shown in Figure 5.3B and of erythrocytes in Figure 5.3D. It is clear that the lognormal model is superior to both the exponential and linear fits for both the platelet and erythrocyte data sets as it is able to capture both the initial linear decrease (which an exponential function cannot capture) and the curved tail (which is missed by a linear fit). The superiority of the lognormal model is clear both from a visual inspection of the quality of the fits obtained (Figure 5.3A and C) and from a comparison of the weighted mean squared error generated from the three fits (*Platelets*: lognormal – 0.45; linear – 8.90; exponential – 72.92 and *Erythrocytes*: lognormal – 13.73; linear - 126.62; exponential – 718.72). Thus, all subsequent analyses of the data used the lognormal model to calculate lifespans.

Platelet and erythrocyte lifespans obtained in wild type C57BL/6 mice using *in vivo* CFSE labelling and curve fitting using the lognormal model were 87.2 ± 2.3 hr (mean ± SEM) and 35.0 ± 0.5 days respectively (Figure 5.4A and 5.4E; Table 5.1). In comparison with C57BL/6 mice, the platelet lifespan was shorter (67.7 ± 1.8 hr) and the erythrocyte lifespan was longer (42.5 ± 0.4 days) in BALB/c wild type mice (Figure 5.4B and 5.4E; Table 5.1) demonstrating that significant strain-specific differences in lifespans can occur. It should be noted that the lifespan values obtained using the CFSE labelling technique are highly reproducible between experiments (15 x C57Bl/6

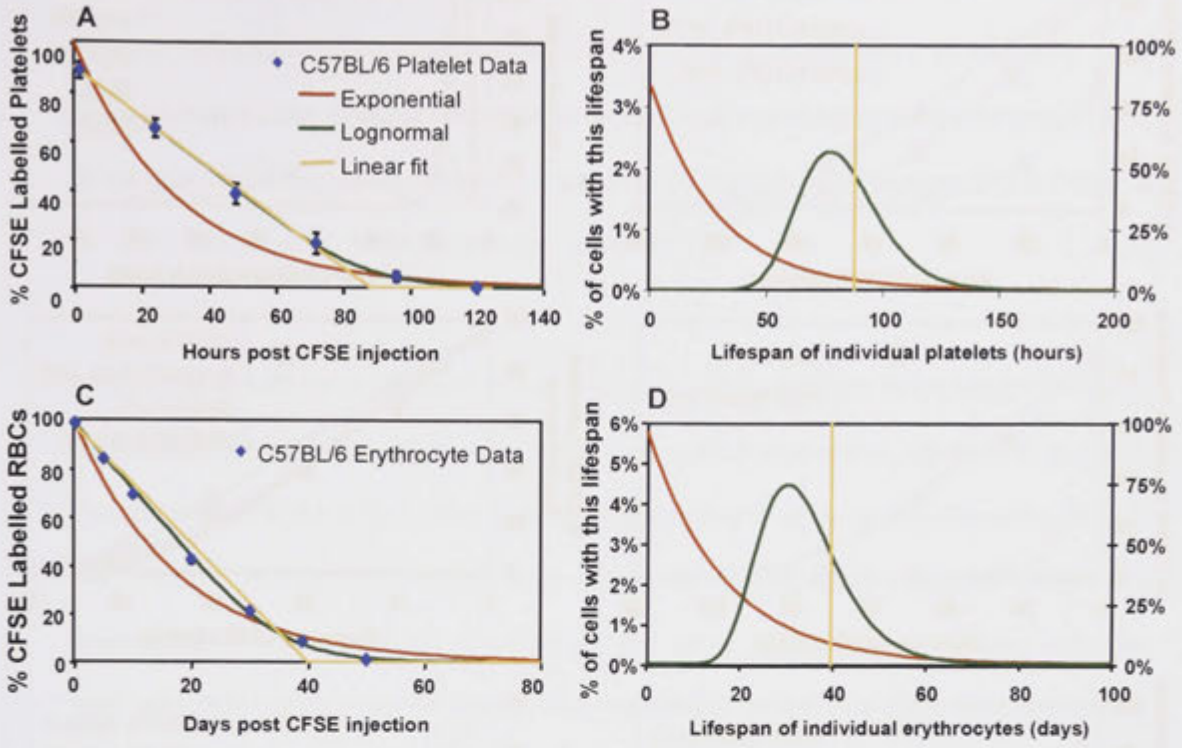

Figure 5.3: Mathematical modelling of labelled platelet and erythrocyte (RBC) data from wild-type C57BL/6 mice. Mean values for proportion of labelled platelets **(A)** and erythrocytes **(C)**, present in C57BL/6 mice following *in-vivo* carboxyfluorescein diacetate succinimidyl ester (CFSE) labelling, were fitted using linear (yellow), exponential (red), and lognormal (green) distribution models. The lifespan distribution obtained with these models is shown in **(B)** for platelets and **(D)** for erythrocytes with the left-hand Y-axis representing the exponential fit and lognormal model, and the right-hand Y-axis representing the linear fit. It can be seen that the lognormal model gave a superior fit to the platelet and erythrocyte survival data and was therefore used for subsequent analyses.

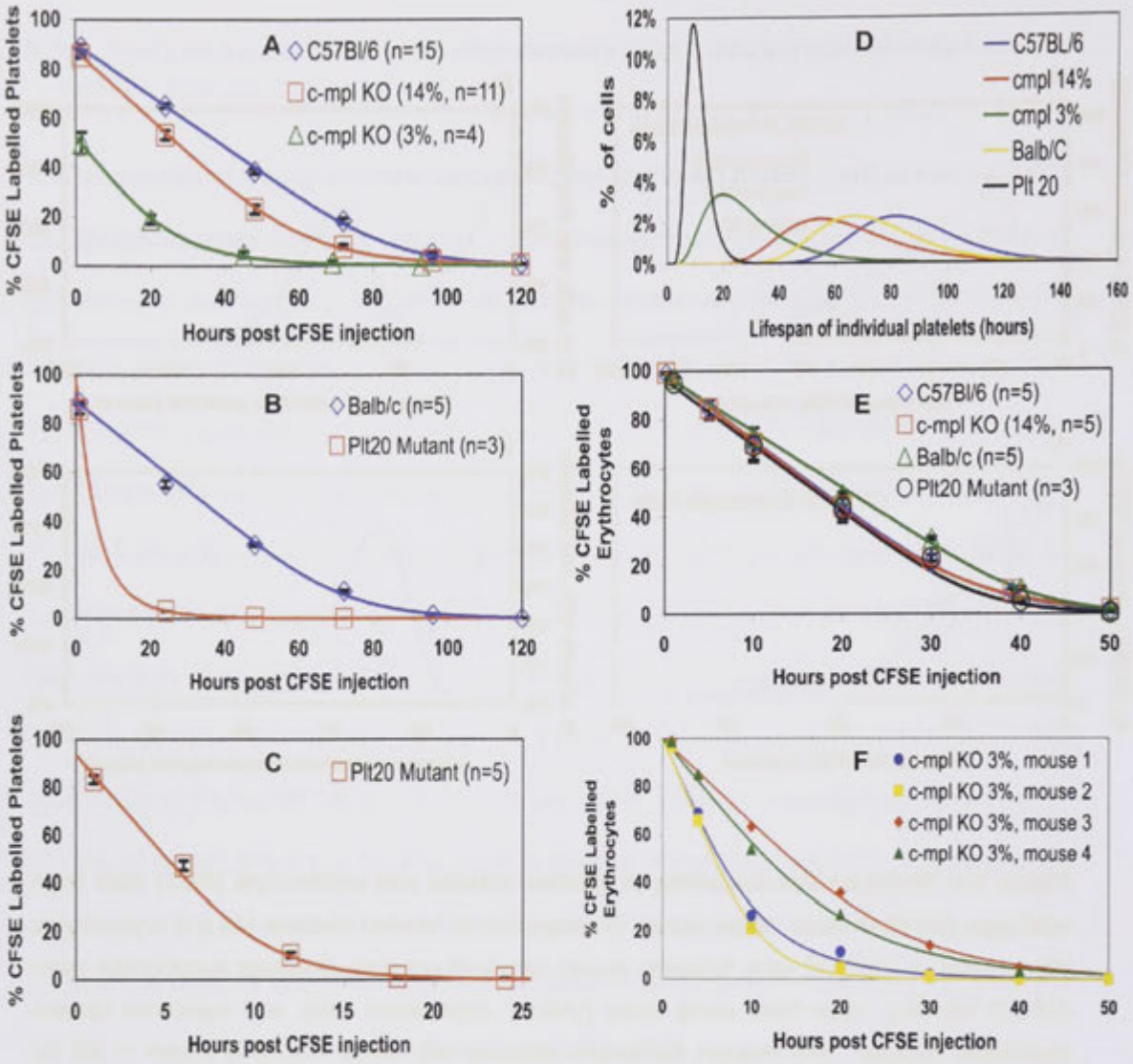

Figure 5.4: Lognormal modelling of labelled platelet and erythrocyte survival data in wild-type, *c-mpl* knockout (KO), and Plt20 mutant mouse strains. Mice received an intravenous injection of carboxyfluorescein diacetate succinimidyl ester (CFSE) and blood samples were collected at the time points indicated in each X axis. Platelets and erythrocytes were identified and counted by flow cytometry as in Figure 5.1, and the CFSE-labelled populations of each followed over time. The lognormal model was applied to the data to generate the curves shown in this figure and to estimate mean lifespans (Table 5.1). Mean values of experimental groups are shown with error bars representing standard error of mean. (**A**) Labelled platelet data over 5 days in wild-type C57BL/6 mice, c-mpl KO mice with mean platelet levels 14% that of controls, and c-mpl KO mice with mean platelet levels 3% that of controls. (**B**) Labeled platelet data in wild-type BALB/c and BALB/c Plt20 mutant mice (platelets 30% that of control levels) during a 5-day period. (**C**) Labelled platelet data in Plt20 mutant mice during a 24-hours period. (**D**) Platelet lifespan distribution calculated using the lognormal model with datasets for wild-type C57BL/6, c-mpl KO (platelets 14% and 3% normal) and Plt20 mutant mice. (**E**) Labelled erythrocyte data in wild-type C57BL/6, *c-mpl* KO (platelets 14% normal), wild-type BALB/c and BALB/c Plt20 mutant mice. (**F**) Labelled erythrocyte data for individual c-mpl KO mice (platelets 3% normal).

mice in Figure 5.4A representing 3 separate experiments) and are within the range of lifespan values previously published, although these values vary significantly most probably due to the different methodologies and mouse strains used (Van Putten 1958; Goodman and Smith 1961; Abbrecht and Littell 1972; Ault and Knowles 1995; Baker *et al.* 1997; Berger *et al.* 1998; Marinkovic *et al.* 2007).

In contrast to wild type C57BL/6 mice, in *c-mpl-/-* mice that lack thrombopoietin (TPO) receptors, platelet and erythrocyte lifespans varied depending upon the baseline platelet levels of the mice. Two phenotypes commonly arise within the same litter of the *c-mpl-/-* mouse strain, one with extremely low platelet numbers which are approximately 3% of normal levels, and the other with platelet numbers that are approximately 14% of normal levels. This phenotypic variation is not genetically stable as the breeding of mice with extremely low platelet levels results in offspring with platelet numbers either 3% or 14% of normal. The explanation for this variation is unknown and has been observed by others (personal communication Dr Ben Kile, WEHI, Australia).

Mice with platelet levels 14% that of wild type controls had a substantially shorter mean platelet lifespan (61.8 ± 2.9 versus 87.2 ± 2.3 hr), a difference that was highly significant ($p < 0.0001$)(Figure 5.4A, Table 5.1). In contrast, the mean erythrocyte lifespan in these mice was not significantly different from control values (36.4 ± 1.4 versus 35.0 ± 0.5 days)(Figure 5.4E, Table 5.1), indicating that the shortened platelet lifespan in these mutant mice is due to an intrinsic defect resulting from a lack of c-mpl signalling and not due to blood loss. Platelet lifespans in *c-mpl-/-* mice with very low (3% of control) endogenous platelet numbers had an even shorter mean platelet lifespan (32.1 ± 6.6 versus 87.2 ± 2.3 hr, $p < 0.0001$), which was accompanied by a significantly ($p<0.02$) reduced erythrocyte lifespan (18.7 ± 4.1 days compared with 35.0 ± 0.5 days), a result indicative of blood loss (Figures 5.4A and 5.4F, Table 5.1). Thus,

in these highly thrombocytopenic mutant mice, platelet lifespan is determined by both extrinsic and intrinsic factors. Platelet production in *c-mpl-/-* mice was, as would be expected, dramatically reduced when compared with wild type mice (Figure 5.5A), but no impairment in erythrocyte production was seen (Figure 5.5B).

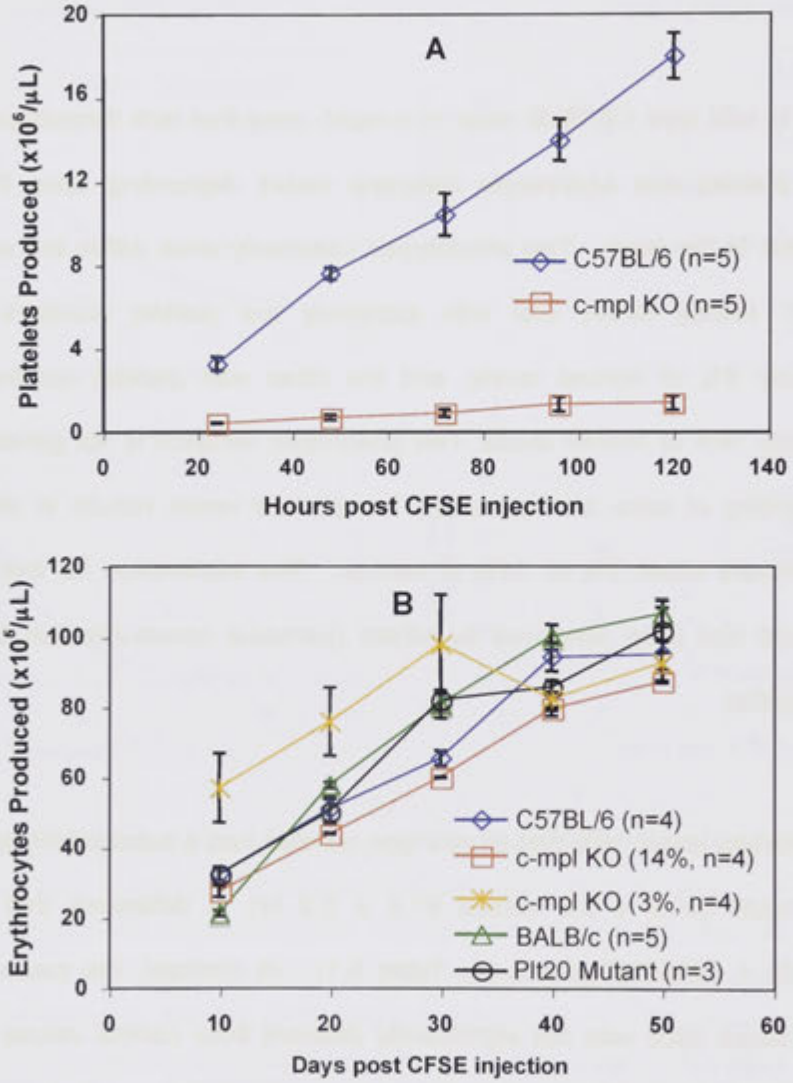

Figure 5.5: Platelet and erythrocyte production in wild-type, *c-mpl* KO and Plt20 mutant mouse strains. Mice received an intravenous injection of CFSE and blood samples were collected at the time points indicated on each X axis. Platelets and erythrocytes were identified and counted by flow cytometry as in Figure 5.1, and the CFSE-dull population of each followed over time. (**A**) Platelet production (cumulative total of absolute numbers x 10^5/μL) in wild-type C57BL/6 and *c-mpl* KO mice (platelets 14% normal). (**B**) Erythrocyte production (cumulative total of absolute numbers x 10^5/μL) in wild-type C57BL/6, *c-mpl* KO (platelets 14% normal) *c-mpl* KO (platelets 3% normal), wild-type BALB/c and BALB/c Plt20 mutant mice.

Table 5.1: Platelet and erythrocyte lifespans in wild-type and platelet-deficient mouse strains

Mouse Strain	Platelet Lifespan hr (mean +/- SEM)	Erythrocyte Lifespan days (mean +/- SEM)	*P*-value *vs* wild-type (platelets; erythrocytes)
Wild-type C57BL/6	87.2 ± 2.3	35.0 ± 0.5	*NA*
c-mpl KO C57BL/6 (14%)	61.8 ± 2.9	36.4 ± 1.4	$p < 0.0001$; p = ns
c-mpl KO C57BL/6 (3%)	32.1 ± 6.6	18.7 ± 4.1	$p < 0.0001$; $p < 0.02$
Wild-type BALB/c	67.7 ± 1.8	42.5 ± 0.4	$p < 0.0001$ [a]; $p < 0.0001$ [a]
Plt20 BALB/c mutant	11.0 ± 0.7	37.2 ± 1.1	$p < 0.0002$; $p < 0.0017$

Lifespan values obtained from lognormal curve fitting of data as shown in Figure 5.3.

SEM indicates standard error of the mean; *NA* indicates not applicable.

[a] Compared with wild-type C57BL/6.

Plt20 mice, generated by ENU mutagenesis, have a shortened platelet lifespan due to the production of an unstable Bcl-X_L protein resulting in a pro-apoptotic phenotype (Mason *et al.* 2007). Platelet lifespan in the Plt20 mutant strain was found to be substantially shorter ($p < 0.0002$) than wild type BALB/c mice (11.0 ± 0.7 versus 67.7 ± 1.8hr) (Figures 5.4B and 5.4C, Table 5.1) which is consistent with previously published work (Mason *et al.* 2007). The erythrocyte lifespan in the Plt20 mutant mice (Figure 5.4E, Table 5.1) was also slightly but significantly ($p = 0.0017$) shorter than in the BALB/c controls (37.1 ± 1.1 versus 42.5 ± 0.4 days).

The shortened platelet lifespans measured in the Plt20 mutant mouse and *c-mpl-/-* mice allowed us to test the ability of the lognormal model to accurately describe extreme platelet data sets. Fits using the lognormal model are shown in Figure 5.4A (*c-mpl* 3% and *c-mpl* 14%) and Figure 5.4B and 5.4C (Plt20 mice). We observed that the lognormal model is able to the fit the *c-mpl* 14%, *c-mpl* 3% and Plt20 platelet data sets extremely well. Additionally, the erythrocyte survival data obtained from the *c-mpl-/-* mice with very low platelet numbers was extremely variable between individual mice.

This gave us an ideal opportunity to test the curve fitting ability of the lognormal model using extreme data sets from individual mice. It can be seen in Figure 5.4F that, in each case, the lognormal model accurately fitted the erythrocyte survival data.

5.3.3 Aged-Associated Changes to Erythrocytes

The CFSE labelling method can not only be used to track platelet and erythrocyte lifespans, but can also be used to follow the changes in the flow cytometry characteristics of old and new erythrocytes. New erythrocytes were determined as those with negligible CFSE fluorescence (CFSE dull) and, therefore, 10 days following CFSE injection were between 0 and 10 days of age. Old erythrocytes were determined as those erythrocytes that still exhibited high CFSE fluorescence (CFSE bright), 40 days following CFSE injection and were therefore 40+ days of age. When the FSC and SSC parameters of these erythrocyte populations were examined it was found that the old erythrocytes had a significantly reduced mean FSC ($p = 0.0001$) and coefficient of variation of SSC ($p = 0.0079$) compared with young erythrocytes (Figure 5.6). These results suggest that aged erythrocytes are smaller in size and have a reduced intracellular complexity, a result consistent with earlier studies of aging erythrocytes (Waugh *et al.* 1992; Willekens *et al.* 2003).

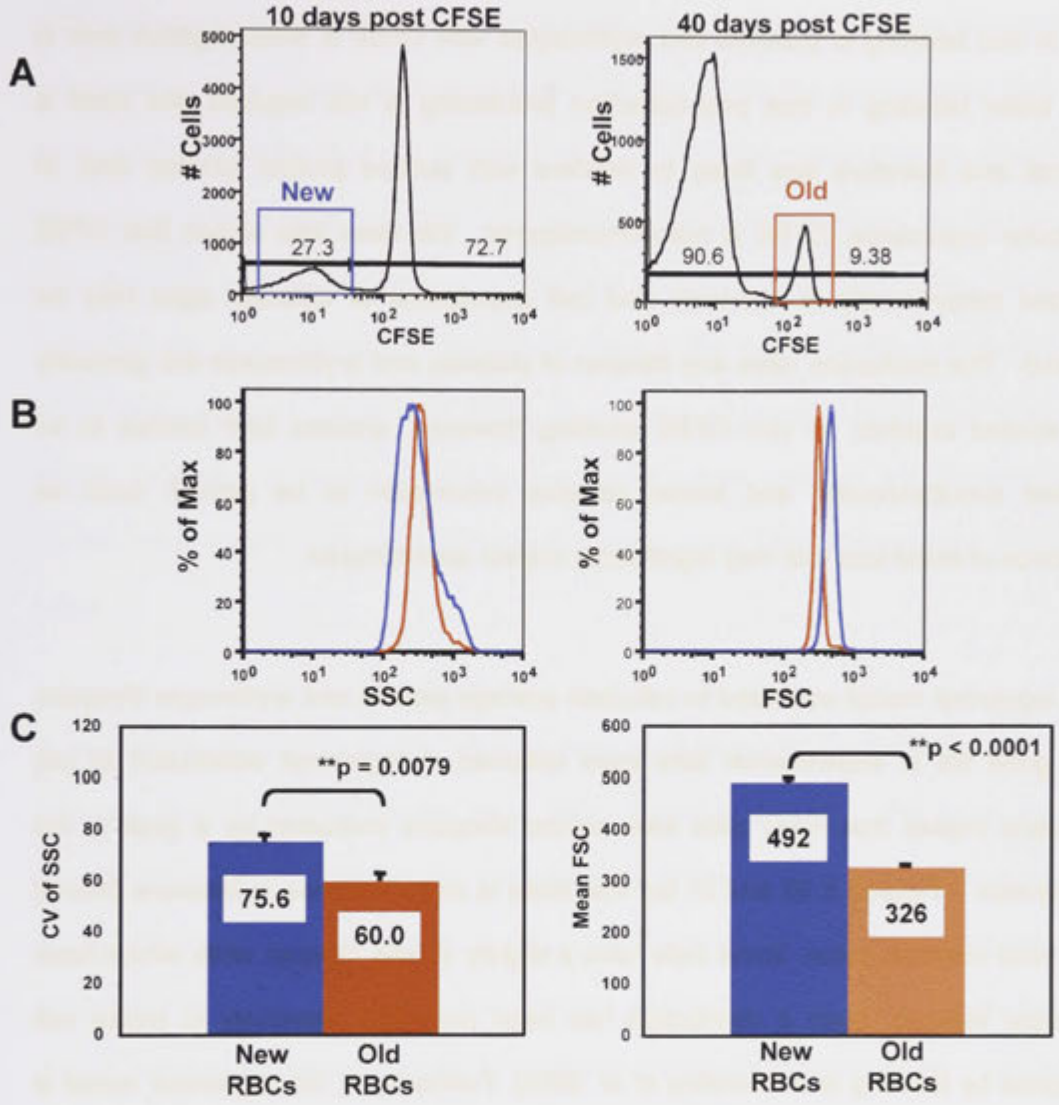

Figure 5.6. Ability of the *in-vivo* CFSE labelling method to detect age-related changes to erythrocytes. Erythrocytes (RBCs) were studied for changes in forward (FSC) and side scatter (SSC) parameters at 10 days and 40 days following *in-vivo* CFSE labelling, with erythrocytes being gated as in Figure 5.1A. (**A**) Selection of newly generated, CFSE dull RBCs (Blue Gate) at 10 days post injection, and old, CFSE bright RBCs (Red Gate) at 40 days post injection. Numbers represent the percentage of CFSE dull and CFSE bright erythrocytes. (**B**) Comparison of SSC and FSC histograms between New and Old RBCs in a single mouse. (**C**) Comparison of coefficient of variation (CV) of SSC, and mean FSC between New and Old RBCs in C57BL/6 mice. Values represent the mean and error bars represent the SEM (n = 5).

5.4 Discussion

The *in vivo* labelling of platelets and erythrocytes with CFSE is advantageous over *in vivo* biotin labelling in that post-collection processing is not required, the label is internal and therefore less likely to interfere with surface protein function and, of particular importance, CFSE is non-immunogenic. We have also shown that CFSE injected intravenously is non-toxic and cell populations of different ages may be studied. The production rates and lifespan of platelets and erythrocytes are generally not studied together. *In vivo* CFSE labelling, however, enables both entities to be studied simultaneously, and allows valuable information to be gained, such as evidence of blood loss that may significantly impact upon lifespan.

The lognormal model was used to calculate average platelet and erythrocyte lifespans and good fits to experimental data were obtained. A lognormal distribution of cell lifespans implies that many cells have similar lifespans (indicated by a peak in the distribution – Figures 5.3B and D) but that there is some variance in lifespans around this most common value. Some cells have a slightly shorter lifespan while others have a longer lifespan. Such a distribution has been proposed previously to model cell lifespans by Dowling *et al* (Dowling *et al.* 2005). Furthermore, the lognormal model is able to fit both the normal and more extreme platelet and erythrocyte survival data sets very well.

A number of other functions have been used previously to model platelet lifespans, from simple linear and exponential functions (Hoffmann-Fezer *et al.* 1993; Baker *et al.* 1997), to more complicated models (Lotter *et al.* 1986). Like the lognormal model, a linear fit to labelled data also assumes that cell destruction is age dependent. However, a linear fit assumes that all cells die after exactly one lifespan, *L*. In contrast, a

lognormal distribution allows for variation in the platelet lifespan about the most common value of *L*. The result is that the survival curves for the lognormal model have what appears to be a linear early part followed by a curved tail that matches well with experimental data. It was also found that a far better fit to the experimental data was obtained by assuming that cell lifespans have a lognormal, rather than an exponential distribution. This is clear both from a visual inspection of the quality of the fits obtained (Figures 5.3A and C) and from a comparison of the mean squared error generated from both fits. It should also be noted that many of the more complicated models that have been proposed (Lotter *et al.* 1986) do not have a biological basis. The lognormal model, however, corresponds well to a scenario where platelets are created with a certain 'most common' lifespan, but where there is some biological variance about this value.

A multiple-hit, or gamma model has also been used to model platelet lifespans (1977; Tsukada and Tango 1980; Lotter *et al.* 1986; Baker *et al.* 1997). We found that the multiple-hit model gave similar lifespan estimates to the lognormal model, however the fitting procedure took far longer to run. This increase in processing time was not associated with any increase in the accuracy of the fit. Furthermore, the multiple-hit model is based on the assumption that platelet lifespan is determined by a number of injurious hits occurring within the circulation. When fitting data using the multiple-hit model there appeared to be little consistency within each data set between the number of hits required for platelet destruction or the waiting time between these hits. This calls into question the biological validity of the model's assumptions.

It is likely that a combination of intrinsic and extrinsic factors determine platelet and erythrocyte lifespan, hence, a mathematical model that makes no assumptions about the events causing platelet destruction but that has a biological basis would be more appropriate for widespread use. The excellent fit of the lognormal model to the

extremely thrombocytopenic *c-mpl-/-* mice and the Plt20 mutant mice demonstrates the versatility of this model in describing lifespans determined by either intrinsic or extrinsic biological events, and hence its use is recommended over the multiple-hit model.

Comparisons between C57BL/6, *c-mpl-/-* and wild type littermate controls demonstrated that the platelet levels within these mice significantly influence the lifespan of platelets and erythrocytes. We infer from the results obtained that when platelet numbers are extremely low (3% of normal), vascular integrity is compromised and microscopic bleeding occurs resulting in reduced platelet and erythrocyte lifespans. This is consistent with the findings of a correlation between platelet lifespan and platelet count in patients with bone marrow hypoplasia (Hanson and Slichter 1985). However, when platelet levels in the *c-mpl-/-* mice are 14% of normal, vascular integrity is maintained, as reflected by a normal erythrocyte lifespan and production rate. The reduced platelet lifespan in these mice, however, suggests that TPO signalling may play some role in the determination of platelet lifespan. It is known that TPO acts as a survival signal for $CD34^+$ stem cells, megakaryocytes and platelets, and it is proposed to do so by altering the intracellular environment to promote cell cycling and proliferation and inhibit apoptosis by altering the balance of proteins such as cyclin D, c-myc, p27, FKHR, Bcl-X_L and Bad (Geddis *et al.* 2002; Majka *et al.* 2002). It is likely, therefore, that in the absence of TPO-R signalling, the few platelets produced have a shortened lifespan, predominantly due to a decrease in Bcl-X_L thus accelerating the Bak-mediated pathway of apoptosis (Mason *et al.* 2007).

As expected, the rate of platelet production in the *c-mpl-/-* mice was considerably reduced and is consistent with the finding that megakaryocyte numbers within the marrow of these mice are very low (Alexander *et al.* 1996). The erythrocyte production rate, however, was not compromised in the *c-mpl-/-* mice despite the finding that there are reduced numbers of erythroid progenitor cells in the marrow and spleen of this

mouse strain (Alexander *et al.* 1996). In *c-mpl-/-* mice with platelet levels 3% of normal, we found elevated rates of erythrocyte production compared to controls, which is consistent with our inference of microscopic blood loss occurring due to a loss of vascular integrity.

In the Plt20 mutant mouse strain, the platelet lifespan was dramatically shortened when compared with normal controls. This is consistent with the findings of Mason *et al* (Mason *et al.* 2007) and has been explained by a reduction of Bcl-X_L signalling causing a pro-apoptotic phenotype in the platelets. The erythrocytes in these mice had a slightly, but significantly, shorter lifespan than their wild type controls. As these mice have a platelet count approximately 30% of normal levels, and the rate of erythrocyte production was not significantly different to that of the wild type controls, it is unlikely that the shortened erythrocyte lifespan was due to microscopic blood loss. A previous study of erythrocytes *in vitro* demonstrated a potential role for membrane-bound Bcl-X_L in erythrocyte survival (Walsh *et al.* 2002). Furthermore, studies on conditional *bcl-x-/-* mice demonstrated apoptosis of a large majority of late-stage erythroblasts and evidence for premature lysis of mature erythrocytes (Wagner *et al.* 2000; Rhodes *et al.* 2005). Our *in vivo* studies of erythrocyte lifespan in the Plt20 mutant mouse would suggest that Bcl-X_L is involved in determining the lifespan of mature erythrocytes as well as late-stage erythroblasts.

Mammalian platelets and erythrocytes are both anucleate in their mature forms, however, platelets retain their mitochondria whereas erythrocytes do not. Platelets therefore have the capacity to utilise mitochondrial-dependent pathways of apoptosis. Indeed, the gross structural alterations occurring in megakaryocytes prior to platelet production, including cytoskeletal alterations, membrane condensation and ruffling, have been compared to cells undergoing apoptosis. The process of programmed cell death in erythrocytes, termed eryptosis, is characterised by a reduction in cell volume,

decoupling of the cytoskeleton from the plasma membrane causing membrane blebbing, the activation of proteases and exposure of phosphatidylserine on the outer membrane following calcium-dependent activation of scramblase (Foller *et al.* 2008). Erythrocyte senescence or aging is characterised by a reduction in cell volume and loss of haemoglobin, cholesterol and phospholipids through vesiculation, the generation of a senescent-specific antigen and exposure of phosphatidylserine (Waugh *et al.* 1992; Willekens *et al.* 2003; Bosman *et al.* 2005). As eryptosis and senescence have similar features it has been suggested that erythrocyte senescence represents an apoptotic pathway(Bosman *et al.* 2005). Our studies of age-associated changes within the erythrocytes demonstrated a reduction in size and cellular complexity consistent with the changes ascribed to senescence and eryptosis.

In conclusion, *in vivo* labelling of erythrocytes and platelets with CFSE overcomes several technical and safety concerns of previously published labelling methods. Additionally, the *in vivo* injection of CFSE in mice was demonstrated to be non-toxic and non-immunogenic. The application of the lognormal model to platelet and erythrocyte survival data using the CFSE labelling method gave an excellent fit to both normal and extreme datasets when lifespan was determined by intrinsic or extrinsic factors. The use of both CFSE labelling and the lognormal model is therefore recommended for future research into erythrocyte and platelet lifespans. Using these novel approaches in *c-mpl-/-* and Bcl-X_L mutant mice it was also demonstrated that TPO-signalling increases platelet lifespan and Bcl-X_L signalling increases erythrocyte lifespan, with both findings having potential clinical relevance.

Chapter 6

Final Discussion

This chapter summarises the major findings arising from the experimental data presented in Chapters 3, 4 and 5 and discusses their implications in terms of current concepts, future research directions and potential avenues for translation.

6.1 Introduction

Platelets are cytoplasmic fragments present in large numbers within the bloodstream that contain a multitude of proteins. For a long time, platelet function was believed to be limited to the essential functions of haemostasis and thrombosis. However, it has become clear in the last decade that platelets play significant roles in both innate and adaptive immunity, inflammatory responses including leukocyte migration, tissue regeneration and angiogenesis. Parallelling the revelation of the diverse physiological functions of platelets, however, has been the association of exacerbated platelet function with numerous thrombotic and chronic inflammatory diseases (Barnes 2002; Klinger 2002; von Hundelshausen and Weber 2007; Jennings 2009; Solanilla *et al.* 2009; Yoshida and Granger 2009).

The aims of this thesis were to examine in detail the following three platelet-associated biological processes:

(i) The role of platelets in tumour cell metastasis, in particular, the kinetics and interrelationship of the pro-metastatic role of platelets and the anti-metastatic role of NK cells, and the relevant contributions to the metastatic process of platelet P-selectin and endothelial P-selectin.

(ii) The determinants and mechanisms of antibody-mediated platelet elimination and the role of inhibitory self-recognition systems in this process.

(iii) The factors influencing platelet and erythrocyte lifespan by establishing appropriate experimental and analytical methodologies.

6.2 The role of platelets in tumour cell metastasis

Platelets have long been implicated in haematogenous tumour cell metastasis, with the purported mechanisms of action including the formation of a thrombus around the tumour cell thus affording protection from haemodynamic stresses, linking tumour cells to the vascular endothelium via adhesion molecules such as P-selectin, assisting the migration of tumour cells across the blood vessel wall through the release of degradative enzymes, and the provision of growth and angiogenic factors enabling the establishment of secondary tumours (Karpatkin and Pearlstein 1981; Karpatkin 2002; Erpenbeck and Schon 2010). It has also been suggested that the only role of platelets in tumour cell metastasis is the provision of a protective cloak from recognition and destruction by immune cells, principally NK cells (Nieswandt *et al.* 1999; Palumbo *et al.* 2005).

The results presented in Chapter 3 obtained using an experimental metastasis model in mice, demonstrated that platelets promoted, whilst NK cells inhibited the lung metastasis of B16F1 melanoma and 4T1.2 breast cancer cell lines. On further examination using the B16F1 melanoma, the pro-metastatic action of platelets and the anti-metastatic action of NK cells were shown to be chronologically distinct and the kinetics of the NK-cell effect was unchanged in the presence or absence of platelets. These data, therefore, unequivocally demonstrate that the role of platelets in tumour cell metastasis occurs within 1 hr of tumour cell entry into the bloodstream and is independent of NK cells. Equally, the anti-metastatic effect of NK cells occurs between 1 and 24 hr following tumour cell injection and is independent of platelets. Previous work on the role of NK cells in the elimination of intraperitoneal B16 melanoma cells also showed an early time frame (3-5 days following injection) for the infiltration and anti-tumoral actions of NK cells (Kurosawa *et al.* 1993). Furthermore, the important role

of IFN-γ produced by early-entry NK cells in activating the anti-tumoral responses of macrophages and T cells was demonstrated (Kurosawa *et al.* 1995; Abe *et al.* 1998).

The data described in Chapter 3 also raise the question of the location of NK cell destruction of tumour cells and suggests that it may be occurring soon after tumour cell attachment to the blood vessel wall. It is possible that endothelial activation, occurring as a result of tumour cell attachment, triggers the recruitment of NK cells to the region of invasion. Indeed, endothelial cells have been demonstrated to secrete TNFα (Imaizumi *et al.* 2000), the principal cytokine for NK cell recruitment into normal and tumour-bearing tissue (Pilaro *et al.* 1994; Smyth *et al.* 1998). The secretion of TNFα also induces the expression of E-selectin on endothelium enabling leukocyte adhesion to the blood vessel wall, however, E-selectin is also implicated in aiding tumour cell metastasis (Biancone *et al.* 1996). Studies by Fogler *et al* also indicate that the VCAM-1:VLA-4 interaction, that is enhanced by TNFα, is likely to support the initial rolling and adhesion of NK cells to the endothelium in the lung, liver and B16 melanoma tumours (Fogler *et al.* 1996). In order to further define the timing and location of NK cell action against metastasising tumour cells, studies in mice with additional time points of NK depletion, such as 6 hr and 12 hr following tumour cell injection, and also NK cell replenishment, such as 48 hrs following tumour cell injection, may be beneficial. Intra-vital microscopy studies may also assist in answering these questions.

To our knowledge, these are the first studies that examine the mechanisms of lung and liver metastasis simultaneously. Using the B16F1 melanoma cells as a model, it was observed that in the absence of platelets, although lung metastasis was significantly reduced, liver metastasis increased. This effect became very obvious in mice depleted of NK cells. Using 4T1.2 breast cancer cells as an additional model, lung metastases decreased in the absence of platelets, however liver metastases remained

undetectable even in the absence of NK cells. These results provide additional evidence that platelets arrest tumour cells within the lung vasculature and, in their absence, a greater number of tumour cells are carried within the bloodstream to the capillary beds of downstream organs. Of equal significance, these data imply that platelets are not required for B16F1 melanoma tumour cell metastasis to the liver and that 4T1.2 breast cancer cells are incapable of metastasising to, or growing within, hepatic tissue. These findings are of particular clinical importance as they suggest that the use of platelet inhibitors to prevent metastasis may result in the redistribution rather than diminution of metastatic spread. Additionally, these results confirm the influence of vascular anatomy, haemodynamic forces and 'seed and soil' interactions on metastatic spread.

Previous studies have consistently demonstrated P-selectin to be involved in tumour cell metastasis, however, this has been attributed to platelet-derived P-selectin (Kim *et al.* 1998) although one study also suggests a possible role for endothelial P-selectin (Ludwig *et al.* 2004). The results of the metastasis experiments described in Chapter 3 clearly demonstrate that both endothelial and platelet-derived P-selectin play significant roles in B16F1 melanoma lung metastasis, and endothelial P-selectin in B16F1 melanoma liver metastasis. These data add to the already substantial evidence supporting the targeting of P-selectin in therapeutic trials to prevent metastasis. Borsig *et al* have studied a number of anticoagulant and non-anticoagulant heparin-like molecules that bind selectins and their administration to mice proved effective in reducing experimental lung metastasis (Stevenson *et al.* 2007). Additionally, low-molecular weight heparins have proven beneficial in a number of human trials in cancer patients with the beneficial effects not only being due to the inhibition of selectin binding, but also the inhibition of the endoglycosidase, heparanase, as well as inhibition of a range of biological processes, such as coagulation, angiogenesis and immune effector function, and induction of apoptosis (Falanga 2004).

The experiments with NK cell and platelet-depleted mice revealed some additional intriguing results that raise further questions. Firstly, a significant number of tumours occurred in the lungs of mice depleted of both NK cells and platelets that were absent from the lungs of mice depleted of platelets alone. This result indicates that a significant population of tumour cells were capable of metastasising to the lungs without the assistance of platelets. The experiments conducted in P-selectin deficient and WT mice depleted of platelets demonstrated that endothelial P-selectin is capable of supporting both lung and liver metastasis in the absence of platelets. However, 20-25% of metastasis to the liver and lungs was observed to occur independently of both platelets and P-selectin. Potential mechanisms of platelet and P-selectin independent metastasis include the physical entrapment of single tumour cells or tumour cell aggregates due to size restrictions within a small capillary despite inherent haemodynamic pressures, and the interaction of other adhesion protein pairs, such as E-selectin with sialylated fucosylated lactosaminoglycans (Biancone *et al.* 1996), VLA-4 with VCAM-1, and hyaluronic acid with CD44 (Zetter 1993).

The role of L-selectin in the promotion of metastasis is of interest when relating the findings of Laubli *et al* to our data on the timing of NK cell anti-metastatic activity. Using B16F1 melanoma cells in an experimental lung metastasis model, these investigators found that L-selectin promoted tumour cell survival, an effect that occurred 12-24 hr following tumour cell injection and could not be attributed to B or T cells as the same results were seen in NOD-SCID mice. However, despite NK cells also expressing L-selectin, in the experiments by Laubli *et al*, NK cell numbers in lung tissue appeared to be unaffected by L-selectin deficiency. It was proposed, therefore, that L-selectin positive leukocytes (granulocytes and/or monocytes) assisted the migration of tumour cells across the vessel wall and the induction of inflammation may provide a protective and nurturing environment for the tumour cells. (Laubli *et al.* 2006).

Taken together, the results described in Chapter 3 suggest a model of lung metastasis wherein tumour cells are dependent upon platelets to a large extent, to assist in establishing resistance to the inherent velocity of blood flow within the lung vasculature and aid attachment to the endothelium. The platelet adhesion molecule, P-selectin, probably plays a dominant cross-linking role in this model through interactions with mucin proteins expressed by tumour cells and PSGL-1 expressed by endothelial cells. A proportion of tumour cells are capable of metastasising independently of platelets and are aided by endothelial P-selectin interactions with tumour-derived mucins. Physical entrapment and other adhesion molecules may also play a role. The majority of tumour cells that succeed in the early stages of metastasis to the lung are rapidly eliminated by NK cells, with only a very small proportion of tumour cells exhibiting NK cell resistance (Figure 6.1). Metastasis to the liver would appear to occur independently of platelets, most likely due to the inherent slow flow of blood and fenestrated endothelium within the hepatic vasculature, and is aided by endothelial P-selectin. Physical entrapment and other adhesion molecules are also likely to play a role. Again, however, NK cells have a major negative impact upon the success of liver metastasis.

6.3 Antibody-mediated platelet depletion and its inhibition

The production of auto-antibodies to platelet surface proteins manifests in a condition known as immune thrombocytopenic purpura (ITP) which affects all age groups and leaves sufferers susceptible to life-threatening haemorrhage. Current treatment strategies have considerable side-effects or associated risks and treatment failures are not uncommon. The predominant mechanism of platelet depletion in ITP is FcR-mediated uptake of antibody-coated platelets by immune effector cells. However, a study by Nieswandt *et al* indicated that FcR-independent mechanisms of platelet depletion existed that were dependent upon the target antigen (Nieswandt *et al.* 2000).

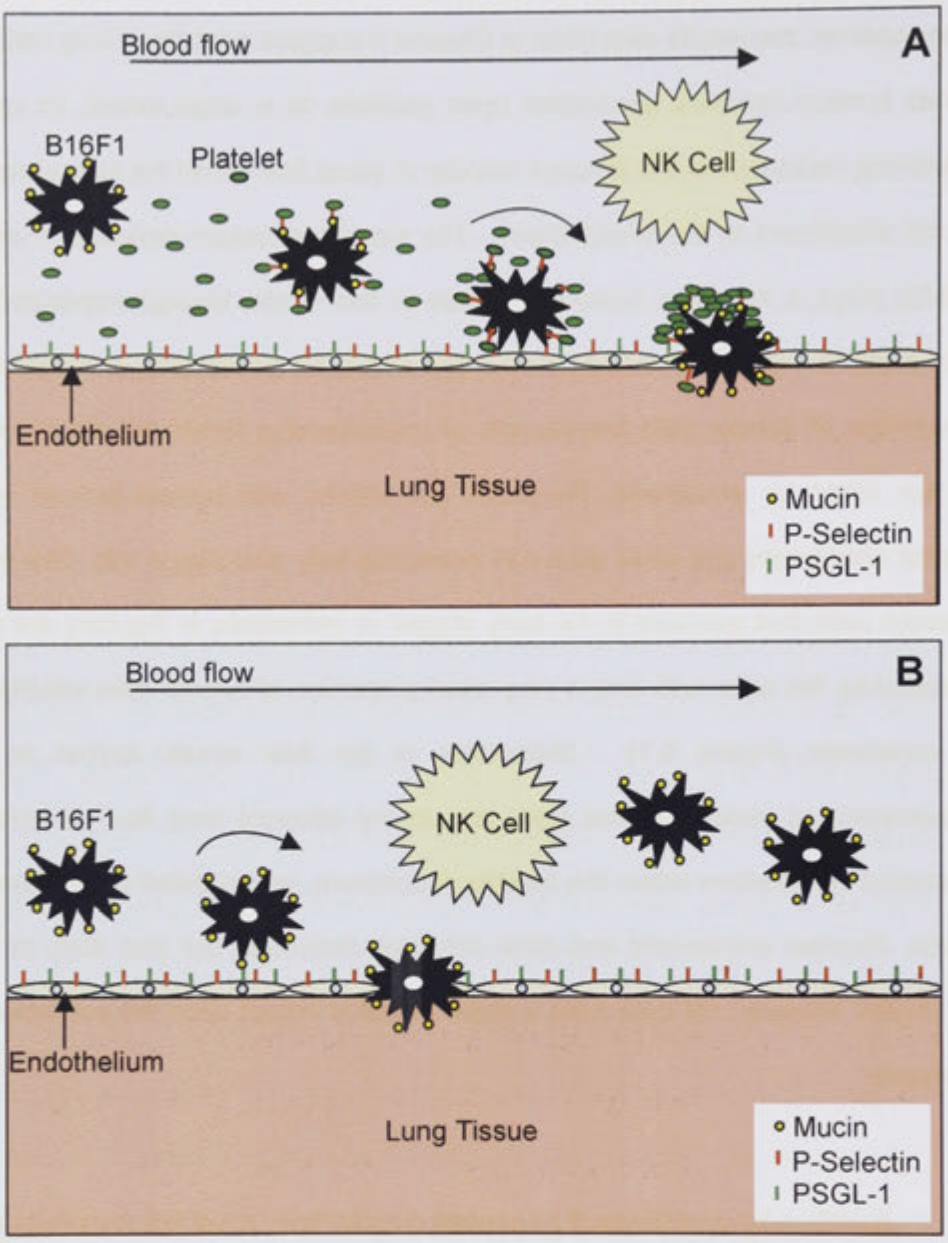

Figure 6.1: B16F1 melanoma metastasis to the lungs may occur through platelet-dependent and independent pathways that involve endothelial P-selectin. (A) Within the bloodstream, activated platelets bind B16F1 melanoma cells via P-selectin:mucin interactions. P-selectin on activated platelets and tumour cell (TC) mucins (e.g. sialyl Lewis ^{x}) interact with PSGL-1 and P-selectin, respectively, on endothelial cells. Additional platelets recruited to the TC provide resistance to haemodynamic forces enabling TC attachment to the blood vessel wall. TNFα released from activated endothelial cells recruit highly-effective anti-tumoral NK-cells that destroy >90% attached TC. **(B)** In the absence of platelets, a proportion of TC interactions with endothelial P-selectin are sufficiently strong to resist haemodynamic forces thus enabling TC attachment to the vessel wall. A proportion of TC will also attach to the vessel wall through platelet and P-selectin independent processes involving other adhesion proteins or physical entrapment (not shown). Unattached TC are swept through the lung capillary bed to downstream organs such as the liver.

Furthermore, studies by Olsson *et al* using a mAb to an unidentified platelet antigen implicated the self-recognition protein pair, CD47:SIRPα, in the regulation of ITP (Olsson *et al.* 2005).

The results of experiments described in Chapter 4, conducted to investigate both of the above findings in greater detail, yielded several significant findings. The mechanism of platelet depletion induced by the majority of mAbs studied was principally FcγR-mediated, but in some cases occurred through direct activation and fragmentation of platelets or via complement-mediated destruction. Furthermore, the level of FcγR-mediated platelet depletion was usually greater following the administration of IgG2b mAbs than IgG1 mAbs. Direct activation and fragmentation of platelets was observed following the administration of both IgG1 and IgG2b mAbs to GpIbα and this process was shown to be both FcγR and complement independent. It is likely, therefore, that mAb binding to GpIbα triggered the receptor resulting in platelet activation and degranulation. Interestingly, the fragmentation of ~80% of the platelet population within a 2 hr period did not have any apparent health consequences such as thrombosis or acute inflammation. A similar effect of platelet fragmentation following Ab binding has been observed in human studies and was attributed to the engagement of the FcγR present on human platelets but absent on mouse platelets (Nardi *et al.* 2001; Li *et al.* 2008). This appears to be the first report, however, of the involvement of GpIbα in this process of mAb-induced platelet activation. With the majority of mAbs studied, complement did not play a role, suggesting that complement-inhibitory proteins present on the platelet surface prevented complement-mediated destruction. In the case of the IgG2b mAb targeting GpIa, however, complement was shown to play a significant role in platelet destruction. Therefore, in treatment refractory cases of ITP, the trial of complement inhibitors may be worthwhile. Treating ITP that involves mAb-induced-platelet fragmentation, however, may prove a much greater challenge.

The more severe ITP induced by rat IgG2b mAbs compared to their rat IgG1 counterparts suggested the preferential binding of rat IgG2b mAb to high-affinity FcγR and rat IgG1 mAbs to low-affinity FcγR. Structural comparisons between mouse and rat IgG confirmed that this was more than likely the case (Hulett and Hogarth 1994).

The administration to mice of mAbs specific for different platelet membrane proteins did not always induce ITP and this effect appeared to be antigen specific. Upon further investigation, the ability of a mAb specific for a particular platelet antigen to induce ITP did not correlate with the density of binding of the mAb to the platelet surface nor the degree of saturation of the platelet surface antigen by the mAb. However, the rate of platelet depletion induced by IgG1 mAbs appeared to be influenced by the density of the mAb on the platelet surface. These data suggested that, in the situation of a non-depleting mAb, the Fc portion of the mAb was incapable of interacting with FcR due to steric hindrance, the mAb exhibited a higher binding affinity for the inhibitory than the activating FcγR, or that FcR-mediated uptake of the mAb coated platelets was being regulated by the presence of additional inhibitory signals.

The most well described self-recognition protein pairs involved in the regulation of the effector function of macrophages are CD47:SIRPα and CD200:CD200R. Since in most cases ITP appears to be induced by FcγR-dependent phagocytosis of mAb coated platelet by macrophages, the function of these inhibitory protein pairs in the regulation of ITP was investigated. Administration of the non-ITP inducing GpIX-specific mAb to mice deficient in CD47 resulted in ITP although at a relatively slow rate of induction. These data suggested that the inhibition of CD47:SIRPα interactions by mAb binding may have been a determinant of ITP induction. Indeed, CD47 is associated on the surface of platelets with the integrins GpIIb/IIIa and GpIa thus it is possible that ITP induction by IgG1 mAbs specific for these CD47-associated proteins occurred as a

result of the disruption of the CD47:SIRPα interaction. This hypothesis could be tested by assessing the capacity of recombinant SIRPα to bind to platelets in the presence of a panel of anti-platelet mAbs including the IgG1 mAbs specific for GpIa and GpIIb/IIIa. The effect of stimulating the inhibitory receptor, SIRPα, using a specific mAb *in vivo* to prevent FcγR-mediated ITP was investigated and discovered to not only prevent, but reverse rat IgG1 mAb induced, FcγR-mediated ITP. This effect was not observed, however, with ITP induced by rat IgG2b mAbs.

The mechanism by which SIRPα signalling inhibits phagocytosis was elucidated by Tsai and Discher (Tsai and Discher 2008). Their studies on the phagocytosis of foreign cells have demonstrated that in response to FcR engagement, actin and non-muscle myosin fibres are recruited in the formation of the phagocytic cup. The binding of autologous CD47 with SIRPα results in the inactivation of myosin through dephosphorylation thus preventing this process from occurring (Tsai and Discher 2008) (Figure 6.2).

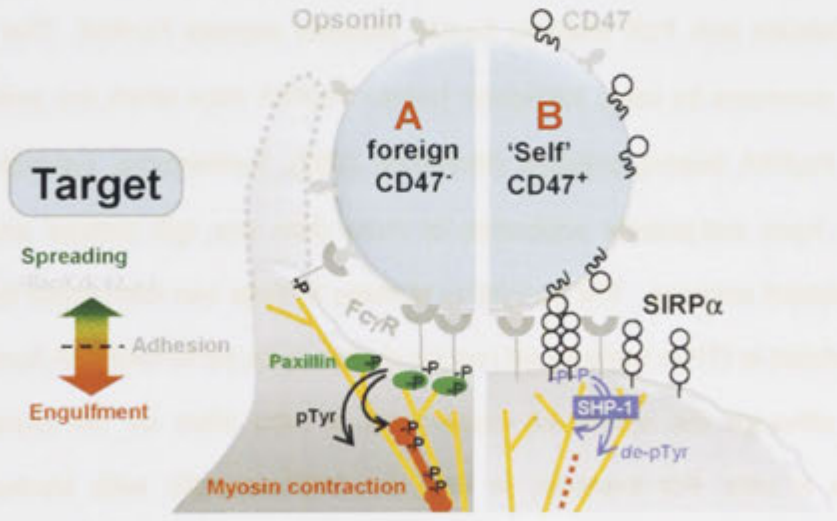

Figure 6.2: Inhibition of phagocytosis by CD47:SIRPα signalling. **(A)** Foreign cells deficient in CD47 are opsonised by IgG and subsequent Fc:FcγR interactions on macrophages initiates the assembly of paxillin, F-actin, and nonmuscle myosin IIA in the formation of a phagocytic cup. **(B)** In contrast, CD47 present on IgG-opsonised 'self' cells signals through SIRPα to inhibit myosin assembly through dephosphorylation thus preventing phagocytosis.

From Tsai R K , Discher D E J Cell Biol 2008;180:989-1003 with minor modification

The results in Chapter 4 imply that signalling induced by the SIRPα mAb regulates low-affinity activating FcγR and that triggering this receptor with a specific mAb or chimeric CD47 protein may be an effective treatment for pathologies involving the binding of low-affinity FcγR. Unlike the low-affinity activating FcγR, SIRPα signalling clearly does not regulate high-affinity activating FcγR. Furthermore, the macrophage inhibitory receptor, CD200R, did not appear to regulate low- or high-affinity activating FcRs. The identification of proteins that negatively regulate high-affinity activating FcγR would be of significant clinical benefit in the treatment of antibody-mediated pathologies including ITP and, therefore, represents a vital area for future research. Until the identification of other such inhibitory proteins, future studies should assess the efficacy of combination therapy using a SIRPα-specific mAb and intravenous pooled immunoglobulin to overcome the pro-phagocytic signalling mediated by both low affinity and high-affinity activating FcγR.

An important limitation of the mouse models of ITP described in this thesis is that mouse platelets lack FcR whereas human platelets express FcγRIIA. This limitation could be overcome by using transgenic human FcγRIIA mice which are available and possess FcγRIIA bearing platelets (McKenzie 2002). Furthermore, patients with ITP generally have anti-platelet antibodies of more than one IgG isotype and against several platelet antigens. The translation of these findings into information that can be directly related to ITP in humans will require studies to be performed with human tissue *in vitro*, although the results of experiments *in vitro* often do not correlate with outcomes *in vivo*. For example, *in vitro* the SIRPα-specific mAb blocked SIRPα signalling by CD47 whereas our *in vivo* experiments using the same antibody appeared to trigger SIRPα signalling (Olsson *et al.* 2005). The use of a chimeric human/mouse model, as has recently been developed by Liang *et al* for the study of drug-induced

thrombocytopenia (Liang *et al.* 2010), in combination with human FcγRIIA transgenic mice, may help to overcome such experimental quandaries.

Taken together, the results of Chapter 4 suggest a model of FcγR-mediated ITP whereby anti-platelet mAbs binding low-affinity FcγR-binding will induce ITP if they sterically hinder CD47:SIRPα interactions. If, however, CD47:SIRPα interactions prevail the balance of signalling from activating and inhibitory FcγR will determine whether phagocytosis occurs. In either of the above scenarios, use of a SIRPα-specific mAb *in vivo* restores the inhibitory signalling pathway thus preventing phagocytosis (Figure 6.3).

6.4 *In vivo* CFSE labelling and mathematical modelling of platelet and erythrocyte lifespans

Little progress has been made in identifying factors that determine the production, lifespan and destruction of platelets and it occurred to us this may be due to deficiencies in the methodologies available for measuring these parameters. It also became clear that prior work in this area focused on either platelet- or erythrocyte lifespans but not on both despite the likelihood of there being common molecular pathways and the potential for one to affect the other. We, therefore, set out to establish a new method for the simultaneous *in vivo* labelling and tracking of platelets and erythrocytes, and to determine the most appropriate mathematical model for the analysis of platelet and erythrocyte lifespan data.

The results described in Chapter 5 demonstrate that *in vivo* CFSE labelling of platelets and erythrocytes requires no post-collection processing, proved to be stable, non-toxic and non-immunogenic, and the lifespans obtained were highly reproducible. CFSE has been used extensively in the study of the migration and division of lymphocytes

Figure 6.3: Potential role of SIRPα signalling in the inhibition of phagocytosis induced by mAbs binding low-affinity FcγR. (A) Following mAb binding to a platelet antigen, Fc portions of the Ab interact with both low-affinity activating (green) and low-affinity inhibitory (red) FcγRs and CD47 on the platelet surface (orange) interacts with SIRPα on the immune effector cell (orange). The balance of signalling is inhibitory and therefore phagocytosis does not occur. **(B)** If the anti-platelet mAb is specific for a protein closely associated with CD47, such as GpIIb-IIIa and GpIa, steric hindrance of the CD47:SIRPα interaction shifts the balance of signals towards a pro-phagocytic outcome. **(C)** Use of a SIRPα-specific mAb triggers the inhibitory SIRPα receptor restoring the inhibitory signalling and thus preventing phagocytosis.

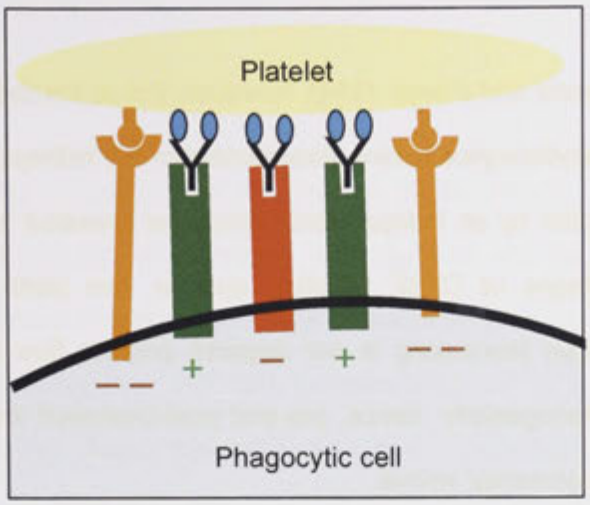

A

No platelet phagocytosis

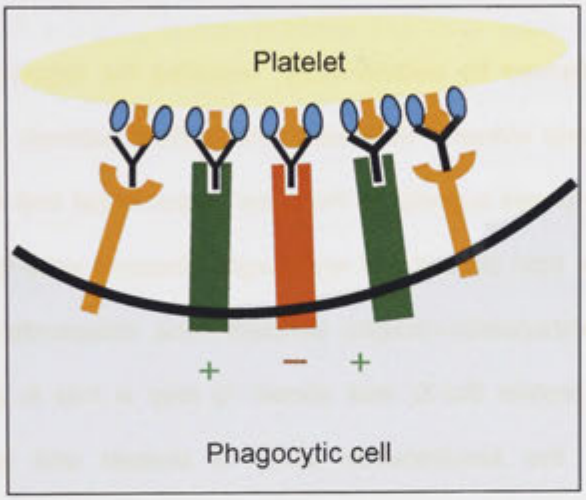

B

Platelet phagocytosis

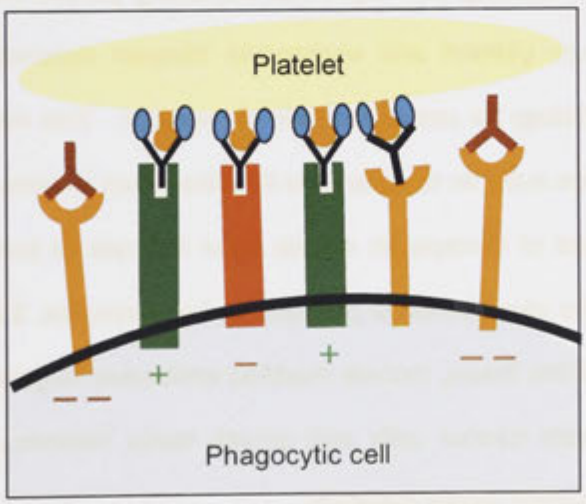

C

No platelet phagocytosis

(Weston and Parish 1990; Lyons and Parish 1994), however, this is the first report of its use to label platelets and erythrocytes *in vivo*. Assessment of the kidneys and livers of mice following CFSE injection by an independent pathologist revealed no signs of organ toxicity. The advantages of CFSE labelling over *in vivo* biotin labelling, therefore, is that post-collection processing is not required prior to flow cytometric analysis and the lack of immunogenicity, hence, pre-and post-treatment studies may be performed in the same experimental animal.

Mathematical modelling, performed by collaborators, revealed the lognormal model gave a robust fit to control and extreme data sets when either extrinsic or intrinsic factors determined lifespan and was superior to the linear, exponential and multiple-hit models. Using these methods, both platelet and erythrocyte lifespans were found to be significantly shortened in thrombopoietin-receptor deficient mice, independent of blood loss, and the anti-apoptotic protein Bcl-X_L was shown to play a role in prolonging erythrocyte lifespans. Thus, the simultaneous study of platelet and erythrocyte lifespans using *in vivo* CFSE labelling with lognormal modelling yielded insights into common intrinsic and extrinsic platelet and erythrocyte lifespan determinants and provides an improved methodology for use in this field of research. This methodology has many potential applications such as to determine the circulation kinetics of tumour cells and to assess the impact of therapeutic agents upon the rate of bone marrow production, the lifespan and the senescence of platelets and erythrocytes. Examples of such agents, in the context of this thesis, include modified antibodies targeting specific platelet protein interactions with tumour cells and growth factor mimetics aimed at boosting platelet or RBC production and/or longevity.

6.5 Conclusion

Platelets are critical for the preservation of life through their maintenance of vascular integrity, immunity, inflammation, wound repair and angiogenesis. The experimental data presented in this thesis has shed some light on three aspects of platelet biology, namely, proving their NK cell independent role in the promotion of tumour cell metastasis that closely resembles their role in assisting leukocyte migration; identifying not only likely determinants and mechanisms of immune-mediated platelet destruction but also an inhibitor of this process that may have therapeutic potential; and the development of robust methods that may be used to better understand those factors influencing the production, lifespan and senescence of platelets. As with most research, whilst the results presented in this thesis have answered some questions, they have also raised many more upon which future research may be based.

References

(1977). "Recommended methods for radioisotope platelet survival studies: by the panel on Diagnostic Application of Radioisotopes in Hematology, International Committee for Standardization in Hematology." Blood **50**(6): 1137-44.

(1988). "Recommended method for indium-111 platelet survival studies. International Committee for Standardization in Hematology. Panel on Diagnostic Applications of Radionuclides." J Nucl Med **29**(4): 564-6.

Abbrecht, P. H. and J. K. Littell (1972). "Erythrocyte life-span in mice acclimatized to different degrees of hypoxia." J Appl Physiol **32**(4): 443-5.

Abe, K., M. Harada, et al. (1998). "Early-appearing tumor-infiltrating natural killer cells play an important role in the nitric oxide production of tumor-associated macrophages through their interferon production." Cancer Immunol Immunother **45**(5): 225-33.

Aghajanian, A., E. S. Wittchen, et al. (2008). "Endothelial cell junctions and the regulation of vascular permeability and leukocyte transmigration." J Thromb Haemost.

Akl, E. A., G. Kamath, et al. (2007). "Oral anticoagulation for prolonging survival in patients with cancer." Cochrane Database Syst Rev(2): CD006466.

Alexander, W. S., A. W. Roberts, et al. (1996). "Deficiencies in progenitor cells of multiple hematopoietic lineages and defective megakaryocytopoiesis in mice lacking the thrombopoietic receptor c-Mpl." Blood **87**(6): 2162-70.

Alterman, A. L., D. M. Fornabaio, et al. (1985). "Metastatic dissemination of B16 melanoma: pattern and sequence of metastasis." J Natl Cancer Inst **75**(4): 691-702.

Alugupalli, K. R., A. D. Michelson, et al. (2001). "Serial determinations of platelet counts in mice by flow cytometry." Thromb Haemost **86**(2): 668-71.

Alves, C. S., S. Yakovlev, et al. (2009). "Biomolecular characterization of CD44-fibrin(ogen) binding: distinct molecular requirements mediate binding of standard and variant isoforms of CD44 to immobilized fibrin(ogen)." J Biol Chem **284**(2): 1177-89.

Amirkhosravi, A., M. Amaya, et al. (1999). "Blockade of GpIIb/IIIa inhibits the release of vascular endothelial growth factor (VEGF) from tumor cell-activated platelets and experimental metastasis." Platelets **10**: 285-292.

Anborgh, P. H., J. C. Mutrie, et al. "Role of the metastasis-promoting protein osteopontin in the tumor microenvironment." J Cell Mol Med.

Arguello, F., R. B. Baggs, et al. (1988). "A murine model of experimental metastasis to bone and bone marrow." Cancer Res **48**(23): 6876-81.

Ault, K. A. and C. Knowles (1995). "In vivo biotinylation demonstrates that reticulated platelets are the youngest platelets in circulation." Exp Hematol **23**(9): 996-1001.

Australian Institute of Health and Welfare, A. G. (2008). "Cancer survival shows significant improvement." Retrieved 24th June, 2010, from http://www.aihw.gov.au/mediacentre/2008/mr20080822.cfm.

Australian Institute of Health and Welfare, A. G. (2010). "Cancer Control - Health Priority Areas." Retrieved 24th June 2010, 2010, from http://www.aihw.gov.au/nhpa/cancer/index.cfm.

Baker, G. R., P. M. Sullam, et al. (1997). "A simple, fluorescent method to internally label platelets suitable for physiological measurements." Am J Hematol **56**(1): 17-25.

Bakewell, S. J., P. Nestor, et al. (2003). "Platelet and osteoclast beta3 integrins are critical for bone metastasis." Proc Natl Acad Sci U S A **100**(24): 14205-10.

Barclay, A. N., G. J. Wright, et al. (2002). "CD200 and membrane protein interactions in the control of myeloid cells." Trends Immunol **23**(6): 285-90.

Barnes, J. L. (2002). Renal Disease. Platelets. A. D. Michelson, Elsevier Academic Press: 447 - 457.

Barthel, S. R., J. D. Gavino, et al. (2007). "Targeting selectins and selectin ligands in inflammation and cancer." Expert Opin Ther Targets **11**(11): 1473-91.

Bartlett, M. R., P. A. Underwood, et al. (1995). "Comparative analysis of the ability of leucocytes, endothelial cells and platelets to degrade the subendothelial basement membrane: evidence for cytokine dependence and detection of a novel sulfatase." Immunol Cell Biol **73**(2): 113-24.

Bastida, E., L. Almirall, et al. (1987). "Tumor-cell-induced platelet aggregation is a glycoprotein-dependent and lipoxygenase-associated process." Int J Cancer **39**(6): 760-3.

Bates, R. C., L. F. Lincz, et al. (1995). "Involvement of integrins in cell survival." Cancer Metastasis Rev **14**(3): 191-203.

Bayless, K. J., G. A. Meininger, et al. (1998). "Osteopontin is a ligand for the alpha4beta1 integrin." J Cell Sci **111 (Pt 9)**: 1165-74.

Ben-Baruch, A. (2008). "Organ selectivity in metastasis: regulation by chemokines and their receptors." Clin Exp Metastasis **25**(4): 345-56.

Berger, G., D. W. Hartwell, et al. (1998). "P-Selectin and platelet clearance." Blood **92**(11): 4446-52.

Berger, M. (1975). "Production of antibodies that bind biotin and inhibit biotin containing enzymes." Biochemistry **14**(11): 2338-42.

Biancone, L., M. Araki, et al. (1996). "Redirection of tumor metastasis by expression of E-selectin in vivo." J Exp Med **183**(2): 581-7.

Blair, P. and R. Flaumenhaft (2009). "Platelet alpha-granules: basic biology and clinical correlates." Blood Rev **23**(4): 177-89.

Bonder, C. S., S. R. Clark, et al. (2006). "Use of CD44 by CD4+ Th1 and Th2 lymphocytes to roll and adhere." Blood **107**(12): 4798-806.

Borsig, L., R. Wong, et al. (2002). "Synergistic effects of L- and P-selectin in facilitating tumor metastasis can involve non-mucin ligands and implicate leukocytes as enhancers of metastasis." Proc Natl Acad Sci U S A **99**(4): 2193-8.

Bosman, G. J., F. L. Willekens, et al. (2005). "Erythrocyte aging: a more than superficial resemblance to apoptosis?" Cell Physiol Biochem **16**(1-3): 1-8.

Bouillard, J. B. and S. Bouillaud (1823). "De l'Obliteration des veines et de son influence sur la formation des hydropisies partielles: consideration sur la hydropisies passive et general." Arch Gen Med **1**: 188-204.

Boyman, O., C. Ramsey, et al. (2008). "IL-7/anti-IL-7 mAb complexes restore T cell development and induce homeostatic T Cell expansion without lymphopenia." J Immunol **180**(11): 7265-75.

Braet, F. and E. Wisse (2002). "Structural and functional aspects of liver sinusoidal endothelial cell fenestrae: a review." Comp Hepatol **1**(1): 1.

Brodt, P., L. Fallavollita, et al. (1997). "Liver endothelial E-selectin mediates carcinoma cell adhesion and promotes liver metastasis." Int J Cancer **71**(4): 612-9.

Caligiuri, M. A., A. Zmuidzinas, et al. (1990). "Functional consequences of interleukin 2 receptor expression on resting human lymphocytes. Identification of a novel natural killer cell subset with high affinity receptors." J Exp Med **171**(5): 1509-26.

Camerer, E., A. A. Qazi, et al. (2004). "Platelets, protease-activated receptors, and fibrinogen in hematogenous metastasis." Blood **104**(2): 397-401.

Cameron, M. D., E. E. Schmidt, et al. (2000). "Temporal progression of metastasis in lung: cell survival, dormancy, and location dependence of metastatic inefficiency." Cancer Res **60**(9): 2541-6.

Cao, Y. (2005). "Opinion: emerging mechanisms of tumour lymphangiogenesis and lymphatic metastasis." Nat Rev Cancer **5**(9): 735-43.

Carman, C. V., P. T. Sage, et al. (2007). "Transcellular diapedesis is initiated by invasive podosomes." Immunity **26**(6): 784-97.

Carpinelli, M. R., D. J. Hilton, et al. (2004). "Suppressor screen in Mpl-/- mice: c-Myb mutation causes supraphysiological production of platelets in the absence of thrombopoietin signaling." Proc Natl Acad Sci U S A **101**(17): 6553-8.

Chambers, A. F., A. C. Groom, et al. (2002). "Dissemination and growth of cancer cells in metastatic sites." Nat Rev Cancer **2**(8): 563-72.

Chambers, A. F., G. N. Naumov, et al. (2001). "Critical steps in hematogenous metastasis: an overview." Surg Oncol Clin N Am **10**(2): 243-55, vii.

Chang, M., P. A. Nakagawa, et al. (2003). "Immune thrombocytopenic purpura (ITP) plasma and purified ITP monoclonal autoantibodies inhibit megakaryocytopoiesis in vitro." Blood **102**(3): 887-95.

Chang, Y. S., Y. Q. Chen, et al. (1992). "Increased expression of alpha IIb beta 3 integrin in subpopulations of murine melanoma cells with high lung-colonizing ability." Int J Cancer **51**(3): 445-51.

Chang, Y. S., E. di Tomaso, et al. (2000). "Mosaic blood vessels in tumors: frequency of cancer cells in contact with flowing blood." Proc Natl Acad Sci U S A **97**(26): 14608-13.

Chen, G., Y. W. Dang, et al. (2008). "Expression of heparanase in hepatocellular carcinoma has prognostic significance: a tissue microarray study." Oncol Res **17**(4): 183-9.

Chen, M., M. Sinha, et al. (2009). "Integrin alpha6beta4 controls the expression of genes associated with cell motility, invasion, and metastasis, including S100A4/metastasin." J Biol Chem **284**(3): 1484-94.

Chen, Y. Q., X. Gao, et al. (1992). "Identification of the alpha IIb beta 3 integrin in murine tumor cells." J Biol Chem **267**(24): 17314-20.

Chen, Y. Q., M. Trikha, et al. (1997). "Ectopic expression of platelet integrin alphaIIb beta3 in tumor cells from various species and histological origin." Int J Cancer **72**(4): 642-8.

Chong, B. H. (2009). "Primary immune thrombocytopenia: understanding pathogenesis is the key to better treatments." J Thromb Haemost **7**(2): 319-21.

Chung, J., A. G. Gao, et al. (1997). "Thrombspondin acts via integrin-associated protein to activate the platelet integrin alphaIIbbeta3." J Biol Chem **272**(23): 14740-6.

Chung, J., X. Q. Wang, et al. (1999). "Thrombospondin-1 acts via IAP/CD47 to synergize with collagen in alpha2beta1-mediated platelet activation." Blood **94**(2): 642-8.

Cines, D. B. and V. S. Blanchette (2002). "Immune thrombocytopenic purpura." N Engl J Med **346**(13): 995-1008.

Cines, D. B. and V. S. Blanchette (2006). Idiopathic Thrombocyopenic Purpura. Thrombocytopenia. K. R. McCrae. New York, Taylor-Francis Group: 115-144.

Clemetson, K. J. (2002). Platelet Receptors. Platelets. A. D. Michelson. San Diego, CA, Elsevier Science: 65-84.

Cohen, I. R., A. D. Murdoch, et al. (1994). "Abnormal expression of perlecan proteoglycan in metastatic melanomas." Cancer Res **54**(22): 5771-4.

Coller, B. S. and S. J. Shattil (2008). "The GPIIb/IIIa (integrin alphaIIbbeta3) odyssey: a technology-driven saga of a receptor with twists, turns, and even a bend." Blood **112**(8): 3011-25.

Condeelis, J. and J. E. Segall (2003). "Intravital imaging of cell movement in tumours." Nat Rev Cancer **3**(12): 921-30.

Cooper, N. and J. Bussel (2006). "The pathogenesis of immune thrombocytopaenic purpura." Br J Haematol **133**(4): 364-74.

Coradini, D., S. Zorzet, et al. (2004). "Inhibition of hepatocellular carcinomas in vitro and hepatic metastases in vivo in mice by the histone deacetylase inhibitor HA-But." Clin Cancer Res **10**(14): 4822-30.

Coussens, L. M. and Z. Werb (2002). "Inflammation and cancer." Nature **420**(6917): 860-7.

Coxon, A., P. Rieu, et al. (1996). "A novel role for the beta 2 integrin CD11b/CD18 in neutrophil apoptosis: a homeostatic mechanism in inflammation." Immunity **5**(6): 653-66.

Crissman, J. D., J. S. Hatfield, et al. (1988). "Morphological study of the interaction of intravascular tumor cells with endothelial cells and subendothelial matrix." Cancer Res **48**(14): 4065-72.

Crow, A. R., S. Song, et al. (2006). "Mechanisms of action of intravenous immunoglobulin in the treatment of immune thrombocytopenia." Pediatr Blood Cancer **47**(5 Suppl): 710-3.

Curran, S. and G. I. Murray (2000). "Matrix metalloproteinases: molecular aspects of their roles in tumour invasion and metastasis." Eur J Cancer **36**(13 Spec No): 1621-30.

Dale, G. L., P. Gaddy, et al. (1994). "Antibodies against biotinylated proteins are present in normal human serum." J Lab Clin Med **123**(3): 365-71.

DiCorleto, P. E. and C. A. de la Motte (1989). "Thrombin causes increased monocytic-cell adhesion to endothelial cells through a protein kinase C-dependent pathway." Biochem J **264**(1): 71-7.

Ding, L., M. Sunamura, et al. (2001). "In vivo evaluation of the early events associated with liver metastasis of circulating cancer cells." Br J Cancer **85**(3): 431-8.

Dowling, M. R., D. Milutinovic, et al. (2005). "Modelling cell lifespan and proliferation: is likelihood to die or to divide independent of age?" J R Soc Interface **2**(5): 517-26.

Elkin, M. and I. Vlodavsky (2001). "Tail vein assay of cancer metastasis." Curr Protoc Cell Biol **Chapter 19**: Unit 19 2.

Elzey, B. D., D. L. Sprague, et al. (2005). "The emerging role of platelets in adaptive immunity." Cell Immunol **238**(1): 1-9.

Eppihimer, M. J., B. Wolitzky, et al. (1996). "Heterogeneity of expression of E- and P-selectins in vivo." Circ Res **79**(3): 560-9.

Erpenbeck, L. and M. P. Schon (2010). "Deadly allies: the fatal interplay between platelets and metastasizing cancer cells." Blood **115**(17): 3427-36.

Ewing, J. (1928). Neoplastic Diseases. Philadelphia, USA, W.B. Saunders.

Falanga, A. (2004). "The effect of anticoagulant drugs on cancer." J Thromb Haemost **2**(8): 1263-5.

Felding-Habermann, B., R. Habermann, et al. (1996). "Role of beta3 integrins in melanoma cell adhesion to activated platelets under flow." J Biol Chem **271**(10): 5892-900.

Feng, D., J. A. Nagy, et al. (2002). "Ultrastructural studies define soluble macromolecular, particulate, and cellular transendothelial cell pathways in venules, lymphatic vessels, and tumor-associated microvessels in man and animals." Microsc Res Tech **57**(5): 289-326.

Feng, D., J. A. Nagy, et al. (1998). "Platelets exit venules by a transcellular pathway at sites of F-met peptide-induced acute inflammation in guinea pigs." Int Arch Allergy Immunol **116**(3): 188-95.

Fogler, W. E., K. Volker, et al. (1996). "NK cell infiltration into lung, liver, and subcutaneous B16 melanoma is mediated by VCAM-1/VLA-4 interaction." J Immunol **156**(12): 4707-14.

Foller, M., S. M. Huber, et al. (2008). "Erythrocyte programmed cell death." IUBMB Life **60**(10): 661-8.

Frenette, P. S., C. V. Denis, et al. (2000). "P-Selectin glycoprotein ligand 1 (PSGL-1) is expressed on platelets and can mediate platelet-endothelial interactions in vivo." J Exp Med **191**(8): 1413-22.

Frenette, P. S., R. C. Johnson, et al. (1995). "Platelets roll on stimulated endothelium in vivo: an interaction mediated by endothelial P-selectin." Proc Natl Acad Sci U S A **92**(16): 7450-4.

Fridman, W. H. (1991). "Fc receptors and immunoglobulin binding factors." Faseb J **5**(12): 2684-90.

Friedl, P. and K. Wolf (2003). "Tumour-cell invasion and migration: diversity and escape mechanisms." Nat Rev Cancer **3**(5): 362-74.

Furie, B. and B. C. Furie (2004). "Role of platelet P-selectin and microparticle PSGL-1 in thrombus formation." Trends Mol Med **10**(4): 171-8.

Fuse, C., Y. Ishida, et al. (2007). "Junctional adhesion molecule-C promotes metastatic potential of HT1080 human fibrosarcoma." J Biol Chem **282**(11): 8276-83.

Garcia, J., N. Callewaert, et al. (2007). "P-selectin mediates metastatic progression through binding to sulfatides on tumor cells." Glycobiology **17**(2): 185-96.

Gasic, G. J. (1984). "Role of plasma, platelets, and endothelial cells in tumor metastasis." Cancer Metastasis Rev **3**(2): 99-114.

Gasic, G. J., T. B. Gasic, et al. (1968). "Antimetastatic effects associated with platelet reduction." Proc Natl Acad Sci U S A **61**(1): 46-52.

Gassmann, P., M. L. Kang, et al. (2010). "In vivo tumor cell adhesion in the pulmonary microvasculature is exclusively mediated by tumor cell--endothelial cell interaction." BMC Cancer **10**: 177.

Geddis, A. E., H. M. Linden, et al. (2002). "Thrombopoietin: a pan-hematopoietic cytokine." Cytokine Growth Factor Rev **13**(1): 61-73.

Geiger, T. R. and D. S. Peeper (2009). "Metastasis mechanisms." Biochim Biophys Acta **1796**(2): 293-308.

Girard, J. P. and T. A. Springer (1995). "High endothelial venules (HEVs): specialized endothelium for lymphocyte migration." Immunol Today **16**(9): 449-57.

Golino, P., P. R. Maroko, et al. (1987). "Efficacy of platelet depletion in counteracting the detrimental effect of acute hypercholesterolemia on infarct size and the no-reflow phenomenon in rabbits undergoing coronary artery occlusion-reperfusion." Circulation **76**(1): 173-80.

Gong, N. and S. Chatterjee (2003). "Platelet endothelial cell adhesion molecule in cell signaling and thrombosis." Mol Cell Biochem **253**(1-2): 151-8.

Goodman, J. W. and L. H. Smith (1961). "Erythrocyte life span in normal mice and in radiation bone marrow chimeras." Am J Physiol **200**: 764-70.

Gorelik, E., W. W. Bere, et al. (1984). "Role of NK cells in the antimetastatic effect of anticoagulant drugs." Int J Cancer **33**(1): 87-94.

Goto, S., N. Tamura, et al. (2002). "Involvement of glycoprotein VI in platelet thrombus formation on both collagen and von Willebrand factor surfaces under flow conditions." Circulation **106**(2): 266-72.

Grivennikov, S. I. and M. Karin (2010). "Inflammation and oncogenesis: a vicious connection." Curr Opin Genet Dev **20**(1): 65-71.

Grossi, I. M., L. A. Fitzgerald, et al. (1987). "Inhibition of human tumor cell induced platelet aggregation by antibodies to platelet glycoproteins Ib and IIb/IIIa." Proc Soc Exp Biol Med **186**(3): 378-83.

Guarino, M., B. Rubino, et al. (2007). "The role of epithelial-mesenchymal transition in cancer pathology." Pathology **39**(3): 305-18.

Guo, Y. L., D. Q. Liu, et al. (2009). "Down-regulation of platelet surface CD47 expression in Escherichia coli O157:H7 infection-induced thrombocytopenia." PLoS One **4**(9): e7131.

Guyer, D. A., K. L. Moore, et al. (1996). "P-selectin glycoprotein ligand-1 (PSGL-1) is a ligand for L-selectin in neutrophil aggregation." Blood **88**(7): 2415-21.

Hanley, W. D., S. L. Napier, et al. (2006). "Variant isoforms of CD44 are P- and L-selectin ligands on colon carcinoma cells." Faseb J **20**(2): 337-9.

Hanna, N. and I. J. Fidler (1980). "Role of natural killer cells in the destruction of circulating tumor emboli." J Natl Cancer Inst **65**(4): 801-9.

Hanson, S. R. and S. J. Slichter (1985). "Platelet kinetics in patients with bone marrow hypoplasia: evidence for a fixed platelet requirement." Blood **66**(5): 1105-9.

Harrington, W. J., V. Minnich, et al. (1951). "Demonstration of a thrombocytopenic factor in the blood of patients with thrombocytopenic purpura. ." J Lab Clin Med **38**: 1-10.

Hato, T., M. H. Ginsberg, et al. (2002). Integrin αIIbβ3 Platelets. A. D. Michelson. California, USA, Acadmic Press: 105-116.

Heilmann, E., P. Friese, et al. (1993). "Biotinylated platelets: a new approach to the measurement of platelet life span." Br J Haematol **85**(4): 729-35.

Henn, V., J. R. Slupsky, et al. (1998). "CD40 ligand on activated platelets triggers an inflammatory reaction of endothelial cells." Nature **391**(6667): 591-4.

Herberman, R. B., M. E. Nunn, et al. (1975). "Natural cytotoxic reactivity of mouse lymphoid cells against syngeneic and allogeneic tumors. II. Characterization of effector cells." Int J Cancer **16**(2): 230-9.

Herbst, R. S. (2004). "Review of epidermal growth factor receptor biology." Int J Radiat Oncol Biol Phys **59**(2 Suppl): 21-6.

Herrera-Galeano, J. E., D. M. Becker, et al. (2008). "A novel variant in the platelet endothelial aggregation receptor-1 gene is associated with increased platelet aggregability." Arterioscler Thromb Vasc Biol **28**(8): 1484-90.

Hidalgo, A. and P. S. Frenette (2007). "Leukocyte podosomes sense their way through the endothelium." Immunity **26**(6): 753-5.

Hoek, R. M., S. R. Ruuls, et al. (2000). "Down-regulation of the macrophage lineage through interaction with OX2 (CD200)." Science **290**(5497): 1768-71.

Hoffmann, A. C., R. Mori, et al. (2008). "High expression of heparanase is significantly associated with dedifferentiation and lymph node metastasis in patients with pancreatic ductal adenocarcinomas and correlated to PDGFA and via HIF1a to HB-EGF and bFGF." J Gastrointest Surg **12**(10): 1674-81; discussion 1681-2.

Hoffmann-Fezer, G., H. Maschke, et al. (1991). "Direct in vivo biotinylation of erythrocytes as an assay for red cell survival studies." Ann Hematol **63**(4): 214-7.

Hoffmann-Fezer, G., J. Mysliwietz, et al. (1993). "Biotin labeling as an alternative nonradioactive approach to determination of red cell survival." Ann Hematol **67**(2): 81-7.

Hoffmeister, K. M., T. W. Felbinger, et al. (2003). "The clearance mechanism of chilled blood platelets." Cell **112**(1): 87-97.

Hofmann, U. B., J. R. Westphal, et al. (2000). "Matrix metalloproteinases in human melanoma." J Invest Dermatol **115**(3): 337-44.

Hofmann, U. B., J. R. Westphal, et al. (2000). "Coexpression of integrin alpha(v)beta3 and matrix metalloproteinase-2 (MMP-2) coincides with MMP-2 activation: correlation with melanoma progression." J Invest Dermatol **115**(4): 625-32.

Honn, K. V., D. G. Tang, et al. (1992). "Platelets and cancer metastasis: a causal relationship?" Cancer Metastasis Rev **11**(3-4): 325-51.

Horsewood, P., C. P. Hayward, et al. (1991). "Investigation of the mechanisms of monoclonal antibody-induced platelet activation." Blood **78**(4): 1019-26.

Houwerzijl, E. J., N. R. Blom, et al. (2004). "Ultrastructural study shows morphologic features of apoptosis and para-apoptosis in megakaryocytes from patients with idiopathic thrombocytopenic purpura." Blood **103**(2): 500-6.

Houwerzijl, E. J., N. R. Blom, et al. (2006). "Megakaryocytic dysfunction in myelodysplastic syndromes and idiopathic thrombocytopenic purpura is in part due to different forms of cell death." Leukemia **20**(11): 1937-42.

Hulett, M. D. and P. M. Hogarth (1994). "Molecular basis of Fc receptor function." Adv Immunol **57**: 1-127.

Hulett, M. D., J. R. Hornby, et al. (2000). "Identification of active-site residues of the pro-metastatic endoglycosidase heparanase." Biochemistry **39**(51): 15659-67.

Imaizumi, T., H. Itaya, et al. (2000). "Expression of tumor necrosis factor-alpha in cultured human endothelial cells stimulated with lipopolysaccharide or interleukin-1alpha." Arterioscler Thromb Vasc Biol **20**(2): 410-5.

Israels, S. J., J. M. Gerrard, et al. (1992). "Platelet dense granule membranes contain both granulophysin and P-selectin (GMP-140)." Blood **80**(1): 143-52.

Itoh, Y. and H. Nagase (2002). "Matrix metalloproteinases in cancer." Essays Biochem **38**: 21-36.

Jackson, S. P. (2007). "The growing complexity of platelet aggregation." Blood **109**(12): 5087-95.

Jain, S., M. Zuka, et al. (2007). "Platelet glycoprotein Ib alpha supports experimental lung metastasis." Proc Natl Acad Sci U S A **104**(21): 9024-8.

Janowska-Wieczorek, A., L. A. Marquez-Curtis, et al. (2006). "Enhancing effect of platelet-derived microvesicles on the invasive potential of breast cancer cells." Transfusion **46**(7): 1199-209.

Janowska-Wieczorek, A., M. Wysoczynski, et al. (2005). "Microvesicles derived from activated platelets induce metastasis and angiogenesis in lung cancer." Int J Cancer **113**(5): 752-60.

Jennings, L. K. (2009). "Role of platelets in atherothrombosis." Am J Cardiol **103**(3 Suppl): 4A-10A.

Jiang, X., H. Multhaupt, et al. (2004). "Essential contribution of tumor-derived perlecan to epidermal tumor growth and angiogenesis." J Histochem Cytochem **52**(12): 1575-90.

Jiang, Y., S. Hirose, et al. (2000). "Polymorphisms in IgG Fc receptor IIB regulatory regions associated with autoimmune susceptibility." Immunogenetics **51**(6): 429-35.

Kalluri, R. and R. A. Weinberg (2009). "The basics of epithelial-mesenchymal transition." J Clin Invest **119**(6): 1420-8.

Kaplan, R. N., R. D. Riba, et al. (2005). "VEGFR1-positive haematopoietic bone marrow progenitors initiate the pre-metastatic niche." Nature **438**(7069): 820-7.

Karpatkin, S. (2002). Tumor Growth and Metastasis. Platelets. A. D. Michelson, Elsevier Science: 491-502.

Karpatkin, S. and E. Pearlstein (1981). "Role of platelets in tumor cell metastasis." Ann Intern Med **95**(5): 636-641.

Karpatkin, S., E. Pearlstein, et al. (1988). "Role of adhesive proteins in platelet tumor interaction in vitro and metastasis formation in vivo." J Clin Invest **81**(4): 1012-9.

Karsan, A. and J. M. Harlan (1999). The Blood Vessel Wall. Hematology: Basic Principles and Practice. R. Hoffman, E. J. J. Benz, S. J. Shattilet al. New York, Churchill Livingstone: 1770 - 1782.

Kennel, S. J., T. K. Lankford, et al. (1993). "CD44 expression on murine tissues." J Cell Sci **104 (Pt 2)**: 373-82.

Kereiakes, D. J., J. H. Essell, et al. (1996). "Abciximab-associated profound thrombocytopenia: therapy with immunoglobulin and platelet transfusion." Am J Cardiol **78**(10): 1161-3.

Khotskaya, Y. B., Y. Dai, et al. (2009). "Syndecan-1 is required for robust growth, vascularization, and metastasis of myeloma tumors in vivo." J Biol Chem **284**(38): 26085-95.

Kiessling, R., O. Haller, et al. (1978). "Mouse natural killer (NK) cell activity against human cell lines is not influenced by superinfection of the target cell with xenotropic murine C-type virus." Int J Cancer **21**(4): 460-5.

Kikkawa, H., D. Miyamoto, et al. (1998). "Role of sialylglycoconjugate(s) in the initial phase of metastasis of liver-metastatic RAW117 lymphoma cells." Jpn J Cancer Res **89**(12): 1296-305.

Kim, S., K. Iizuka, et al. (2000). "In vivo natural killer cell activities revealed by natural killer cell-deficient mice." Proc Natl Acad Sci U S A **97**(6): 2731-6.

Kim, Y. J., L. Borsig, et al. (1999). "Distinct selectin ligands on colon carcinoma mucins can mediate pathological interactions among platelets, leukocytes, and endothelium." Am J Pathol **155**(2): 461-72.

Kim, Y. J., L. Borsig, et al. (1998). "P-selectin deficiency attenuates tumor growth and metastasis." Proc Natl Acad Sci U S A **95**(16): 9325-30.

Klinger, M. H. F. (2002). Inflammation. Platelets. A. D. Michelson. San Diego, CA, Elsevier Science: 459-467.

Klintman, D., X. Li, et al. (2004). "Important role of P-selectin for leukocyte recruitment, hepatocellular injury, and apoptosis in endotoxemic mice." Clin Diagn Lab Immunol **11**(1): 56-62.

Konstantopoulos, K. and S. N. Thomas (2009). "Cancer Cells in Transit: The Vascular Interactions of Tumor Cells." Annu Rev Biomed Eng.

Kopp, H. G., T. Placke, et al. (2009). "Platelet-derived transforming growth factor-beta down-regulates NKG2D thereby inhibiting natural killer cell antitumor reactivity." Cancer Res **69**(19): 7775-83.

Kretz-Rommel, A., F. Qin, et al. (2008). "Blockade of CD200 in the presence or absence of antibody effector function: implications for anti-CD200 therapy." J Immunol **180**(2): 699-705.

Kuderer, N. M., A. A. Khorana, et al. (2007). "A meta-analysis and systematic review of the efficacy and safety of anticoagulants as cancer treatment: impact on survival and bleeding complications." Cancer **110**(5): 1149-61.

Kuligowski, M. P., A. R. Kitching, et al. (2006). "Leukocyte recruitment to the inflamed glomerulus: a critical role for platelet-derived P-selectin in the absence of rolling." J Immunol **176**(11): 6991-9.

Kurosawa, S., M. Harada, et al. (1995). "Early-appearing tumour-infiltrating natural killer cells play a crucial role in the generation of anti-tumour T lymphocytes." Immunology **85**(2): 338-46.

Kurosawa, S., G. Matsuzaki, et al. (1993). "Early appearance and activation of natural killer cells in tumor-infiltrating lymphoid cells during tumor development." Eur J Immunol **23**(5): 1029-33.

Laubli, H., J. L. Stevenson, et al. (2006). "L-selectin facilitation of metastasis involves temporal induction of Fut7-dependent ligands at sites of tumor cell arrest." Cancer Res **66**(3): 1536-42.

Lee, W. Y. and P. Kubes (2008). "Leukocyte adhesion in the liver: distinct adhesion paradigm from other organs." J Hepatol **48**(3): 504-12.

Lejtenyi, D., D. G. Osmond, et al. (2003). "Natural killer cells and B lymphocytes in L-selectin and Mac-1/LFA-1 knockout mice: marker-dependent, but not cell lineage-dependent changes in the spleen and bone marrow." Immunobiology **207**(2): 129-35.

Lelekakis, M., J. M. Moseley, et al. (1999). "A novel orthotopic model of breast cancer metastasis to bone." Clin Exp Metastasis **17**(2): 163-70.

Lengweiler, S., S. S. Smyth, et al. (1999). "Preparation of monoclonal antibodies to murine platelet glycoprotein IIb/IIIa (alphaIIbbeta3) and other proteins from hamster-mouse interspecies hybridomas." Biochem Biophys Res Commun **262**(1): 167-73.

Li, F., P. P. Wilkins, et al. (1996). "Post-translational modifications of recombinant P-selectin glycoprotein ligand-1 required for binding to P- and E-selectin." J Biol Chem **271**(6): 3255-64.

Li, Z., M. A. Nardi, et al. (2008). "Platelet fragmentation requires a specific structural conformation of human monoclonal antibody against beta3 integrin." J Biol Chem **283**(6): 3224-30.

Liang, S. X., M. Pinkevych, et al. (2010). "Drug-induced thrombocytopenia: development of a novel NOD/SCID mouse model to evaluate clearance of circulating platelets by drug-dependent antibodies and the efficacy of IVIG." Blood **116**(11): 1958-60.

Lindberg, F. P., D. C. Bullard, et al. (1996). "Decreased resistance to bacterial infection and granulocyte defects in IAP-deficient mice." Science **274**(5288): 795-8.

Liotta, L. A. (1992). "Cancer cell invasion and metastasis." Sci Am **266**(2): 54-9, 62-3.

Liotta, L. A., J. Kleinerman, et al. (1974). "Quantitative relationships of intravascular tumor cells, tumor vessels, and pulmonary metastases following tumor implantation." Cancer Res **34**(5): 997-1004.

Liu, L. and P. Kubes (2003). "Molecular mechanisms of leukocyte recruitment: organ-specific mechanisms of action." Thromb Haemost **89**(2): 213-20.

Lopez, J. A. and M. C. Berndt (2002). The GPIb-IX-V Complex. Platelets. A. D.Michelson. Massachusetts, Academic Press**:** 85-104.

Lotter, M. G., A. D. Heyns, et al. (1986). "Evaluation of mathematic models to assess platelet kinetics." J Nucl Med **27**(7): 1192-201.

Ludwig, R. J., B. Boehme, et al. (2004). "Endothelial P-selectin as a target of heparin action in experimental melanoma lung metastasis." Cancer Res **64**(8): 2743-50.

Luscinskas, F. W., G. S. Kansas, et al. (1994). "Monocyte rolling, arrest and spreading on IL-4-activated vascular endothelium under flow is mediated via sequential action of L-selectin, beta 1-integrins, and beta 2-integrins." J Cell Biol **125**(6): 1417-27.

Luzzi, K. J., I. C. MacDonald, et al. (1998). "Multistep nature of metastatic inefficiency: dormancy of solitary cells after successful extravasation and limited survival of early micrometastases." Am J Pathol **153**(3): 865-73.

Lyons, A. B. and C. R. Parish (1994). "Determination of lymphocyte division by flow cytometry." J Immunol Methods **171**(1): 131-7.

Magnusson, S., M. Hou, et al. (1998). "Biotinylated platelets have an impaired response to agonists as evidenced by in vitro platelet aggregation tests." Thromb Res **89**(2): 53-8.

Majka, M., J. Ratajczak, et al. (2002). "Thrombopoietin, but not cytokines binding to gp130 protein-coupled receptors, activates MAPKp42/44, AKT, and STAT proteins in normal human CD34+ cells, megakaryocytes, and platelets." Exp Hematol **30**(7): 751-60.

Mandybur, T. I. (1981). "Metastatic brain tumors induced by injected of syngeneic tumor cells into cerebral circulation in rats." Acta Neuropathol **53**(1): 57-63.

Mannori, G., P. Crottet, et al. (1995). "Differential colon cancer cell adhesion to E-, P-, and L-selectin: role of mucin-type glycoproteins." Cancer Res **55**(19): 4425-31.

Marinkovic, D., X. Zhang, et al. (2007). "Foxo3 is required for the regulation of oxidative stress in erythropoiesis." J Clin Invest **117**(8): 2133-44.

Mason, K. D., M. R. Carpinelli, et al. (2007). "Programmed anuclear cell death delimits platelet life span." Cell **128**(6): 1173-86.

Massberg, S., G. Enders, et al. (1999). "Fibrinogen deposition at the postischemic vessel wall promotes platelet adhesion during ischemia-reperfusion in vivo." Blood **94**(11): 3829-38.

May, A. E., T. Kalsch, et al. (2002). "Engagement of Glycoprotein IIb/IIIa on Platelets Upregulates CD40L and Triggers CD40L-Dependent Matrix Degradation by Endothelial Cells." Circulation **106**: 2111-2117.

May, F., I. Hagedorn, et al. (2009). "CLEC-2 is an essential platelet-activating receptor in hemostasis and thrombosis." Blood **114**(16): 3464-72.

McDonald, B., E. F. McAvoy, et al. (2008). "Interaction of CD44 and hyaluronan is the dominant mechanism for neutrophil sequestration in inflamed liver sinusoids." J Exp Med **205**(4): 915-27.

McEver, R. P., K. L. Moore, et al. (1995). "Leukocyte trafficking mediated by selectin-carbohydrate interactions." J Biol Chem **270**(19): 11025-8.

McKenzie, S. E. (2002). "Humanized mouse models of FcR clearance in immune platelet disorders." Blood Rev **16**(1): 3-5.

McMillan, R., L. Wang, et al. (2004). "Suppression of in vitro megakaryocyte production by antiplatelet autoantibodies from adult patients with chronic ITP." Blood **103**(4): 1364-9.

Merten, M. and P. Thiagarajan (2000). "P-selectin expression on platelets determines size and stability of platelet aggregates." Circulation **102**(16): 1931-6.

Meyer, T. and I. R. Hart (1998). "Mechanisms of tumour metastasis." Eur J Cancer **34**(2): 214-21.

Mezzano, D., V. Matus, et al. (2008). "Tissue factor storage, synthesis and function in normal and activated human platelets." Thromb Res **122 Suppl 1**: S31-6.

Michelson, A. D., M. R. Barnard, et al. (1996). "In vivo tracking of platelets: circulating degranulated platelets rapidly lose surface P-selectin but continue to circulate and function." Proc Natl Acad Sci U S A **93**(21): 11877-82.

Mikami, S., M. Oya, et al. (2008). "Expression of heparanase in renal cell carcinomas: implications for tumor invasion and prognosis." Clin Cancer Res **14**(19): 6055-61.

Miles, F. L., F. L. Pruitt, et al. (2008). "Stepping out of the flow: capillary extravasation in cancer metastasis." Clin Exp Metastasis **25**(4): 305-24.

Moore, K. L., S. F. Eaton, et al. (1994). "The P-selectin glycoprotein ligand from human neutrophils displays sialylated, fucosylated, O-linked poly-N-acetyllactosamine." J Biol Chem **269**(37): 23318-27.

Mummert, M. E., D. I. Mummert, et al. (2003). "Functional roles of hyaluronan in B16-F10 melanoma growth and experimental metastasis in mice." Mol Cancer Ther **2**(3): 295-300.

Murphy, E. A. and M. E. Francis (1969). "The Estimation of Blood Platelet Survival I. General Principles of the Study of Cell Survival." Thrombosis and Haemostasis **22**: 281-295.

Murphy, E. A. and M. E. Francis (1971). "The estimation of blood platelet survival. II. The multiple hit model." Thromb Diath Haemorrh **25**(1): 53-80.

Muzykantov, V. R., J. C. Murciano, et al. (1996). "Regulation of the complement-mediated elimination of red blood cells modified with biotin and streptavidin." Anal Biochem **241**(1): 109-19.

Nakhaei-Nejad, M., A. M. Hussain, et al. (2007). "Endothelial PI 3-kinase activity regulates lymphocyte diapedesis." Am J Physiol Heart Circ Physiol **293**(6): H3608-16.

Nanda, N., M. Bao, et al. (2005). "Platelet endothelial aggregation receptor 1 (PEAR1), a novel epidermal growth factor repeat-containing transmembrane receptor, participates in platelet contact-induced activation." J Biol Chem **280**(26): 24680-9.

Nardi, M., S. Tomlinson, et al. (2001). "Complement-independent, peroxide-induced antibody lysis of platelets in HIV-1-related immune thrombocytopenia." Cell **106**(5): 551-61.

National Cancer Institute, U. S. N. I. o. H. "Metastatic Cancer: Questions and Answers." Retrieved 24th June, 2010, from http://www.cancer.gov/cancertopics/factsheet/Sites-Types/metastatic.

Naumov, G. N., L. A. Akslen, et al. (2006). "Role of angiogenesis in human tumor dormancy: animal models of the angiogenic switch." Cell Cycle **5**(16): 1779-87.

Nguyen, D. X., P. D. Bos, et al. (2009). "Metastasis: from dissemination to organ-specific colonization." Nat Rev Cancer **9**(4): 274-84.

Nicolson, G. L. (1993). "Cancer progression and growth: relationship of paracrine and autocrine growth mechanisms to organ preference of metastasis." Exp Cell Res **204**(2): 171-80.

Nierodzik, M. L., F. Kajumo, et al. (1992). "Effect of thrombin treatment of tumor cells on adhesion of tumor cells to platelets in vitro and tumor metastasis in vivo." Cancer Res **52**(12): 3267-72.

Nieswandt, B., W. Bergmeier, et al. (2000). "Identification of critical antigen-specific mechanisms in the development of immune thrombocytopenic purpura in mice." Blood **96**(7): 2520-7.

Nieswandt, B., M. Hafner, et al. (1999). "Lysis of tumor cells by natural killer cells in mice is impeded by platelets." Cancer Res **59**(6): 1295-300.

Nimmerjahn, F., P. Bruhns, et al. (2005). "FcgammaRIV: a novel FcR with distinct IgG subclass specificity." Immunity **23**(1): 41-51.

Noble, S. and J. Pasi (2010). "Epidemiology and pathophysiology of cancer-associated thrombosis." Br J Cancer **102 Suppl 1**: S2-9.

Nourshargh, S., P. L. Hordijk, et al. (2010). "Breaching multiple barriers: leukocyte motility through venular walls and the interstitium." Nat Rev Mol Cell Biol **11**(5): 366-78.

Nurden, A. T., P. Nurden, et al. (2008). "Platelets and wound healing." Front Biosci **13**: 3532-48.

Nurden, A. T., J. F. Viallard, et al. (2009). "New-generation drugs that stimulate platelet production in chronic immune thrombocytopenic purpura." Lancet **373**(9674): 1562-9.

Nurden, P., G. Clofent-Sanchez, et al. (2004). "Delayed immunologic thrombocytopenia induced by abciximab." Thromb Haemost **92**(4): 820-8.

Offermanns, S., C. F. Toombs, et al. (1997). "Defective platelet activation in G alpha(q)-deficient mice." Nature **389**(6647): 183-6.

Oldenborg, P. A., H. D. Gresham, et al. (2001). "CD47-signal regulatory protein alpha (SIRPalpha) regulates Fcgamma and complement receptor-mediated phagocytosis." J Exp Med **193**(7): 855-62.

Oleksowicz, L., Z. Mrowiec, et al. (1995). "Characterization of tumor-induced platelet aggregation: the role of immunorelated GPIb and GPIIb/IIIa expression by MCF-7 breast cancer cells." Thromb Res **79**(3): 261-74.

Olsson, M., P. Bruhns, et al. (2005). "Platelet homeostasis is regulated by platelet expression of CD47 under normal conditions and in passive immune thrombocytopenia." Blood **105**(9): 3577-82.

Orian-Rousseau, V. (2010). "CD44, a therapeutic target for metastasising tumours." Eur J Cancer **46**(7): 1271-7.

Paget, S. (1889). "The distribution of secondary growths in cancer of the breast." Lancet **1**: 571-573.

Palma-Nicolas, J. P., E. Lopez, et al. (2010). "Thrombin stimulates RPE cell motility by PKC-zeta- and NF-kappaB-dependent gene expression of MCP-1 and CINC-1/GRO chemokines." J Cell Biochem **110**(4): 948-967.

Palumbo, J. S., K. W. Kombrinck, et al. (2000). "Fibrinogen is an important determinant of the metastatic potential of circulating tumor cells." Blood **96**(10): 3302-9.

Palumbo, J. S., K. E. Talmage, et al. (2005). "Platelets and fibrin(ogen) increase metastatic potential by impeding natural killer cell-mediated elimination of tumor cells." Blood **105**(1): 178-85.

Panis, Y., B. Nordlinger, et al. (1990). "Experimental colorectal liver metastases. Influence of sex, immunological status and liver regeneration." J Hepatol **11**(1): 53-7.

Parish, C. R. (2006). "The role of heparan sulphate in inflammation." Nat Rev Immunol **6**(9): 633-43.

Parish, C. R., C. Freeman, et al. (1999). "Identification of sulfated oligosaccharide-based inhibitors of tumor growth and metastasis using novel in vitro assays for angiogenesis and heparanase activity." Cancer Res **59**(14): 3433-41.

Parish, C. R., C. Freeman, et al. (2001). "Heparanase: a key enzyme involved in cell invasion." Biochim Biophys Acta **1471**(3): M99-108.

Patel, D., H. Vaananen, et al. (2003). "Dynamics of GPIIb/IIIa-mediated platelet-platelet interactions in platelet adhesion/thrombus formation on collagen in vitro as revealed by videomicroscopy." Blood **101**(3): 929-36.

Pauli, B. U., H. G. Augustin-Voss, et al. (1990). "Organ-preference of metastasis. The role of endothelial cell adhesion molecules." Cancer Metastasis Rev **9**(3): 175-89.

Pilaro, A. M., D. D. Taub, et al. (1994). "TNF-alpha is a principal cytokine involved in the recruitment of NK cells to liver parenchyma." J Immunol **153**(1): 333-42.

Pitchford, S. C., S. Momi, et al. (2008). "Allergen induces the migration of platelets to lung tissue in allergic asthma." Am J Respir Crit Care Med **177**(6): 604-12.

Pitchford, S. C., S. Momi, et al. (2005). "Platelet P-selectin is required for pulmonary eosinophil and lymphocyte recruitment in a murine model of allergic inflammation." Blood **105**(5): 2074-81.

Pitchford, S. C., H. Yano, et al. (2003). "Platelets are essential for leukocyte recruitment in allergic inflammation." J Allergy Clin Immunol **112**(1): 109-18.

Plow, E. F. and M. H. Ginsberg (1999). The Molecular Basis for Platelet Function. Hematology: Basic Principles and Practice. R. Hoffman, E. J. J. Benz, S. J. Shattilet al. New York, N.Y., Churchill Livingstone: 1741-1752.

Ponta, H., L. Sherman, et al. (2003). "CD44: from adhesion molecules to signalling regulators." Nat Rev Mol Cell Biol **4**(1): 33-45.

Poujol, C., W. Bergmeier, et al. (2003). "Effect of infusing rat monoclonal antibodies to the murine GPIb-IX-V complex on platelet and megakaryocyte morphology in mice." Platelets **14**(1): 35-45.

Prevost, N., D. Woulfe, et al. (2002). "Interactions between Eph kinases and ephrins provide a mechanism to support platelet aggregation once cell-to-cell contact has occurred." Proc Natl Acad Sci U S A **99**(14): 9219-24.

Provan, D., R. Stasi, et al. (2009). "International consensus report on the investigation and management of primary immune thrombocytopenia." Blood.

Psaila, B. and D. Lyden (2009). "The metastatic niche: adapting the foreign soil." Nat Rev Cancer **9**(4): 285-93.

Quah, B. J., H. S. Warren, et al. (2007). "Monitoring lymphocyte proliferation in vitro and in vivo with the intracellular fluorescent dye carboxyfluorescein diacetate succinimidyl ester." Nat Protoc **2**(9): 2049-56.

Rabinovitz, I. and A. M. Mercurio (1996). "The integrin alpha 6 beta 4 and the biology of carcinoma." Biochem Cell Biol **74**(6): 811-21.

Raju, T. S. (2008). "Terminal sugars of Fc glycans influence antibody effector functions of IgGs." Curr Opin Immunol **20**(4): 471-8.

Ravetch, J. V. and S. Bolland (2001). "IgG Fc receptors." Annu Rev Immunol **19**: 275-90.

Reed, G. L. (2002). Platelet Secretion. Platelets. A. D. Michelson. San Diego, CA, Elsevier Science: 181-195.

Rhodes, M. M., P. Kopsombut, et al. (2005). "Bcl-x(L) prevents apoptosis of late-stage erythroblasts but does not mediate the antiapoptotic effect of erythropoietin." Blood **106**(5): 1857-63.

Riccardi, C., A. Santoni, et al. (1980). "In vivo natural reactivity of mice against tumor cells." Int J Cancer **25**(4): 475-86.

Rickles, F. R., S. Patierno, et al. (2003). "Tissue factor, thrombin, and cancer." Chest **124**(3 Suppl): 58S-68S.

Roos, E. (1991). "Adhesion molecules in lymphoma metastasis." Cancer Metastasis Rev **10**(1): 33-48.

Ruffell, B. and P. Johnson (2009) "The regulation and function of hyaluronan binding by CD44 in the immune system." Hyaluronan Today **Volume**, DOI:

Salter, J. W., C. F. Krieglstein, et al. (2001). "Platelets modulate ischemia/reperfusion-induced leukocyte recruitment in the mesenteric circulation." Am J Physiol Gastrointest Liver Physiol **281**(6): G1432-9.

Samanna, V., H. Wei, et al. (2006). "Alpha-V-dependent outside-in signaling is required for the regulation of CD44 surface expression, MMP-2 secretion, and cell migration by osteopontin in human melanoma cells." Exp Cell Res **312**(12): 2214-30.

Samuelsson, A., T. L. Towers, et al. (2001). "Anti-inflammatory activity of IVIG mediated through the inhibitory Fc receptor." Science **291**(5503): 484-6.

Sanderson, R. D. (2001). "Heparan sulfate proteoglycans in invasion and metastasis." Semin Cell Dev Biol **12**(2): 89-98.

Santoso, S., V. V. Orlova, et al. (2005). "The homophilic binding of junctional adhesion molecule-C mediates tumor cell-endothelial cell interactions." J Biol Chem **280**(43): 36326-33.

Seiffert, M., P. Brossart, et al. (2001). "Signal-regulatory protein alpha (SIRPalpha) but not SIRPbeta is involved in T-cell activation, binds to CD47 with high affinity, and is expressed on immature CD34(+)CD38(-) hematopoietic cells." Blood **97**(9): 2741-9.

Sheibani, N. and W. A. Frazier (1999). "Thrombospondin-1, PECAM-1, and regulation of angiogenesis." Histol Histopathol **14**(1): 285-94.

Sheikh, S., R. S. Parhar, et al. (2004). "Immobilization of rolling NK cells on platelet-borne P-selectin under flow by proinflammatory stimuli, interleukin-12, and leukotriene B4." J Leukoc Biol **76**(3): 603-8.

Shulman, N. R., V. J. Marder, et al. (1965). "Similarities between known antiplatelet antibodies and the factor responsible for thrombocytopenia in idiopathic purpura. Physiologic, serologic and isotopic studies." Ann N Y Acad Sci **124**(2): 499-542.

Shultz, L. D., B. L. Lyons, et al. (2005). "Human lymphoid and myeloid cell development in NOD/LtSz-scid IL2R gamma null mice engrafted with mobilized human hemopoietic stem cells." J Immunol **174**(10): 6477-89.

Singh, I., G. B. Zibari, et al. (1999). "Role of P-selectin expression in hepatic ischemia and reperfusion injury." Clin Transplant **13**(1 Pt 2): 76-82.

Smyth, M. J., Y. Hayakawa, et al. (2002). "New aspects of natural-killer-cell surveillance and therapy of cancer." Nat Rev Cancer **2**(11): 850-61.

Smyth, M. J., J. M. Kelly, et al. (1998). "An essential role for tumor necrosis factor in natural killer cell-mediated tumor rejection in the peritoneum." J Exp Med **188**(9): 1611-9.

Snelgrove, R. J., J. Goulding, et al. (2008). "A critical function for CD200 in lung immune homeostasis and the severity of influenza infection." Nat Immunol **9**(9): 1074-83.

Solanilla, A., J. Villeneuve, et al. (2009). "The transport of high amounts of vascular endothelial growth factor by blood platelets underlines their potential contribution in systemic sclerosis angiogenesis." Rheumatology (Oxford) **48**(9): 1036-44.

Somanath, P. R., N. L. Malinin, et al. (2009). "Cooperation between integrin alphavbeta3 and VEGFR2 in angiogenesis." Angiogenesis **12**(2): 177-85.

Stevenson, J. L., A. Varki, et al. (2007). "Heparin attenuates metastasis mainly due to inhibition of P- and L-selectin, but non-anticoagulant heparins can have additional effects." Thromb Res **120 Suppl 2**: S107-11.

Suzuki-Inoue, K. (2011). "Essential in vivo roles of the platelet activation receptor CLEC-2 in tumour metastasis, lymphangiogenesis and thrombus formation." J Biochem **150**(2): 127-32.

Taichman, D. B., M. I. Cybulsky, et al. (1991). "Tumor cell surface alpha 4 beta 1 integrin mediates adhesion to vascular endothelium: demonstration of an interaction with the N-terminal domains of INCAM-110/VCAM-1." Cell Regul **2**(5): 347-55.

Takada, A., K. Ohmori, et al. (1993). "Contribution of carbohydrate antigens sialyl Lewis A and sialyl Lewis X to adhesion of human cancer cells to vascular endothelium." Cancer Res **53**(2): 354-61.

Takai, T., M. Li, et al. (1994). "FcR gamma chain deletion results in pleiotrophic effector cell defects." Cell **76**(3): 519-29.

Tang, D. G. and K. V. Honn (1994). "Adhesion molecules and tumor metastasis: an update." Invasion Metastasis **14**(1-6): 109-22.

Tomiyama, Y., M. Shiraga, et al. (2002). Platelet membrane proteins. Platelets in thrombotic and non-thrombotic disorders. P. Gresele, C. P. Page, V. Fuster and J. Vermylen. Cambridge, UK, Cambridge University Press: 80-92.

Townson, J. L. and A. F. Chambers (2006). "Dormancy of solitary metastatic cells." Cell Cycle **5**(16): 1744-50.

Tremblay, P. L., J. Huot, et al. (2008). "Mechanisms by which E-selectin regulates diapedesis of colon cancer cells under flow conditions." Cancer Res **68**(13): 5167-76.

Trikha, M., Z. Zhou, et al. (2002). "Multiple roles for platelet GPIIb/IIIa and alphavbeta3 integrins in tumor growth, angiogenesis, and metastasis." Cancer Res **62**(10): 2824-33.

Trousseau, A. (1865). Phlegmasia alba dolens. Clinique Medicale de l'Hotel-Dieu de Paris. Paris, J-B Balliere. **3 (94):** 652-695.

Tsai, R. K. and D. E. Discher (2008). "Inhibition of "self" engulfment through deactivation of myosin-II at the phagocytic synapse between human cells." J Cell Biol **180**(5): 989-1003.

Tse, J. C. and R. Kalluri (2007). "Mechanisms of metastasis: epithelial-to-mesenchymal transition and contribution of tumor microenvironment." J Cell Biochem **101**(4): 816-29.

Tsukada, T. and T. Tango (1980). "On the methods calculating mean survival time in 51Cr-platelet survival study." Am J Hematol **8**(3): 281-90.

Tzanakakis, G. N., K. C. Agarwal, et al. (1993). "Prevention of human pancreatic cancer cell-induced hepatic metastasis in nude mice by dipyridamole and its analog RA-233." Cancer **71**(8): 2466-71.

VanDeWater, L., P. B. Tracy, et al. (1985). "Tumor cell generation of thrombin via functional prothrombinase assembly." Cancer Res **45**(11 Pt 1): 5521-5.

Van Putten, L. M. (1958). "The life span of red cells in the rat and the mouse as determined by labeling with DFP32 in vivo." Blood **13**(8): 789-94.

Vidal-Vanaclocha, F. (2008). "The prometastatic microenvironment of the liver." Cancer Microenviron **1**(1): 113-29.

Virchow, R. (1858). Die Cellularpathologie in ihrer Begründung auf physiologische und pathologische Gewebenlehre. Berlin.

Vivier, E., E. Tomasello, et al. (2008). "Functions of natural killer cells." Nat Immunol **9**(5): 503-10.

Vlodavsky, I., A. Eldor, et al. (1992). "Expression of heparanase by platelets and circulating cells of the immune system: possible involvement in diapedesis and extravasation." Invasion Metastasis **12**(2): 112-27.

Vlodavsky, I. and Y. Friedmann (2001). "Molecular properties and involvement of heparanase in cancer metastasis and angiogenesis." J Clin Invest **108**(3): 341-7.

Vlodavsky, I., M. Mohsen, et al. (1994). "Inhibition of tumor metastasis by heparanase inhibiting species of heparin." Invasion Metastasis **14**(1-6): 290-302.

von Hundelshausen, P. and C. Weber (2007). "Platelets as immune cells: bridging inflammation and cardiovascular disease." Circ Res **100**(1): 27-40.

Voulgaraki, D., R. Mitnacht-Kraus, et al. (2005). "Multivalent recombinant proteins for probing functions of leucocyte surface proteins such as the CD200 receptor." Immunology **115**(3): 337-46.

Wagner, D. D. and P. S. Frenette (2008). "The vessel wall and its interactions." Blood **111**(11): 5271-81.

Wagner, K. U., E. Claudio, et al. (2000). "Conditional deletion of the Bcl-x gene from erythroid cells results in hemolytic anemia and profound splenomegaly." Development **127**(22): 4949-58.

Wahrenbrock, M., L. Borsig, et al. (2003). "Selectin-mucin interactions as a probable molecular explanation for the association of Trousseau syndrome with mucinous adenocarcinomas." J Clin Invest **112**(6): 853-62.

Waldhauer, I. and A. Steinle (2008). "NK cells and cancer immunosurveillance." Oncogene **27**(45): 5932-43.

Walsh, M., R. J. Lutz, et al. (2002). "Erythrocyte survival is promoted by plasma and suppressed by a Bak-derived BH3 peptide that interacts with membrane-associated Bcl-X(L)." Blood **99**(9): 3439-48.

Wang, H. S., Y. Hung, et al. (2005). "CD44 cross-linking induces integrin-mediated adhesion and transendothelial migration in breast cancer cell line by up-regulation of LFA-1 (alpha L beta2) and VLA-4 (alpha4beta1)." Exp Cell Res **304**(1): 116-26.

Waugh, R. E., M. Narla, et al. (1992). "Rheologic properties of senescent erythrocytes: loss of surface area and volume with red blood cell age." Blood **79**(5): 1351-8.

Webster, M. L., E. Sayeh, et al. (2006). "Relative efficacy of intravenous immunoglobulin G in ameliorating thrombocytopenia induced by antiplatelet GPIIbIIIa versus GPIbalpha antibodies." Blood **108**(3): 943-6.

Wessels, M. R., P. Butko, et al. (1995). "Studies of group B streptococcal infection in mice deficient in complement component C3 or C4 demonstrate an essential role for complement in both innate and acquired immunity." Proc Natl Acad Sci U S A **92**(25): 11490-4.

Weston, S. A. and C. R. Parish (1990). "New fluorescent dyes for lymphocyte migration studies. Analysis by flow cytometry and fluorescence microscopy." J Immunol Methods **133**(1): 87-97.

Weyrich, A. S. and G. A. Zimmerman (2004). "Platelets: signaling cells in the immune continuum." Trends Immunol **25**(9): 489-95.

Willekens, F. L., B. Roerdinkholder-Stoelwinder, et al. (2003). "Hemoglobin loss from erythrocytes in vivo results from spleen-facilitated vesiculation." Blood **101**(2): 747-51.

Wohner, N. (2008). "Role of cellular elements in thrombus formation and dissolution." Cardiovasc Hematol Agents Med Chem **6**(3): 224-8.

Wojtukiewicz, M. Z., D. G. Tang, et al. (1992). "Thrombin enhances tumor cell adhesive and metastatic properties via increased alpha IIb beta 3 expression on the cell surface." Thromb Res **68**(3): 233-45.

Wong, S. Y. and R. O. Hynes (2006). "Lymphatic or hematogenous dissemination: how does a metastatic tumor cell decide?" Cell Cycle **5**(8): 812-7.

Woulfe, D., J. Yang, et al. (2002). Signal Transduction During the Inititation, Extension and Perpetutation of Platelet Plug Formation. Platelets. A. D. Michelson. San Diego, C.A., Elsevier Science: 197-213.

Xue, K. X. and J. Gao (1989). "A study of the formation of liver metastasis and its mechanism using the intrasplenic inoculation of cancer cells." Chinese Journal of Cancer Research **1**(2): 8-12.

Yamao, T., T. Noguchi, et al. (2002). "Negative regulation of platelet clearance and of the macrophage phagocytic response by the transmembrane glycoprotein SHPS-1." J Biol Chem **277**(42): 39833-9.

Yeaman, M. R. and A. S. Bayer (2002). Antimicrobial Host Defense. Platelets. A. D. Michelson, Elsevier Science: 469-490.

Yoshida, H. and D. N. Granger (2009). "Inflammatory bowel disease: A paradigm for the link between coagulation and inflammation." Inflamm Bowel Dis.

Yu, Y., X. D. Zhou, et al. (2002). "Platelets promote the adhesion of human hepatoma cells with a highly metastatic potential to extracellular matrix protein: involvement of platelet P-selectin and GP IIb-IIIa." J Cancer Res Clin Oncol **128**(5): 283-7.

Zetter, B. R. (1993). "Adhesion molecules in tumor metastasis." Semin Cancer Biol **4**(4): 219-29.

Zhang, L., C. B. Underhill, et al. (1995). "Hyaluronan on the surface of tumor cells is correlated with metastatic behavior." Cancer Res **55**(2): 428-33.

Zhang, Y., L. Li, et al. (2007). "Downregulating the expression of heparanase inhibits the invasion, angiogenesis and metastasis of human hepatocellular carcinoma." Biochem Biophys Res Commun **358**(1): 124-9.

Zijlstra, M., M. Bix, et al. (1990). "Beta 2-microglobulin deficient mice lack CD4-8+ cytolytic T cells." Nature **344**(6268): 742-6.

Zucker-Franklin, D. and C. S. Philipp (2000). "Platelet production in the pulmonary capillary bed: new ultrastructural evidence for an old concept." Am J Pathol **157**(1): 69-74.